КОЛЛОИДНЫЙ ЖУРНАЛ

COLLOID JOURNAL

(KOLLOIDNY ZHURNAL)

(1957)

IN ENGLISH TRANSLATION

WITHDRAWN
POSTMASTER:
IF NOT DELIVERABLE NOTIFY
Chemical Abstracts
OHIO STATE UNIV., COLUMBUS 10, O.
AND POSTAGE WILL BE SENT
REC'D. MAR 24 1958 C. A. LIBRARY
ABSTRACTOR:
PLEASE RETURN PROMPTLY TO
CHEMICAL ABSTRACTS
OHIO STATE UNIV., COLUMBUS 10, O.

VOL. 19 NO. 3

CONSULTANTS BUREAU, INC.
227 WEST 17TH STREET, NEW YORK 11, N. Y.

an agency for the interpretation of international knowledge

JOURNAL OF

GENERAL CHEMISTRY

OF THE USSR

(Obshchei Khimii.)

in complete English translation

The most important Russian chemical journal, with broad coverage of all aspects of investigation, from the purely theoretical and experimental, to the most practical, including industrial applications, covers: Organic and inorganic research, pharmacology, petroleum, textiles, biology, medicine, dyes, and fuels, etc.

Sample articles: Two forms of gramicidin, their mutual transformations and structure; the change of the chemical heterogeneity of cellulose xanthate during the ripening of viscose; investigation in the field of tantomeric compounds; the lability of hydrogen atoms of the quinaldine methyl group; the problem of experimental proof of the Baker-Nathan effect; polarographic study of the kinetics of polymerization processes.

Annual subscription, 12 issues,
approx. 3600 pages, $170.00.

Single articles available—Tables of Contents on request.

CONSULTANTS BUREAU, INC.
227 WEST 17th STREET, NEW YORK 11, N.Y. — U.S.A.
Telephone: ALgonquin 5-0713 • Cable Address: CONBUREAU, NEW YORK

COLLOID JOURNAL

(KOLLOIDNY ZHURNAL)

Journal of Theoretical and Applied Physics and

Chemistry of Colloids

Volume XIX

(Number 3, May-June, 1957)

Editor

A. V. Dumansky

Editorial Board

P. N. Antipov-Karataev, B. V. Deryagin, B. A. Dogadkin (Deputy Editor), A. V. Dumansky,
V. A. Kargin, S. M. Lipatov, P. A. Rebinder, I. P. Serdobolsky (Secretary), M. P. Volarovich

Publication of the Academy of Sciences of the USSR

IN ENGLISH TRANSLATION

Copyright, 1957

CONSULTANTS BUREAU, INC.
227 West 17th Street
New York 11, N. Y.

Printed in the United States

Annual Subscription . . . . $ 80.00
Single issue 20.00

Note: The sale of photostatic copies of any portion of this copyright translation is expressly prohibited by the copyright owners. A complete copy of any paper in this issue may be purchased from the publisher for $ 7.50.

HEATS OF SWELLING AND SOLUTION OF POLYMERS IN RELATION TO MOLECULAR WEIGHTS AND TEMPERATURE

K. S. Akhmedov and S. M. Lipatov

The heat effects of interaction of polymers with organic solvents and plasticizers have been studied by a number of workers. Lipatov and his associates [1] established that acetylcellulose fractions in methyl acetate, and gelatin fractions in water, each have the same heats of swelling and solution at room temperature, irrespective of molecular weight. Kargin and Tager [2] showed that the heats of solution of different nitrocellulose fractions in acetone are equal. However, it has also been found that in a number of instances heats of solution or swelling depend on the molecular weight and the strength of the structure of the polymer. Lipatov and Morozov [3] showed as long ago as 1935 that agar fractions have different heats of swelling and solution. For an agar fraction of molecular weight 6050 the heat of swelling was 36.9 cal./g, and for molecular weight 25,380, the value was 44.6 cal./g, or higher by 7.5 cal./g. Recently Schulz [4] found that the heat of solution of polystyrene fractions depends on the molecular weight. Tager [5] obtained a similar result for the same polymer.

However, as has been shown in a number of papers by Lipatov et al. [6], studies of heat effects at room temperature cannot reveal the structural characteristics of different polymers in relation to their chemical structure, molecular weight, etc. In these papers [6] it was established that structural problems can be solved conclusively only by studying variations of the heats of solution with temperature. This approach has been increasingly used in recent years; it was successfully utilized by Schulz [4] in studying the heats of solution of polystyrenes of different molecular weight, and by Tager [2] in studies of the same polymer.

While it was previously believed that problems of polymer structure could be definitely solved by the simultaneous use of X-ray and electron diffraction methods [7], at the present time the calorimetric method can be regarded as a method for studying structure together with these [6, 8]. Thus, the thermodynamic and structural criteria of the phase state not only do not diverge in the case of polymers, as has been asserted quite recently [9], but they are firmly interconnected, as for substances of low molecular weight.

EXPERIMENTAL

Polyvinyl chloride and perchlorovinyl (chlorinated PVC). To study the effect of molecular weight on the heat of solution of polymers at different temperatures, polyvinyl chloride and two of its fractions were used; for this, polyvinyl chloride was fractionated from 4% solution in dichloroethane by additions of various amounts of absolute alcohol. The chlorine contents of the polyvinyl chloride samples were determined by the Carius combustion method; the value for our samples was 56.2% by weight, corresponding to the following composition: $-CH_2-CHCl-CH_2-CHCl-$.

The molecular weights of the polyvinyl chloride samples were determined viscosimetrically from the intrisic $M^{0.67}$ viscosities of their solutions in dichloroethane at 30°, and calculated from the formula

$$[\eta] = 3 \cdot 10^{-4}\ M^{0.67}.$$

The viscosimetric determinations were performed with a capillary hanging level viscosimeter, adapted for use with volatile liquids, convenient for studies of viscosity over a wide temperature range.

The heats of swelling and solution were determined by means of an adiabatic calorimeter, in adiabatic or isothermal conditions depending on the duration of the swelling and solution processes. The tables and graphs give average values for 2-3 parallel determinations. The determinations were accurate to within ± 0.25 cal./g.

TABLE 1

Intrinsic Viscosities and Molecular Weights of Polyvinyl Chloride Samples in Dichloroethane at 30°

Polymer	Intrinsic viscosity in poises	Molecular weight
Nonfractionated polyvinyl chloride	0.75	117 900
Polyvinyl chloride, Fraction I	0.65	95 500
Ditto, Fraction II	1.15	223 100

Polyvinyl chloride. The behavior of Fractions I and II in two solvents – dichloroethane and nitrobenzene – was studied as a function of the temperature. The heats of swelling and solution of the low and high molecular weight fractions of polyvinyl chloride in dichloroethane and nitrobenzene at various temperatures are given in Figs. 1 and 2.

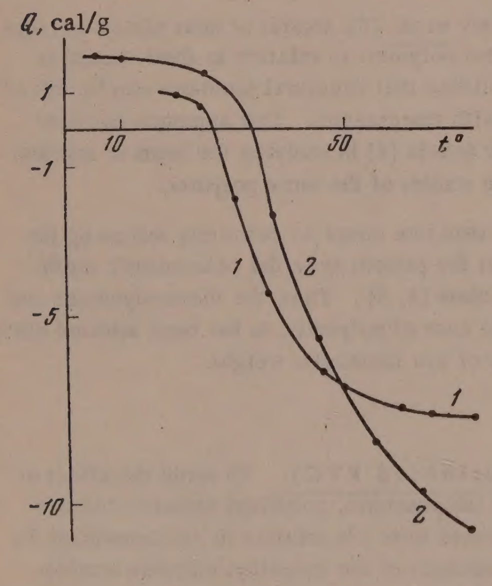

Fig. 1. Variation of the heats of swelling and solution of polyvinyl chloride in dichloroethane with temperature: 1) soluble fraction; 2) insoluble fraction.

It is seen in Figs. 1 and 2 that with increase of temperature the structural differences between the fractions, and the influence of the nature of the solvent on the heat effect and its temperature relationship, become more prominent. Figure 1 shows that the two polyvinyl chloride fractions differ considerably in their behavior in dichloroethane. In the temperature range of 25-50° the first fraction dissolves with a greater negative heat effect than the second, while at temperature above 50-55° a clearly pronounced opposite is seen. Thus, at 70° the first fraction dissolves with absorption of 8 cal./g, and the second, with absorption of 14 cal./g. This is not found with nitrobenzene as solvent (Fig. 2). In the 20-70° temperature range the heats of solution of the two fractions differ sharply, while above 70° they are equal.

Here we have a case in which, for the same packing density, the heat of solution varies greatly at different temperatures according to the nature of the solvent.

Ftorlon.* A similar study was made of the heats of swelling and solution of three fluorinated polymer samples with equal fluorine contents, but with different specific viscosities in 0.25% solutions in acetone** (η_{sp}).

---

* "Ftorlon" derives its name from "ftor", Russian from fluorine, and is one of the fluorinated hydrocarbon polymers.

** The fluorinated polymers with definite characteristics were kindly supplied by Z. A. Rogovin, to whom we express our gratitude.

The heats of solution of the fluorinated polymers in acetone at different temperatures are given in Table 2 and Fig. 3.

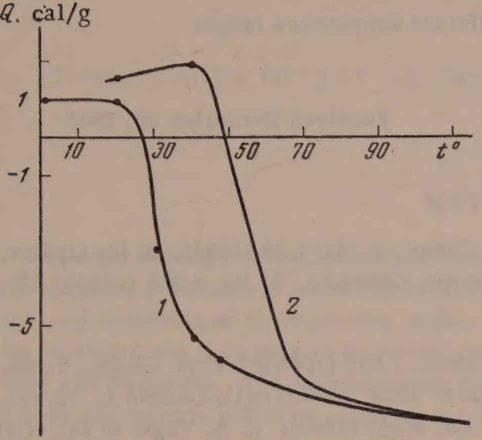

Fig. 2. Variation of the heats of swelling and solution of polyvinyl chloride in nitrobenzene with temperature: 1) soluble fraction; 2) insoluble fraction.

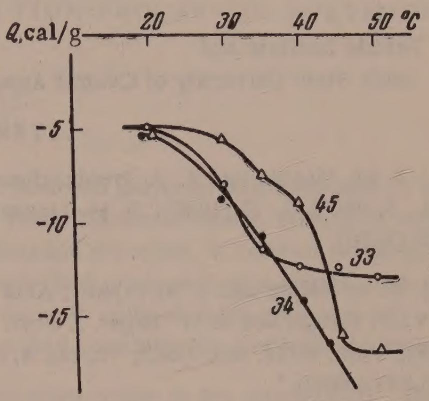

Fig. 3. Variation of the heats of swelling and solution of three fluorinated polymer samples (33, 34, 45) with temperature.

TABLE 2

Heats of Solutions of Fluorinated Polymers (Q cal./g) in Acetone at Different Temperatures

Temperature in °C	Heats of solution in cal./g		
	Sample 33 $\eta_{sp} = 0.26$	Sample 45 $\eta_{sp} = 0.705$	Sample 34 $\eta_{sp} = 0.94$
20	— 5.14	— 5.10	— 5.14
30	— 8.20	— 5.33	— 8.80
35	—11.75	— 7.60	—10.65
40	—12.35	— 9.00	—14.45
45	—12.44	—16.37	—16.5
50	—13.2	—17.0	—22.5

As Table 2 shows, the heats of solution of the fluorinated polymers in acetone in the 20 to 50° temperature range are negative. Samples 34 and 45 show a gradual decrease of the heat effect of solution with temperature, the decrease being greater with higher solution viscosity. Sample 33, with considerably lower solution viscosity, shows a sharp decrease of the heat of solution between 20 and 35°, but from 35° the heat of solution remains constant. These results demonstrate the influence of molecular weight on the heats of swelling and solution as a function of the temperature. However, the influence of the molecular weight greatly depends on the chemical composition and physical state of the polymers.

The heat effect for amorphous polystyrene increases with increasing molecular weight, and the curves lie higher for greater molecular weights [4]. At 20°, despite the molecular weight differences, the heats of swelling of the polymers are equal, but a 50° increase in the molecular weight of the polymer results in an increasing negative value of the heat of solution.

SUMMARY

1. The effect of temperature on the heats of swelling and solution of polyvinyl chloride and ftorlon of different molecular weights has been studied.

2. The increasing negative heat effect cannot be attributed to changes of packing density.

3. The influence of the molecular weight differs in different temperature ranges.

Moscow Textile Institute and
the V. I. Lenin State University of Central Asia

Received December 28, 1956

LITERATURE CITED

[1] S. M. Lipatov and Z. A. Preobrazhenskaya, J. Gen. Chem., 4, No. 1,59 (1934); S. M. Lipatov, Colloid J., 8, No. 1-2, 73 (1946); S. M. Lipatov and S. I. Meerson, Colloid J., 8, No. 4,233 (1946); 12, No. 2,122 (1950).

[2] V. A. Kargin and S. A. Papkov, Acta Physicochim. URSS, 3,839 (1935); J. Phys. Chem., 7, No. 4,483 (1936); V. A. Kargin and A. A Tager, J. Phys. Chem., 15, No. 9, 1029, 1036 (1941); Colloid J., 10, No. 6, 455 (1948); Proc. Acad. Sci. USSR, 72, No. 4,725 (1950); 73, No. 5,967 (1950); A. A. Tager et al., Colloid J., 14, No. 5,367 (1952).*

[3] S. M. Lipatov and A. A. Morozov, J. Gen. Chem., 5, No. 8, 1120 (1935).

[4] G. V. Schulz, Naturwissensch. 40, 164, 1953; Z. phys. Chem. 192, 221, 1955.

[5] A. A. Tager, R. V. Krivokorytova, and P. M. Khodorov, Proc. Acad. Sci. USSR, 100, No. 4, 741 (1955).

[6] S. M. Lipatov, Proc. Acad. Sci. USSR, 48, No. 6,434 (1945); S. M. Lipatov and S. I. Meerson, Colloid J., 8, No. 4,233 (1946); 12, No. 2,125 (1950); S. I. Meerson, Dissertation (Moscow, 1945).

[7] G. L. Slonimsky, Mechanical Properties of Polymers and the Properties of their Solutions (State Light Ind. Press, Moscow, 1951).

[8] N. V. Mikhailov and E. Z. Fainberg, Proc. Acad. Sci. USSR, 109, 1160 (1956).

[9] B. A. Kargin and G. L. Slonimsky, Progr. Chem., 24, 785 (1955).

---

* Original Russian pagination, see C. B. Translation.

TWO STAGES OF THE NETWORK FORMATION PROCESS IN POLYMERS

G. M. Bartenev

The cross linking (structurization) of linear and slightly branched polymers forms the basis of a number of technological processes, of which the most important are: vulcanization of rubber, tanning of collagen and gelatin, and hardening of thermosetting resins. These structurization processes, in contrast to aging processes, can be regulated and they play an important part in the technological production of materials with required structure and properties. The structurization processes which occur in aging develop spontaneously and in most cases have and adverse effect by changing the desired structure and worsening the properties of the materials.

It has been shown that the process of spatial network formation occurs in two stages [1-3]. The two-stage nature of the process was observed in the first two investigations [1, 2]. In the third [3], the importance of the initial molecular weight of the polymer was established. It was shown that the start of network formation corresponds to a certain quite definite amount of bound sulfur, which depends on the molecular weight of the polymer. The first general views on the two-stage nature of the process were probably put forward by Flory [4].

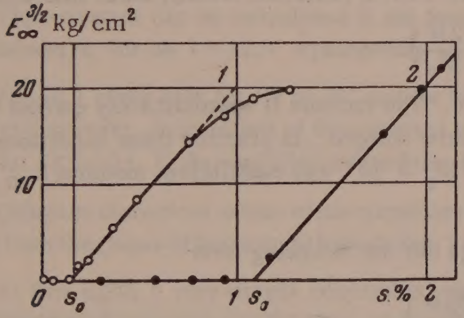

Fig. 1. Relationship between the equilibrium modulus and the amount of bound sulfur (in weight percentages on the vulcanizate): 1) NR (natural rubber); 2) SKS-30A.

The general mechanism of spatial network formation in the structurization of linear polymers, for the case of rubber vulcanization, is discussed below. The chemical aspects of polymer network formation are discussed in a recent review [5].

1. The two-stage nature of the network formation process is seen in Fig. 1, which shows, as an illustration, the variation of the equilibrium modulus (to the power 3/2) with the amount of sulfur bound during vulcanization of an unfilled natural rubber composition (NR), of molecular weight 150,000, modulus at 20°, from N. M. Novikova's data, and a synthetic SKS-30A rubber fraction of molecular weight 140,000, modulus at 70°, from the data of F. A. Galil-Ogly. The choice of the equilibrium modulus to characterize the spatial network [6, 7] is explained by the fact that the equilibrium modulus E_∞ bears a definite relationship to the number of chains in the network N per unit volume. In Fig. 1, values of $E_\infty^{3/2}$, which, according to [6], is proportional to N, are taken along the ordinate axis. If the amount of bound sulfur is proportional to the number of cross links, then the relationship between $E_\infty^{3/2}$ and the amount of bound sulfur must be linear; this is found to be so for all fractions of SKS-30A at the second stage of cross linking [3]. Natural rubber shows a deviation from linearity at the end of the second stage; this is explained by superposition of thermooxidative degradation processes on the vulcanization.

At the first stage a single spatial network is not yet formed, as the equilibrium modulus is zero. At the first stage the material is in a plastic, and at the second, in an elastic state. At the first structurization stage the molecular chains are not yet joined in a single spatial network, but individual molecules are cross-linked into larger formations. Only after these molecular aggregates have reached a definite size does the subsequent cross linking lead to the formation of a continuous spatial network.

2. Let us consider the cross linking of a linear polymer with initial molecular weight M_0, assuming that the cross links have a statistically uniform distribution throughout the volume. Let M be the molecular weight of a chain in the network (segment of a linear molecule between two cross links). Corresponding to these are N_0 and N, the numbers of original molecules and network chains per unit volume; n is the total number of cross links per unit volume of the polymer; ν is the number of cross links per unit volume.

At the first stage of structurization the cross links join individual linear molecules, which results in an increase of the average molecular weight of the polymer. As has been reported [1, 4, 8], network formation begins not at once, but after all (or nearly all) the molecules of the original material have been joined by cross links. At this stage long branched chains are formed, much larger than the original linear molecules. Thus, cross linking of individual molecules leads to formation of long branched chains, the molecular weight M of which increases to values greatly exceeding M

The material remains plastic until enough cross links have been formed to join the original molecules into a spatial network. We shall term this number of cross links per unit volume the "critical" number, and shall denote it by $n_k = \beta N_0$, where β is a coefficient which depends on the molecular weight distribution, and the degree of coiling and intertwining of the molecules in the original material (the meaning of the coefficient β is discussed below).

It is evident that when $n < n_k$, $\nu = 0$; when $n \geq n_k$, $\nu = n - n_k$.

The number of chains N determines the equilibrium properties and is included in the formulas of the molecular theory of network polymers. Since each new cross link forms two new chains, $N = 2\nu$, and therefore when $n \geq n_k$

$$N = 2(n - n_k) = 2(n - \beta N_0), \tag{1}$$

and when $n < n_k$, $N = 0$.

The Flory formula [4, 8] derived (for $\beta = 1$) with network defects (terminal chains) taken into account

$$N = \frac{\rho_0 N_A}{M}\left(1 - \frac{2M}{M_0}\right)$$

is not suitable for the whole $n \geq n_k$ range of network formation. The formula is approximately correct when $M \ll M_0$, that is, for dense networks and high original molecular weights. In practice these conditions are probably satisfied for network polymers with molecular weight $M_0 > 10^5$ and equilibrium modulus E_∞ greater than 10 kg / cm^2.

The general formula valid over the entire $n \geq n_k$ range has the following form

$$N = 2n \Big/ \left(1 + \frac{2\beta\rho M}{\rho_0 M_0}\right),$$

where ρ is the density for the active part of the rubber; ρ_0 is the density for the whole rubber, including the regions of the molecules which did not enter the network. Calculation of ρ is the main difficulty in the use of this formula.

3. To illustrate the application of these relationships, let us consider the vulcanization of butadiene – styrene SKS-30A and natural (NR) rubber. Let j be the number of sulfur atoms per cross link both between different molecules and between parts of the same molecule. The total and "critical" numbers of cross links are expressed in terms of the amount of bound sulfur by the following formulas:

$$n = \frac{\rho N_A}{\mu j}\frac{s}{100}; \qquad n_k = \frac{\rho N_A}{\mu j}\frac{s_0}{100}, \tag{2}$$

where $\mu = 32{,}1$ is the atomic weight of sulfur; s and s_0 are the total and "critical" amounts of bound sulfur in percentages by weight (on the vulcanizate).

For the "critical" amount of bound sulfur we have the formula

$$s_0 = \beta j/\mu \cdot 100 \frac{1}{M_0}, \tag{3}$$

which is in good agreement with the data [3] given in Fig. 2.

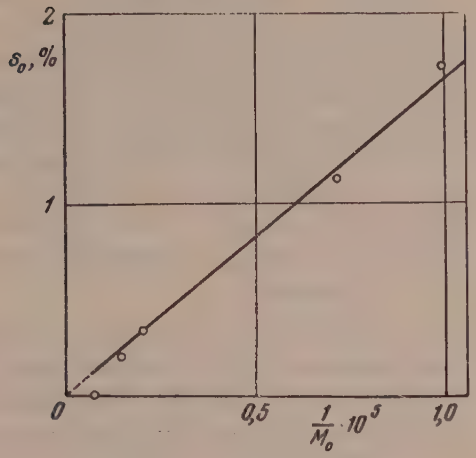

Fig. 2. Relationship between the "critical" amount of sulfur added during vulcanization, and the reciprocal molecular weight of the original polymer (from data in [3]).

The value of s_0 is determined from the intercept cut off (Fig. 1). For NR, s_0 is 0.15% at M_0 = 150.000, which gives βj = 7. For SKS-30A the value, found from the straight line in Fig. 2, is βj = 50.

It is not possible to determine the number of sulfur atoms in the cross link, j, by the intercept method, as the coefficient β is not known. It is possible to find j from the slope of the straight line in the coordinates of Fig. 1.

From Equations (1) and (2) it follows that

$$N = \frac{2\rho N_A}{\mu j} \frac{\Delta s}{100}, \tag{4}$$

where $\Delta s = s - s_0$.

For further calculations by this formula it is necessary to know the relationship between N and E_∞. For this we use the relationship $N = CE_\infty^{3/2}$ [6], where C is a constant which depends on the physical properties of the polymer molecules and the temperature.

This constant can be calculated if the length of the chain segment in the Kuhn model is known. According to Vishnitskaya, for NR l = 12.0 Å (according to Kuhn l = 13 Å), and for SKS-30A l = 12.6 Å.

Figure 1 gives data for NR at 20° and for SKS-30A (fraction of molecular weight 140,000) at 70°. For these temperatures, calculation of the constant gives the following values: $C = 2.29 \cdot 10^{18}$ for NR, and $C = 1.96 \cdot 10^{18}$ for SKS-30A, if the equilibrium modulus is expressed in kilograms per 1 cm^2.

Using the numerical values of the quantities in Formula (4) (ρ = 0.96 for NR, ρ = 0.94 for SKS-30A vulcanizates), we find from the slopes of the straight lines in Fig; 1 (for NR) and Fog. 3 (for SKS-30A that $j \approx 7$ for both rubbers.

At first sight, a very simple conclusion suggests itself: each cross link is formed by the opening of an eight-membered molecular sulfur ring, as in vulcanization without accelerators [9]. However, this cannot be asserted, in view of the possible deviations from the ideal vulcanization process. There are data [9] showing that j should be smaller in vulcanization with an accelerator *.

Network defects (in contrast to the ideal network formed by cross linking of a linear polymer of the maximum molecular weight) include closed loops, end of molecules not included in the network, mechanical entanglement of two chains (according to Flory [4]), cross links in close proximity to each other, and branching of the polymer chains. These "defects" can be taken into account only roughly and qualitatively. It has been shown for NR [6] that the ends of the original rubber molecules which do not enter into the network do not influence the equilibrium modulus if the initial molecular weight is high enough (150,000) and the modulus is not too low. It is evident that defects like ends and closed loops depend on the initial molecular weight. It follows from the data in Fig. 3 that for SKS-30A rubber these defects are not significant, as the initial molecular weight has practically no influence on the equilibrium modulus.

---

* It must be taken into account that part of the added sulfur does not form cross links [1], and this may lead to a decrease of j. From the experimental results given (Figs. 1, 3, 4) it follows that the amount of sulfur which does not form cross links is proportional to the total amount of bound sulfur.

Cross links in close proximity arise with increasing frequency as the spatial network becomes denser and with greater irregularity of distribution of the sulfur molecules through the vulcanizate. Such defects should lead to deviations from the linear relationship shown in Fig. 3 only with high contents of bound sulfur. For thin networks, such as are represented by the data in Figs. 1-3, these defects can probably also be ignored. If ends, loops, and closely situated cross links are taken into account, the value of $\bar{j}$ should decrease (to only a slight extent for the vulcanizates in question).

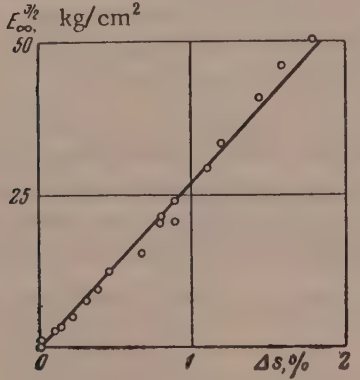

Fig. 3. Variation of equilibrium modulus with the amount of bound sulfur added in the second stage of vulcanization, for different fractions of SKS-30A rubber with molecular weights from 100,000 to 1,170,000, from F. A. Galil-Ogly's data (equilibrium modulus determined at 70°).

Other "defects", such as mechanical entanglement and branching, result in formation of additional cross bonds in the spatial network and therefore $\bar{j}$ would increase if they are taken into account. For NR and SKS-30A branching may be neglected. Mechanical entanglements are not fixed cross links in the network, as the points of contact continuously change because of thermal motion. These have not been taken into consideration in the deformation theory of network polymers.

The views put forward above provide an explanation for the "critical" molecular weight of rubber, for which the first vulcanization stage is not found [3]. The material before vulcanization usually contains a certain number n' of cross links of various origins. With a high enough molecular weight of the rubber this number may reach the critical value, and the critical molecular weight is therefore $M'_0 = \beta \rho N_A / n'$.

The different coefficients for NR and SKS-30A ($\beta = 1$ and $\beta = 7$) were somewhat unexpected. The probable explanation for the difference lies in the technological preparation of the materials for vulcanization. Fractions of SKS-30A rubber were prepared in the form of films from a solution of the rubber and other ingredients in benzene, while the natural rubber mix was made in the usual way on rolls. The same result as for NR ($\beta = 1$), was obtained for SKS-30A and SKS-30 mixes made on rolls. This probably indicates that the molecules become globulized in solution [10], in contrast to processing on rolls, * when the chain molecules become ruptured and entangled.

In a globular structure a considerable proportion of the cross links is used in intramolecular cross linking, and the rest in intermolecular, which prolongs the first structurization stage.

4. In rubber technology attention has been devoted mainly to studies of the vulcanization optimum. The initial stage of vulcanization has been studied only recently. In two investigations [11, 12] the conditions and duration of the initial stage of vulcanization were studied both from the technological and the chemical aspects (chemical kinetics of cross link formation).

The first vulcanization stage determines the correct technological production of molded rubber articles. The flow of the rubber mix and filling of the mold depend on the existence of this stage. The pressure in the vulcanization press and in pressure molding makes for a more rapid filling of the mold. Absence of the first vulcanization stage leads to the undesirable effect known as "scorching", **

---

* In this case the molecular weight M_0 refers not to the original rubber but to the material after treatment on rolls.

** At vulcanization temperatures (130 – 150°, as has been shown [9, 13, 14]), irreversible flow occurs in network polymers also, but the rate of plastic deformation at the second vulcanization stage is low and the mold is filled mainly during the first stage of the process.

The duration of the first vulcanization stage $t = \int_0^{s} \frac{ds}{W}$ depends on the sulfur addition rate $W = ds/dt$. critical amount of sulfur s_0, and therefore on the type of accelerator group, vulcanization temperature, technological preparation, and the molecular weight of the starting material. Absence of the first vulcanization stage is a result of the fact that a critical or larger number of cross links is formed in the original material before vulcanization, owing to thermooxidation processes, scorching, and other structurization processes. The existence of a prolonged first vulcanization stage (like its absence) is undesirable, and is caused by a low rate of sulfur addition, low molecular weight, absence of high molecular weight fractions in the rubber, globular structure of the polymer, etc.

Correct technology of vulcanization of rubber mixes in molding presses should correspond to a quite definite optimum duration of the first stage of the process. At present the composition of the technological rubber mixes for the production of molded articles is based on the results of practical experience. Therefore the technological potentialities will be increased by the use of a method whereby the duration of the first stage can be determined.

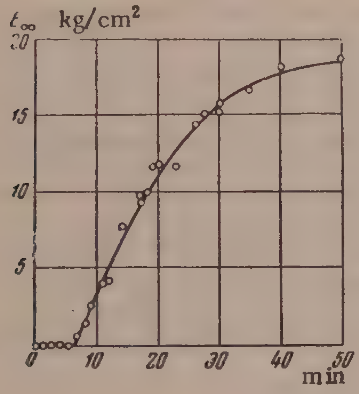

Fig. 4. Variation of the equilibrium modulus with vulcanization time for unfilled SKS-30 rubber, from data in [2].

The duration of the first stage can be determined by measurements of the equilibrium modulus for different times of vulcanization of the mix*. As an illustration of this method, Fig. 4 shows the variation of the equilibrium modulus with vulcanization time for an unfilled mixture made on rolls from SKS-30 rubber with 3 parts of sulfur and 1 part of mercaptobenzothiazole by weight, at a vulcanization temperature of 143°.

At the present time the optimum value of the first vulcanization stage is chosen indirectly – by plasticity tests on the mixes and by selection of rubbers of suitable molecular weight distribution**, by addition of antioxidants, and by suitable selection of vulcanizing groups, mixing conditions, and vulcanization temperature.

The effectiveness of the proposed method should be verified by further investigations on technical rubbers. Applications of the method to studies of structurization processes in gelatin and resins [15, 16] are of undoubted interest.

SUMMARY

1. The two-stage nature of network formation in polymers is discussed, and a formula is derived connecting the number of chains in the network with the initial molecular weight of the polymer and the number of cross links. It is shown that below a certain critical number of cross links a network is not formed.

2. The application of the derived relationships in determination of the number of sulfur atoms in the cross links, the critical molecular weight, and the degree of globulization of the rubber, has been studied in the case of rubber vulcanization.

3. The first vulcanization stage is shown to be of considerable practical importance, as it determines the correct technological conditions for the vulcanization of rubber in molding presses, multilayer articles, etc. For this reason, determinations of the vulcanization optimum in rubber technology must be augmented by studies of the initial stage of the process. A method for determining the duration of the first stage of vulcanization is described.

---

* The nonequilibrium (technological) modulus is unsuitable for this purpose, as it is not zero for the plastic state.

** The simultaneous presence of fractions of low and high molecular weight ensures plasticity of the mixture at the first stage and a high rate of network formation at the second stage.

I express my gratitude to B. A. Dogadkin for discussion of the work.

Scientific Research Institute for the Rubber Industry
Moscow

Received May 4, 1956

LITERATURE CITED

[1] B. A. Dogadkin, G. M. Bartenev, and N. M. Novikova, Colloid J., 10, No. 2,94 (1948).

[2] G. M. Bartenev and G. I. Belostotskaya, J. Tech. Phys., 24, No. 10, 1773 (1954).

[3] A. S. Novikov, G. M. Bartenev, and F. A. Galil-Ogly, Proc. Acad, Sci. USSR, 94, No. 22, 253 (1954).

[4] P. Flory, Chem. Rev. 35, 51, (1944).

[5] B. A. Dogadkin and M. M. Reznikovsky, Progr. Chem. 24, No. 7, 801 (1955).

[6] G. M. Bartenev, J. Tech. Phys., 22, No. 7, 1154 (1952); Proc. Sci.-Tech. Conf. All-Union Sci. Tech. Soc. Rubber Technologists, 1953 (State Chem. Press, 1954) pp. 196-207.

[7] L. A. Vishnitskaya, Trans. Inst. Rubber Ind., 1,53 (1954).

[8] L. Treloar, Physics of Rubber Elasticity (Foreign Lit. Press, 1953) p. 69. [Russian Translation.]

[9] B. A. Dogadkin and Z. N. Tarasova, Colloid J., 15, No. 5, 347 (1953).*

[10] A. S. Novikov, T. V. Dorokhina, and P. I. Zubov, Proc. Acad. Sci. USSR, 105, No. 3, 514 (1955).

[11] B. A. Dogadkin, M. Feldhstein, and D. Pevzner, J. Appl. Chem., 28, 533, (1955).

[12] B. A. Dogadkin, Bond Strength Between the Layers of Rubber-Fabric Multilayer Articles (State Chem. Press, 1956) pp. 16-28.

[13] A. Tobolsky, I. Prettymann, J. Dillon, Appl. Phys. 15, 380, (1944).

[14] G. L. Slonimsky, V. A. Kargin, G. N. Buiko, E. V. Reztsova, and M. Lyuis-Riera, Proc. Acad. Sci. USSR, 93, 523 (1953).

[15] P. I. Zubov, Z. N. Zhrukina, and V. A. Kargin, Colloid J., 16, 109, 345 (1954).*

[16] G. L. Slonimsky, V. A. Kargin, and L. I. Golubenkova, Proc. Acad. Sci. USSR, 93, 311 (1953).

---

* [Original Russian pagination. See C. B. Translation].

THE ELECTROCHEMISTRY OF HIGH-POLYMER DISPERSIONS

4. INFLUENCE OF CATIONS OF DIFFERENT VALENCIES ON THE ELECTROKINETIC POTENTIAL OF SYNTHETIC LATEX GLOBULES

S. S. Voyutský and R. M. Panich

The influence of univalent ions on the zeta-potential of negatively charged latex globules has been studied in considerable detail [1]. In contrast to this, the action of multivalent ions on the electrokinetic potential of latex globules has hardly been studied at all. This question has only been touched upon in our investigations [2, 3], but as the zeta-potential was determined by an imperfect method without allowance for the ionic strengths of the solutions, the results obtained require correction.

Investigation of the action of multivalent cations on the zeta-potential of latex globules is of great interest, as electrolytes with such cations are the usual latex coagulant in industry. Moreover, as was first shown by our investigations, introduction of multivalent cations into the latex results in reversal of the globule charge, which may also be of great practical importance.

The object of the present investigation was a more detailed comparative study of the effects of cations of different valencies on the zeta-potential of synthetic latex globules, with due attention to all the requirements of the experimental technique for determination of electrophoretic mobility. Considerable attention was also paid to charge reversal on the latex particles by means of multivalent ions.

Determination of the thresholds of coagulation of latex by electrolytes.

First, the maximum electrolyte concentrations were determined at which the latex is still stable and does not contain floccules which hinder electrophoresis. The material studied was dialyzed BD1 latex, containing ammonium napthenate stabilizer. Fuller details of this latex were given in an earlier communication [4].

TABLE 1

Threshold of Coagulation of Latex BD1 by Electrolytes with Cations of Different Valencies

Electrolyte	Coagulation threshold in millimoles/liter	Ratio of coagulation thresholds
NH_4Cl	440	245
$CaCl_2$	6.7	3.75
$AlCl_3$	1.8	1.0

The electrolytes used were ammonium chloride, calcium chloride, and aluminum chloride. The first was chosen because the latex contained ammonium ions; the second, because calcium ions are usually present in industrial water; and the third because, in industry, aluminum salts are generally used for latex coagulation. These electrolytes all had the same anion. The coagulation threshold was determined by mixing equal volumes of latex and electrolyte solutions of various concentrations. The concentration of BD1 latex used for the experiments was 1%. The results are given in Table 1, where the concentrations given for calcium and aluminum chlorides correspond to irreversible coagulation, while the aluminum chloride concentration corresponds to reversible flocculation, which disappears on dilution of the latex with water.

Table 1 shows that, for latexes with negatively charged particles, the valency of the cation has a very strong influence on the coagulation threshold; i. e., the Schulze – Hardy rule for lyophobic colloidal systems is obeyed. Table 1 shows also that the coagulation thresholds for uni- and bivalent ions are inversely proportional to the sixth power of the valency, which is in agreement with the formula derived by Deryagin and Landau [6] from the theory of stability of Lyophobic sols, and which is a quantitative refinement of the Schulze – Hardy rule. The deviation from this rule for the trivalent cation may be attributed either to the effects of hydrolysis, or to approach to charge reversal.

Effect of electrolytes on the zeta-potential of latex globules. The experiments to determine the effect of electrolytes on the zeta-potential of latex globules were carried out by the macro-electrophoretic technique described in an earlier communication [5]. The dialyzed BD1 latex, diluted with distilled water to 1% solid content, was mixed with an equal volume of buffer solution with ionic strength 0.02 and pH 9.9, to which the required amount of electrolyte had previously been added. In contrast to the experiments described in the preceding section, the electrolyte with a univalent cation was sodium chloride. The auxiliary liquid in the apparatus was a mixture of buffer and electrolyte diluted with an equal volume with distilled water.

The zeta-potential was calculated by means of the Henry formula [7] with corrections for electrical relaxation. The numerical coefficient in the formula was found from the appropriate curves in the diagram given in Overbeek's paper [8], which shows the variation of the coefficient with a certain criterion κa. For sodium and aluminum chlorides, the coefficient was determined from the curve for a uni-univalent electrolyte, and for calcium chloride, from the curve for a bi-univalent electrolyte.

The curve for a uni-univalent electrolyte was used in the case of aluminum chloride because, as has been shown by Nikolsky and Paramonova [9], this salt is hydrolyzed at pH 4 and above to the hydroxide, while the hydroxide is ionized to give univalent ions. At pH > 8, these are mainly the anions $Al(OH)_2O^-$ or AlO_2^-, and at pH < 8, $Al(OH)_2^+$ cations. Trivalent aluminum ions can only appear in solution at pH < 4.

The results of the electrophoretic determinations are given in Table 2.

It is seen from Table 2 that addition of increasing amounts of electrolytes with uni- and trivalent cations leads first to some increase and then to a decrease of the zeta-potential of the latex globules. Increase of the concentration of bivalent electrolyte results in a steady fall of the potential.

As was to be expected, if the results are calculated per unit concentration of the added electrolyte, aluminum chloride lowers the zeta-potential to a greater extent than the other electrolytes, while sodium chloride has the least effect. It is important that coagulation of the latex by aluminum and calcium chlorides began not at the zeta-potential which corresponds to the appearance of floccules on addition of sodium chloride, but at a much higher value.

Charge reversal of the latex globules by addition of aluminum chloride to the latex. It might have been expected that multivalent cations, having higher adsorption potentials, reverse the charge on latex globules as effectively as hydrogen ions, which are readily adsorbed [9]. In fact, our experiments showed that additions of definite amounts of aluminum chloride solution to 2-4% latexes resulted only in partial coagulation and charge reversal of the globules remaining in the latex. It should be pointed out, however, that in such cases charge reversal took place only when equal volumes of aluminum chloride solution with a concentration of 1 millimole/liter and over were added to the latex. Additions of aluminum chloride at lower concentrations did not result in charge reversal, but merely lowered the electrokinetic potential of the latex globules and decreased the stability of the system.

As is seen in Fig. 1, as increasing amounts of aluminum chloride are added to latex BD1, the zeta-potential of the globules first increases very lightly, then falls, and at a certain not very high electrolyte concentration (~ 1 millimole / liter of the final solution) the latex coagulates. The coagulum so formed is quite unlike the coagulum formed by acidification of the latex, but consists of a fine powder or loose lumps, easily rubbed apart by the fingers. However, the range of aluminum chloride concentrations causing coagulation of the latex is not wide. If this concentration is exceeded slightly, the latex is not coagulated and charge reversal takes place. Still larger amounts of aluminum chloride decrease the positive zeta-potential only slightly. It is significant that on addition of very large amounts of aluminum chloride (46 millimoles/liter and over) the latex again becomes unstable, and coagulates.

TABLE 2

Effect of Electrolytes on the Zeta-Potential of BD1 Latex Globules

Electrolyte	Electrolyte concentration, millimoles/liter	pH	Ionic strength	Electrophoretic mobility in $\frac{\mu/\text{sec}}{\text{v / cm}}$	Coefficient in the Henry equation	Zeta-potential in mv
NaCl	0	9.9	0.01	—4.87	4.9	—83.2
	80	9.8	0.09	—6.05	4.55	—95.5
	170	9.8	0.18	—3.93	4.45	—61.0
	260	9.8	0.27	—2.12	4.35	—32.0
$CaCl_2$	0	9.9	0.01	—4.87	4.9	—83.2
	1.12	9.6	0.013	—3.85	5.7	—76.5
	2.25	9.3	0.017	—3.70	5.55	—71.5
	4.5	9.2	0.026	—2.76	5.3	—51.0
$AlCl_3$	0	9.9	0.01	—4.87	4.9	—83.2
	0.23	9.7	0.011	—5.38	4.9	—92.0
	0.46	9.5	0,018	—5.25	4.9	—90.0
	0.92	9.2	0,015	—4.00	4.7	—65.5

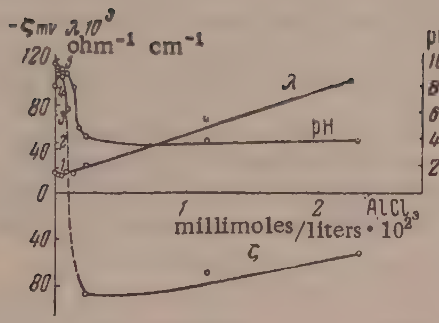

Fig. 1. Variations of the zeta-potential of the globules, pH, and specific conductance (λ) of BD1 latex on addition of aluminum chloride.

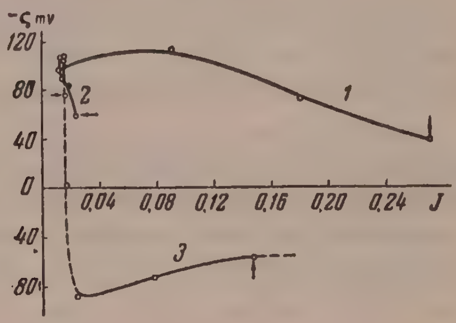

Fig. 2. Effect of ionic strength (J) on the zeta-potential of BD1 latex globules on addition of various electrolytes : 1 – NaCl; 2 – $CaCl_2$; 3 – $AlCl_3$

DISCUSSION OF RESULTS

For a clearer picture of the effect of electrolytes on the zeta-potential of latex globules and latex stability, let us examine the curves in Fig. 2, based on the data in Table 2 and Fig. 1. The ionic strengths of BD1 latex samples diluted with buffer solution and containing various amounts of electrolytes are taken along the abscissa axis, while the ordinates represent the corresponding electrokinetic potentials of the latex globules. The last points on the curves, indicated by arrows, correspond to the highest electrolyte concentrations at which the zeta-potential could still be determined. These maximum concentrations decrease sharply with increasing valency of the cation.

With increasing sodium chloride content in the latex the zeta-potential first increases somewhat, then begins to fall. An increase of the zeta-potential of latex globules on addition of small amounts of electrolytes with univalent cations has been reported by other investigators [11, 12]. The cause of this effect probably lies in adsorption of the anions present in the system by the globules. The glycine anion in the buffer mixture, or the chloride anion, may habe this effect. The subsequent decrease of the zeta-potential is probably to be explained by compression of the electric double layer.

Addition even of small amounts of calcium chloride to the system results in a sharp decrease of the zeta-potential. Addition of aluminum chloride produces first a slight increase of the zeta-potential, and then a sharp decrease and coagulation. If excess aluminum chloride is added, in certain conditions the latex globules may undergo charge reversal. There are two complicating factors, to which reference was already made earlier, in the action of aluminum chloride on the latex.

1. Then aluminum chloride is added to the latex it is hydrolyzed, and the system therefore becomes more acid. Thus, when aluminum chloride is added, the zeta-potential of the globules is influenced not only by the aluminum ions but also by the change in the solution pH as the result of hydrolysis.

2. From pH 4 and above a colloidal suspension of insoluble aluminum hydroxide is formed in the system, stabilized by ions which may arise during its ionization. The structure of the aluminum hydroxide micelles on each side of the isoelectric point, according to Nikolsky and Paramonova [9], is shown schematically in Fig. 3.

It follows from the foregoing that at pH < 8 latex to which aluminum chloride had been added contains positively charged colloidal particles of aluminum hydroxide. These, in becoming adsorbed on the as yet negatively charged globules, cause, in our opinion, a sharp decrease of the zeta-potential, and in certain conditions also charge reversal. Evidence of the adsorption of aluminum hydroxide by the latex particles is provided by the fact that the coagulum formed in these conditions differs in appearance from the coagulum formed when the latex is acidified. The explanation for the powderlike nature of the coagulum is that a layer of aluminum hydroxide is formed around the globules, protecting them against direct contact and thereby preventing the formation of the usual compact aggregates.

In our opinion, adsorption of colloidal aluminum hydroxide particles, having a high adsorption potential, on the surface of the negatively charged latex globules also accounts for the increase in the zeta-potential of the globules on addition of small amounts of aluminum chloride to the latex, when the pH of the medium is still fairly high (Curve 3, Fig. 2). As in this case the polymer globules and the colloidal aluminum hydroxide particles have charges of the same sign, adsorption is not too rapid and the zeta-potential increases only slightly.

Figure 4 can conveniently be used to take into account the influence of aluminum chloride only on the latex, excluding the influence of pH changes; Fig. 4 shows the variation of the electrokinetic potential of the latex globules as a function of pH on addition of increasing amounts of aluminum chloride to the system, and also on addition of different amounts of hydrochloric acid. These curves are based on data from the present and preceding communications [10].

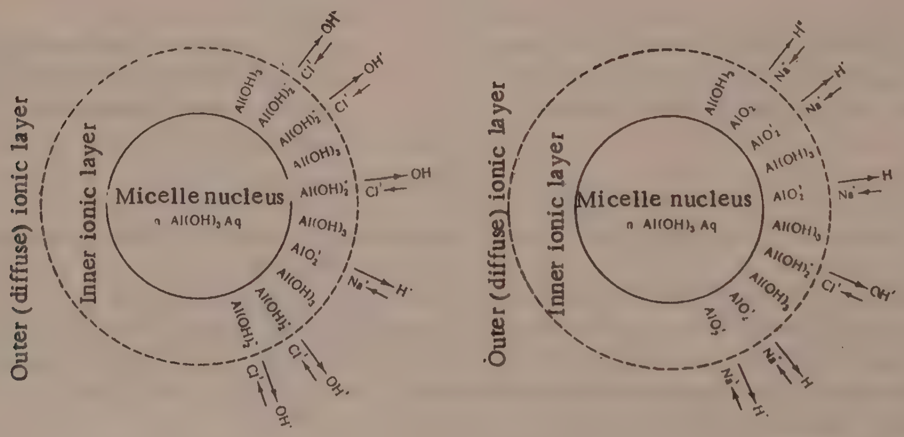

Fig. 3. Structure of aluminum hydroxide micelle: 1) at pH < 8; 2) at pH > 8.

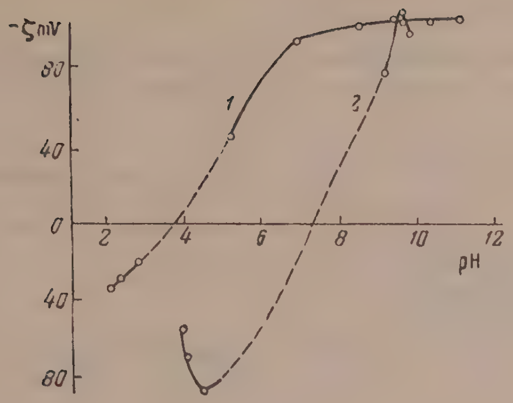

Fig. 4. Zeta-potential of BD1 latex globules as a function of pH in experiments with additions of: 1) hydrochloric acid; 2) aluminum chloride.

Comparison of Curves 1 and 2 (Fig. 4) shows that addition of aluminum chloride to the system shifts the zera-potential – pH curve for the latex in the direction of higher pH values than the curve obtained for the addition of hydrochloric acid. The curve for the addition of aluminum chloride to the latex cuts the abscissa axis at pH ~ 8, which coincides with the isoelectric point of aluminum hydroxide. Evidently the electrical properties of the particles below pH 8 are wholly determined by the aluminum hydroxide layer adsorbed on the globules.

Adsorption of aluminum hydroxide accounts for the certain difference in shape between Curves 1 and 2 in Fig. 4. Curve 2 has a minimum as a result of the fact that on further decrease of pH the hydroxide dissolves, the adsorbed layer of hydroxide on the latex globules becomes less dense, and the positive zeta-potential decreases.

It should also be noted that, for dialyzed latex, the positive zeta-potential is much higher in presence of aluminum chloride than in presence of hydrogen ions, which indicates that the positively charged colloidal aluminum hydroxide particles have a high adsorption potential.

SUMMARY

1. The coagulation of latexes stabilized by soaps, by electrolytes with cations of different valencies entirely conforms to the Schulze – Hardy rule, established for typical colloidal systems.

2. Addition of electrolytes to latexes in general decreases the zeta-potential of the latex globules, the decrease being greater with higher valency of the electrolyte cation.

3. Uni- and divalent cations are not capable of effecting charge reversal on soap-stabilized latex globules, while trivalent cations can change the sign of the charge on the latex globules. Such charge reversal, like the charge reversal resulting from acidification, occurs only in latexes containing not more than 2-4% solids.

4. With increasing amounts of added aluminum chloride the zeta-potential of the latex globules increases somewhat, and then falls sharply, reaching zero (at the isoelectric point), and then becomes positive. Subsequently it decreases again at high electrolyte concentrations in the system. Addition of aluminum chloride to the latex gives rise to two regions of aggregative instability, corresponding to two regions of low zeta-potential.

5. When aluminum salts are added to latexes, the zeta-potential of the globules is influenced not only by the ions formed by ionization of these salts, but also by the pH changes resulting from their hydrolysis. To establish the effect of the aluminum ions only, zeta-potential – pH curves for latex acidified by different amounts of HCl should be compared with similar curves for latex containing different amounts of aluminum chloride.

6. When aluminum chloride is added to latexes, the active ions are apparently not Al^{3+} ions but, at pH > 8, $Al(OH)_2O^-$ or AlO_2^- ions, and at pH < 8, $Al(OH)_2^+$ ions formed from aluminum hydroxide which is produced in the hydrolysis of aluminum chloride. At pH < 8, in latexes to which aluminum chloride has been added, positively charged colloidal particles of aluminum hydroxide are probably formed. These are adsorbed on the latex globules and cause a sharp decrease of the negative electrokinetic potential, followed by charge reversal.

The Moscow Institute of Fine Chemical Technology

Received April 4, 1956

LITERATURE CITED

[1] S. S. Voyutsky and R. M. Panich, Progr. Chem., 25, No. 1, 57 (1956).

[2] S. S. Voyutsky, R. M. Panich, and K. A. Kalyanova, Collected Papers of the Central Sci. Res. Inst. for Leather Substitutes on the Theory and Practice of Sizing and Impregnation (State Light Ind. Press, 1952) p. 90.

[3] S. S. Voyutsky, R. M. Panich, and K. A. Kalyanova, Trans. Lomonosov Inst. Fine Chem. Technol., Mosco, vol. 5 (State Chem. Press 1953) p. 30.

[4] S. S. Voyutsky and R. M. Panich, Colloid J., 18, 326 (1956).*

[5] S. S. Voyutsky and R. M. Panich, Colloid J., 18, 647 (1956).*

[6] B. V. Deryagin and L. D. Landau, J. Exp. Theoret. Phys., 11, 802 1941; 15, 662 (1941); Acta Phys. Chim. URSS 14, 633, 1941.

[7] D. C. Henry, Proc. Roy. Soc., 133, 106, (1931).

[8] T. G. Overbeek, Adv. Coll. Sci. 8, 97, (1950).

[9] B. P. Nikolsky and V. I. Paramonova, J. Phys. Chem., 2, 687 (1931).

[10] R. M. Panich and S. S. Voyutsky, Colloid J., 19, 113 (1957).*

[11] E. A. Hauser, M. Bender, Proceedings of the Rubber Technology Conference, 1938, p. 101.

[12] S. H. Maron, D. Turnbull, M. E. Elder, J. Am. Chem. Soc. 70, 582, (1948).

---

* [Original Russian pagination. See C. B. Translation].

ADHESION OF HIGH POLYMERS

3. EFFECTS OF THE SIZE, SHAPE, AND POLARITY OF HIGH-POLYMER MOLECULES ON THEIR ADHESION TO CELLOPHANE

S. S. Voyutsky, A. I. Shapovalova, and A. P. Pisarenko

The effects of the nature of high polymers on their adhesive properties have been the subject of several investigations [1-4]. However, the question still remains obscure, as most of the investigations in this direction have been based on faulty methods. In particular, much harm was done in the earlier investigations because it was not strictly determined whether in the tests the joints were broken at the adhesive – substrate boundary or within the adhesive itself; i. e., whether true adhesion or the cohesive strength of the adhesive was being measured. Because of this, a number of experimental investigations of adhesion are rendered valueless, and the development of the physical chemistry of adhesion in general has been slow for this reason.

The present communication contains certain data on the effect of the nature of high polymer adhesives on adhesion to a polymeric substrate, obtained by means of a technique developed by us earlier [5], in which the usual methodological defects have largely been eliminated. This method essentially consists of determination of the force or work expended in gradual peeling-off of a film of adhesive applied in solution form to the substrate. Special attention is paid to determining whether the peeling is adhesive or cohesive in character.

The substrate used in the present investigation was a cellulose model – Cellophane from which the glycerol plasticizer had been washed out. Adhesion of high polymers to cellulose is important in impregnation of tire cords, gluing of paper and board, production of fabric-based leather substitutes, etc. Cellophane is the most convenient of all the cellulose materials because of its mirror-smooth surface, so that it is possible to assume the area of nominal contact equal to the area of true contact, and to determine the character of the peeling visually.

The adhesives tested were several elastomers used in industry. The solvents used in applying the adhesives to the substrate were the solvents generally used in the production of rubber adhesives – gasoline, benzene, dichloroethane.

The joints were made and peeled apart under strictly standardized conditions [5].

Effect of the size of the macromolecules on adhesion. Table 1 contains our data on the force required to peel isobutylenes of different molecular weights from Cellophane.

As Table 1 shows, the peeling resistance of polyisobutylene of molecular weight 7000 is practically zero, and the peeling is purely cohesive, i. e., it occurs in the layer of adhesive. With increase of molecular weight to 20,000 the resistance to separation increases sharply, and the separation is of the mixed type. Evidently in this case the cohesive strength of the adhesive is equal to the force required to peel the adhesive from the substrate. With molecular weights of 100,000 and over, the peeling is purely adhesive; the absolute value of the resistance to separation is the same in all cases, approximately 70 g/cm.

Table 1 also gives the results of experiments on the peeling from Cellophane of polyisoprenes of molecular weight 20,000 – 150,000 (synthetic product) and 150,000 – 300,000 (natural rubber). Here again the polymer of lower molecular weight had considerably greater adhesion. The mixed type of separation of synthetic polyisoprene from Cellophane shows that the cohesive strength of this polymer is approximately equal to the adhesive force.

TABLE 1

Resistance to Separation of Cellophane and Polyisobutylenes of Different Molecular Weight

Adhesive	Molecular weight	Type of separation	Separation resistance in g/cm		
			minimum	maximum	average
Polyisobutylene	7 000	Cohesive	0	0	0
	20 000	Mixed	307	386	369
	100 000	Adhesive	61	70	67
	150 000	Ditto	59	73	67
	200 000	Ditto	60	71	68
Polyisoprene	20 000—150 000	Mixed	1112	1617	1379
	150 000—300 000	Adhesive	13	25	18

At first sight it seems strange that natural rubber had such poor adhesion to Cellophane. It is generally considered that natural rubber is an excellent adhesive. However, poor adhesion of natural rubber to Cellophane has also been reported by others [3].

Table 1 shows that polymer adhesion increases with decreasing molecular weight. However, as the cohesive strength of a polymer decreases with decreasing molecular weight, the optimum gluing powers should probably be found in polymers of moderate molecular weight, which ensures adequate adhesion together with sufficient strength of the adhesive layer.

Effect of the structure and shape of the macromolecules on adhesion. Table 2 gives data on the separation of various nonpolar or weakly polar polymers from Cellophane.

Table 2 shows that adhesion of polybutadiene to cellophane is greater when the elastomer molecule has a more regular structure. Increase of the number of vinyl side chains in the molecule greatly diminishes adhesion. From the nature of the separation in this case it may be concluded that polymers with more regular structure have higher cohesive strength. This is in entire agreement with the modern views on the relationship between the mechanical properties and molecular structure of polymers. Styrene side chains in the butadiene polymer molecule have an analogous influence on adhesion.

A comparison of the adhesion of the copolymer containing 70% butadiene and 30% styrene, and of the copolymer containing 70% butadiene and 30% methylstyrene, to Cellophane shows that adhesion is considerably lower in the latter case. This is probably to be attributed to the presence of a methyl group in the styrene residue.

The adverse effect of methyl groups in adhesion can also be seen from a comparison of the resistance of butyl rubber and polyisobutylene, of similar molecular weight, to separation from Cellophane. The presence in the butyl rubber molecule of even a small number of isoprene groups, containing only one methyl group per four carbon atoms in the main chain, results in a sharp increase of adhesion. However, the increase of adhesion may also be the consequence of the presence of a small content of low molecular weight polymer fractions in the synthetic product.

The general conclusion to be drawn from the data in Table 2 is that the adhesion of a polymeric adhesive to Cellophane decreases with increasing number of short side chains in the molecule.

Effect of the presence of polar groups in the macromolecule on adhesion. The data in Table 3 show how the resistance to separation of Cellophane from butadiene – acrylonitrile copolymers varies with the contents of polar acrylonitrile groups.

Table 3 shows that the resistance to separation for butadiene – acrylonitrile copolymers decreases with increasing contents of polar nitrile groups in the molecule. The type of separation also alters from cohesive to pure adhesive.

TABLE 2

Resistance to Separation of Various Nonpolar or Weakly Polar Elastomers from Cellophane

Adhesives and their characteristics	Type of separation	Resistance to separation in g/cm		
		minimum	maximum	average
Polybutadiene containing 50% butadiene groups in 1,4 position and 50% in 1,2 position	Adhesive	1433	1484	1445
Polybutadiene of the same molecular weight, containing 20% butadiene groups in the 1,4 position and 80% in the 1,2 position	Mixed	498	594	550
Copolymer containing 70% butadiene and 30% styrene	Cohesive	1153	1652	1368
Copolymer containing 50% butadiene and 50% styrene	Adhesive	3	22	14
Copolymer containing 70% butadiene and 30% methylstyrene	Mixed	274	1727	771
Butyl rubber, mol. wt. 60,000-80,000	Adhesive	272	307	298
Polyisobutylene, mol. wt. 80,000-100,000	Adhesive	61	70	67

TABLE 3

Resistance to Separation of Butadiene — Acrylonitrile Copolymers of Different Polarities from Cellophane

Adhesives and their characteristics	Type of separation	Resistance to separation in g/cm		
		minimum	maximum	average
Butadiene—acrylonitrile copolymer containing 18.4% acrylonitrile groups	Cohesive	1380	1735	1638
Ditto, containing 28.6% acrylonitrile groups	Mixed	1144	1717	1382
Ditto, containing 37.7% acrylonitrile groups	Adhesive	125	138	132

DISCUSSION OF RESULTS

Up to the present adhesion has been thought to be caused either by the action of molecular forces [3, 6] or by formation of an electric double layer at the interphase [7-9]. However, as we have shown [10], neither of these viewpoints is valid when both the adhesive and the substrate are high polymers.

It our theory, both adhesion of high polymers to each other and autohesion consists of diffusion of chain molecules or sections of them from one polymer into the other to form a stable bond constituting a gradual transition from one polymer to the other. It is quite obvious that the interdiffusion of two high polymers in contact is none other than mutual solution. Therefore adhesion of high polymers to each other is closely related to their mutual solubilities, which, as we have shown [11], is largely determined by their polarity relationships.

If our diffusion theory of adhesion is correct, the adhesion of high polymers to each other should depend very largely on the ability of the macromolecules to diffuse into solids and on the mutual solubility of the high polymers. Unfortunately, almost nothing is known at the present time about these important characteristics of high polymers, and therefore verification of the views put forward above must be confirmed to finding the relationships between adhesion and molecular structure (molecular weight, form of the macromolecules, presence of polar groups) of the contacting polymers.

In our experiments the same substrate, Cellophane, was used. Cellophane, like cellulose, consists of macromolecules containing polar hydroxyl groups. Because of the size and rigidity of these macromolecules, and the molecular forces acting between them, they are not capable of any appreciable diffusion into elastomers. Conversely, the molecules of the elastomers used in our investigations are fairly flexible and capable of diffusion. Therefore in our case it is sufficient to correlate the adhesion between Cellophane and elastomers with the molecular structure of the latter.

Effect of molecular size and shape of nonpolar elastomers on their adhesion to Cellophane. We have seen that, with the same contact time, the adhesion of polyisobutylene to Cellophane first decreases with increasing molecular weight, and then becomes practically constant. Experiments with polyisoprenes of different molecular weight do not contradict this result. The fact that adhesion ceases to be dependent on the molecular weight after the latter has reached a certain value has been reported by others for other materials [4]. In our theory, this can be explained in the same way as in the case of autohesion [12]: as the molecular weight increases, the number of free ends of molecules, capable of diffusing especially easily, diminishes. When the molecular weight is high, mainly chain segments diffuse, and their penetration into the spaces between the substrate molecules is difficult. Therefore a less stable bond will be formed in a given time between two high polymers in contact, and as the segment size does not depend on the length of the macromolecule, the adhesion ceases to depend on the molecular weight.

Another explanation of the fact that adhesion becomes independent of molecular weight above a certain value is the higher plasticity of the adhesives with lower molecular weight which, of course, favors diffusion. There are reports in the literature [3] that introduction of not too large amounts of plasticizers into high polymer adhesives improves adhesion. It is possible, of course, that the increase of adhesion with diminishing molecular weight is to be explained by the combined action of both these factors.

It should be noted here that the increase of adhesion with decreasing molecular weight does not contradict the observed fact that bond strength increases with increasing molecular weight of the adhesive. The reason is that in most instances the joints are broken not at the adhesive – substrate boundary but within the adhesive layer. In such conditions the resistance to separation will, of course, increase with increasing molecular weight of the adhesive.

Thus, the question of the influence of molecular weight on adhesion needs to be reviewed in the light of the foregoing data. There are adequate grounds for believing that decrease of molecular weight, which decreases the cohesive strength of the substance, favors increased adhesion. This view is quite understandable from the viewpoint of the diffusion theory of adhesion – as the molecular size decreases the capacity of the molecule for diffusion increases, and adhesion should therefore increase also.

We have seen that determination of the adhesion of polybutadiene to Cellophane showed that an increase of the number of butadiene groups in the 1,2 position in the adhesive molecule worsens the adhesion. The probable explanation is that, as the number of butadiene groups in the 1,2 position increases in the molecule, the ability of the molecule to diffuse becomes less on purely steric grounds (increased number of side groups).

Another example of the influence of side groups is provided by the adhesion of butadiene – styrene copolymers, with different proportions of the components, to Cellophane. A small amount of styrene groups in the copolymer increases adhesion, but a large amount produces a decrease. Similar changes of adhesion with different proportions of the components in copolymer molecules have been observed by others [4]. The explanation again is that the copolymer molecules with a low styrene group content are largely regular in structure and therefore diffuse more easily into the substrate. A large number of styrene groups in the copolymer molecule decreases the ability to diffuse because of the presence of a large number of cumbersome side chains in the macromolecule and decreased chain flexibility.

As we have seen, replacement of styrene by methylstyrene groups in the copolymer molecule decreases adhesion. The probable reason for this is the considerable decrease of the diffusion capacity of the macromolecules owing to the presence of additional methyl groups. The results of experiments with polyisobutylene and butyl rubber lead to similar conclusions.

Reference was made earlier to the adverse effect of short side chains in the macromolecule on adhesion. However, if these side chains are long enough, they may act as individual chains which, for steric reasons, diffuse more readily into the substrate than do the middle regions of the molecular chains [12]. This is quite understandable, as the probability of entry of such a molecular end into a space between the substrate molecules is certainly higher than the probability of entry of a middle part of a molecule into the same space. This view is confirmed by the results of McLaren [3], who showed that adhesion to Cellophane increases in the polymethacrylate series from n-methyl methacrylate polymer to n-butyl methacrylate polymer. McLaren also showed that isopropyl and isobutyl methacrylate polymers have considerably lower adhesion to Cellophane than the corresponding normal methacrylate polymers. This is in full agreement with our views on the influence of molecular shape on adhesion.

Effect of polarity of the adhesive on adhesion to Cellophane. First it must be pointed out that it is found experimentally that such nonpolar or weakly polar high polymers as polyisobutylene and polybutadiene have fairly high adhesion to polar Cellophane. The reason, in our view, is the insufficiently close packing of the cellulose molecules, owing to which the flexible and mobile molecules of the adhesive can diffuse into the cellulose. Another interpretation of the effect is that the hydrocarbon chains of the nonpolar adhesive are capable of dissolving in cellulose to a certain extent, thus forming a bond between the adhesive and substrate. Further, it has been found that butadiene – acrylonitrile copolymers have decreasing adhesion to Cellophane with increasing contents of polar acrylonitrile groups in their molecules. Others [3] have also reported that high polymers containing nitrile groups in their molecules have poor adhesion to Cellophane. Since Cellophane molecules are strongly polar, this result seems at first sight incomprehensible – it would seem that the more strongly polar nitrile groups the polymer contains, the better would it dissolve in Cellophane and the stronger would be the bond formed between the adhesive and the substrate. However, the contradiction is easily explained because, with increasing contents of polar groups in the macromolecules of the adhesive, the rigidity of the macromolecular chains increases and therefore their diffusion capacity diminishes. Moreover, adhesion decreases owing to the presence of often cumbersome polar side chains in the molecules, which hinder diffusion for steric reasons. Finally, the polar groups present in the polymer molecules may themselves interact by intermolecular forces, and this would also hinder diffusion.

Thus, the decrease of adhesion with increasing polarity of the adhesive in our experiments must be explained as a purely kinetic effect. It is important that if instead of the polar Cellophane a nonpolar substrate was used, the adhesion would also decrease with increasing polarity of the adhesive. However, the interpretation of this effect would be different – in this case increase of the polarity of the adhesive would result in a decrease of the solubility of the adhesive in the substrate, i.e., it would be explained purely on thermodynamic grounds.

It should be noted that adhesion does not always diminish with increasing polarity of the high polymer. For example, McLaren [3] found that, with increasing chlorine content in chlorinated polyethylene, the adhesion of the polymer to Cellophane first increases, then begins to decrease. McLaren also found that moderate contents of polar groups – chlorine, carboxyl, carbonyl, and hydroxyl – in the macromolecules may improve adhesion to Cellophane. The possible explanation is that, for a moderately polar high polymer, the improvement of adhesion as the result of better solubility exceeds the decrease of adhesion caused by increased rigidity of the molecules and decreased diffusion of the polymer.

SUMMARY

1. The method developed by the authors has been used to study the influence of size, form, and polarity of macromolecules on the adhesion of high polymers to Cellophane.

2. Adhesion of high polymers to Cellophane increases with decreasing molecular weight. However, for maximum bond strength, the cohesive properties of the polymer must also be taken into account.

3. Increase of the number of short side chains in the polymer molecule lowers its adhesion.

4. The adhesion of a polymer to Cellophane decreases with increasing contents of polar groups in its macromolecules.

5. The results are explained on the basis of the diffusion theory of high polymer adhesion developed by the authors.

Central Scientific Research Institute for the Leather
Substitutes Industry, Moscow

Received May 3, 1956

LITERATURE CITED

[1] O. Gerngross, Z. ang. Chem. 44, 33, (1942).

[2] K. Thinius, Kunststoffe 37, 36,(1947).

[3] A. D. McLaren, C. H. Hofrichter, Paper Trade J. 125, 96, (1947); A. D. McLaren, J. Pol. Sci. 3, 652, (1948).

[4] C. J. Seiler, Paper Trade J. 126, 37, (1938).

[5] A. I. Shapovalova, S. S. Voyutsky, and A. P. Pisarenko, Colloid J., 18, 485 (1956).*

[6] J. Remond, Rev. Produits Chim. 57, 469, (1954); 58, 70, (1955).

[7] B. V. Deryagin and N. A. Krotova, Adhesion (Acad. Sci. USSR Press, Moscow, 1949).

[8] B. V. Deryagin, J. Acad. Sci. USSR, No. 7, 10 (1954).

[9] S. M. Skinner, R. L. Savage, J. E. Rutzler, J. Appl. Phys. 24, 438, (1953).

[10] S. S. Voyutsky, A. I. Shapovalova, and A. P. Pisarenko, Proc. Acad. Sci. USSR, 105, 1000 (1955).

[11] V. I. Alekseenko, I. U. Mishustin, and S. S. Voyutsky, Colloid J., 17, 3, (1955)*; Proc. Acad. Sci. USSR, 95, 93, (1954).

[12] S. S. Voyutsky and B. V. Shtarkh, Colloid J., 16, 3, (1954).*

---

* [Original Russian pagination. See C. B. Translation].

STUDIES OF THE PHYSICAL CHEMISTRY OF AGAR

2. THEORY AND PRACTICE OF AGAR FRACTIONATION

S. A. Glikman and I. G. Shubtsova

It is known that agar obtained from different seaweeds and by different technological processes varies greatly in chemical composition (contents of proteins, ash elements, etc.) [1]. The principal component which determines the properties of agar is a polygalactan in the linear molecules of which some of the galactose residues are esterified by sulfuric acid which, in turn, is combined with various cations, mainly calcium and potassium. According to the literature [2, 3], different samples of agar contain on the average from 18 to 57 d-galactopyranose units per sulfate ester group, while in carrageenins nearly every galactose unit is esterified by sulfuric acid [4].

However, the physicochemical properties of different agar samples are evidently determined not only by the average chemical composition of the polysaccharide and its average degree of polymerization, but also by its molecular heterogeneity. Attempts to fractionate agar have not hitherto given the desired results. By washing with cold water, electrodialysis, or precipitation by alcohol – water mixtures [5-8], soluble fractions could be separated from the sparingly soluble portion, but the latter, which comprises more than 70% of the original substance, could not in practice be separated into fractions. An interesting fact is that similar results were obtained by a number of workers [9, 10] in the fractionation of another polyelectrolyte, pectin. In this case also the main part of the material, comprising ~ 70% of the total, could not be fractionated by extraction with mixtures of variable composition.

The method, often used for the fractionation of other high polyners, of solution at increasing temperatures has as yet not been used for agar, because of its supposed instability to the action of heat. However, the literature data on the effects of prolonged heating on the properties of agar solutions are very contradictory [2, 11, 12]. There is reason to believe that only solutions of partially dialyzed agar, containing free sulfate ester groups, are unstable to high temperatures, the agar molecules being hydrolyzed [2]. Our own experiments have shown that when nondialyzed solutions of agar were heated for five hours at 100° their viscosity decreased only slightly (by about 4%).

Two nondialyzed agar samples were used in our investigation: Sample I, Japanese fibrous, extracted from Gelidium seaweed, and Sample II, Far Eastern film agar, obtained from Ahnfeltia plicata seaweed by the freezing process. The fractionation was effected by consecutive extraction with water at 25, 45, 60, 75, 85 and 90°. The material was usually washed four times, until the fraction soluble in the given conditions was completely extracted. All the washings were combined in the one fraction. The durations of the washings were: at 25°, 10 hours, at 45 and 60°, 1 hour, and at 75,85, and 90°, 30 minutes. The solutions were evaporated at 50° and the residues were finally dried at 80°. The high-temperature extracts were not evaporated but were dehydrated by the freezing method.

Most of the water-soluble free impurities of mineral and organic origin were extracted with the first fraction. Therefore the physicochemical characteristics determined for the first fraction must be regarded as provisional. The insoluble impurities remained in the fraction insoluble at 90°, which comprised 3.7% of the weight of Sample I and 11.7% of sample II, and which was not investigated.

Calcium was determined by the Grossfeld method [13], verified for agar by Starostina [7]. The determination of SO_4^{2-} ions by oxidation with HNO_3 was carried out by Pavlov's method [14], and these ions were also determined in a hydrochloric extract of the ash obtained in presence of excess cations [13].

The table shows that the sulfate group content in Sample I and all its fractions (except the 90° fraction) is considerably higher, and the calcium content considerably lower, than in Sample II. The ratio of the equivalents shows that in Sample I not all the sulfate groups are saturated with calcium, while Sample II contains calcium in excess. This is confirmed by qualitative analysis of the ash, which showed that in addition to calcium Sample I contains considerable amounts of other cations (Na^+, K^+, Mg^{2+}, Al^{3+}, Fe^{3+}), while Sample II contains only Na^+, K^+, and Fe^{3+}, the first two being present only in the first two fractions. The ash and SO_4^{2-} contents of the fractions decrease progressively in both samples.

Fractionation Yield and Characteristic Fraction

Samples		Yield of fraction, %	Moisture, %	Ash, % of dry agar	Ash constituents, % of dry agar		Relative numbers of esterified residues	Ratio of $\frac{Ca}{SO_4}$ equivalents	$[\eta]_\infty$
					SO_4^{2-}	Ca^{2+}			
Sample I		—	16.6	3.95	3.48	0.75	1 : 16	0.55	1.48
Its fraction at	25°	26.2	18.3	10.72	10.20	1.47	1 : 6	0,34	0.72
″	45°	5.7	15.9	3.96	3.46	0.64	1 : 16	0.44	0.80
″	60°	5.4	—	—	—	—	—	—	0.84
″	75°	14.5	17.0	1.90	1.69	0.48	1 : 34	0.68	0.96
″	85°	16.1	16.7	0.86	1.04	0.26	1 : 58	0.60	1.05
″	90°	16.2	16.9	0.75	0.67	0.24	1 : 88	0.87	1.18
Residue		13.7	—	—	—	—	—	—	—
Sample II		—	14.0	3.89	1.06	1.64	1 : 56	3.73	2,25
Its fraction at	25°	6.9	12.1	24.65	4.36	8.27	1 : 18	4.79	—
″	60°	11.2	17.3	4.10	1.24	2.27	1 : 47	4.28	1.50
″	75°	19.1	17.4	2.33	0.79	1.39	1 : 74	4.24	2.22
″	85°	23.8	17.5	2.02	0.65	0.95	1 : 90	3.50	2.44
″	90°	28.2	17.4	2.05	0.69	0.98	1 : 86	3.40	2.60
Residue		11.7	—	—	—	—	—	—	—

The intrinsic viscosities given in the table were determined by the method described in the preceding communication * from the experimental data in Figs. 1 and 2. For the two samples studied, the values of $[\eta]_\infty$ increase consecutively from the low to the high temperature fractions. The value of $[\eta]_\infty$ for the original Sample II is close to that of its 75° fraction, and for Sample I, it is higher than the value for its 90° fraction. The values found for $[\eta]_\infty$ cannot accurately reflect the relative molecular weights of the fractions, as their chemical composition differs both in the sulfate ester group contents and in the cation contents. For the same molecular weight, the molecules of a polyelectrolyte should become straighter with increasing numbers of sulfate groups in the molecules, and therefore the effective volume (bulk) and viscosity should increase. A decrease in the content of these groups should produce the opposite effect.

It is this effect – a consecutive decrease in the frequency of the sulfate ester groups – that is seen in the transition from the low to the high temperature fractions of Sample I. Therefore the consecutive increase of intrinsic viscosity found for this series of fractions probably does not correspond completely to increasing molecular weights, but is somewhat diminished owing to the lower contents of sulfate groups in the high temperature fractions.

Sample II differs from Sample I by a lower content of sulfate ester groups and a considerably higher calcium content. The decrease in the frequency of sulfate groups in the transition from the low-molecular 25° fraction to the higher fractions is not so rapid in Sample I as in Sample II. Therefore the discrepancy between the molecular weight and viscosity changes is less prominent in Sample I. Indeed, in the case of Sample II the $\eta_{sp}/c - c$ curve and the value of $[\eta]_\infty$ for the original sample are not higher than for all the

---

* Colloid J., 19, 172 (1957). [C. B. Translation, p. 183].

fractions, but are similar to those for the intermediate 75° fraction.

The nature of the cations replacing hydrogen in the acid groups in agar should also have a definite influence on the form of the polyelectrolyte molecule and therefore on the viscosity of the agar. This influence depends on the possibility of formation of intramolecular bonds on replacement of hydrogen by bivalent cations, and also on the different degrees of solvation of the cations in solution. Samples I and II differ considerably in their cation contents and the degree of substitution in the acid groups. In Sample I, on the average, only half the sulfate ester groups are saturated with calcium, and the degree of substitution only reaches 0.85 in the highest 90° fraction. On the other hand, in Sample II the number of calcium equivalents is on the average 4 times as great as the number of sulfate ester groups, and this proportion varies relatively little for the different fractions. With the greater homogeneity of Sample II, both in respect of the sulfate group contents and of cation substitution, its values of $[\eta]_\infty$ probably reflect molecular weight differences of the fractions more accurately than in the case of Sample I.

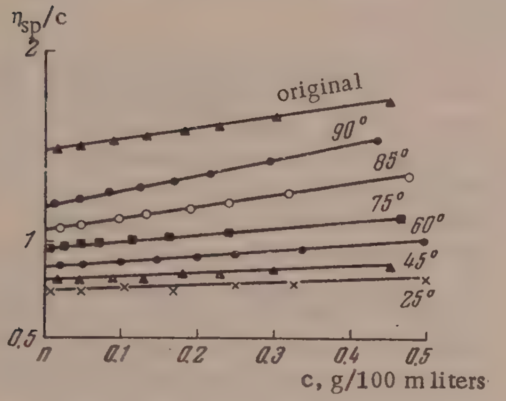

Fig. 1. Viscosity of Japanese agar and its fractions in presence of KCl solution containing 0.1 equiv. / liter.

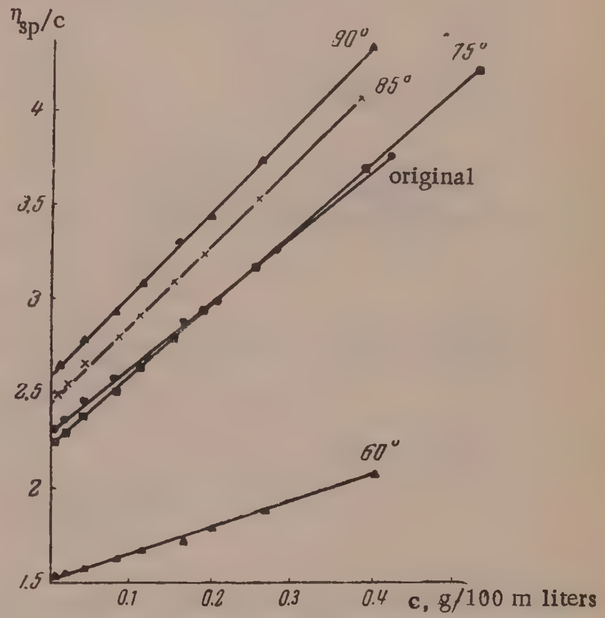

Fig. 2. Viscosity of Far Eastern agar and its fractions in presence of KCl solution containing 0.1 equiv. / liter.

To characterize the hydrophilic nature of the fractions and the stability of their aqueous solutions, the thresholds of coagulation of these solutions by alcohol were determined. The method consisted of measurement of the relative viscosities (at 60°) of 0.15% aqueous solutions of the agar and of the same solutions after addition of increasing amounts of alcohol. The curves in Fig. 3 show that the reduced specific viscosity of the solutions remains almost unchanged up to a certain critical alcohol concentration, and then decreases sharply, evidently as the result of coagulation. The critical concentrations of alcohol for the original agar and all the fractions studied are very similar (~ 60% alcohol). This accounts for the failure of attempts to fractionate agar by variations of the solvent composition.

In order to explain the very different effects of two parameters of state – temperature and solvent composition – on equilibrium in the system agar – solvent, it is necessary to consider briefly the modern theories of high polymer fractionation. As is known, the phase equilibrium theory advanced by Gee and Huggins is based on the assumption of a homogeneous force field around the polymer molecule, and does not take into account specific interaction between the different functional groups of these molecules. In the solution and fractionation of polymers containing polar groups, the energy factor plays a greater role than the entropy factor. The Gee and Huggins theory is evidently not applicable to such systems.

The Brønsted equation should provide a better explanation of the observed effects. The applicability of this equation to negative heat effects only does not prevent its use for positive heats of swelling, since the heat of solution, which represents the difference between the heat expended in separating the polymer chains and the heat of solvation, may be negative. If the heat of solution is also positive, it is necessary to take into account that the characteristic which determines the phase equilibrium conditions is not the absolute value of q, but the difference between the heats of solvation of the polymer in a mixture of the given composition (q_x) and in a mixture of optimum composition (q_n), in which all the functional groups of the polymer molecule are solvated to the maximum; this difference $q = q_x - q_n$ will always be negative.

A defect of the Brønsted equation is that it is applicable only to regular solutions. This has been taken into account by Meyer [15], who introduces into the Brønsted equation a correction term for entropy

$$N_2^{\text{sat}} = e^{z\,(q + Ts)/RT}$$

where N_2^{sat} is the mole fraction of the polymer in a saturated solution; z is the number of units in the molecule; $s = (\Delta S - \Delta S^{\text{id}})/z = \Delta S^{\text{exc}}/z$ is the excess of the entropy change over the ideal value, per monomer unit, when a polymer molecule is transferred into another phase. Meyer points out that s must be very small, as it represents the difference between two values of S^{exc} corresponding to excesses, over the ideal entropy of solution, of two polymer molecules differing by one monomer unit.

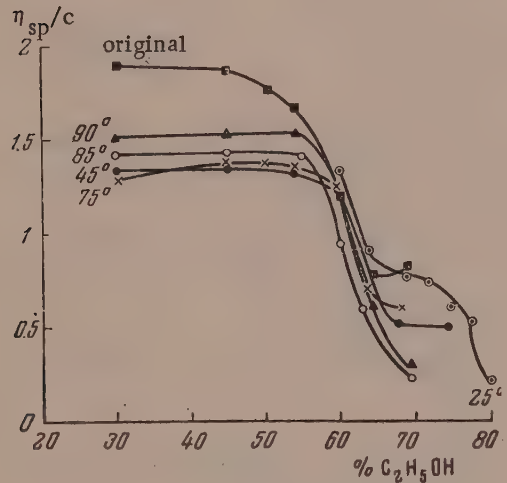

Fig. 3. Thresholds of coagulation of Japanese agar and its fractions by alcohol.

In considerations of the question of agar fractionation, it must primarily be borne in mind that while change of temperature results in a change of the cohesive energy, changes of solvent composition mainly influence the energy of adhesion (solvation) and have relatively little effect on the cohesive energy. Increase of alcohol concentration in agar solutions leads to partial desolvation and coagulation of the agar in consequence of the changed energy relationships. Coagulation evidently occurs when the heat effect q of a unit in the polymer chain reaches a negative value greater in absolute magnitude than the entropy effect T_s, as follows from the Brønsted — Meyer equation $N_2^{\text{sat}} = \exp[z(q + T_s)/RT]$.

Since the values of q are determined by the difference between the solvation and cohesive energies of all active groups, capable of hydrogen bonding (i.e., mainly hydroxyl groups), in the agar molecules, it naturally follows that the coahulation threshold should be practically the same for all agar fractions differing in degree of esterification or in the nature of the substitution in the sulfate ester groups, if the number of such goups in all the fractions is small relative to the number of hydroxyl groups. As regards the molecular weight differences, if (q + Ts), is similar for all the fractions, only large differences in the degree of polymerization can result in separate precipitation of the fractions.

Variation of the solvent composition affects not only the energy relationship in high polymer solutions, but also the entropy of solution, which should be reflected in a change in the term Ts in the Brønsted — Meyer equation. If this change was at all considerable, then agar fractions differing in molecular weight would be precipitated at different maximum concentrations of alcohol. This is not so, probably because the molecules of agar, as of other polymeric carbohydrates, are greatly extended and fairly rigid. Therefore their flexibility should not greatly change at constant temperature with the solvent composition.

The situation should be different with variations of the solution temperature of agar in a solvent of constant composition or in pure water. In such cases not only the hydration energy but the cohesive energy is changed considerably. Moreover, as the cohesive energy decreases with increase of temperature, even small differences of cohesive energy, depending on the relative contents of sulfate ester groups in the macromolecule, should appreciably influence the magnitude of the aggregate effect. Therefore fractionation of agar by variation of the temperature is quite feasible, and the fractions so obtained differ both in molecular weight and in chemical composition.

SUMMARY

1. It has been shown for two agar samples that, by consecutive extraction at increasing temperatures (from 25 to 90°), agar can be separated into a series of fractions differing in intrinsic viscosity, sulfate ester group contents, and substituent cations, but differing little in their hydrophilic nature.

2. The results of fractionation by varying the temperature with a solvent of constant composition, and by varying the solvent composition at constant temperature, are explained thermodynamically on the basis of the Brønsted equation as modified by Meyer.

The N. G. Chernyshevsky State University
Saratov

Received September 10, 1955

LITERATURE CITED

[1] I. Kizevetter, J. Far Eastern Branch Acad. Sci. USSR, 26, 53 (1957); Bull. Pacific Sci.-Res. Inst. Fisheries, 36, 265 (1952).

[2] M. Samec, V. Isajevic, Koll. Beih. 16, 285, (1922).

[3] W. Hoffman, R. Gortner, Biol. Chem. 65, 371, (1925).

[4] H. Kruyt, Coll. Sci. 2, 187, (1949).

[5] S. Lipatov, Problems of the Science of Lyophilic Colloids (Acad. Sci. Byelorussian SSR Press, 1941). pp. 53, 84-85.

[6] A. Morozov and V. Rudi, Colloid J., 15, 117 (1953).*

[7] V. Gryuner and K. Starostina, Trans. All-Union Sci. Res. Inst. Confectionery Ind. 3, 1, (1941).

[8] S. Glikman and M. Lipovsky, Sci. Mem. Saratov State Univ. 30, 46 (1952).

[9] G. Schneider, H. Bock, Ber., 70, 1617, (1937.)

[10] S. Glikman and S. Orlov, Proc. Acad. Sci. USSR, 71, 895 (1950).

[11] W. Cooper, B. Cantal, W. Nuttal, Pharm. J. 26, 688, (1908).

[12] S. Levites, Koll.-Z. 2, 237, (1907).

[13] I. Grossfeld, Manual for the Investigation of Food Products (Food Ind. Press, 1937) p. 93.

[14] S. Pavlov, J. Appl. Chem., 5, 877 (1932).

[15] K. Meyer, Natural and Synthetic High Polymers, Second Ed., (New York, 1950), p. 709

---

* [Original Russian pagination. See C. B. Translation].

~~THE~~ EFFECT OF SWELLING ON THE STRENGTH OF VULCANIZATES

B. A. Dogadkin, D. L. Fedyukin, and V. E. Gul

Data on the influence of temperature, deformation conditions and swelling on the strength characteristics of high polymers are important in relation to the theory of the mechanism of the rupture of these materials. The relationship between the tensile strength of vulcanizates and the temperature and deformation rate [1] indicates the important role of intermolecular interaction in the mechanism of the rupture of high polymers with a spatial structure.

The observed relationships are difficult to explain if it is assumed that the resistance of a material to rupture is determined by principal chemical valency forces only. On the other hand, if the tensile strength of a vulcanizate is regarded as the sum of the principal valency forces P_X and intermolecular forces P_M all the known relationships between strength characteristics and the temperature and extension rate can be interpreted with a certain degree of approximation [2]. To determine the role of intermolecular forces in the mechanism of vulcanizate rupture it was of special interest to study the influence of swelling on tensile strength. This is of great practical as well as theoretical interest. The addition of substances of low molecular weight, known as softeners or plasticizers, to mixtures based on high polymers, is a widely used technological procedure. The substances used as plasticizers or softeners are generally well compatible with the polymers and can swell them.

Various chemical processes can take place between the plasticizers and the other ingredients in the production of a finished article from a raw mixture. In particular, softeners influence vulcanization and oxidation processes. Therefore in most cases a distinction must be made between chemical and physical interaction of plasticizers and the components of the mixture. The present paper deals mainly with the determination of the influence of physical interaction between the plasticizer and high polymer (swelling) on the tensile strength of vulcanizates.

One method whereby intermolecular interaction can be varied is swelling. This method is very convenient as by its means it is possible to vary intermolecular interaction without affecting interaction by the principal chemical valency forces. It is shown [3] that even in one and the same vulcanizate (and still more so in different vulcanizates) chemical and intermolecular bonds differing in nature and intensity are present. Consequently, different solvents should have different effects on the intermolecular interaction of a vulcanizate swollen in them. Therefore the materials chosen for the investigation were carbon-filled vulcanizates based on rubbers differing in chemical composition and structure, namely: natural (smoked sheet), butadiene—styrene (with 70: 30 butadiene—styrene ratio), and butadiene—acrylonitrile (with 62: 40 butadiene—acrylonitrile ratio); while the solvents used were dimethyl phthalate, dibutyl phthalate, dioctyl phthalate, dibutyl sebacate, dioctyl sebacate, and Vaseline oil. These substances differ both in molecular size and structure, and in polarity.

The swelling was effected by immersion of spade-shaped test specimens either directly into the solvent or into its alcoholic solution. To ensure uniform distribution of the solvent through the vulcanizate at different degrees of swelling, the specimens were kept between sheets of paper for 7-8 days after being extracted from the solvents, before the tensile tests. The degree of swelling was expressed in percentages on the weight of vulcanizate. The tensile and relative elongation tests were carried out according to State All-Union Standard 270-41. The number of parallel tests was not less than 25 in each case. The changes in the specimen dimensions caused by swelling were not taken into account in calculations of the cross section. The results for filled vulcanizates based on natural, styrene (SKS-30) and acrylonitrile (SKN-40) rubbers are given in Figs. 1,2, and 3 respectively. These figures show that the tensile strength varies in different ways for different combinations of vulcanizate and swelling agent. In some cases the often described steady decrease of tensile strength with increasing swelling is observed. This is found for natural rubber vulcanizate swollen in dimethyl and dioctyl phthalates, and for SKS-30 vulcanizate swollen in dibutyl and dioctyl phthalates and in dibutyl and dioctyl sebacates (Figs. 1, 2). In contrast to these typical cases, when filled vulcanizates of natural rubber are swollen in dibutyl phthalate and dibutyl sebacate, of styrene rubber in dimethyl phthalate, and of nitrile rubber in dimethyl ,dibutyl, and dioctyl phthalates and dibutyl sebacate, the tensile strength does not change steadily but passes through a maximum at a definite degree of swelling. When natural rubber vulcanizate is swollen in dimethyl phthalate, the tensile strength falls sharply, while SKN-40 vulcanizate swollen in this solvent shows an initial considerable increase of tensile strength. Dimethyl phthalate is the most polar of the solvents used. When natural rubber vulcanizate is swollen in a less polar solvent, dibutyl sebacate, the greatest increase of tensile strength is found. The relative elongation of the vulcanizates varies similarly with the degree of swelling. A steady decrease of relative elongation is found for natural rubber vulcanizate swollen in dimethyl phthalate (Fig. 4) and for butadiene–styrene (SKS-30) rubber vulcanizates swollen in dibutyl phthalate, dioctyl phthalate, dibutyl sebacate, and dioctyl sebacate (Fig. 5). Variation of the relative elongation which passes through a maximum is found for swollen butadiene–acrylonitrile rubber (SKN-40) in all solvents (Fig. 6). The curves in Fig. 7 show that the variations of tensile strength and elongation at break for swollen vulcanizates follow a similar course.

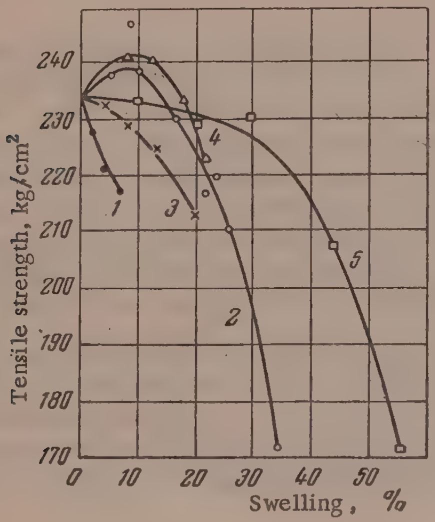

Fig. 1. Variation of tensile strength of filled natural rubber vulcanizate with the degree of swelling: 1) in dimethyl phthalate; 2) in dibutyl phthalate; 3) in dioctyl phthalate; 4) in dibutyl sebacate; 5) in Vaseline oil.

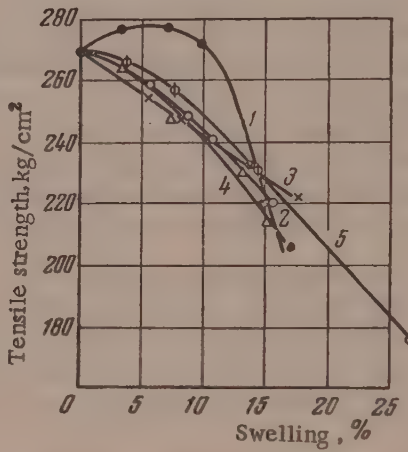

Fig. 2. Variation of tensile strength of filled SKS-30 vulcanizate with the degree of swelling: 1) in dimethyl phthalate; 2) in dibutyl phthalate; 3) in dioctyl phthalate; 4) in dibutyl sebacate; 5) in dioctyl sebacate.

Thus, the steady variation of static strength and relative elongation of swollen vulcanizates, described in the literature, is only a particular case of the influence of solvents on the mechanical properties of vulcanizates. Cases of unsteady variation, with increasing strength at low degrees of swelling, such as described here, are met quite often.

This course of strength and relative elongation variations during swelling of vulcanizates can be explained as follows. Swelling, on the one hand, increases the flexibility of the chain molecules, which facilitates their orientation during extension and therefore increases the tensile strength of the specimen. A direct relationship between the degree of orientation (in the limit, the degree of crystallization) and strength of vulcanizates has been demonstrated in a series of papers [4]. On the other hand, penetration of the solvent molecules during swelling weakens the forces between the molecular polymer chains, leading to a decrease of the vulcanizate strength. The consequence of the superposition of these opposing influences is that, in the general case, the relationship between strength and degree of swelling will show extreme values. If the positive influence of the

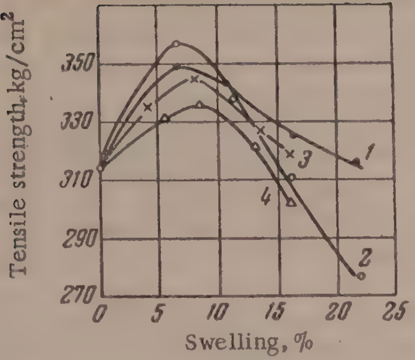

Fig. 3. Variation of tensile strength of filled SKN-40 vulcanizate with the degree of swelling: 1) in dimethyl phthalate; 2) in dibutyl phthalate; 3) in dioctyl phthalate; 4) in dibutyl sebacate.

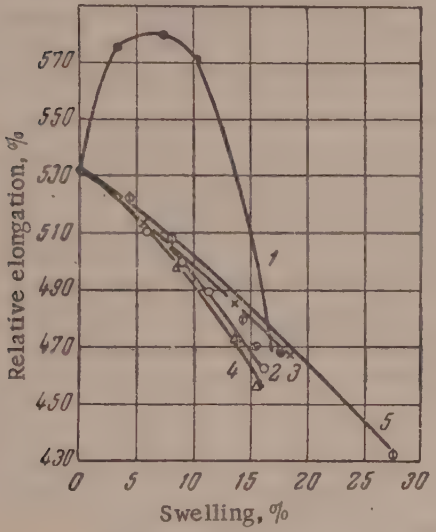

Fig. 5. Variation of relative elongation of filled SKS-30 vulcanizate with degree of swelling: 1) in dimethyl phthalate; 2) in dibutyl phthalate; 3) in dioctyl phthalate; 4) in dibutyl sebacate; 5) in dioctyl sebacate.

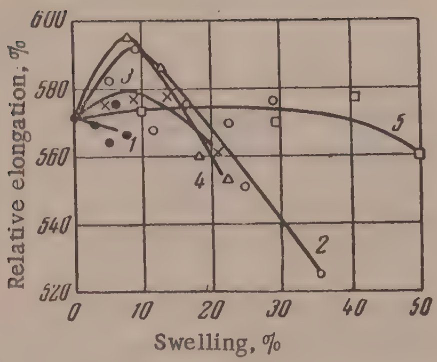

Fig. 4. Variation of relative elongation of filled natural rubber vulcanizate with the degree of swelling: 1) in dimethyl phthalate; 2) in dibutyl phthalate; 3) in dioctyl phthalate; 4) in dibutyl sebacate; 5) in Vaseline oil.

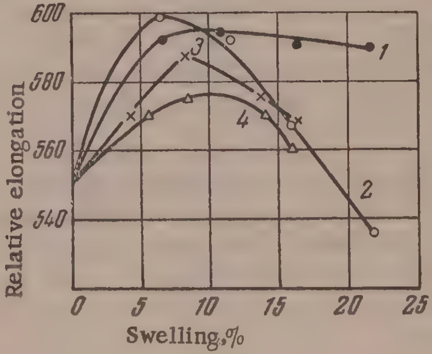

Fig. 6. Variation of relative elongation of filled SKN-40 vulcanizate with degree of swelling: 1) in dimethyl phthalate; 2) in dibutyl phthalate; 3) in dioctyl phthalate; 4) in dibutyl sebacate.

chain flexibility increase prevails, an increase of strength and elongation at break will be found at low degrees of swelling.

In the experiments described this was the case for butadiene–acrylonitrile rubber, the molecular chains of which are less flexible than those of natural rubber, swollen in all the solvents used. In the case of natural rubber the increase in chain flexibility as the result of swelling is slight, and for most solvents the more pronounced effect is decrease of strength owing to decreased energy of intermolecular interaction. Natural rubber vulcanizates show decreases of strength and relative elongation even at low degrees of swelling. Natural rubber has high chain flexibility and the action of solvents on it largely consists of changes in the energy of interaction between the molecular chains.

The effect of changes of molecular chain flexibility on the strength of swollen vulcanizates becomes evident when Figs. 3 and 8 are compared. It is seen that the glass transition temperature, which characterizes molecular chain flexibility, falls up to 12% swelling; further addition of solvent does not lower the glass transition temperature. The strength maximum corresponds to the degree of swelling which gives the lowest glass transition temperature.

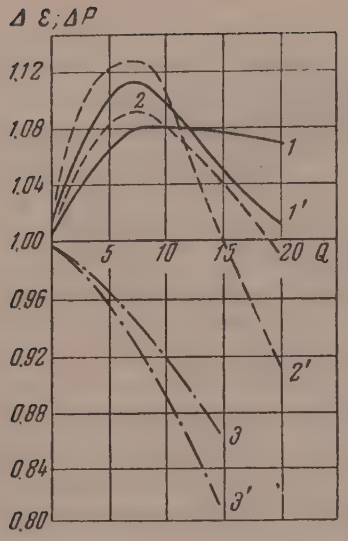

Fig. 7. Relative changes of tensile strength and elongation at break for different degrees of swelling: 1) SKN-40 in dimethyl phthalate; 2) SKN-40 in dibutyl phthalate; 3) SKS-30 in dibutyl sebacate (the symbols 1, 2, 3, and 1', 2', 3' refer to the tensile strength and relative elongation respectively).

It must be pointed out that, as has already been reported by us [5], maximum values of tensile strength and relative elongation during swelling are also found in the case of fatigue (dynamic) strength of vulcanizates. It was to be expected that similar maxima in the influence of the solvent on strength and relative elongation would be found when the solvent (softener) is introduced into the composition during milling before vulcanization. In fact, as Fig. 9 shows, when such softeners as dimethyl, dibutyl, and dioctyl phthalate are added to a butadiene–acrylonitrile SKN-40 rubber composition, the strength–softener content curve shows a maximum. The strength maximum lies in the region of softener concentration (~ 10%) corresponding to the strength maximum for the swollen vulcanizate. Additions of dibutyl and dioctyl sebacate result in steady decrease of strength with increasing softener concentration. Thus, the low molecular compounds act similarly as softeners (plasticizers) and as swelling agents. However, since softeners introduced into the composition may interact chemically with its ingredients during vulcanization, the results of their action on the mechanical properties of the vulcanizate evidently will not coincide completely.

The effect of swelling of vulcanizates on their strength characteristics, caused by the influence of swelling on the molecular chain flexibility, degree of orientation, packing density, energy of intermolecular interaction, and other parameters, is primarily determined by the molecular characteristics of the rubber–solvent (softener) pair. Unfortunately, the attempts to correlate the swelling effect with various molecular characteristics of the components of the system, which have been reported in the literature, have not yielded sufficiently definite results. We found the following values for the dielectric constants of the solvents (swelling agents) studied: dimethyl phthalate 6.56; dibutyl phthalate 5.03; dioctyl phthalate 4.17; dibutyl sebacate 3.71; dioctyl sebacate 3.37.

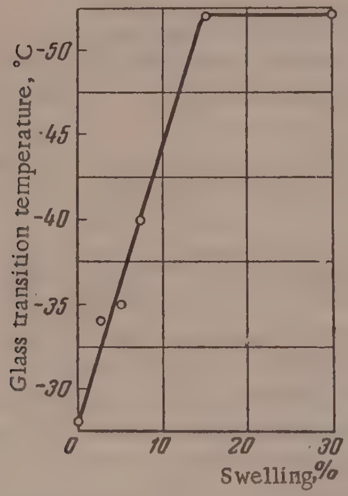

Fig. 8. Variation of the glass transition temperature of SKN-26 vulcanizate with degree of swelling in dibutyl phthalate.

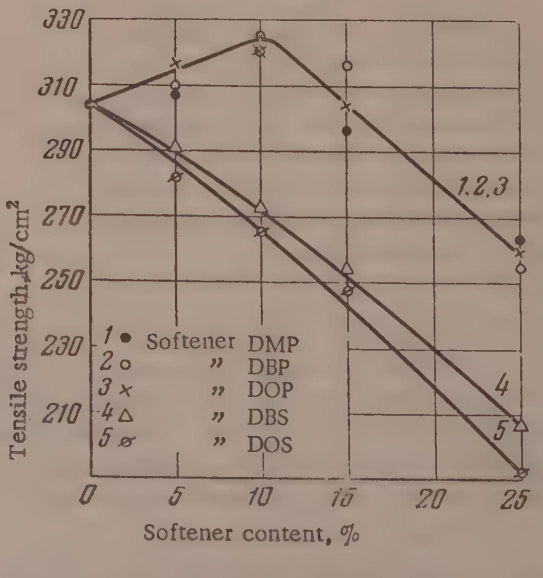

Fig. 9. Variation of tensile strength of butadiene–acrylonitrile rubber vulcanizates with amounts of softener added during milling: 1, 2, 3) dimethyl, dibutyl, and dioctyl phthalates; 4) dibutyl sebacate; 5) dioctyl sebacate.

It is not possible to correlate the dielectric constant of a solvent with the effects of its action on the strength characteristics of swollen vulcanizates [6]. There is no doubt that, in addition to the polarity of the solvent and the magnitude of the cohesive energy, the size and configuration of the solvent molecules which affect the packing of the rubber molecules are also important in relation to these effects.

SUMMARY

1. It is shown that, in addition to the previously described steady decrease of tensile strength of vulcanizates during swelling, there are cases in which the strength passes through a maximum at low degrees of swelling.

2. Variations of a similar character during swelling are also found for the relative elongation of vulcanizates.

3. Such variations of tensile strength and relative elongation are found when the increase of chain flexibility and the associated increased orientation effect is greater than the effect of weakened intermolecular bonding in the polymer caused by penetration of the solvent molecules into the polymer.

4. A strength maximum may also be found if the swelling agent (softener) is introduced into the rubber composition on rolls before vulcanization.

LITERATURE CITED

[1] B. A. Dogadkin and D. M. Sandomirsky, Colloid J., 12, 267 (1950); S. N. Zhurkov and B. N. Narzulaev, J. Tech. Phys., 23, 1677 (1953).

[2] V. E. Gul, Proc. Acad. Sci. USSR, 85, 145 (1952); 96, 953 (1954).

[3] B. Dogadkin, Trans. III All-Union Conf. Colloid Chem., (Acad. Sci. USSR Press, 1953) p. 136.

[4] A. P. Aleksandrov and Yu. S. Lazurkin, Proc. Acad. Sci. USSR, 7, 308 (1944); B. A. Dogadkin and B. K. Karlin, Colloid J., 9, 348 (1947); V. I. Kasatochkin and B. V. Lukin, J. Tech. Phys., 19, 76 (1950).

[5] B. A. Dogadkin and V. E. Gul, Colloid J., 12, 184 (1950); V. E. Gul, V. L. Fedyukin, and B. A. Dogadkin, Colloid J., 15, 11 (1953).*

[6] V. E. Gul, Colloid J., 13, No. 2, 99 (1951).

The M. V. Lomonosov Institute of Fine
Chemical Technology
Moscow

Received May 25, 1956

---

* [Original Russian pagination. See C. B. Translation].

ELASTIC DEFORMATION OF WOOD

Yu. M. Ivanov

A peculiarity of the deformation of wood is that as the stress increases there are two consecutive regions of characteristic deformation [1]: the first is the region of ordinary elasticity, while in the second, after-effect (creep) deformations develop rapidly, accompanied by a decrease of the "instantaneous" deformation modulus. The boundary between these two regions corresponds to the stress σ_{pf}, formerly termed the plastic flow limit.

In the first region the deformation of wood is mainly elastic with a fairly high "instantaneous" modulus of the order of $1-1.5 \cdot 10$ kg/cm^2 (in the air-dry state at room temperature) which remains constant during the development of the elastic-after effect type, the modulus for which is 5-6 times as great as the elastic deformation modulus. When σ_{pf} is exceeded the situation changes abruptly – the rapid development of after-effect deformation is accompanied by a continuous irreversible decrease of the elasticity modulus, which retains a constant decreased value on subsequent application of a force less than σ_{pf}, i.e., in the first region.

These deformation regions are clearly seen in the compression of wood in the direction of the fibers. Micromechanical studies have shown that considerable deformations in the second region do not cause any microscopic changes in the structure of wood, and must be attributed entirely to submicroscopic changes in the secondary walls, consisting mainly of cellulose, which take the main part of the force [2]. A more detailed investigation of after-effect deformations on compression in the second region is of considerable interest. Such an investigation could provide much additional information on the behavior of native cellulose on compression along the direction of the principal anisotropic axis, which cannot be effected in cellulose fibers, the deformation of which in longitudinal extension has been extensively studied [3].

It is possible that the decrease of the elasticity modulus, i.e., an increase in the flexibility of the system, is the result of bond cleavage in the cellulose complex of the secondary walls; if so, this effect should be more prominent as the result of a decrease of the intermolecular interaction, for example in swelling. To verify this view, experiments were performed on swollen wood; the results are detailed below.

Methods. Specimens of beech, oak and larch 20 × 20 × 40 mm in size, with moisture contents above the fiber saturation values, were subjected to compression in the direction of the fiber length at constant temperatures in the range between +15 and +40°. Measures were taken to avoid contact deformation at the end planes of the specimens, which could introduce considerable errors into the results. Metal stops were glued to the opposite end faces of each specimen, with 20-26 mm distance between their axes, i.e., the deformation measurement base. Scales with 0.001 and 0.01 mm divisions were placed on the steel balls of the stops; the former were used for absolute deformations of up to 0.7-0.8 mm, and the latter for larger deformations. The stops were glued to the air-dry wood by means of synthetic glue, either on the cold wood or with heating to not over +60° for 1-2 hours. Then (usually after a day) the specimen was gradually humidified during several days to a state of saturation and tested, immersed in water, by means of the reversing device of the lever testing machine. The general testing procedure was as follows. A load was rapidly applied to the end of the lever and the specimen was left for some time under a constant stress. After the unloading the specimen was completely released, centered again if necessary, and the loading was repeated.

Results of the experiments. Typical deformation–time curves in the second region for beech, oak, and larch wood specimens are given in Figs. 1, 2, and 3. It is seen that the deformation increase rapidly at constant stress; the "instantaneous" deformation on unloading is greater than on loading, indicating increased flexibility of the system. The total deformation Y_2 in the last cycle is 10-20 times as large as the initial "instantaneous" deformation, Y_1 and in other experiments it is 30-45 times as large, reaching 5-8 % of the original length. As the experiments were continued, with the same (or somewhat smaller) load applied to the specimen in the second region, the deformation increased further. For example, one beech specimen tested as described four times at +20° in two months showed a total deformation (including residual) of 11.1%, with an "instantaneous" deformation of 5.5%; another beech specimen tested three times at +38° during 13 days gave a total deformation of 8.9%, with an "instantaneous" deformation of 5%. Despite these large deformations, there were no signs of any damage to the wood structure. The residual deformation was largely restored after the specimens were heated in water at +90° for 4 hours. The equilibrium modulus was about 2 orders of magnitude lower than the initial elastic modulus. The very low values found for the modulus persisted for long periods. For example, repeated tests on beech specimens in the first region (at a stress of 87.5 kg/cm^2) during 7 months, accompanied by periodic drying and wetting of the specimens, gave approximately the same values for the modulus; heating of the specimens in water at +90° for 4-5 hours also had no influence on the modulus.

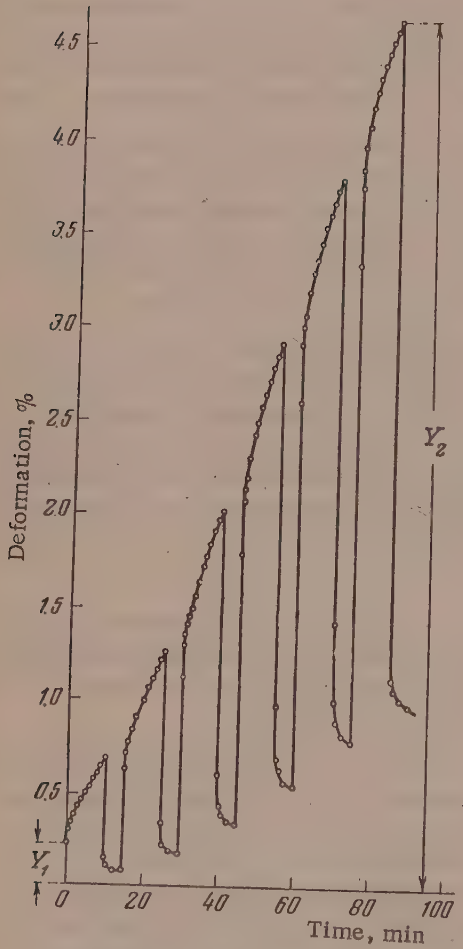

Fig. 1. Deformation–time curves for swollen beech wood compressed longitudinally in the second region; stress 262 kg/cm^2; σ_{pf} = 238 kg/cm^2; temperature +17.6°.

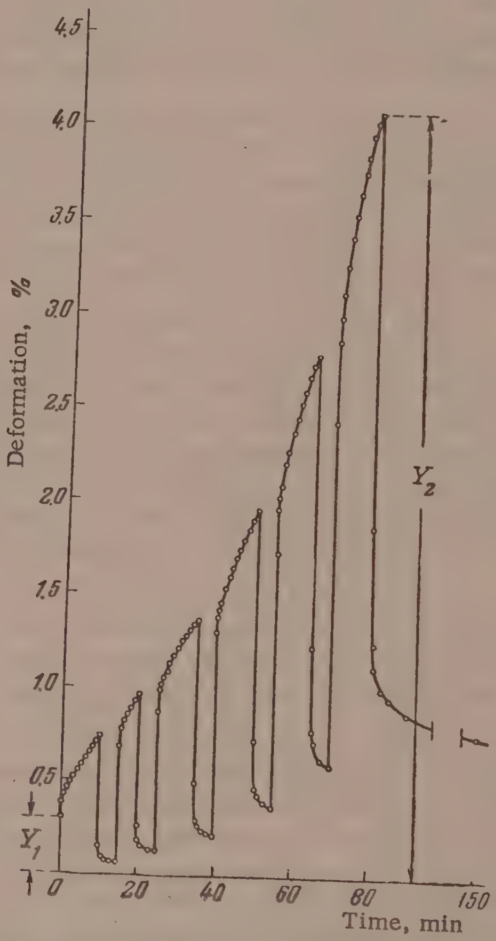

Fig. 2. Deformation–time curves for swollen oak wood compressed longitudinally in the second region; stress 214 kg/cm^2; σ_{pf} = 203 kg/cm^2; temperature +17.6°.

Thus it has been shown that large deformations in the second region can arise in wood; the corresponding low values of the equilibium modulus persist for long periods of time. The excess of the stress over σ_{pf} is significant. This follows from the fact that, for the same conditions of swelling, temperature, and mechanical stress conditions, the deformations in the first region are of a totally different character – the "instantaneous" deformation remains practically constant (Fig. 4, a), the equilibrium elastic modulus is almost 4 times as large as the "instantaneous" equilibrium elastic modulus is almost 4 times as large as the "instantaneous" modulus, while the residual deformation in swollen wood is restored after 1-2 days, without increase of temperature. The deformations remain similarly constant on application of a stress $\sigma < \sigma_{pf}$ to a specimen previously subjected to a considerable deformation – up to 3.5% of the original length in the second region (Fig. 4,b).

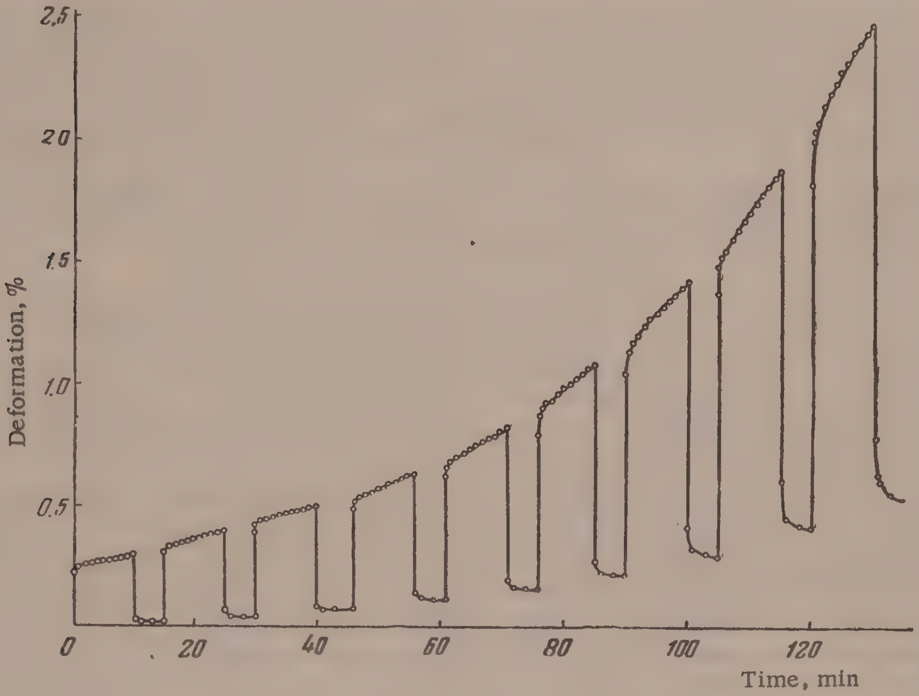

Fig. 3. Deformation–time curves for swollen larch wood compressed longitudinally in the second region; stress 242 kg/cm^2; σ_{pf} = 228 kg/cm^2; temperature + 16.0°.

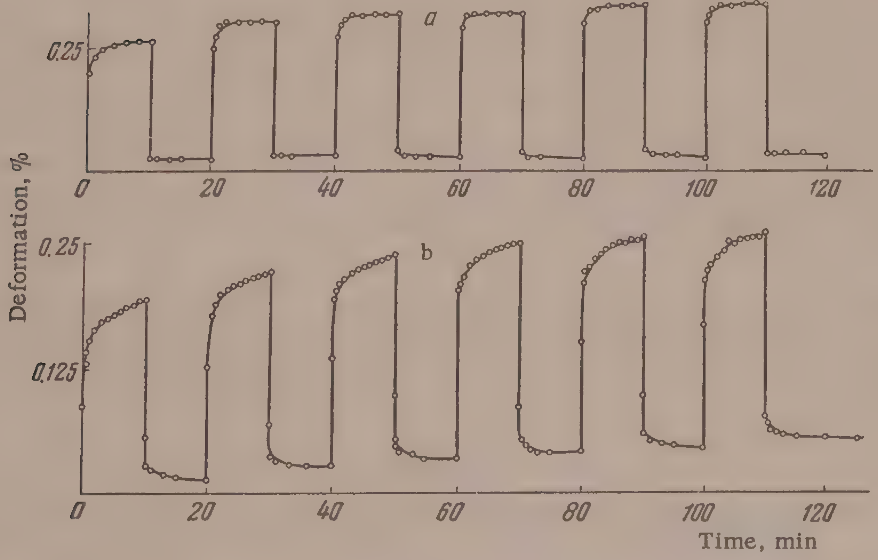

Fig. 4. Deformation–time curves for swollen beech wood compressed longitudinally in the first region: a) natural; stress 180 kg/cm^2; σ_{pf} = 225 kg/cm^2; temperature 16.1 °C; b) previously subjected to 3.5% deformation in the second region; stress 85 kg/cm^2; σ_{pf} = 225 kg/cm^2; temperature 19.0°C.

DISCUSSION OF RESULTS

Analysis of the foregoing results leads to the conclusion that after-effect deformations on compression of wood in the direction of the fibers in the second region are elastic deformations with the characteristic feature that they are accompanied by an irreversible increase in the flexibility of the system. Residual deformations in the second region, which we erroneously considered to be irreversible, are delayed elastic deformations, i.e., reversible by their nature.*

The deformations in the second region are generally similar in character to high elastic deformations of linear polymers, including cellulose fibers; they distinctly show: 1) the relaxation character of the deformations; 2) two principal relaxation time distributions – the first of short times, relating to rapid changes of deformation during loading and unloading, and the second of long times, seen in the slow restoration of deformations after unloading, and 3) a thermoreversible residual deformation of considerable magnitude.

This result is of great theoretical importance, and provides a clear description of the behavior of wood in the two deformation regions, the independent significance of which is emphasized by the above results: these regions differ not only in the magnitude but in the nature of the deformations.

The behavior of wood under stress $\sigma > \sigma_{pf}$, i.e., in the first region, resembles that of polymers in the glassy state. This resemblance is the consequence of the high degree of orientation which is produced in the cellulose of the secondary cell walls during biosynthesis. Strongly polar polymers such as cellulose are characterized by an increase of intermolecular interaction as the result of orientation. Having a fixed structure with almost total loss of high elastic properties, they are in a peculiar form of glassy state [4]. Because of this, deformations in the first region are largely determined by changes in the distances between the particles, and the plasticizing action of moisture influences only the magnitude of the deformation. Under the action of greater stresses in the second region, the state of natural "vitrification" of the cellulose in the secondary cell walls is gradually overcome. This process is effected when intermolecular interaction is weakened by swelling. It seems likely that the molecular mechanism whereby the elastic deformation is irreversibly changed (i.e., increased) consists of an increase of chain mobility owing to rupture of intra- or intermolecular bonds in the cellulose. A gradual increase of chain mobility during isothermal deformation of wood begins from the instant a definite value σ_{pf} of the stress is exceeded, as the result of a lowering of the potential barrier of bond rupture in the force field. The stress σ_{pf}, which is more correctly described as the start of irreversible increase of elasticity σ_{ie}, evidently cannot be a constant quantity, but should decrease not only with increase of moisture content and temperature, but with increased time during which the force acts; this is confirmed experimentally.

The irreversible increase of elastic deformation observed for wood is therefore the result of mechanical activation of an increase of the mobility of the cellulose chains in the secondary cell walls. The high elasticity observed in this case, however, differs from typical high elasticity of polymers in increasing irreversibly in isothermal conditions. Transition of polymers into the state of high elasticity is reversible – a polymer heated above the glass transition temperature T_g passes into the high elastic state, and returns to the glassy state when cooled below T_g. In the present instance the cellulose of the secondary cell walls leaves the natural "glassy" state on application of a force field $\sigma > \sigma_{pf}$, but removal of this field does not result in the loss of the high elastic properties in the cellulose, which does not return to the "glassy" state. On the contrary, the acquired high elasticity is retained for prolonged periods, indicating the irreversible nature of the bond rupture caused by the force field.

Further study is needed to determine the causes of the irreversible transition of the cellulose in the secondary cell walls from the natural "glassy" state. In our opinion, the explanation should be sought in the theory of the amorphous structure of cellulose, which demonstrates the nonequilibrium nature of its highly oriented state [5].

SUMMARY

1. It is shown that under certain conditions, when wood is compressed in the direction of the fibers in the second region, large deformations are produced, reaching 5-10% of the original length. The corresponding low values of the equilibrium modulus persist for a considerable time.

---

* The residual deformations obtained in the second region in longitudinal compression are also prevented in air-dry wood after it has been swollen in water.

2. It is shown that these deformations are reversible; they have the characteristic features of high elastic deformation in polymers – a relaxational character, two main relaxation time distributions, and retarded thermoreversible residual deformation.

3. It is suggested that these large elastic deformations produced when swollen wood is longitudinally compressed in the second region are caused by transition of the cellulose in the secondary cell walls from a natural "glassy" state, owing to increased mobility of the cellulose chains resulting from bond rupture under the action of the force field.

4. These results emphasize the significance of the two regions of the deformation of wood which had been established earlier, as mechanical activation of bond rupture only begins after a certain stress, which can be termed the start of irreversible elasticity increase σ_{ie}, has been exceeded.

In conclusion, the author expresses this deep gratitude to Academician V. A. Kargin, O. P. Golova, and N. V. Mikhailov for valuable comments in the course of discussion of the results of this investigation.

LITERATURE CITED

[1] Yu. M. Ivanov, Proc. Acad. Sci. USSR, 19, No. 6-7, 549 (1938); J. Tech. Phys., 16, No. 11, 1357 (1946); Trans. Inst. Wood Acad. Sci. USSR, 9, 431 (1953).

[2] Yu. M. Ivanov, Trans. Inst. Wood Acad. Sci. USSR, 9, 89 (1953).

[3] N. V. Mikhailov and V. A. Kargin, Trans. IV Conf. High Mol. Compounds, (Acad. Sci. USSR Press, 1949) p. 138.

[4] A. P. Aleksandrov, Trans. 1st and 2nd Conf. High Mol. Compounds (Acad. Sci. USSR Press, 1945) p. 49; V. A. Kargin, N. V. Mikhailov, and V. I. Elinek, Investigations of High Molecular Compounds (Acad. Sci. USSR Press, 1949) p. 315; U. S. Usmanov and V. A. Kargin, Chemistry and Physical Chemistry of High Molecular Compounds, (Acad. Sci. USSR Press, 1952) p. 169.

[5] V. A. Kargin, V. L. Karpov, Yu. S. Lipatov, G. S. Markov, and T. A. Koretskaya, Proc. Acad. Sci. USSR, 101, 707 (1955).

Moscow Received June 22, 1956

THIXOTROPIC AND STRUCTUROMECHANICAL PROPERTIES OF ASKANGEL SUSPENSIONS IN RELATION TO THE COMPOSITION OF THE EXCHANGE COMPLEX

E. I. Kobakhidze, M. E. Shishniashvili, and N. N. Serb-Serbina

One of the most important factors to influence the thixotropic properties of clay suspensions is the composition of their exchange complex, which mainly affects the strength and nature of the thixotropic structure formed in the system [1]. Studies of the influence of the composition of the exchange complex on the thixotropic properties of clay suspensions are both of independent scientific significance in relation to the mechanism and basic laws of this effect, and of practical value for determining the rational conditions for the production of drilling muds with the required structromechanical properties.

Rational production and use of clay suspensions with the necessary structuromechanical properties is important e.g. deep oil drilling. Thus, the main purpose of the present investigation was to carry out a qualitative and quantitative study of the thixotropic and structuromechanical properties of bentonite suspensions in relation to the composition of the exchange complex and to the equilibrium pH values established on addition of alkaline electrolytes.

The material studied was a highly disperse askangel fraction, which was converted into Na- and Ca-askangels, Al (electrodialyzed) askangel, and Na-askangel prepared by replacement of the bases absorbed by the electrodialyzed product by Na ions.

The sodium, calcium, and sodium-substituted electrodialyzed askangels were prepared by the Gedroits method [3], consisting of treatment of the natural and electrodialyzed clays by 1 N NaCl and $CaCl_2$ solutions. The saturated samples were purified by ordinary dialysis in Cellophane bags. Electrodialyzed askangel was prepared by electrodialysis of askangel pastes in three-compartment electrodialyzers at an electrode potential of 600 v (39-37 v/cm). The electrodialysis was continued for about two months and was terminated after the transfer of detectable amounts of electrolyte into the side compartments of the dialyzer, in the form of the corresponding acids or bases, had ceased. According to most investigators [4], electrodialyzed bentonite is to be regarded as "hydrogen bentonite" (H-bentonite), i.e., it is assumed that it contains hydrogen ions only, instead of alkali metal or alkaline earth cations, in the exchange complex. These authors ascribe to H-bentonite the properties of a strong acid.

However, in recent years it has been shown in our laboratory [5] that when askangel is electrodialyzed a considerable decrease of pH of the suspensions occurs in the central compartment of the apparatus, with a simultaneous substantial increase of exchange aluminum in the exchange complex. It has been shown by numerous experiments that electrodialyzed askangel has high exchange acidity and that its exchange capacity is almost entirely determined by exchange aluminum. A similar effect was also found by Shishniashvili and Batsanadze [6] in the purification of aluminosilicate gels by electrodialysis. At low degrees of purification, the aluminosilicate gels contained considerable amounts of exchange aluminum. At high degrees of purification (at electrode potentials of 7000 v), aluminosilicate gels, in contrast to clays, contained no exchange aluminum. Thus, according to the results of our laboratory, electrodialysis of askangel yields Al-bentonite and not H-bentonite.

The samples of askangel derivatives so obtained were made into aqueous suspensions and the following physicochemical characteristics were determined: viscosity, water loss, specific conductance, and pH; the degree of swelling and the swelling kinetics were also determined for all the samples.

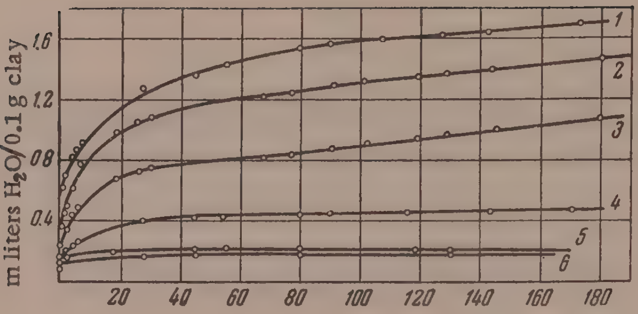

Fig. 1. Swelling kinetics of: 1) Na-askangel; 2) highly disperse fraction of native askangel; 3) native (original) askangel; 4) Oglanli bentonite; 5) Ca-askangel; 6) Al (electrodialyzed) askangel. Time in hours

The viscosities were determined by the falling sphere method by means of the Höppler viscosimeter. Water loss was determined by filtration of the suspensions under vacuum at a residual pressure of 18 mm Hg. In our experiments the standard funnel (d = 9 cm) was replaced by a smaller funnel (d = 5 cm). It was thus possible to carry out experiments with relatively small volumes of suspension (40 ml).

The Freundlich, Schmidt, and Landau method as simplified by Kister [7] was used for studying the kinetics of swelling.

The results of the determinations are given in Table 1 and Fig. 1. For comparison, Table 1 also gives data for suspensions of Oglanli and Na-substituted Oglanli bentonite.

It is seen from Table 1 that the viscosity, water loss, specific conductance, and pH of askangel suspensions greatly depend on the composition of the exchange complex.

The results of studies of the swelling kinetics of askangel and Oglanli bentonite show that Na-askangel has the greatest swelling capacity followed by highly disperse native askangel and then by native (original) askangel. Oglanli bentonite swells considerably less, and Ca- and Al (electrodialyzed) askangels show practically no swelling.

The thixotropic properties of these suspensions were studied by means of the Veiler—Rebinder apparatus [8], by measurement of the increase of the structural strength P_m with time. The results of these measurements were used to plot kinetic curves for thixotropic buildup.

As has been stated, Ca- and Al-askangels do not swell in water, and therefore they form suspensions containing large aggregated particles which show visible sedimentation. Structure formation in suspensions of Ca- and Al-askangels occurs only at a high solid phase content (>30 %), when the particles come into direct contact with one another. The structural strength, for example, of 32% Ca-askangel paste ($P_m = 3.7 \cdot 10^4$ dynes/ /cm^2), is lower than the strength of 10% native askangel paste ($P_m = 5 \cdot 10^4$ dynes/cm^2).

The properties of Na-askangel are different. Because of its high swelling in water, Na-askangel forms fairly stable, but nonthixotropic suspensions even at a low solid phase content (3%).

These results are in agreement with earlier findings. Serb-Serbina and Rebinder [1] showed that, with increasing contents of Na ions in bentonite clays, structure formation passes through a maximum and then gradually diminishes or ceases completely.

It has been shown in the present investigation that thixotropic structure formation does not occur to any practical extent in suspensions of askangel saturated with Na ions, irrespective of the concentration of the solid phase. It is shown in Figs. 2 and 3 that the shearing stress for Na-askangel suspensions does not vary with time.

Introduction of increasing amounts of Na cations into other bentonites also decreases thixotropic structure formation. However, as has been reported in the literature [9, 10], suspensions of Na-bentonites, such as Na-Oglanli bentonite, do not lose their thixotropic properties. The thixotropic buildup of Na-askangel differs significantly in character from that of Na-Oglanli bentonite, as it is evidently determined by the colloidochemical properties and mineralogical composition of these clays.

TABLE 1

Viscosity, Water Loss, pH, and Specific Conductance of 4% Suspensions of Askangel and 10% Suspensions of Oglanli Bentonite in Relation to the Composition of the Exchange Complex

Sample	Viscosity at 20° in centipoises	Water loss in 30 min., in ml	Specific conductivity at 25° 10^4 ohm^{-1} cm^{-1}		pH	
			suspension	filtrate	suspension	filtrate
Native askangel	7.5	9.0	6.83	4.96	8.95	8.50
Na-askangel	11.3	7.5	3.0	1.04	6.96	7.9
Ca-askangel	Kinetically unstable suspension		1.08	1.06	8.18	7.86
Al (electrodialyzed) askangel	ditto	—	0.29	0.19	3.72	4.82
Na-substituted electrodialyzed askangel	39.5	6.5	1.96	0.71	5.27	7.43
Oglanli bentonite	3.0	12.0	10.82	9.6	8.85	8.27
Na-substituted Oglanli bentonite	5.16	5.5	4.4	2.79	8.9	7.79

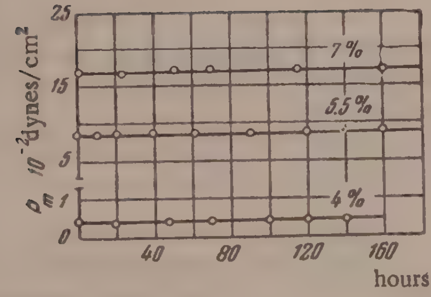

Fig. 2. $P_m \sim f(\tau)$ curves for Na-askangel suspensions.

We also studied the thixotropic properties of suspensions of Na-substituted electrodialyzed askangel. Figure 4 shows the thixotropic buildup curves for a 7% suspension of Na-substituted electrodialyzed askangel; in contrast to the Na-askangel suspensions, this shows thixotropic buildup. The time of thixotropic buildup for a 7% suspension of Na-substituted electrodialyzed askangel is ~ 70 hours.

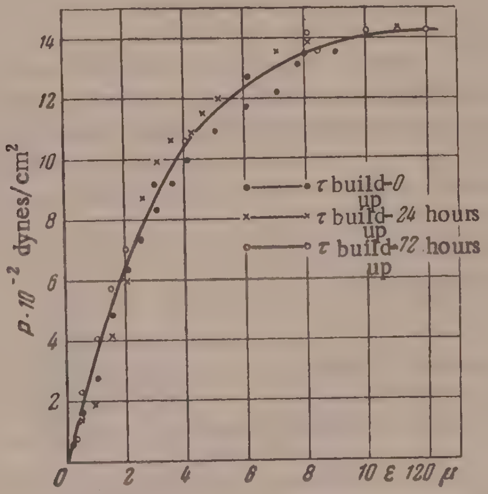

Fig. 3. Variation of shearing deformation with shearing stress in 7% Na-askangel suspensions for different times of thixotropic buildup.

Quantitative investigations of the composition of the exchange complex of Na-askangel and Na-substituted electrodialyzed askangel showed that the total exchange capacity and the amount of exchange sodium are the same for both these materials, but the Na-substituted electrodialyzed askangel has a much lower calcium content, and also contains 3.7 mg-equiv. of exchange aluminum per 100 g (Table 2).

TABLE 2

Composition of the Exchange Complex in Na-Derivatives of Bentonites

Exchange cations	Total exchange capacity in mg-equiv./100 g clay		
	Na-askangel	Na-substituted electrodialyzed askangel	Na-Oglanli bentonite
Sodium	71.75	75.7	56.28
Calcium	14.25	2.78	10.47
Magnesium		Trace	
Aluminum	—	3.72	—
Total exchange capacity	86.0	82.2	66.75

Thus, the thixotropic properties of suspensions of Na-derivatives of bentonites depend not only on the composition of the exchange complex, but also on the conditions of preparation. In particular, thixotropic structure formation in Na-substituted askangel suspensions made from electrodialyzed askangel is probably the consequence of the chemical changes in the particle surfaces which always occur during electrodialysis [5].

For studies of the effect of the equilibrium pH on the thixotropic and structuromechanical properties of askangel, nonthixotropic 4% suspension of Na-askangel and 5% suspension of Ca-askangel were treated with 1 N NaOH solution at different pH values. The treatment of the suspensions was continued until equilibrium pH was established. The curves for the kinetics of thixotropic buildup in these systems are shown in Figs. 5 and 6. Treatment of nonthixotropic suspensions of Na-askangel and of kinetically unstable suspensions of Ca-askangel with NaOH solution induces structure formation, which increases with increasing pH. The structure is completely broken down by mechanical action, but is restored during rest. Formation of a thixotropic structure in Ca-askangel suspensions on addition of NaOH is caused by the dispersing action of this electrolyte, which is the result of partial substitution of the Ca ions by Na ions in the exchange complex. As is known, dispersion, i.e., increase in the number of kinetic elements per unit volume of suspension, favors thixotropic structure formation. The formation of a thixotropic structure in Na-askangel suspensions on addition of NaOH is probably caused by the coagulating action of excess alkali.

Quantitative investigation of the structuromechanical properties of these systems showed that they belong to quasisolid plastic systems, characterized by a conventional flow limit P_{k1}, below which the system flows at a high constant viscosity. Above the conventional flow limit the viscosity falls sharply and the system continues to flow with decreasing viscosity (giving S-shaped curves for the deformation kinetics).

In illustration, the corresponding kinetic deformation curves are shown in Figs. 7 and 8. The elasticoviscous parameters of suspensions of Na- and Ca-askangels at different equilibrium pH values are given in Table 3. From the data in Table 3, P_{k1} for these suspensions is 28.5, 124, and 140 dynes/cm^2 respectively.

At shearing stresses $< P_{k1}$ all the eleasticoviscous parameters are invariant and increase with pH. Evidently, at such stresses either no structural breakdown takes place, or the individual disrupted bonds have time to reform thixotropically during flow.

However, a slight increase of the shearing stress produces an abrupt fall of viscosity as the result of commencing breakdown of the structural skeleton. At such stresses the disrupted bonds do not have time to be thixotropically restored, and breakdown develops rapidly. Thus, structure formation in nonthixotropic Na-askangel

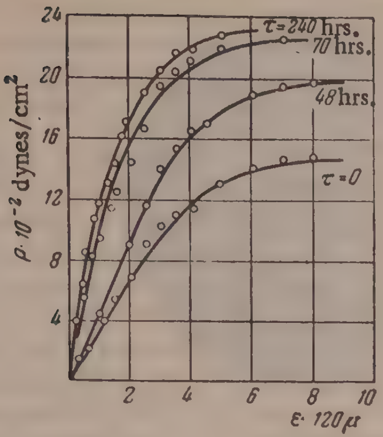

Fig. 4. Variation of shearing deformation with shearing stress in 7% suspensions of Na-substituted electrodialyzed askangel for different times of thixotropic buildup.

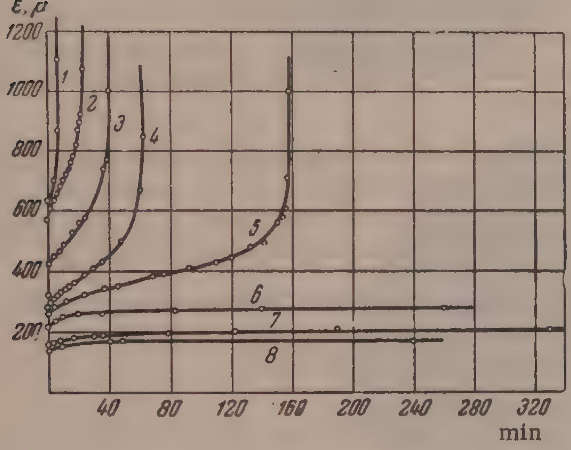

Fig. 7. Curves for the deformation kinetics of 4% suspension of Na-askangel of pH 10.5, for P: 1) 268; 2) 242; 3) 224; 4) 190; 5) 137; 6) 111; 7) 85; 8) 69 dynes/cm^2.

suspensions and kinetically unstable Ca-askangel suspensions on addition of NaOH consists of the formation of a continuous structure in which the structural elements are held together by weak and labile coagulation forces.

The structure formation process in askangel suspensions in relation to the composition of the exchange complex was also studied by means of the electron miscroscope. Owing to the high resolving power of the microscope, this method allows visual

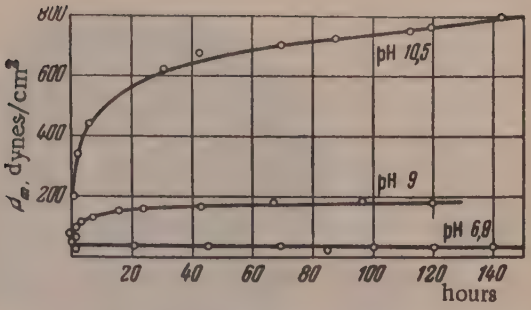

Fig. 5. Curves for the kinetics of thixotropic buildup in 4% Na-askangel suspensions at different equilibrium pH.

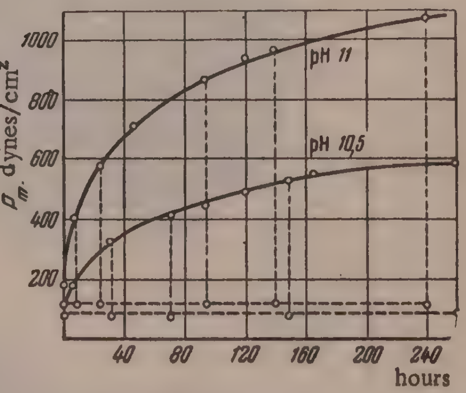

Fig. 6. Curves for the kinetics of thixotropic buildup in 5% Ca-askangel suspensions at different equilibrium pH.

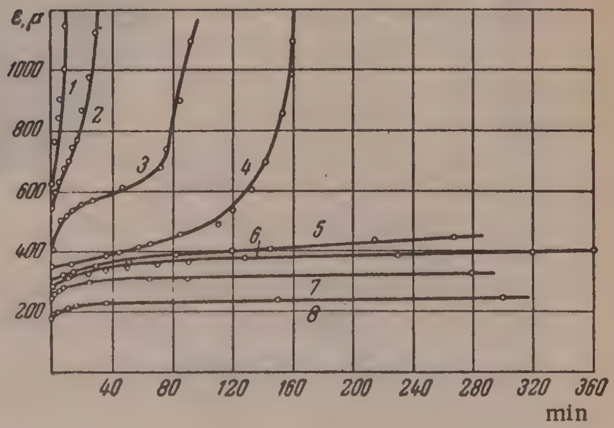

Fig. 8. Curves for the deformation kinetics of 5 % suspension of Ca-askangel of pH 11.0, for P: 1) 194; 2) 180; 3) 167; 4) 153; 5) 127; 6) 100; 7) 75; 8) 59 dynes/cm^2.

TABLE 3

Elasticoviscous Properties of Alkali-Treated Suspensions of Na- and Ca-Askangel at Different pH Values

4% Na-askangel; pH 9.0					4% Na-askangel; pH 10.5					5% Ca-askangel; pH 11				
P in dynes/cm^2	$E_1 \cdot 10^{-4}$ in dynes/cm^2	$E_2 \cdot 10^{-4}$ in dynes/cm^2	$\eta_1 \cdot 10^{-8}$ in poises	$\eta_2 \cdot 10^{-7}$ in poises	P in dynes/cm^2	$E_1 \cdot 10^{-4}$ in dynes/cm^2	$E_2 \cdot 10^{-4}$ in dynes/cm^2	$\eta_1 \cdot 10^{-8}$ in poises	$\eta_2 \cdot 10^{-9}$ in poises	P in dynes/cm^2	$E_1 \cdot 10^{-4}$ in dynes/cm^2	$E_2 \cdot 10^{-4}$ in dynes/cm^2	$\eta_1 \cdot 10^{-8}$ in poises	$\eta_2 \cdot 10^{-7}$ in poises
15	0.18	0.9	1.3	0.7	69	0.59	3.31	1.19	0.63	25	0.4	1.76	4.8	2.8
33	0.17	0.9	1.3	0.65	85	0.63	3.40	1.01	0.65	59	0.38	1.77	5.1	2.2
24	0.19	1.0	0.47	0.7	111	0.60	3.33	1.04	0.63	75	0.36	1.80	5.0	2.25
42	0.18	1.0	0.24	0.69	137	0.63	3.29	0.07	—	100	0.41	1.71	5.1	2.11
48	0.18	—	0.02	—	190	0.62	—	0.03	—	127	0.43	—	3.4	—
—	—	—	—	—	224	0.54	—	0.02	—	153	0.43	—	0.94	—
—	—	—	—	—	—	—	—	—	—	167	0.47	—	0.56	—
—	—	—	—	—	—	—	—	—	—	180	0.37	—	—	—
—	—	—	—	—	—	—	—	—	—	194	0.37	—	—	—

observation of the finest collidal particles in askangel, and of structure formation in askangel suspensions. The investigations were performed with the aid of 100 kv electron microscope by the direct preparation method, with electrono-optical magnification of 13-15 · 10^3. Fig. 9 shows electron micrographs of these suspensions.

Electron micrographs (a) of native askangel showed that askangel consists mainly of very small, semitransparent, isometric particles of rounded shape with diffuse outlines. This diffuseness is probably caused by the high swelling power of askangel particles in water. In Micrograph (a) bonds between individual particles can be seen in a number of places, forming kinds of individual chains, the spatial arrangement of which probably gives rise to the structural networks which penetrate the whole volume of the thixotropic suspension.

Particles of Na-askangel (b) also have diffuse outlines, evidently caused by the high degree of dispersion and strong swelling in water. In contrast to native askangel, no structural networks are seen in Na-askangel.

The particles in Ca-askangel (c) and electrodialyzed Al-askangel (d) consist of large coagulated aggregates up to 2.5 μ in size. In Al-askangel individual structural networks can be seen, consisting of very small particles, probably formed during electrodialysis.

Substitution of aluminum by sodium ions in electrodialyzed Al-askangel results in dispersion of the aggregates down to particles 48-96 mμ in size, interconnected into continuous structural networks (e).

Thus, the electron microscope data are in full agreement with the results obtained in the study of thixotropic structure formation.

SUMMARY

1. The thixotropic and structuromechanical properties of askangel suspensions in relation to the composition of the exchange complex have been studied. It is shown that substitution of the exchange complex of askangel by Na ions causes peptization of the particles, and in consequence a thixotropic structure is not formed in Na-askangel suspensions, irrespective of the concentration of the solid phase.

2. Suspensions of Na-substituted electrodialyzed askangel, in contrast to Na-askangel suspensions, show thixotropic structure formation.

3. Suspensions of Ca- and Al (electrodialyzed)

---

* This part of the work was carried out jointly with Scientific Assistant A. I. Mumladze.

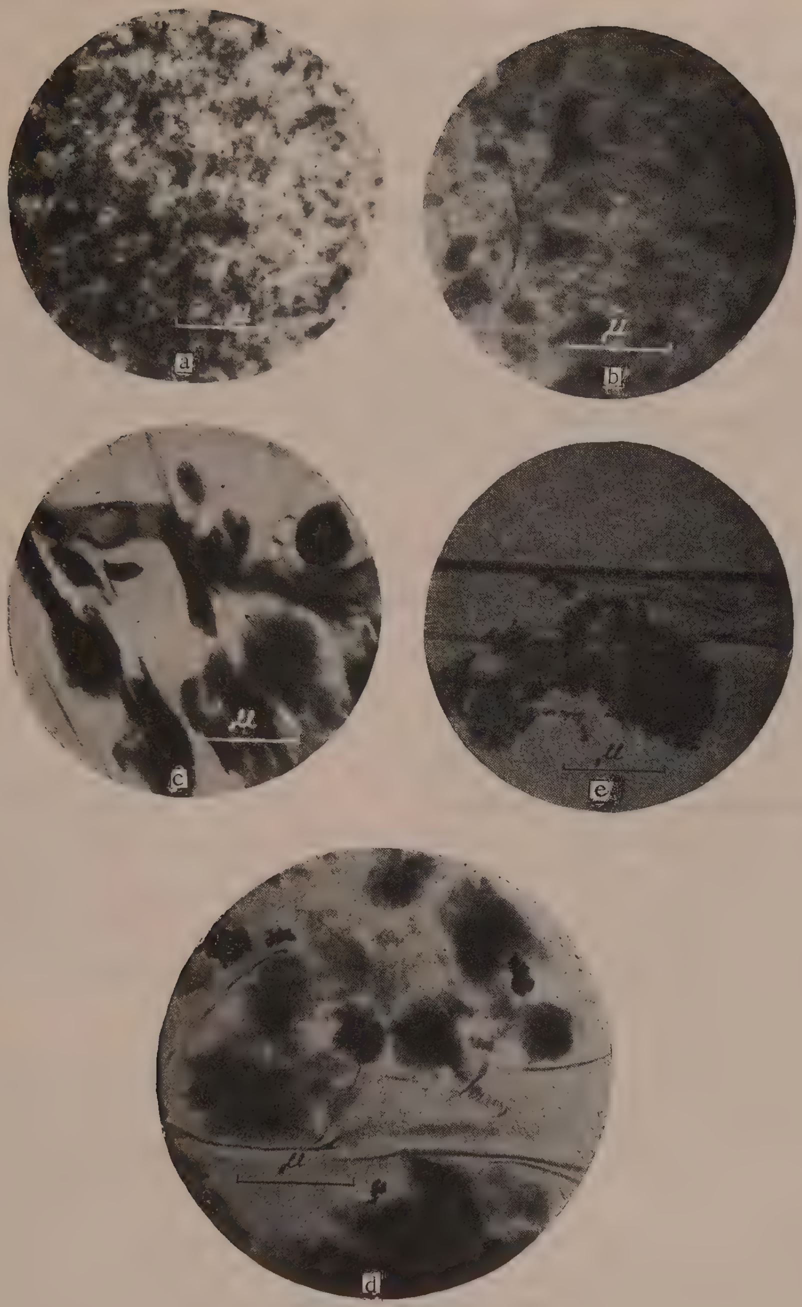

Fig. 9. Electron micrographs: a) native askangel; b) Na-askangel; c) Ca-askangel; d) Al-askangel (electrodialyzed); e) Na-substituted electrodialyzed askangel.

askangel are kinetically unstable, sedimenting suspensions. Structure formation in these systems occurs only with high contents of the solid phase.

4. Treatment of nonthixotropic Na-askangel suspensions and of kinetically unstable Ca-askangel suspensions by 1 N NaOH solution leads to formation of thixotropic structures. Structure formation in Na-askangel suspensions is caused by the coagulant action of excess alkali. Structure formation in Ca-askangel suspensions is the result of the dispersant action of NaOH.

5. Suspensions of Na- and Ca-askangel treated with NaOH solution have the structuromechanical properties of quasisolid or practically solidlike (plasticoviscous) systems.

LITERATURE CITED

[1] N. N. Serb-Serbina and P. A. Rebinder, Colloid J., 9, 381 (1947).

[2] E. I. Kobakhidze and M. E. Shishniashvili, Colloid J., 19 No. 1 (1957).*

[3] K. K. Gedroits, Chemical Analysis of Soil (State Agric. Press, 1929).

[4] W. Lewis, L. Squires, and G. Broughton, Industrial Chemistry of Colloidal and Amorphous Materials (Foreign Lit. Press, Moscow, 1948) p. 216. [Russian Translation.]

[5] S. N. Papuashvili, M. E. Shishniashvili, and L. D. Agladze, Trans. Inst. Chem. Acad. Sci. Georgian SSR, 12,23 (1956).

[6] M. E. Shishniashvili and A. L. Batsanadze, Colloid J., 15, 130 (1953).*

[7] E. G. Kister, Petroleum Economy, 12, 63 (1947).

[8] S. Ya. Veiler and P. A. Rebinder, Proc. Acad. Sci. USSR, 49, 354 (1945); S. Ya. Veiler, Factory Lab. No. 4, 432 (1948).

[9] L. A. Abduragimova, P. A. Rebinder, and N. N. Serb-Serbina, Colloid J., 17, 184 (1955).*

[10] S. A. Kudrina, Canadidate Dissertation (Tashkent, 1950).

The P. G. Melikishvili Institute of Chemistry,
Acad. Sci. Georgian SSR
Tbilisi

Institute of Physical Chemistry, Acad. Sci. USSR
Division of Disperse Systems
Moscow

Received May 7, 1956

---

* [Original Russian pagination. See C. B. Translation.]

PROPERTIES OF THIN LAYERS OF LIQUID BETWEEN MICA PLATES

G. A. Korchinsky

There are different opinions concerning the distance to which the influence of a solid surface on an adjacent liquid layer extends. According to some determinations, it reaches values of the order of one micron [1]. We have determined this distance by measuring the disjoining pressure of water and aqueous solution of acetic, propionic, and butyric acids at low pressures. The acids were purified by distillation. The solutions were made in redistilled water, and their concentrations were determined by titration.

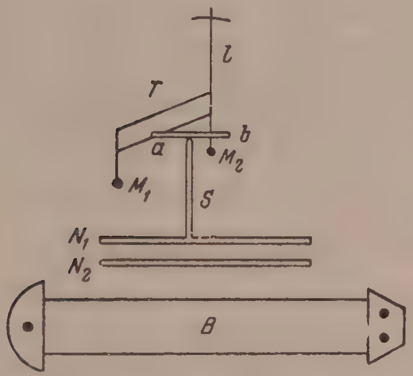

Fig. 1. Diagram of the apparatus.

The thickness of a liquid layer between two mica plates at a definite disjoining pressure was measured by means of the Deryagin and Obukhov apparatus [2] the receiving portion of which had been modified (Fig. 1). The essential part of the apparatus consits of two mica plates, glued onto steel plates N_1 and N_2 (in order to eliminate distortion of the mica). The lower plate N_2 is attached to the bottom of the cell containing the liquid to be studied. The upper plate N_1 is placed on the lower plate beforehand. The rod **S**, an integral part of plate N_1, serves to transmit the displacements. The receiving portion consists of a steel lever **T**, the section ab of which was previously graduated under the microscope. The divisions consist of small notches into which the prism-shaped head to the rod S enters. The sensitivity of the instrument depends on the division in which the head of the rod is held. A fine glass thread 1, which serves as a pointer, is attached on one side of the lever; on the other side counterpoises M_1 and M_2 are attached to stabilize the system. The cell to which the plate N_2 is attached stands on a frame with legs adjustable by screws; these are used to establish the pointer in the zero position. The values were calculated from the ratios of the lever arms. Additional experiments to determine the influence of side factors were performed and necessary precautions taken as described in the paper cited [2].

The experimental data for water and aqueous acid solutions were used to plot disjoining pressure isotherms (Figs. 2,3). Fig. 2 shows that the distance between the mica plates increases with decreasing disjoining pressure of the liquid up to a maximum value, beyond which the distance remains almost unchanged on decrease of pressure. Consequently, repulsion forces cease to act at this distance, or the influence of the solid surface on the liquid layer in contact with it ceases at half this distance. The repulsion forces measured by this method have an appreciable effect at distances of several microns between the two plane parallel surfaces separated by a liquid layer. This does not mean that all this layer constitutes a special phase. Two layers should be distinguished.

1. A surface layer, in which the molecules are fixed in definite positions and in definite mutual orientation. Thereby they form a kind of crystal lattice. This is confirmed by Trillat's experiments [3]. This layer has been named the multimolecular adsorption layer and, as has been shown [4], can be regarded as a separate phase.

2. The second layer, from a thickness of about 0.3μ, does not form a separate phase, but differs in certain respects from the main bulk of the liquid. Above the multimolecular layer there is an ionic atmosphere,

the density of which probably decreases in a direction away from the surface. Our experimental results may be represented by the equation

$$\alpha P^2 + Ph = \text{const},$$

where P is the disjoining pressure; h is the distance between the plates.

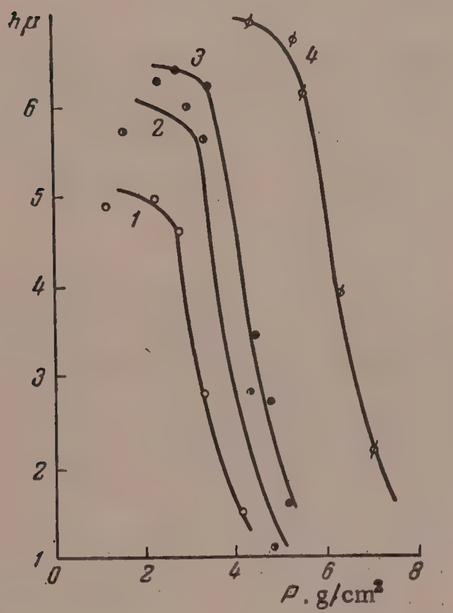

Fig. 2. Disjoining pressure isotherms: 1) water; and aqueous solutions of acetic acid at concentrations: 2) 1.01 mole/liter; 3) 0.505 mole/liter; 4) 0.125 mole/liter.

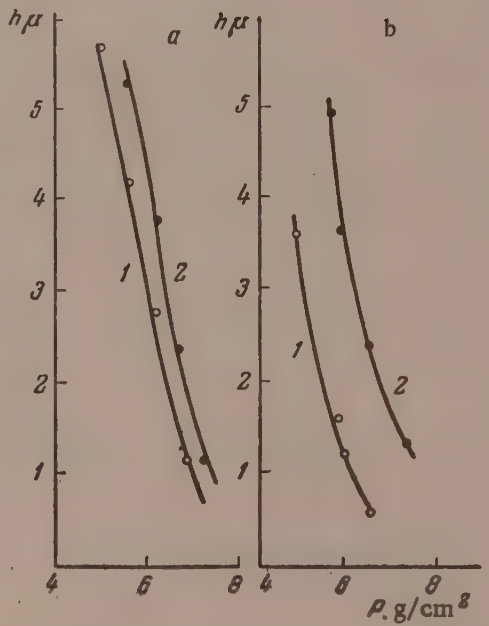

Fig. 3. Disjoining pressure isotherms for aqueous solutions of propionic (a) and butyric (b) acids at concentrations: 1) 0.5 mole/liter; 2) 0.125 mole/liter.

This equation also applies to the data for free films of $2 \cdot 10^{-5}\%$ undecylic acid solution obtained by Deryagin and Titievskaya [5].

The curves in Figs. 2 and 4 show that, as the concentration of acetic acid increases, the orientation energy and the thickness of the liquid layer first increase and then, at considerable concentrations, decrease. This can be attributed to adsorption induced by the field of force of the mica. Water is present on the mica in an adsorbed state, i.e., a multimolecular adsorption layer is formed, above which ions are arranged in a definite manner, forming an ionic atmosphere.

Acetic acid molecules are adsorbed on mica more strongly than water. This is in accordance with the fact that liquids of lower surface tension, for example at the liquid–air interface, wet solid surfaces better. Water is therefore displaced by acetic acid from the mica surface, and both water and acid molecules are present upon it in the adsorbed state. Here the water molecules are held more firmly than in the case of pure water, because water molecules are additionally bound by mica through acetic acid. The water and acid molecules are probably joined by hydrogen bonds.

It is shown in a number of papers [6] that acetic acid molecules are hydrated in a definite region of solution concentrations. In the present instance the concentration in the main volume of the solution is below this region, but, owing to the fact that acetic acid molecules are more strongly adsorbed on the mica surface, the concentration needed for the formation of such compounds is produced in the multimolecular layer; in consequence the multimolecular adsorption layer is increased and the ionic atmosphere also becomes thicker; this leads to an increase of the disjoining pressure effect.

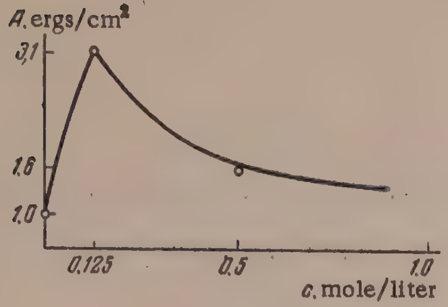

Fig. 4. Variation of particle orientation energy with acetic acid concentration.

On further increase of concentration, acetic acid tends to displace water completely. A kind of hydrophobic surface is formed; i.e., the particles are almost isolated from the force field of the mica, and the multimolecular adsorption layer and the ionic atmosphere both diminish; this ultimately leads to a decrease of the disjoining pressure effect, similarly to the compression of the diffuse layer on increase of electrolyte concentration. The variation of the orientation energy with concentration resembles the variation of zeta-potential with concentration. The variation of orientation energy (Fig. 4) as a function of the concentration of surface active substances indicates variations in the strength of the films separating plane parallel surfaces.

For concentrations of 0.5 mole/liter, the work of orientation of the molecules increases with increasing hydrocarbon chain length in the acids studied (Fig. 4), while at a concentration of 0.125 mole/liter it decreases. The orientation energy varies between 2 and 3 ergs//cm². The explanation is that with decreasing concentration the distances between the solute particles increase, and therefore their interaction weakens. Solute–solvent interaction decreases with increasing length of the hydrocarbon chains in the acid molecules. In general, the structure of the adsorption layer both at the liquid–gas interface [7] and at the solid–liquid interface depends on the nature of interaction of the solute molecules with each other and with the solvent molecules, while the thickness of the ionic atmosphere, in its turn, depends on the structure of the adsorption layer.

In conclusion, I express my deep gratitude to Prof. A. V. Pamfilov for his constant interest in this work.

SUMMARY

1. The influence of a mica surface on an adjoining liquid layer extends to distance up to 4 μ; the distance depends on the nature and the concentration of the surface active substance present.

2. The results obtained in measurements of the disjoining pressure of water and aqueous solutions of acetic, propionic, and butyric acids can be represented by the equation $\alpha P^2 + Ph = \text{const}$.

3. The orientation energy of the molecules in water and aqueous acids solutions can serve to characterize the state of a fine layer on a solid surface.

LITERATURE CITED

[1] J. C. Henniker, Rev. of modern Phys. 21, 322 (1949).

[2] B. V. Deryagin and E. Obukhov, Colloid J., 1, 385 (1935).

[3] I. Trillat, Phys. Radium 10, 32, (1929); J. Z. Phys. 6, 191 (1930).

[4] B. V. Deryagin and Z. M. Zorin, J. Phys. Chem. 29, 1755 (1955).

[5] B. V. Deryagin and A. S. Titievskaya, Colloid J. 15, 416 (1953).*

[6] A. N. Glagoleva, J. Gen. Chem. 18, 1005 (1946); S. Ya. Levitman and N. F. Ermolenko, J. Gen. Chem., 18, 1567 (1948).

[7] A. V. Pamfilov, G. G. Devyatykh and L. V. Shirshova, J. Phys. Chem. 24, 292, 1832 (1950).

Chernovits State University

Received June 17, 1956

---

* [Original Russian pagination. See C. B. Translation.]

INVESTIGATION OF THE MECHANICAL PROPERTIES OF PLASTIC DISPERSE SYSTEMS IN CONDITIONS OF UNIAXIAL EXTENSION AND COMPRESSION

E. P. Mosikhin and G. V. Vinogradov

Because of the existence of a fairly rigid structural framework in such soft plastic materials as clay pastes, solid greases, and similar materials, it is possible to study their mechanical properties by the same methods as are used for typical solids. As the result of investigations carried out by Vinogradov and Klimov [1] on lubricants and congealed oils, considerable success has been attained in the study of the elasticoplastic and strength properties of such plastic disperse systems, test methods have been worked out in detail, and the typical characteristics of these properties have been described. The most important data have so far been obtained in investigations in which pure shear conditions were realized.

The lack of information on the resistance of soft plastic bodies to normal stresses, and on the role of normal stresses in deformation processes in general, is a significant gap, as under actual conditions of use many disperse systems are subjected not only to shearing deformations but are often in a state of complex stress. In such conditions the deformation and destruction processes may be determined not only by tangential but also by normal stresses.

In shearing deformations effected in instruments with concentric gaps visual observation of destruction of the structural framework is difficult, and difficulties therefore arise in defining the conditions in which the yield value is passed. Moreover, in this test method the deformation process may be obscured by the wall effect. The method, described in the present paper, for studying soft plastic bodies in conditions of uniaxial extension and compression is free from most of these defects, and makes possible the determination of the true volume mechanical properties of such materials.

It must be remembered, however, that plastic disperse systems show the properties of solids only at low shearing stresses. Experiments on the extension of plastic disperse systems involve considerable practical difficulties because of their ease of deformation, with the consequent difficulties of suitable design for the clamps, of specimen molding, and a number of other factors. Devices designed for this purpose and some of the results obtained are described below.

A conventional diagram of the simplest proposed apparatus is shown in Fig. 1. The test specimen 1 is molded in the band holders 2 by means of the graduated tube 3. The lower holder, in one piece with the massive stand 4, is stationary. The upper holder is joined by the thread 5 to the balance arm 6. Weights 8 are placed on the pan 7 suspended from the arm.

Molding of the specimen begins with filling the tube with thoroughly homogenized grease. The band holders are then introduced simultaneously into the tube, and the grease is partially extruded through the hole, as shown by arrows in Fig. 1. The position of the graduated tube at this stage in the preparation of the test specimen is shown in Fig. 1 by a dotted line. The movement of the upper holder into the tube stops when the thread has become slightly tensed. To complete the molding of the specimen the graduated tube is slowly lowered onto the base of the stand with the lower holder. Extension of the specimen is determined by displacement of the pointer 9 attached to upper holder (Fig. 1). The readings are taken by means of the measuring microscope 10, to an accuracy of 5 μ. The angles of the slip lines and the planes along which the specimens are destroyed (ruptured) are measured to an accuracy of 1'.

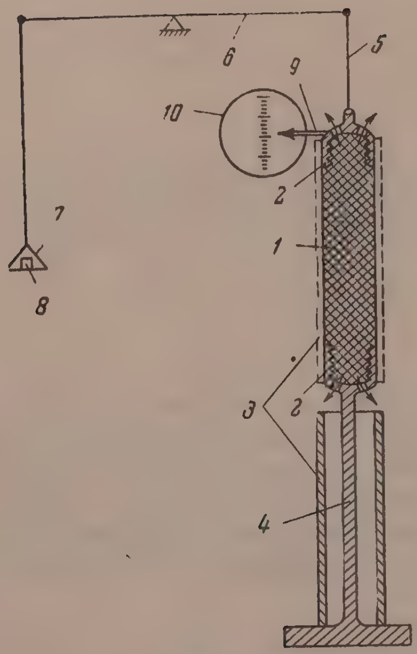

Fig. 1. Simplified apparatus for extension of plastic bodies.

Some results of the use of this apparatus for testing "solidol" grease, a plastic material the rheological properties of which have been studied in detail by Vinogradov, Klimov, and Pavlov [2], are given below. Fig. 2 shows photographs corresponding to different stages of deformation of solidol at a load rate of 2 g/minute. Photograph a shows the original specimen; b shows the beginning of local constriction or neck formation. This stage corresponds to the end of uniform plastic deformation. After a neck has been formed, deformation increases at constant load to failure. Formation and further development of local constriction is accompanied by appearance of slip lines, inclined at about 45° to the specimen axis.

The deformation and destruction of specimens of plastic disperse systems after the formation of a neck differ in some respects from the effects observed in metals which form a neck on extension. In specimens made from homogenized grease the cross section of the neck at right angles to the axis is oval in shape; the neck from the sides of the major and minor axes of the oval is shown in Photographs c and d respectively. A typical specimen after destruction is shown in e. The start of destruction is easily recognized by the appearance of cracks in the region of the neck (Photo f).

The final destruction – separation of the specimen into two parts – is explained in Fig. 3. The rupture surface is an oval (shown in Fig. 3 by a shaded area), the plane of which is inclined at 45° to the specimen axis. Figure 3 shows the direction of the shear plane which coincides with the direction of the minor axis of the oval. Thus, destruction of grease specimens occurs in the direction of the greatest tangential stresses. According to Bartenev's classification [3], this is a case of plastic rupture. In all the experiments the neck was formed near the upper holder, which shows that the weight of the specimen itself exerted an appreciable effect.

A typical extension diagram, in nominal stress – relative extension coordinates, is shown in Fig. 4, Curve 1. The linear portion of this curve, starting from the coordinate origin, up to $\sigma = 10$ g/cm^2 (elastic limit) corresponds to purely elastic deformation. In fact, experiments with decreasing loads showed that at stresses less than 10 g/cm^2 the loading and unloading lines for solidol practically coincide. The relative extension in purely elastic deformation is a few tenths of one per cent. Young's modulus is of the order of $3 \cdot 10^3$ g/cm^2. Beyond the region of purely elastic deformation, homogenized greases undergo fairly considerable elongation and show appreciable plasticity. The point K on the diagram represents the nominal strength, which is determined from the ratio of the maximum load sustained by the specimen to its original cross section.

Comparison of the tensile strength σ_t with the maximum shearing strength τ_s, determined by shearing experiments, showed that $\sigma_t/\tau_s \sim 2$. This fact, in the first approximation (because a nominal value of the tensile strength was used), confirms the applicability of the plasticity theory to plastic disperse systems.

Clearly defined hysterisis effects are observed in the plastic deformation region. This is illustrated by the data in Fig. 4, which also shows that the unloading Curves 2 are nearly linear, and that with repeated loadings increase of load results in smaller extensions, i.e., the test specimens exhibit less plasticity. Repeated loadings to values above the elastic limit and below the strength limit produce a decrease of the strength limit – the weakening effect discovered by Vinogradov and Klimov [4] in experiments on greases in conditions of pure shear; this is illustrated by Curve 2 in Fig. 4.

After several loading – unloading cycles the system reached a strength limit at the point E, i.e., the resistance of the specimen to tensile deformation decreased considerably. Rest produced the opposite effect. A specimen which, after the same loading – unloading cycles, was rested for one hour before the last loading,

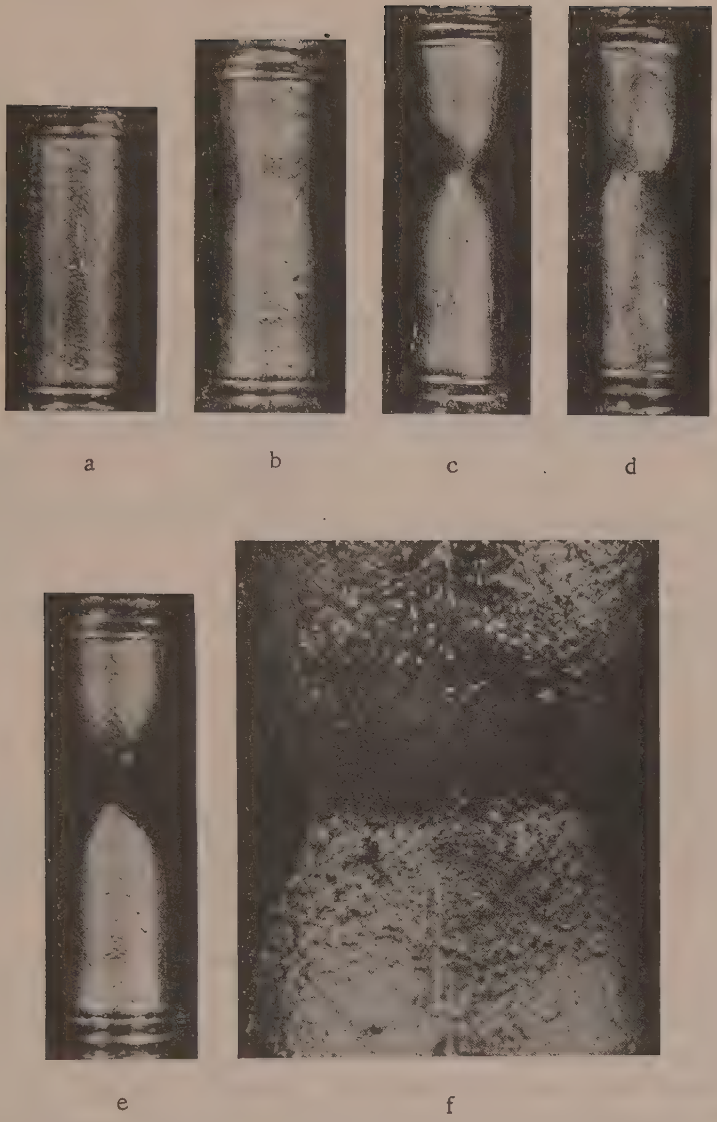

Fig. 2. Photographs of a solidol specimen at different stages of extension: a) original state; b) start of neck formation; c) view of neck in the direction of the major axis of the oval; d) ditto, in the direction of the minor axis; e) after destruction; f) cracks in the neck region.

reached, as the result of thixotropic buildup, a strength limit not at the point E but at the point F, i.e., at higher stresses and accordingly at a greater plastic deformation. The broken region EF of the curve therefore represents the increase of strength as the result of one hour of rest. These results show that the weakening effect and thixotropy in plastic disperse systems may appear not only when the strength limit has been exceeded, but generally as the result of plastic deformations at stresses below the strength limit. The above method for studying soft plastic bodies under uniaxial extension has certain defects.

1. The apparatus, with direct loading, is of the absolutely yielding type and does not record decreased resistance of the specimens to deformation on formation of local constrictions. Therefore loads and extensions should be measured only up to the moment of neck formation.

2. The weight of the specimen itself results in an inhomogeneous stressed state, which is intensified

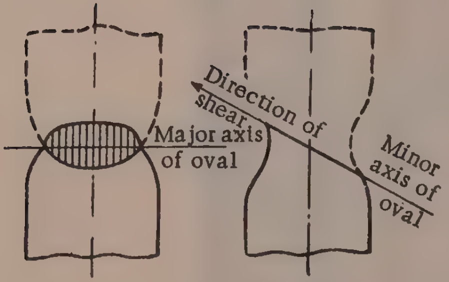

Fig. 3. Destruction of specimens of plastic disperse systems in extension.

owing to concentration of stresses at the point of transition from the specimen surface to the inner surface of the tube, and the true strength limit is therefore difficult to determine. Therefore the elastic and plastic characteristics determined by this method are average values.

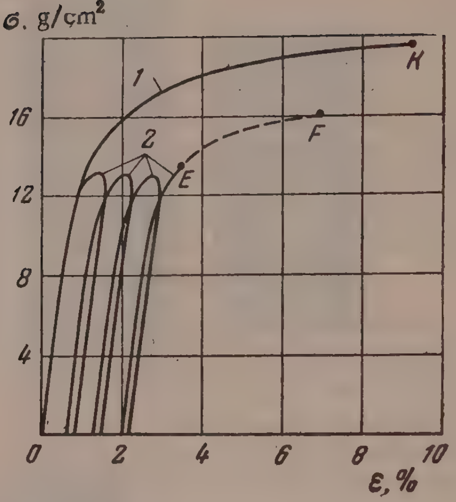

Fig. 4. Extension diagram for solidol.

3. Because of the limited speed at which extensions can be read off through the microscope, tests cannot be carried out at any considerable rates of loading.

4. In the use of this apparatus it is difficult to prepare and test specimens of plastic disperse systems with length (l) – diameter (d) ratio greater than 3-3.6. It is therefore difficult to compare the results of tests on plastic disperse systems with results for such typical solids as metals, specimens of which usually have $l/d = 5$.

In view of these defects, an improved apparatus was designed for testing plastic disperse systems in conditions of uniaxial extension and compression, by means of which different deformation rates can be obtained, the extension (or compression) diagrams are automatically recorded, and thermostatic control is provided. The specimens can be tested either in a vertical or a horizontal position. In the latter case the specimen is contained in a liquid of the same or similar density, whereby the influence of the weight of the specimen is largely excluded and stress inhomogeneity is avoided. In consequence, specimens with $l/d = 5$ can be tested.

The apparatus consists of an electric drive, loading and load measuring mechanisms, recording mechanism, and a bath containing a liquid. The apparatus is shown diagrammatically in Fig. 5.

The bath is a rectangular vessel 340 mm long, 150 mm wide, and 140 mm high; the electric drive consists of a direct current motor 2 and worm reducing gear 3. The speed of the motor shaft is measured by means of a stroboscopic disk 4 and neon lamp 5. A rheostat (not shown) in the shunt winding circuit is used to vary the speed from 50 to 3000 revolutions per minute. The gear ratio of the reducing gear is 60. The loading mechanism consists of a step pulley 6, thread 7, a movable holder 8 with a connecting rod, and a return spring 9. The step pulley is fixed on the shaft by means of a cotter, and can be moved along the shaft, so that the thread can be moved onto any of the steps. The moving holder is in one piece with the rod. The external diameter of the holder is 20 mm, internal – 17 mm, length – 25 mm, internal thread (right hand) pitch – 1.5 mm; The rod diameter is 10 mm, and length 175 mm. The rod can move within the tube. The return spring 9 is used for moving the holder during unloading.

For compressive testing, a reversing device shown separately in Fig. 5,b is screwed into the holders 8 and 12.

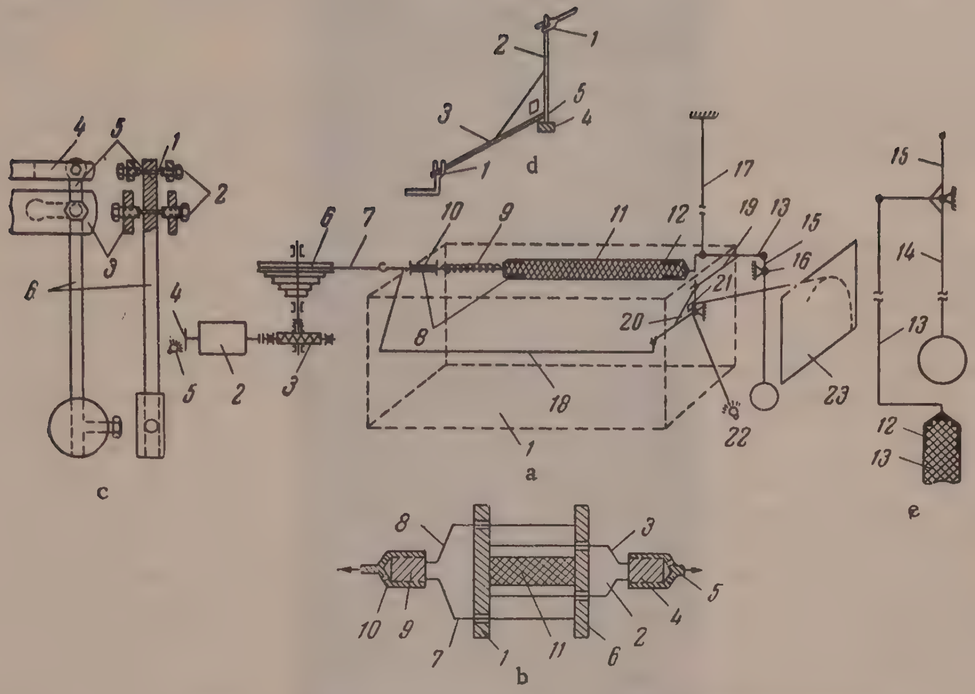

Fig. 5. Apparatus for investigation of extension and compression in plastic disperse systems: a) kinematic scheme; b) reversing mechanism for compressive testing; c) pendulum device for extension and compression tests; d) frame for mirror readings of deformations and loads; e) arrangement of the pendulum for testing plastic bodies in a vertical position.

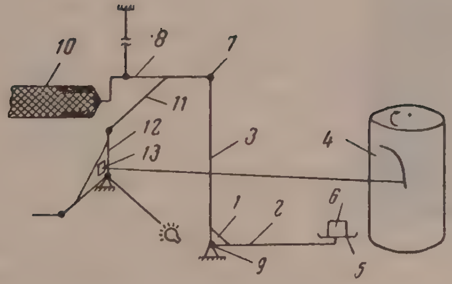

Fig. 6. Diagram of device for automatic recording of deformation—time curves.

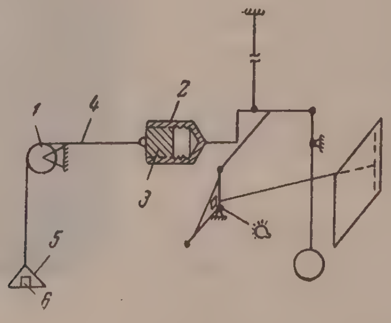

Fig. 7. Diagram of device for constructing the loading scale.

The load measuring mechanism (Fig. 5,a) consists of the holder 12 this holder has a left hand thread and is of the same dimensions as the movable holder) pendulum connecting rod 13, a pendulum consisting of a long arm 14 and a short arm 15, a bracket 16, and a suspension thread 17. The connecting rod 13 joins the holder 12 to the short arm 15 of the pendulum. The suspension thread acts as an additional support. The point of attachment of the thread 17 to the rod 13 is found after this rod has reached equilibrium with the holder in the free state in order to decrease excess pressure on the pendulum supports. When a load is applied to the

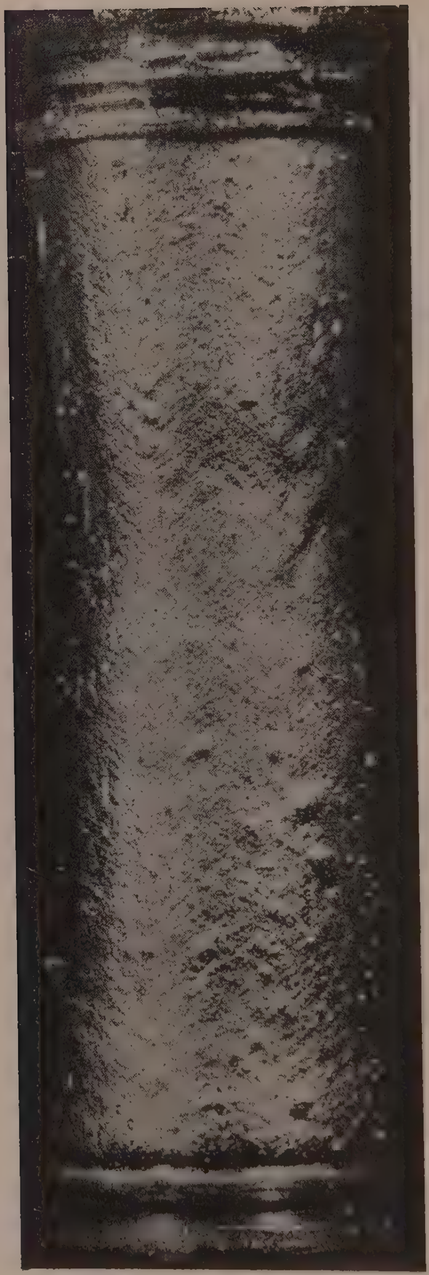

Fig. 8. Slip lines on the surface of a solidol specimen subjected to extension.

specimen, the pendulum connecting rod moves, while the point of suspension of the rod 13 and thread 17 describes an arc of radius equal to the length of the thread; in consequence, the holders are no longer coaxial. To decrease this effect, the suspension thread was 500 mm in length; the suspension point is then displaced by not more than 0.05 mm with a maximum displacement of 3.5 mm of the rod. Interchangeable disks of different weight (from 20 to 150 g) are used for testing specimens with different strength limit.

The reversing device (Fig. 5,b) consists of a plate 1, joined by the connectors 2 and 3 to the bung 4, screwed into the "stationary" holder 5. The plate 6 is joined by connectors 7 and 8 to the bung 9, which is screwed into the movable holder 10. The plates have suitable openings to allow free movement of the connectors 2,3,7, and 8. The specimen 11 is molded between the plates 1 and 6. Because of the right hand internal thread in holder 10 and left hand in holder 5, and corresponding right and left hand external threads on the bungs 9 and 4, the device can be screwed into both holders simultaneously. Thus, with the use of this reversing device it is possible to perform compressive tests, with the holders moving the same direction as in extension tests.

The stationary pendulum support is shown in Fig. 5,c. The tempered steel needles 1 rest in steel conical sockets in the ends of the screws 2. The contact between each needle and the socket is regulated by turning the screw in the bracket 3. A support of similar design is used for joining the rod 6 to the short arm 5 of the pendulum (13,15, and 14 in Fig. 5,a).

The recording mechanism consists of the transmission levers 18 and 19 (Fig. 5,a), a three-support frame 20 carrying a mirror 21, a light source 22, and a photosensitive screen 23. The transmission lever 18 is rigidly linked to the rod 8 of the movable holder and hinged to the horizontal rod of the three-support frame. The transmission lever 19 is rigidly linked to the connecting rod 13 of the pendulum and hinged to the vertical rod of the same frame. The lengths of the frame rods (horizontal 80 mm, vertical 40 mm) were so chosen as to give an extension diagram 200× 200 mm on the screen. The specimen 11 is molded between the holders 8 and 12 (Fig. 5,a) as described for the apparatus shown in Fig. 1.

Fig. 5,d shows the hinged joints between the transmission levers and the frame rods; these are effected by means of the small forks 1. The gap between the rods and the forks 1 does not exceed 0.05 mm, allowing the rods 2 and 3 to turn about the fixed frame support 4 by not more then 14°. The fixed frame support 4 is also a metallic conical socket in which rests a steel needle 5 with a conical tip.

Let us consider the operation of some of the mechanisms of the instrument. When the motor 2 (Fig. 5,a) is switched on, the rotation is transmitted through the reducing gear 3 to the step pulley shaft, the thread is wound onto the pulley 6, and the rod of the movable holder 8 moves at a definite speed. The test specimen 11 is deformed and transmits the load to the short arm 15 of the pendulum through the connecting rod 13, displacement of which deflects the pendulum by a definite angle. The transmission lever 19, which moves together with the rod 13, turns, by means of the fork, the vertical rod of the frame 20 with its attached mirror 21. The ray of light reflected by the mirror moves upward on the screen and records the increase of load on a definite scale. The transmission lever 18 moves together with the movable holder 8, and turns the horizontal rod of the frame by means of the fork. The reflected ray is displaced to the right (if the screen is viewed from the side of the drive) and registers, again on a definite scale, the change in the length of the specimen. In this way an extension (of compression) diagram is recorded in load—extension coordinates. It should be remembered that the total deformation includes the deformation of the specimen itself, elastic deformations of the instrument parts, and displacement of the rod 13 during the experiment. To exclude the elastic deformation of the instrument parts and displacement of the rod, a metal specimen screwed into the two holders is "squeezed",, and a "squeezing" diagram is recorded. The elastic deformations of the instrument parts and the rod displacement are substracted from the total deformation, which gives the corrected extension (or compression) diagram.

For extension tests with the specimen in the vertical position, the pendulum is proveded with two short arms of equal length at right angles to each other (the second short arm is not shown in Fib. 5,a). The whole apparatus is then placed in the vertical position. Fig. 5,e shows the method of connecting the immovable holder 12 to the pendulum, the rod 13 being connected to the second short arm of the pendulum.

To obtain curves showing the deformation kinetics, the pendulum is replaced by a special angle bracket 1 with levers 2 and 3 and a photorecording drum 4 fitted with a clock mechanism (Fig. 6). One end of the horizontal lever 2 carries a pan 5 for weights 6; its other end is connected by means of a point support 7 with the pendulum rod 8. The support 9 of the angle bracket 1 is of the fixed hinge point type. When the load is applied by the weights 6, the lever 2 and the rigidly linked lever 3 turn about the hinge 9. The transmitted force causes deformation of the specimen 10 and therefore displacement of the rod 8. The transmission lever 11, rigidly linked to the rod 8, turns the vertical rod 12 of the frame and with it, the mirror 13. The ray reflected from the mirror moves downward along the slit of the drum and records the deformation of the specimen. The drum 4 with photographic paper attached on it is rotated by means of the clock mechanism, thus provides a time axis on the diagram.

The instrument is calibrated in order to determine the load and extension scales. The holders 8 and 12 (Fig. 5,a) are first set in the zero position, so that the "fixed" holder 12 was not under any load, and the movable holder 8 was 100 mm away from it.

The device shown in Fig. 7 is used to construct the loading scale. It consists of a pulley 1 rotating on needle supports of the type described above. A light bung fitted with a ring is screwed into the "fixed" holder 2. The thread 4 is joined to the ring at one end and to the pan 5 with weights 6 at the other. The position of the point of light corresponding to the zero position of the holders is marked on the screen. The first load is then put on the pan 5, the light spot being thereby displaced upward on the screen; the new position is marked on the screen. A second load is applied and the position of the light spot is again marked, etc. The calibration is continued up to the maximum load (150 g). When the loading scale is completed, and unloading scale is constructed in a similar way. Friction in the pulley bearings 1 (Fig. 7) is allowed for by previous calibration of the pulley itself.

To construct the extension scale, the holder 8 (Fig. 5,a) is moved from the zero position by means of a micrometer, the light spot being displaced horizontally on the screen; its new position is marked. The positions of the light spot are again noted with successive loadings, etc. The points so obtained are used to construct a coordinate grid which is photographed to natural size on sensitive film.

After the testing of each specimen the coordinate grid is photographed onto the paper which is used to record the extension curve (care is taken that the zero points of the curve and coordinate grid coincide). The sensitive paper thus carries an image of the extension curve and the coordinate grid.

To illustrate the use of the extension method, the results of an investigation of a homogenized solidol grease are given. Figure 8 shows a photograph of the specimen after a stress corresponding to plastic deformation has been reached. The photograph clearly shows shearing lines at an angle of 45° to the specimen axis, similar to the lines found after extension of metal specimens.

SUMMARY

1. A new method is described for investigating the rheological properties of plastic disperse systems by testing them in conditions of uniaxial extension and compression. Two instruments designed for such tests are described.

2. Homogenized Ca solidol greases have been used to demonstrate that tensile failure of specimens of plastic disperse systems occurs in the direction of the maximum tangential stress, i.e., by a plastic failure mechanism. Slip lines (Lüders lines) are observed in the direction of the maximum tangential stress. At failure, the neck of the specimen is in the shape of an oval in a direction at right angles to the specimen axis.

3. The uniaxial extension instrument has been used to determine Young's modulus for solidol ($3 \cdot 10^3$ g/cm^2), and it has been shown that in the region of pure elastic deformation the relative extensions comprise tenths of one per cent. The greases showed appreciable plasticity in deformation beyond the pure elastic region.

4. It was found that the ratio of the tensile strength to the shearing strength (determined by means of rotational elastometers) is approximately two. Hysteresis effects in loading and unloading in the plastic deformation region have been examined, and it is shown that plastic disperse systems may exhibit strength loss and thixotropy at stresses below the strength limit.

LITERATURE CITED

[1] G. V. Vinogradov and K. I. Klimov, Proc. Acad. Sci. USSR, 57, 911; 58, 1677 (1947).

[2] G. V. Vinogradov, V. P. Pavlov, K. I. Klimov, and M. M. Gvozdev, Trans. Military Acad. Armored and Tank Forces, No. 11-12 (88-89) 27 (1951).

[3] G. M. Bartenev, Progr. Chem. 24, No. 7, 815 (1955); G. M. Bartenev and G. I. Belostotskaya, J. Tech. Phys. 24, 1773 (1954).

[4] G. V. Vinogradov and K. I. Klimov, J. Tech. Phys., 18, 355 (1948).

The I. V. Stalin Military Academy of
Armored and Tank Forces

Received May 21, 1956

ELECTRON-MICROSCOPE AND X-RAY INVESTIGATIONS OF DISPERSE PHASES IN ORGANOSOLS OF LEAD—TIN ALLOYS

E. M. Natanson, V. P. Chalyi, N. N. Kozachek, and A. P. Kaban

Electron microscope investigations of the disperse phases in nonstabilized organosols of lead—tin alloys, made electrolytically [1] from alkaline electrolytes, were carried out in order to study the particle form in these alloys in relation to the component ratio and current density during their formation at the cathode.

The Em-100 electron microscope, giving ~ 18,000 magnification, was used for these investigations. The specimens were prepared by application of microdrops of the organosols onto thin collodion films, which were then dried at 30-40°.

The materials studied were disperse phases of lead and tin organosols and of their alloys, obtained by cathodic deposition with the following atomic ratios of the two metals in the aqueous layer of a two-layer electrolyte: 3: 1, 1: 1, 1: 2, 1: 3 and 1: 7. Cathode deposits were obtained at current densities of 3,5,10,15,20 and 30 amp. /dm^2 from each of these electrolyte compositions.

From the results, which are presented in the form of the most typical photographs (see Plate), it is possible to establish certain characteristics relating to the formation of the particles in the alloy organosols.

For the same atomic ratios of lead and tin in the electrolyte, variations of current density have a significant effect on the structure of the highly disperse metal particles formed at the cathode.

This factor is especially prominent in the formation of disperse phases of lead—tin alloy organosols at the cathode in electrolytes with lead—tin ratios of 1: 2, 1: 1, and 3: 1. As the Photographs 1 (D_c = 5 amp./dm^2, electrolyte ratio Pb: Sn = 1: 2) and 2 (D_c = 10 amp./dm^2, electrolyte ratio Pb: Sn = 1: 1) show, at low current densities between 5 and 10 amp./ dm^2 the cathode deposits are predominantly microdendritic in structure. The branches of such dendrites are often almost perpendicular to the main axial stem, and separate accumulations of dendrites have a more or less ordered structure. It was noted that the axial dendrites do not have a continuous structure but consist of chains of closely adherent individual crystals. In some instances this structure is fairly loose and the distances between individual crystals can be clearly detected in the field of vision of the electron microscope.

Irregular formations, probably consisting of a mechanical mixture of tin and lead particles, are also seen. Here the lead is deposited on the cathode in the form of microdendrites, and tin in the form of irregular amorphous particles. This is confirmed by electron micrographs of highly disperse cathode deposits formed in two-layer electrolytes in total absence of tin (Micrograph 3, D_c = 10 amp./dm^2) and in total absence of lead (Micrograph 4, D_c = 20 amp./dm^2) at current densities from 3 to 30 amp./dm^2.

At current densities from 3 to 10 amp./dm^2 the cathode deposits consist mainly of lead particles. Tin particles are found much less often in the field of vision. The main reason for this is probably that at low current densities tin, even in a two-layer bath, is deposited in the form of coarse lumps.

At current densities from 10 to 20 amp./dm^2 the tin content of the deposits increases sharply. The dendrites in such deposits have a disoriented structure, seen in Micrographs 5,6, and 7 (D_c=10 and 15 amp./dm^2, atomic ratios of Pb to Sn in the electrolyte 3: 1 and 1: 1). This is especially prominent if the position of the side branches relative to the axial stem is examined, as the side branches of the dendrites begin to disintegrate

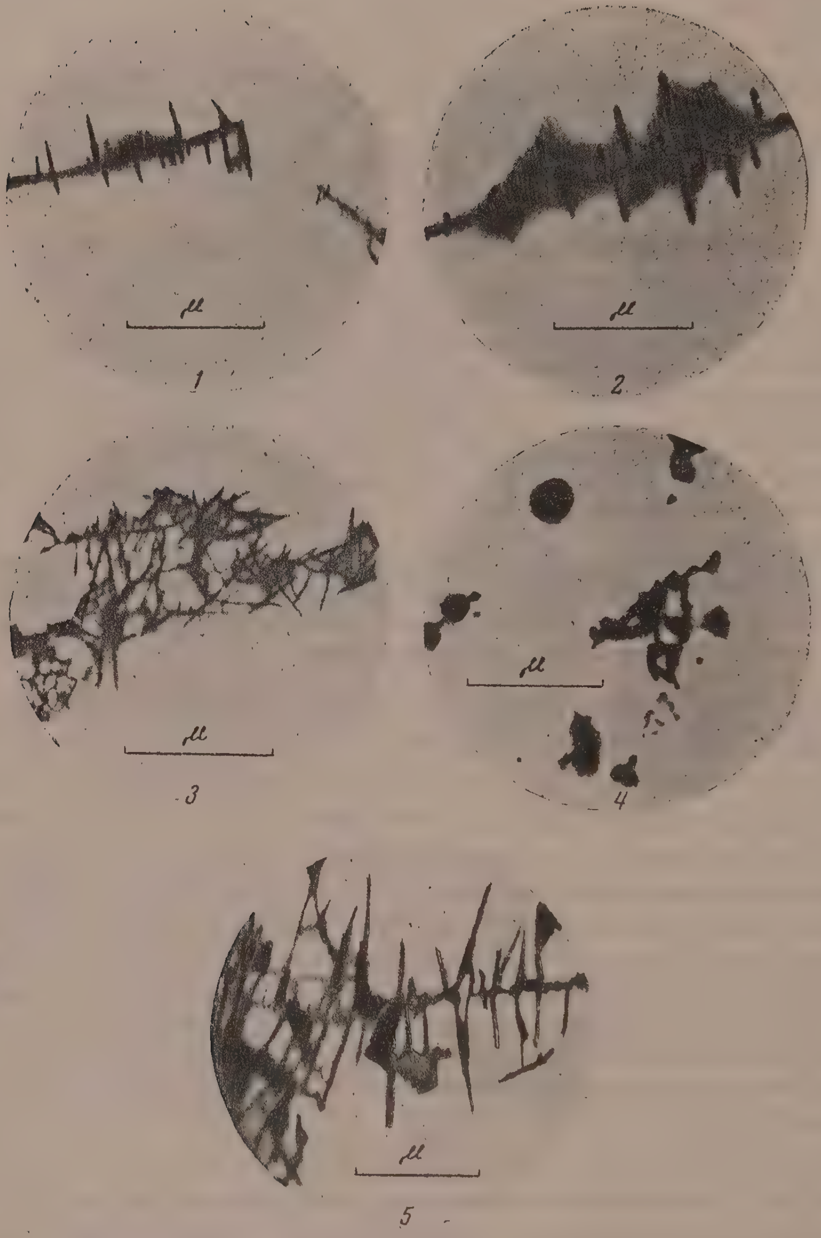

Electron micrographs of the disperse phase of organosols: 1) alloy of Pb: Sn = 63.7: 37.3%, D_c = 5 amp./dm^2; 2) alloy of Pb: Sn = 60: 40%, D_c = 10 amp./dm^2; 3) lead, D_c = 10 amp./dm^2; 4) tin, D_c = 20 amp./dm^2; 5) alloy of Pb: Sn = 75: 25%, D_c = 10 amp./dm^2.

from the base. Disintegration of the dendrites is most pronounced in alloys with Pb: Sn = 1: 2 (Micrograph 9, D_c = 10 amp./dm^2). The process is seen particularly clearly when the current density is increased to 30 amp./dm^2 (Micrograph 8).

Transition from a dendritic to an amorphous structure in the cathodic particles commences at a current density of 10 amp./dm^2 at Pb: Sn = 1: 2, at current density of 15 amp./dm^2 at Pb: Sn ratios of 1: 1 and 3: 1, and is almost complete at a current density of 20 amp./dm^2. In our opinion this process is the result of formation of a lead–tin alloy at the cathode.

At current densities of 25-30 amp./dm^2 (Micrograph 8, atomic ratio Pb: Sn = 1: 2) no dendrites are seen in the cathode deposits of lead–tin alloy. In all probability, at these current densities the two metals form the alloy at once at the cathode, in the form of fine particles, sometimes joined in large loose amorphous aggregates.

It is also important to take into account that the composition of the lead and tin deposits varies with the current density (see Table).

The Table shows that, with increasing cathode current density, the lead content of the cathode deposits decreases in the range from 3 to 15 amp./dm^2, and then remains almost unchanged on further increase of current density up to 25 amp./dm^2.

Micrographs 3,5,2,9, and 10 show that, at the same current density of 10 amp./dm^2, the structure of the cathode deposits greatly depends on the lead–tin ratio in the electrolyte. At a ratio of Pb: Sn = 1: 0 the particles of the highly disperse lead are of clearly defined microdendritic form. These particles aggregate into very loose accumulations, randomly arranged relative to each other. At ratios of Pb: Sn = 3: 1, 1: 1, and 1: 2 the cathode deposits mainly consist of lead particles of an oriented dendritic structure. Most of the branches of these dendrites are almost exactly perpendicular to the main stem. However, in many cases a transition into an amorphous mass can be seen, probably owing to alloy formation (for example, for Pb: Sn = 1: 1 in Micrograph 2). In this case the cathode deposit is probably a mixture of particles of lead–tin alloy and of pure dendritic lead.

At a ratio of Pb: Sn = 1: 2 (Micrograph 9) alloy formation and transition of dendritic into amorphous particles is still more pronounced. At a lead–tin ratio of 1: 3 in the electrolyte the cathode deposit consists mainly of amorphous particles and contains almost no dendritic particles.

Similar results are seen in electron micrographs of disperse phases of organosols obtained at a current density of 15 amp./dm^2.

These facts suggest that increase of the tin content in the electrolyte favors formation of highly disperse lead–tin alloys at the cathode and decreases the current density at which this process begins. For example, at the ratio of Pb: Sn = 1: 3 there are almost no dendrites in the cathode deposits formed at current densities of 3,5, and 10 amp./dm^2.

In conclusion, it may be noted that for any given lead–tin atomic ratio in the electrolyte there is a definite current density range in which particles of lead–tin alloy are formed at the cathode. In this range, the start of alloy formation is indicated by a sort of "swelling" process in the microdendrites; as the current density increases, this leads to the formation of cathode deposits consisting of almost entirely disintegrated dendrites.

X-ray investigations. Specimens of the disperse phases of lead–tin organosols were studied by the x-ray powder method with iron radiation. An ordinary cylindrical camera with a cassette 57.3 mm in diameter was used. The specimens (0.84 mm in diameter) were prepared as described previously by one of us [2].

To determine the phase composition, standard specimens of spectroscopically pure tin and lead were first taken, and the x-ray diagrams of these were compared with the diagrams of the specimens under investigation.

The results showed that with Pb: Sn ratios of 2: 1, 1: 1, 1: 3 and 1: 5 in the electrolyte, and at the same current density of 10 amp./dm^2, the phase composition of the disperse phase of lead–tin organosols is represented by Pb + β-Sn and does not depend on the Pb: Sn ratio in the aqueous layer of the two-layer electrolyte.

At a ratio of Pb: Sn = 1: 2 in the aqueous electrolyte layer, with a gradual decrease of the cathode current density from 3 to 25 amp./dm^2, the phase composition remains unchanged. At 30 amp./dm^2 the disperse phase of the organosol consists of pure lead.

These results show that the phase composition of disperse phases of lead–tin alloy organosols fully corresponds to the phase diagram for the lead–tin system, in which the components form a eutectic [3].

According to x ray data in the literature [4], at 20° lead dissolves 3.5 atomic % of tin; its crystal lattice parameter decreases as a result. Alloys containing 10-95 atomic % of tin give x ray diagrams showing lines for both metals. With tin contents of 98.6 atomic % and higher, a solid solution of lead in tin is formed, the lattice parameter of the latter being changed only slightly.

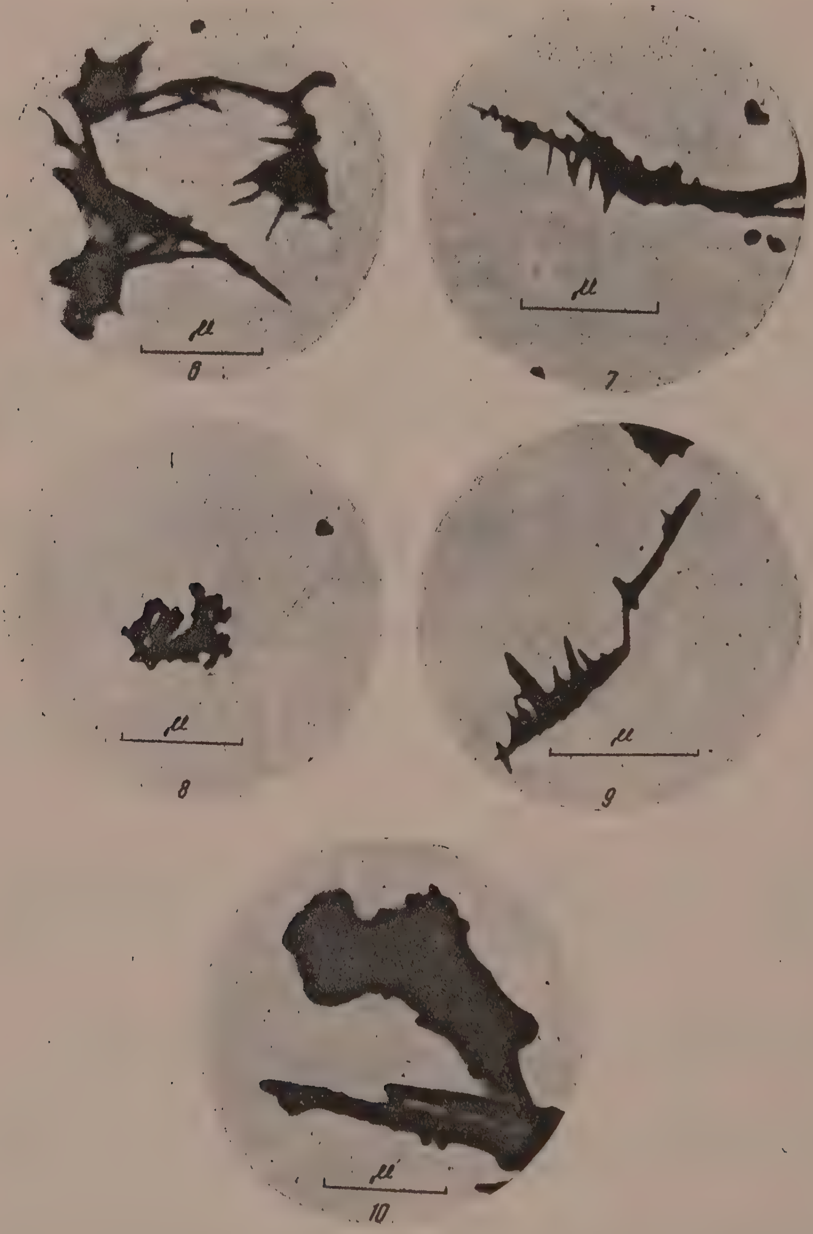

Electron micrographs of the disperse phase of organosols: 6) alloy of Pb: Sn = 48.8; 51.2%, D_c = 15 amp./dm^2, 7) alloy of Pb: Sn = 72; 28%, D_c = 15 amp./dm^2, 8) alloy of Pb: Sn = 23.: 77%, D_c = 30 amp./dm^2, 9) alloy of Pb: Sn = 44.5; 55.5%, D_c = 10 amp./dm^2, 10) alloy of Pb: Sn = 19.8; 80.2%, D_c = 10 amp./dm^2.

With increasing tin content in the electtolyte solution the β-Sn lines on the x ray diagrams become more prominent. Increase of current density causes a weakening of th β-Sn lines, and at 30 amp./dm^2 these lines disappear completely because of the increased degree of dispersion of the tin deposits.

Composition of Cathode Deposits of Lead and Tin Alloys at Different Current Densitites and Component Ratios in the Lower Electrolyte Layer

Atomic Pb : Sn ratio in electrolyte	D_c amp./dm^2	% composition of deposit	
		Pb	Sn
1 : 7	10	16.4	83.6
	15	12.6	87.4
	20	6.0	94.0
	30	5.5	94.5
1 : 3	3	46.1	53.9
	5	40.0	60.0
	10	36.4	63.6
	15	14.7	85.3
	20	12.0	88.0
	30	12.0	88.0
1 : 2	3	71.4	28.6
	5	63.7	36.3
	10	44.5	55.5
1 : 2	15	30.0	70.0
	20	22.0	78.0
	30	23.0	77.0
1 : 1	3	70.0	30.0
	10	60.0	40.0
	15	48.8	51.2
	20	40.7	59.3
	30	30.0	70.0
3 : 1	3	79.5	20.5
	10	75.0	25.0
	15	72.0	28.0
	20	69.3	30.7
	30	61.5	38.5

In the production of metal organosols by the electrolytic method [1], hydrogen is copiously evolved at the cathode. It was therefore desired to investigate whether it enters into the metal lattices, in particular of lead. The (331) and (420) lines were used to calculate the lattice parameter for lead. The measurements were performed by means of sliding calipers, from the centers of the lines (measurement accuracy was ± 0.05 mm). Arithmetic averages of five measurements were taken for the calculations. The value found for the crystal lattice parameter of pure lead was 4.938 A. This is in good agreement with literature data for very pure lead [5]. Thus, it is confirmed once again [2,6] for alloy organosols that when loose (disperse) metal deposits are formed at the cathode, nonequilibrium solid solutions by incorporation of hydrogen into the metal lattice are not formed.

Our investigations showed that the size of the "blocks" (primary crystallites) of lead in lead–tin alloys remains constant under different conditions of electrolysis (salt concentrations and cathode current density). This is an exception to the general rule (see [6]) and is applicable only to loose cathodic deposits of lead and its alloys, at which hydrogen is evolved at a considerable overvoltage. The average "block" size for all the organosol alloys was 308 A.

SUMMARY

1. Electron microscope investigations showed that the disperse phase particles in lead organosols have a dendritic structure, and the tin particles are of indefinite form and of amorphous structure. It is therefore possible to follow, by means of the electron microscope, the course of formation of the colloidal particles of alloys of these metals under various conditions.

2. For a given atomic ratio of lead to tin in the electrolyte, increase of cathode current density favors simultaneous deposition of these metals in the form of an alloy.

3. At a given current density and different lead–tin atomic ratios in the electrolyte, alloy formation depends on the quantitative proportions of the components. Relative increases of the tin content favor alloy formation.

4. X-ray investigations showed that, when lead and tin are simultaneously deposited on the cathode from two-layer electrolytes, a eutectic alloy is formed. The crystal lattice parameter of lead in the alloys is

4.938 A. The size of the primary crystals ("blocks") in the alloys does not vary with the cathode current density or the ratio of the metals in the electrolyte, and has a value of 308 A.

LITERATURE CITED

[1] E. M. Natanson, Mem. Inst. Chem. Acad. Sci. Ukrainian SSSR 7, 311 (1940); Colloid J. 9, 191 (1947); Trans. All-Union Conf. Colloid Chem.*, (Acad. Sci. USSR Press, 1952), p. 113.

[2] V. P. Chalyi, Bull. Acad. Sci. USSR, Phys. Ser. 17, 195 (1953); V. P. Chalyi and E. M. Natanson, Colloid J. 18, No. 1, 127 (1956).*

[3] Landolt-Börnstein, Tabellen, T. 1 (1923), p. 581.

[4] W. C. Phebus, F. C. Blake, Phys. Rev. 25, 107 (1925); G. S. Zhdanov and Ya. S. Umansky, X-ray Crystallography of Metals, II (State United Sci.-Tech. Press, Moscow-Leningrad, 1938), p. 372. **

[5] B. F. Ormont, Structures of Inorganic Substances (State-Tech. Theoret. Press, Moscow-Leningrad, 1950), p. 334. **

[6] V. P. Ghalyi and S. P. Rozhenko, Summaries of Papers at the 5th All-Union Conference on the Use of x-rays for Investigation of Materials (Leningrad, 1955), p. 45.

Institute of General and Inorganic Chemistry
Acad. Sci. Ukrainian SSSR

Received May 29, 1956

---

* [Original Russian pagination. See C. B. Translation.]
** [In Russian.]

PRODUCTION OF TITANIA–SILICA GELS AND THEIR POROUS STRUCTURE

I. E. Neimark, A. I. Rastrenenko, and M. A. Piontkovskaya

Silicate catalysts occupy a prominent position in organic synthesis and the petroleum industry. It has been conclusively shown [1] that the productivity, activity, and often even the selectivity of a catalyst depends considerably on the character of its porous structure. Therefore the rational utilization of catalysts is directly related to the problem of producing them with the desired microstructure.

Processes of gel and porous structure formation have been studied in greatest detail for silicic acid gels [2]. It has been shown that the porous structure of silica gels is determined by the aging, washing, and drying conditions. Advances in the question of formation of a porous structure in silica gels have made it possible to approach the problem of developing methods for the production of optimum porous structures in gels of technically important hydroxides; these include titania–silica gels. Little work has been done on methods for regulating the porous structure of titania–silica gels during their formation, or on production of gels with a given porous structure. The only information available in the literature relates to the production of titanium catalysts by application of titanium dioxide to already prepared silica gels. For example, Graeber and Cryder [3] have described the production of titania–silica gels by application of titanium tetrachloride in paste form to prepared silica gels. These authors did not study the structural characteristics of the titania–silica gels.

The object of the present investigation was to develop methods for producing titania–silica gels of various structural types and to test the possibility of extending the main concepts of the mechanism of porous structure formation in silica gels to these more complex systems.

Methods for the production and investigation of porous structures in titania–silica gels. Titania–silica gels were prepared by simultaneous precipitation of the respective components. The hydrogels were suitably treated to give titania–silica gels with the required porous structure. The treatment was so designed that the main chemical composition did not vary from specimen to specimen in a given series of catalysts. The starting materials were: water glass of 2.7 ratio, sulfuric acid solution, and titanium dioxide or titanium hydroxide prepared from titanium tetrachloride.

Certain factors which might influence the structure of titania–silica gels were studied, namely: pH of the wash water, drying temperature, nature of the intermicellar liquid, etc. The intermicellar liquid in the hydrogels was replaced by n-butyl or isobutyl alcohols, i.e., liquids which do not dissolve the mixed gel components and which have much lower surface tension than water.

Intermediate structure types were also prepared by a combined method, in which the hydrogels were first dried and then treated with alcohols. In this way micropores were produced in the structure in addition to a considerable volume of larger pores.

By variations of the temperature conditions in drying the hydrogels and alcogels, and in the preliminary drying before replacement of water by alcohols in the hydrogels, and also by variations of the pH of the wash waters, we were able to obtain specimens differing in specific surface, total pore volume, and nature of porosity in each series of gels. Four series of titania–silica gels with different titanium contents were prepared.

Production of titania–silica gels of Series I. Titanium dioxide in the form of a fine powder was added to sulfuric acid (d = 1.18) and made into a fine suspension by means of vigorous stirring for several hours. After this, without interruption of the stirring, a water glass solution with a density of 1.18 g/cc was carefully added to the mixture. The respective proportions of sulfuric acid, water glass, and titanium dioxide were: 1 volume, 2.15 volumes, and 12.5 g/liter. The mixture was warmed to 50° to accelerate coagulation. When syneresis commenced, the hydrogel mass was cut into 1.5-2 cm pieces and divided into two portions: one was washed with acidified tap water at pH 3.5 (Specimen T-1), and the other, with ammoniacal water at pH 8 (Specimen T-2). After washing to remove salts, part of the hydrogel washed with ammoniacal water was treated with isobutyl alcohol and dried at 250° (Specimen T-3).

Production of titania–silica gels of Series II. A silicic acid sol was prepared by mixing one volume of sulfuric acid (d = 1.18) with 2.15 volumes of sodium silicate solution (d = 1.18) with vigorous stirring; to this was added a previously prepared suspension of TiO_2, to give 15 g of dry titanium dioxide per 1 liter of the sol. The mixture was then warmed to 75° with uninterrupted stirring, when coagulation ensued. The coagulated mass was cut into 1.5-2 cm pieces and washed with distilled water to remove salts. After being washed by decantation, the hydrogel mass was divided into four portions for subsequent treatment. One portion was dried at room temperature immediately after the washing (Specimen T-21), the second was dried at 200° (Specimen T-22), and the third was treated with n-butyl alcohol at the boil. Complete replacement of the hydrogel water by butyl alcohol was confirmed by the refractive index of the condensate. The product was dried at 200° (Specimen T-23). Finally, the fourth portion of the washed hydrogel was dried at room temperature for 15 days. The dried gel was treated with n-butyl alcohol, then dried at room temperature for 20 days and at 150° for 4 hours (Specimen T-24).

Production of titania–silica gels of Series III. The original hydrogel mass for production of titania–silica gels of Series III was made by the same method as for Series I. The main difference between the two series was the titanium dioxide content, which in Series III was based on a content of 30 g of TiO_2 per liter of the original silicic acid sol. Specimen T-11 was prepared by drying the hydrosol at room temperature for 20 days and then for 6 hours at 200°. Specimen T-13 was obtained from the hydrogel which was washed, treated with n-butyl alcohol, dried at 100° for about 2 hours, and then at 200° for 3 hours. To remove traces of alcohols, the dried gel was heated at 500° for 1 hour. The hydrogel from which Specimen T-14 was prepared was dried for 6 days at room temperature, treated with n-butyl alcohol, then dried at room temperature for 25 days and finally at 150° for 4 hours. Traces of alcohol were removed at 500° for 1 hour.

Production of titania–silica gels of Series IV. The specimens of this series were prepared by simultaneous precipitation. Different volumes of $Ti(OH)_4$ suspensions were added with vigorous stirring to equal volumes of a silicic acid sol prepared by the usual method. The stirring was continued to coagulation. The mixed gel was aged for 24 hours, then cut into 1.5-2 cm pieces and divided into two portions: one was washed with tap water at pH 7.5, and the other with distilled water at pH 6.0. The washed hydrogels were dried at 160°.

Methods of adsorption and structure determination. The porous structure of the titania–silica gels was characterized by determinations of the total pore volume from the difference between the reciprocals of the apparent and true densities, by study of the adsorption isotherms for methyl alcohol vapor at 20°, determined with the aid of vacuum apparatus with a spring quartz balance, and by calculations of the specific surfaces and effective pore sizes. For additional clarity, the adsorption isotherms were converted into differential adsorption isotherms [4].

Structural and adsorption characteristics of titania–silica gels; results and discussion. The structural characteristics of the titania–silica gels are given in Table 1.

Figures 1 and 2 show the adsorption isotherms and pore radius distributions for the specimens of Series I. The data in Table 1 and the adsorption isotherms show sharp differences between the pore structures of different specimens of this series. The lowest capacity was found for Specimen T-1; its isotherm shows only a slight hysteresis loop, indicating that the intermediate pore volume is small and that micropores predominate.

Specimen T-2 has greater capacity and its isotherm shows a large hysteresis loop. The largest pores were found in Specimen T-3; its porosity was nearly 9 times that of the finely porous Specimen T-1. The distribution of the intermediate pore volume by effective radius (Fig. 1) and differential adsorption isotherms (Fig. 2) give a clear picture of the character of the porous structure of titania–silica gels of Series I: Specimen T-1 is homogeneously microporous, with predominant pore radius < 10 A, while Specimen T-2 has a larger average radius, ~30 A. The average pore radius for Specimen T-3 is in the range 60-70 A.

The preparation conditions of T-1 and T-2 titania–silica gels differed by the use of wash waters of different pH. The dried Specimen T-2, washed with alkaline water at pH 7.5, had larger pores than Specimen T-1, washed with water at pH 6. This agrees with data obtained earlier for silica gels [5].

Replacement of hydrogel water in Specimen T-3 by a liquid of low surface tension resulted in the formation of a very coarsely porous specimen; this is also in good agreement with the influence of the same factor on the structure of silica gels [5].

TABLE 1

Structural Characteristics of Titania–Silica Gels

Series	Specimen	Apparent density in g/cc	Total porosity in cc/g	Maximum sorptive capacity in cc/g	Specific surface in m^2/g	Predominant pore radius in A
I (10% TiO_3)	T-1	1.29	0.33	0.36	465	<10
	T-2	0.78	0.84	0.82	260	30
	T-3	0.30	2.89	2.80	400	65
II (13% TiO_2)	T-21	1.39	0.28	0.33	645	<10
	T-22	1.24	0.37	0.38	686	15
	T-23	0.41	2.0	2.04	652	45
	T-24	0.62	1.17	1.18	625	40
III (22% TiO_2)	T-11	1.32	0.34	0.34	539	<10
	T-12	1.28	0.36	0.38	598	<10
	T-13	0.38	2.21	2.20	598	45
	T-14	0.07	0.51	0.52	569	15
IV (4,6% TiO_2)	T-3^d	1.28	0.34	0.34	696	<10
	T-3^b	0.82	0.76	0.77	580	17.5

The structure and adsorption characteristics of titania–silica gel specimens of Series II are illustrated by the data in Table 1 and Figs. 3 and 4. These data show that the specimens in this series, prepared under different conditions, differ considerably in porous structure. The adsorption and desorption isotherms for methyl alcohol are given in Fig. 3. The volume distribution curves for the intermediate pores by effective radius show that Specimen T-23 has the greatest effective pore radius (~ 40 A), and Specimen T-22 has the least (~ 15 A) (Fig. 3). The figure does not show the curve for the pore distribution by radius for the most finely porous Specimen T-21; its pore size lies in the < 10 A region.

Differential isotherms for titania–silica gels of Series II are given in Fig. 4. As already stated, Specimens T-21 and T-22 differed in the temperature at which the hydrogel was dried; the first was dried at room temperature and the second at 200°. The adsorption and desorption branches of the isotherms for Specimen T-21 coincide over the whole range of relative pressures, while the isotherm for Specimen T-22 shows a hysteresis loop, indicating that some of the pores in this specimen are of the intermediate type. The porosity differences between Specimens T-21 and T-22 arose in consequence of the different contracting action exerted by the capillary forces on the gel skeleton during drying, as the difference between the surface tensions of the intermicellar liquid (water) at 18 and 200° is more than 20 dynes/cm. In consequence the hydrogel dried at room temperature was more finely porous than the hydrogel dehydrated at 200°.

Replacement of the water in the hydrogel by n-butyl alcohol, as in the specimens of Series I, gave Specimen T-23, with a very high adsorptive capacity. Preliminary drying followed by replacement of water by alcohol gave T-24, with a lower capacity. The curves for the volume distribution of the intermediate pores by effective radius also differ for the two specimens. The maximum on the curve for T-24 lies further in the direction of smaller radii. The explanation for the change in the porous structure of Specimen T-24 is probably that the hydrogel shrank somewhat during the preliminary drying. The subsequent treatment with n-butyl alcohol halted the shrinkage.

The conditions for the preparation of titania–silica gels of Series III were similar to those for Series II. The difference lay in the different contents of titanium dioxide in the specimens. The structural and adsorptive characteristics of these specimens, given in Table 1 and Figs. 5 and 6, indicate that the structure relationships found in titania–silica gels of Series II apply also to the specimens of Series III with other titanium dioxide contents.

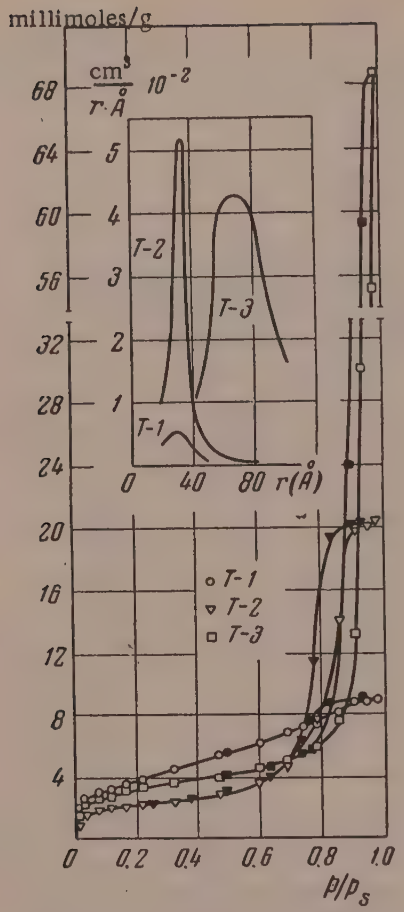

Fig. 1. Isotherms for adsorption of methyl alcohol vapor on titania–silica gel specimens of Series I; black points represent desorption; curves for the volume distribution of intermediate pores by effective radius are shown at the top.

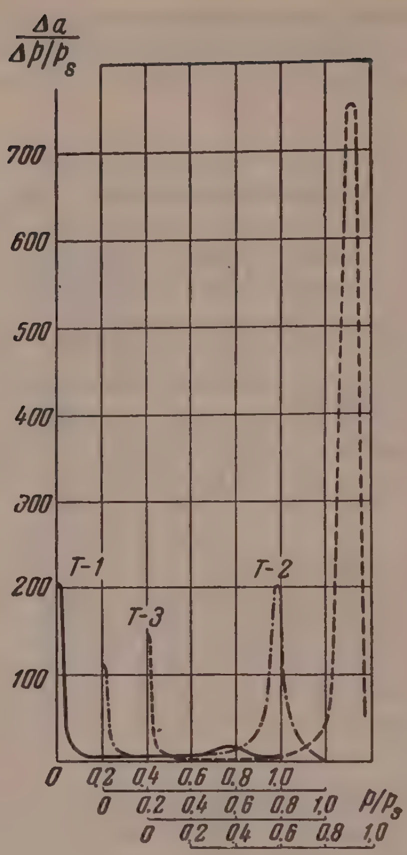

Fig. 2. Differential adsorption isotherms for titania–silica gel specimens of Series I.

The structural characteristics of Specimens T-3^d and T-3^t, washed with water of different pH, differ sharply (Table 1 and Fig. 7). The titania–silica gel washed with water at pH 6.0 is microporous. The isotherm for methyl alcohol adsorption does not show a hysteresis loop. The specimen washed with water at pH 7.5 has larger pores. The isotherm for this specimen has a considerable hysteresis loop.

It is interesting to note that titania–silica gels containing different amounts of titantium dioxide but prepared under the same conditions are almost identical in structure.

Figure 8 shows isotherms for adsorption of methyl alcohol vapor on titania–silica gels with different titanium dioxide contents but washed and dried under the same conditions. It is seen from Fig. 8 that the adsorption isotherms for these specimens practically coincide. The reason is probably the similarity of the chemical and hydrophilic properties of silica and titania.

It was important to determine the influence of some of these factors on the structure of titania gels. The influence of the intermicellar liquid and drying temperature on the porosity of titania gels was studied. Figure 9 gives isotherms for adsorption of methyl alcohol vapor on titania gels, the intermicellar liquid in which was water (Specimen 880^d) and n-butyl alcohol (Specimen 890), respectively. Figure 9 shows that replacement of hydrogel water by a liquid of low surface tension leads to formation of specimens with very large pores.

Increase of the drying temperature, which leads to a decrease of the surface tension of the intermicellar liquid, also results in formation of more coarsely porous gels (Table 2).

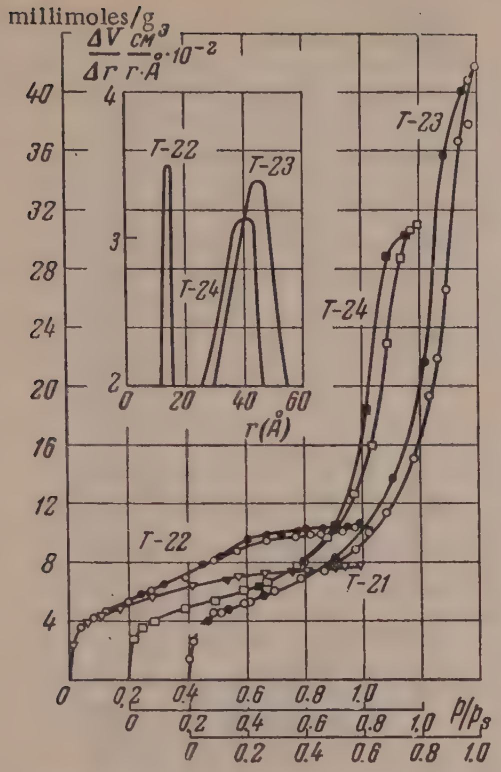

Fig. 3. Isotherms for adsorption of methyl alcohol vapor on titania–silica gel specimens of Series II; black points represent desorption; curves for the volume distribution of pores of effective radius are shown at the top.

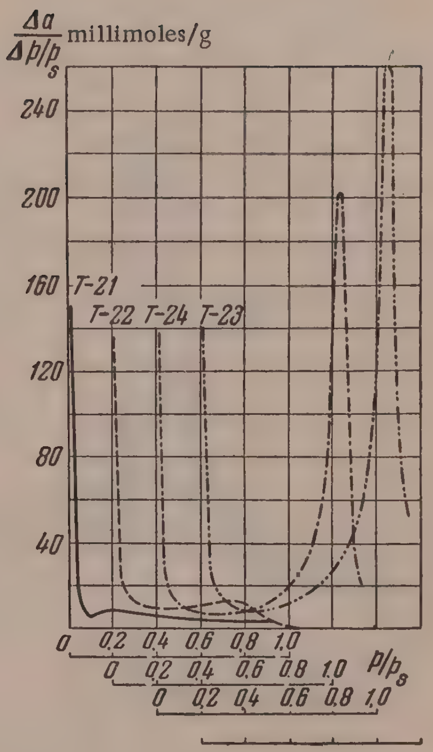

Fig. 4. Differential adsorption isotherms for titania–silica gel specimens of Series II.

These results indicate that the relationships found earlier for the effects of various factors on the structure of silica gels [2, 5, 6] are also applicable to titania–silica gels and titania gels. It is probable that the pore formation mechanism is similar for silica, titania–silica, and titania gels.

TABLE 2

Effect of Drying Temperature on the Structure of Titania Gels

Drying temperature in °C	Apparent density in g/cc	Total pore volume in cc/g	Volume of benzene adsorbed from saturated vapor in cc/g
20	1.78	0.25	0.28
140	1.48	0.38	0.38

An alkaline medium favors ion exchange between the gel hydrogen and the cations of the medium, whereby the bonds between the gel particles and water are weakened, which results in accelerated aggregation of the particles into longer chains and clusters. The framework becomes more rigid and less compressible during drying, and in consequence more coarsely porous titania–silica gels are formed. A weakly acid medium hinders ion exchange, the gel framwork remains hydrophilic and elastic, and this gives a denser packing of the particles when the hydrogels are dried. Decrease of the surface tension of the intermicellar liquid and the associated decrease of capillary forces always leads to formation of coarsely porous specimens.

We have been able to vary the porous structure of titania–silica gels within wide limits on the basis of the theory of the formation of porous structure in silica gels.

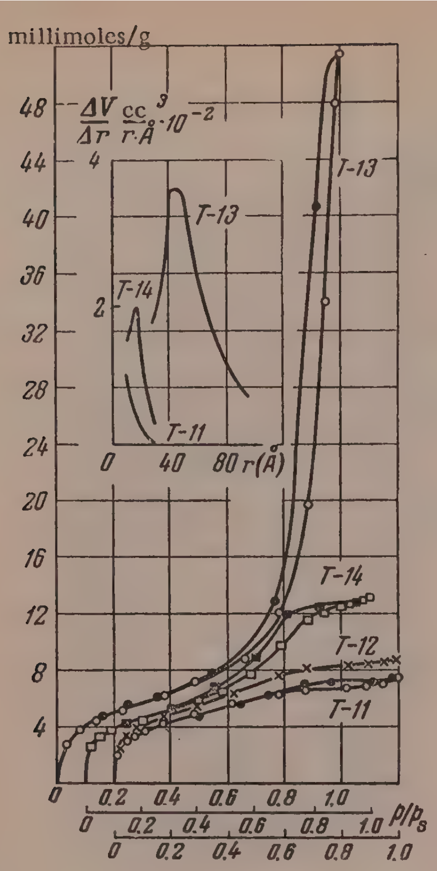

Fig. 5. Isotherms for adsorption of methyl alcohol vapor on titania–silica gel specimens of Series III; black points represent desorption; curves for the volume distribution of the intermediate pores by effective radius are shown at the top.

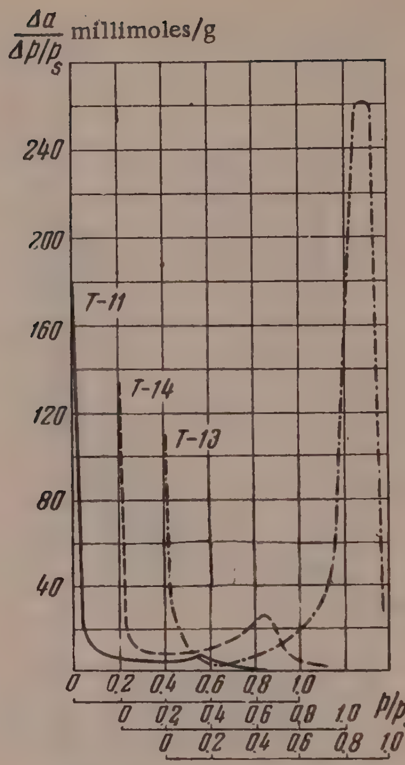

Fig. 6. Differential adsorption isotherms for titania–silica gel specimens of Series III.

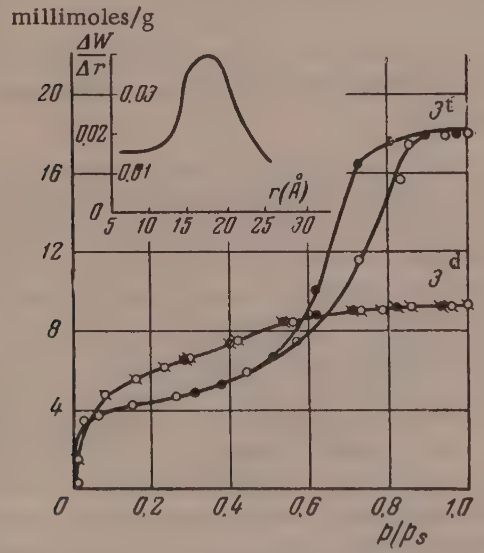

Fig. 7. Isotherms for adsorption of methyl alcohol vapor on titania–silica gels of Series IV; black points represent desorption; curves for the volume distribution of the intermediate pores by effective radius are shown at the top.

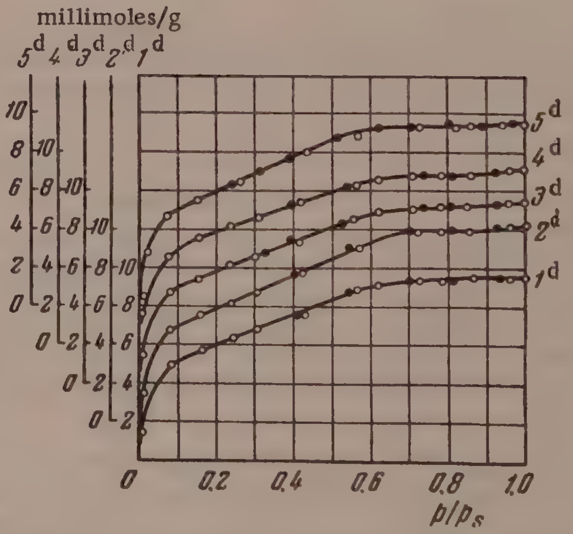

Fig. 8. Isotherms for adsorption of methyl alcohol vapor on titania–silica gels with different titanium dioxide contents; black points represent desorption; 1^d) 2.3% TiO_2; 2^d) 3.4%; 3^d) 4.6%; 4^d) 5.6%; 5^d) 6.7% TiO_2.

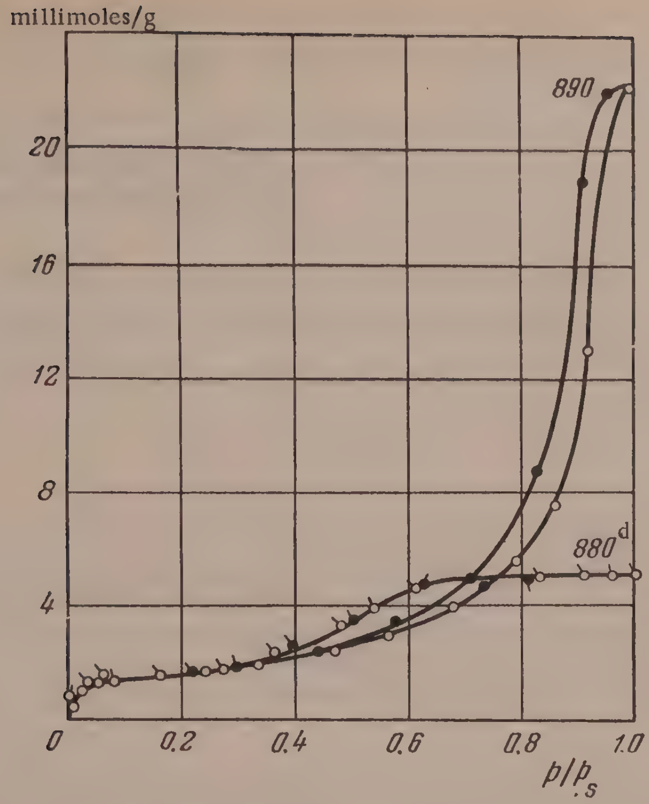

Fig. 9. Isotherms for adsorption of methyl alcohol vapor on titania gels 880^d and 890; black points represent desorption.

SUMMARY

1. Specimens of titania–silica and titania gels of different porous structures have been prepared and their adsorptive and structural properties have been studied in detail.

2. It is shown that the structure and adsorptive properties of titania–silica gels depend on the preparation conditions and are independent of the titanium content (up to 22% TiO_2).

3. On the basis of the parallel influence of preparation conditions on the nature of the porous structure in silica, titania–silica, and titania gels it is shown that our theory of the mechanism of structure formation in hydrophilic adsorbents is applicable to titania gels.

4. Methods have been developed for preparing titania–silica gels with a required porous structure over a wide range of total porosity (from 0.3 to 2.2 cc/g).

LITERATURE CITED

[1] G. K. Boreskov, Chem. Ind. 221 (1947); 257 (1947); I. E. Neimark and R. Sheinfain, J. Phys. Chem. 23, 595 (1949); G. K. Boreskov and V. A. Dzisno, J. Phys. Chem. 24, 1135 (1950); I. E. Neimark, Trans. All-Union Conf. on Catalysis, Kiev (Acad. Sci. Ukr. SSR Press, 1950); I. E. Neimark and L. Kh. Freidlin, Bull. Acad. Sci. USSR, Div. Chem. Sci. No. 3, 311 (1951).

[2] I. E. Neimark, Trans. Commission on Analytical Chemistry 6 (IX) (Acad. Sci. USSR Press, 1955) p. 77; Progr. Chem. No. 6 (1956).

[3] E. G. Graeber and D. S. Cryder, Ind. Eng. Chem. 27, 828 (1935).

[4] V. G. Bykov, Bull. Acad. Sci. USSR, Div. Chem. Sci. No. 6 (1951).

[5] I. E. Neimark and R. Yu. Sheinfain, Colloid J. 15, 145 (1953).*

[6] I. E. Neimark and R. Yu. Sheinfain, Colloid J. 15, 45 (1953).*

Received June 11, 1956

The L. V. Pisarzhevsky Institute of Physical Chemistry,
Acad. Sci. Ukrainian SSR, Kiev

---

* [Original Russian pagination. See C. B. Translation.]

PHASE EQUILIBRIA IN COLLOID SYSTEMS

1. SEPARATION OF A HOMOGENEOUS SOLUTION INTO TWO PHASES AND THE GEL FORMATION PROCESS

S. P. Papkov

Attention was drawn in an earlier paper [1] to the need for a more detailed examination of cases in which equilibrium is established slowly in colloid systems. This is all the more necessary as it is often wrongly concluded that colloidal systems do not obey the phase rule owing to the low rates at which equilibria are established. Moreover, as the result of these low rates the true equilibrium picture is obscured by secondary processes. This is seen especially clearly for such colloid systems as gels. In the present communication an attempt is made to consider gel formation as a specific instance of the separation of a system into two phases, on the assumption that the phase rule is fully obeyed.

General scheme of gel formation. If the equilibrium in a one-phase two-component system is displaced so that the system passes through the critical compatibility point of the components, separation into two phases takes place. The separation passes through the following successive stages: a) formation of nuclei of the new phase; b) growth of these nuclei; c) coalescence of the particles of the new phase owing to the tendency to decrease the interphase to a minimum; and finally, d) hydrostatic (mechanical) equilibrium, as the phases are usually of different densities.

Each of these stages has its own characteristics which depend on the equilibrium composition and physical properties of the coexisting phases. Accordingly the time for complete equilibrium to be established will also differ for different systems.

When gas—liquid or liquid—liquid (with both liquids of low viscosity) phases are formed, the time required for the establishment of complete equilibrium (with respect to the composition and mechanical) is usually short. Completely separated macrophases with a minimum interphase area are formed.

The situation is somewhat different when a liquid solution separates into two phases with formation of a crystalline phase. The time required to reach equilibrium may be relatively long, depending on the number of active centers of crystallization (impurities or spontaneously formed crystal nuclei), and coalescence of the particles of the crystalline phase is generally limited, since natural recrystallization (or crystal growth) depends on the difference of vapor pressures (or solubilities) over crystals of different size. This difference is vanishingly small for large crystals. Therefore systems with crystalline phases are regarded as being practically equilibrium systems even if a microcrystalline precipitate is formed. Hydrostatic equilibrium is usually established comparatively rapidly.

In systems in which the separating phases are amorphous and not crystalline the position is quite different. Such systems include not only most solutions of high polymers, but many solutions of substances of low molecular weight. The peculiar nature of phase separation in such solutions often leads to formation of imperfectly separated systems, with highly disperse phases, with consequent specific physicochemical properties. Such systems are justifiably considered as a separate domain, included in colloid chemistry.

For a clearer picture of the structure of colloids formed in the separation of a one-phase multicomponent system, and for derivation of certain conclusions concerning their specific physicochemical properties, it is necessary to examine in detail the phase separation process leading to formation of amorphous phases in such a system.

Coexisting amorphous phases (in equilibrium with respect to composition) are mutual solutions of the components, differing in concentration. We may arbitrarily call one of the phases a solution of Component B in Component A, and the other a solution of A in B. Restricting ourselves to a consideration of only a particular group of condensed systems, we will for convenience term the substance which has the properties of a solid at normal temperatures Component B, and the substance which has the properties of a liquid (the "solvent") Component A. We shall term a solution of B in A Phase I, and a solution of A in B, Phase II.

In contrast to systems which separate with formation of crystalline phases, Phase II in amorphous systems is never 100% Component B, but contains some Component A in a state of equilibrium. It is important to note that the physical properties of this phase may vary considerably according to the ratio of the components in it. This applies, in particular, to viscosity. At viscosities above 10^{10} poises this phase will have the properties of a solid (it will be brittle under stresses of relatively low frequency). At lower viscosities the second phase is a liquid; i. e., it will change its shape under its own weight in a time comparable with the usual duration of an experiment.

The composition and the corresponding physical properties of Phase II to a great extent determine the course of phase separation in a system, and its structure in incomplete hydrostatic equilibrium. As a rule, Phase I has very low viscosity differing little from the viscosity of Component A ("solvent"), since in most of the systems with which we are concerned the concentration of Component B in it is very low. Therefore Phase I has little influence on the structural characteristics of separating systems.

Let us consider the process of phase separation in greater detail. In the first instant after the change in the parameters of the system (transition through the critical point of total miscibility of the components) nuclei of the new phases are formed. Here attention must be drawn toa point which has generally been neglected. Hitherto, as a rule, the separation only of the "solid" phase (Phase II) from the nonequilibrium solution has been considered. In various investigations [2] the rates of formation and growth of particles of the "precipitated" substance (Component B) have been studied on the assumption that the nonequilibrium solution becomes poorer in Component B as the separation proceeds, and gradually reaches an equilibrium concentration. In this view, the concentration of Component B in the nonequilibrium solution at any instant in the course of precipitation represents the difference between the original amount of Component B and the amount of it present in the "solid" phase formed. However, there are no grounds for assuming that simultaneous separation of equilibrium Phase I does not occur simultaneously, so that the nonequilibrium solution becomes poorer in Component A. Indeed, if formation of stable nuclei of Phase II is possible owing to fluctuation processes, formation and further growth of Phase I nuclei is equally justifiable. These two routes are equivalent from the energy aspect, since either can independently lead to the formation of two equilibrium phases. Therefore we must start with the assumption that displacement of the equilibrium leads to the simultaneous formation of nuclei of Phases II and I.

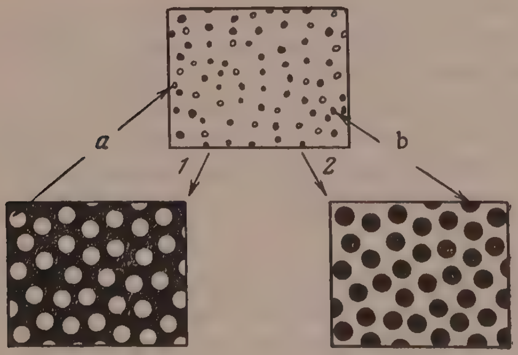

Fig. 1. Separation of a homogeneous solution into two phases. a) Phase I, b) Phase II; 1) growth rate of Phase I nuclei predominates; 3) growth rate of Phase II nuclei predominates.

The next stage is the growth of the nuclei, and the rates of such growth may differ for the two phases. The growth rate of the nuclei depends on many factors, an especially prominent role being played by the mobility of the molecules of the substance which predominates in the composition of the given phase. The greater the difference between the molecular weights of Components A and B, the more probable it is that the Phase I nuclei will grow at the greater rate, since this phase consists mainly of Component A of low molecular weight (the solvent). Certain experimental data lead to the same conclusion.

A system undergoing separation into two phases can be likened to an emulsion, in which the "emulsion medium" is the nonequilibrium solution, and the "emulsified particles" are spherical particles of the new phases. These particles gradually grow, while the volume of "emulsion medium" (the nonequilibrium solution) gradually decreases.

Depending on the relative rates of growth of the particles, the "emulsion medium" (the nonequilibrium solution) will become richer either in Component B or in Component A, gradually approaching the composition of one of the equilibrium phases. For example, if particles of Phase I grow more rapidly, the nonequilibrium solution will become richer in Substance B. When equilibrium with respect to composition is reached, Phase II will have been formed mainly by enrichment of the nonequilibrium solution (emulsion medium) by Component B rather than by growth of its nuclei. The concentration of this, formerly nonequilibrium, solution coincides when equilibrium concentration is reached with the concentration of the particles of the slowly growing phase, and a homogeneous medium is formed, surrounding isolated spherical particles of the rapidly growing phase. Two variants of phase separation of a system are shown schematically in Fig. 1.

The course of the hydrostatic separation and subsequent coalescence of the disperse phase particles will depend on which of the phases is disperse. If both phases are of low viscosity, a completely separated system with a single interface is formed relatively rapidly. If the disperse phase is solid (viscosity greater than 10^{10} poises), a suspension is formed which does not form a continuous layer even on settling, while at very high degrees of dispersion it constitutes a colloidal sol with all its characteristic properties (adsorption processes at the interphase).

In our opinion, the greatest interest attaches to the case in which the disperse phase is a liquid, and the dispersion medium is a solid (with viscosity greater than 10^{10} poises). In such a case a solid continuous framework is formed, consisting of Phase II and containing isolated microregions of liquid Phase I. Both the geometrical form of the microparticles and consequently of the "walls" of the framework, and the physicomechanical properties of the whole system, will vary according to the volumes of the coexisting phases.

If the volume of Phase II (solid) is greater than the volume of Phase I (liquid), Phase I will consist of spherical inclusions separated by thick partitions of Phase II, while the physicomechanical properties of the whole system will differ little from the properties of continuous Phase II. If the volume of Phase II is very small compared with the volume of Phase I, the most probable geometrical configuration of Phase I particles is polyhedral, while the structural "skeleton" consisting of Phase II will resemble a honeycomb structure. This gives a system which is very interesting in its physicomechanical properties, with its framework consisting of thin "walls" of homogeneous composition. Such thin layers of solids, as is known, are capable of elastic bending. With a true elastic deformation of the thin "walls" not exceeding 1-2%, as for any continuous system the total deformation of such a system can reach very high values owing to elastic bending.

Unfortunately, little is known about the mechanics of such systems, consisting of solid thin formations (films, fibers) with very low densities of the substance ("loose" solid systems). Nevertheless, the number of such systems found in practice is very large (paper, leather, cotton, etc.). All these materials behave as "high-elastic" systems at low loads and can undergo large reversible deformations considerably exceeding the elastic deformations of continuous materials.

If, in the separation of a multicomponent solution, the solid phase forms a structural "skeleton" consisting of thin films, the result is a limiting example of a lamellar superelastic system. Such systems are known in colloid chemistry as gels. This mechanism for the formation of gel systems can be extended both to gels of low molecular, including inorganic, substances, and to gels formed by high polymers. Each of these classes has its own specific characteristics, and they are therefore considered separately below.

Gels of low molecular substances. One of the specific characteristics of substances of low molecular weight is their tendency to crystallization. Therefore, before we consider concrete examples of gel formation in inorganic low molecular substances, it is necessary to present briefly certain principles concerning the relationship between crystalline and amorphous equilibria. This is necessary because, as was shown in the preceding section, the gel formation mechanism is based on separation of a homogeneous solution into two amorphous phases.

It is known that many substances are deposited from solution not as crystals but as amorphous formations. Weimarn [2] at one time held the view that external distinctions between the forms in which a solute was deposited are determined only by the degree of dispersion of the crystalline substance. However, Weiser and his associates [3] carried out a series of x-ray investigations of precipitates, in which it was shown that the transition from an amorphous to a crystalline precipitate often requires a long time, sometimes measured in years. After the series of detailed investigations made by Berestneva and Kargin [4] there is no longer any doubt that, at least for sparingly soluble compounds which give rise to colloid systems, primary formation of amorphous particles is characteristic; these particles are subsequently converted into crystalline formations at rates which depend on the nature of the components and the experimental conditions.

It may be assumed that the amorphous and crystalline state are separated by an energy barrier, the magnitude of which determines the practical probability and rate of transition from an amorphous to a crystalline precipitate. This view was put forward in relation to pure substances by Kobeko [5]. It can undoubtedly be extended to multicomponent systems such as amorphous precipitates deposited from solutions.

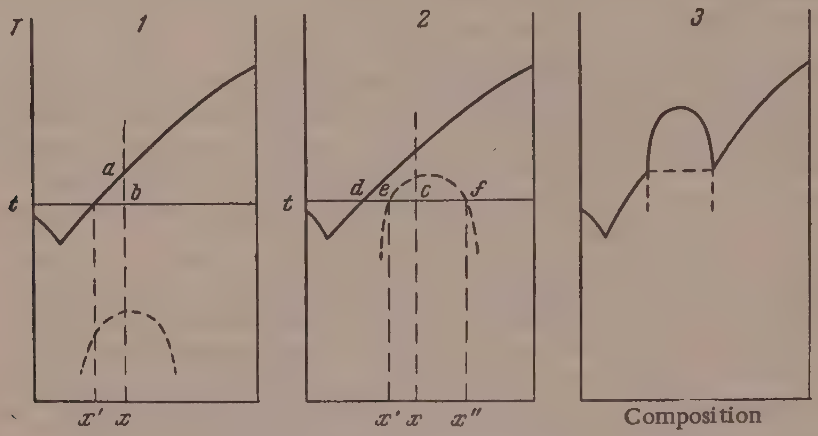

Fig. 2. Crystalline and amorphous equilibrium diagrams.

However, the existence of a potential barrier between the two states in itself indicates that separation of a substance in amorphous form when a one-phase two-component system separates into two phases leads to formation of equilibrium phases such that their composition does not in principle depend on the possibility and rate of a further transition to another equilibrium state with a lower energy level (crystal—solution). Thus, the potential energy minimum of the system, corresponding to amorphous equilibrium, should not depend on the second minimum, which characterizes crystalline equilibrium. This principle of the mutual independence of the two types of equilibrium forms the basis of all the subsequent discussion.

Let us now consider the general equilibrium scheme for a two-component condensed system (with the vapor phase ignored) on the assumption that the rates of transition from one equilibrium state to the other are determined by not very small activation energies of such transitions. In Fig. 2 three variants are given of the relative positions of the curves for crystalline and amorphous equilibrium on composition—temperature diagrams. To simplify the picture, we shall consider only cases in which the crystal—solution equilibrium is not complicated by formation of intermediate molecular compounds.

Figure 2,1 represents the case in which the curve for the equilibrium separation of a two-component solution into amorphous phases lies considerably below the curve for separation into a crystalline phase and a solution over it. If a solution of composition x is cooled, saturation is reached at the point a. Below this point the solution is supersaturated with respect to the crystal-solution equilibrium. For example, at room temperature t (point b) such a solution separates into a crystalline phase consisting of 100% B and a saturated solution of B in A, the composition of which is represented by x'. The rate of this separation is determined by the rates of formation and growth of the crystal nuclei. Amorphous phases cannot be formed at the point b, as the amorphous equilibrium curve lies considerably below the room temperature region and the system is "unsaturated" with respect to such equilibrium. Systems of this kind include many aqueous solutions of highly soluble inorganic salts (sodium chloride, potassium chloride, etc.) and also numerous organic substances of low molecular weight dissolved in organic solvents.

In Fig. 2,2 the amorphous separation curve lies close to the crystal—solution equilibrium curve. When a solution of composition x is cooled down to temperature t, or when substance B is formed, say by an exchange reaction in solution, the system reaches the point c. The solution, supersaturated with respect to crystalline equilibrium, is also supersaturated to amorphous equilibrium. If the potential barrier between the two states is large enough, two stable amorphous phases are formed, with equilibrium compositions x' and x" (Phase I and Phase II).

The "life" of these phases may vary. If the viscosity of Phase II is very high, the rate of crystallization in it may be very low and transition to the crystalline state will occur mainly in Phase I with subsequent gradual crystallization of substance B at the peripheries of the particles in Phase II.

As regards the physical form of the demixing of the system, the considerations in the first section of this paper are applicable. Rapid growth of particles of Phase I leads to formation of a cellular structure, the "framework" of which consists of Phase II, richer in Component B; i. e., a gel is formed. If the total concentration of Component B in the system is very low, the continuous gel structure breaks down and an amorphous "precipitate" is formed, the particles of which are nevertheless of gel form. Similar breakdown of the gel occurs under mechanical action on the system (stirring, convection currents, etc.). These particles, irrespective of the plasticity of Phase II or, more accurately, of the plasticity of the solution which is nonequilibrium at the start of the separation and which approaches Phase II in composition, may assume a rounded shape under the action of surface tension forces; in our opinion this is confirmed by the electron micrographs of precipitates obtained by Shekhter, Roginsky, and Sakharova [6] and similar micrographs given in the papers by Berestneva and Kargin [4].

The lack of quantitative experimental data on amorphous equilibrium curves in the literature is primarily explained by the exceptional difficulties encountered in analysis of the precipitates. Therefore we shall illustrate this type of equilibrium only by certain data reported by Weimarn [2], relating to the water–barium sulfate system. Weimarn gradually increased the initial concentrations of salts forming $BaSO_4$ by a double decomposition reaction, and observed the following characteristic types of precipitation. At very low concentrations of $BaSO_4$, lying within the range of its solubility in water in contact with a crystalline precipitate, a stable aqueous solution is formed (up to the point d on the normal temperature line, see Fig. 2,2). Further increase of concentration leads to formation of a crystalline precipitate, corresponding to the concentrations in the range d–e. At yet higher concentrations (region e–f), the precipitate is no longer crystalline but amorphous, which takes the form of a continuous gel on further increase of concentration, as the "walls" of the gel are already strong enough mechanically. This region corresponds to the region in which the system separates into equilibrium amorphous phases. The relevant data reported by Weimarn are given in the table.

Effect of Total $BaSO_4$ Concentration on the Form of the Precipitate
(After Weimarn [2])

Normality	Form of precipitate
$5 \cdot 10^{-5}$–$1.4 \cdot 10^{-4}$	No precipitate formed in course of a year
$1.4 \cdot 10^{-4}$–$1.7 \cdot 10^{-3}$	Slow precipitation
$1.7 \cdot 10^{-3}$–0.75	Crystalline precipitate
0.75–3.0	Rapid formation of amorphous precipitate
3.0–7.0	Transparent gel

These data do not reflect the exact positions of the transition points for the $BaSO_4$ system, but nevertheless the general type and sequence of the transitions in this system conform completely to the diagram in question.

It is likely that for most systems which form sparingly soluble precipitates the crystalline and amorphous equilibrium curves lie close together. At least, gel structures are formed in hydroxides, sulfates, carbonates, and sulfides of multivalent metals. As is shown by the data of Berestneva and Kargin [4], vanadium pentoxide also first forms an amorphous precipitate; this is fully confirmed by the ease with which this substance forms gels. Efremov [7] observed gel formation in the separation of vanadium pentoxide in instances in which crystallization could not proceed far; this also provides indirect evidence that gel formation is directly related to amorphous deposition.

The third type of relative position of the curves for crystalline and amorphous equilibrium (Fig. 2,3) does not lead to formation of more or less stable colloid systems, as the amorphous separation region lies above the fusion curve and this leads to rapid separation of the liquid phases with formation of macroregions of both phases. A well-known example of such a system is the system water–isovaleric acid.

Characteristics of gel formation in high polymer systems. The concept of high polymer gels as imperfectly separated systems, consisting of two equilibrium phases, the honeycomb structural skeleton being formed by the phase with high viscosity, has been discussed earlier [8]. Therefore in the present paper we shall consider only certain characteristics of high polymer gels as compared with gels of substances of low molecular weight.

The main peculiarities of high polymers are the low kinetic mobility of their molecules and their complex configuration. The consequence of the first of these is that the amorphous equilibrium curve is sharply displaced into the region of low concentrations of the polymer, and in many actual instances Phase I may be regarded as the pure solvent. Nevertheless, it constitutes an equilibrium phase, containing a definite if small amount of the high polymer. This is clearly seen in experiments on the osmotic effects of swelling. This fact also provides the basis for high polymer fractionation when the system approaches the upper critical point of complete mutual solubility, at which the high polymer concentration in Phase I becomes quite appreciable. An example of phase equilibrium in high polymers is provided by the previously studied [9] equilibrium in the system acetal cellulose–chloroform.

Because of the high molecular weights of high polymers, Phase II in a separated system is highly viscous and its properties approach those of a solid even at relatively high concentrations of the "solvent" in it. Therefore hydrostatic equilibrium and coalescence of microregions of the phases are generally reached slowly, and gels are therefore formed exceptionally frequently. In fact, as has already been pointed out (see, for example, [1]), instances of liquid coacervation are very rare cases of equilibrium in high polymers.

A consequence of the complexity of configuration of polymeric macromolecules is that the rates of transition of the amorphous into the crystalline phase are so low that the crystalline state is realized exceptionally rarely. The view is advanced in the paper cited earlier [9] and in a number of papers by Kargin and his associates that for many high polymers it is the amorphous and not the crystalline state which is the state of true equilibrium in many high polymers. This view is quite admissible if the complexity of the spatial configuration of certain high polymers with large side chains is taken into account. Regular packing of such macromolecules may be less favorable from the energy aspect than a random disposition. However, even for high polymers for which the ordered state corresponds to lower values of free energy, the activation energy of the transition to an ordered arrangement of the molecules is so high that equilibrium becomes established between the amorphous phases without intervention of the crystallization process. The question of the relationship between the crystalline and amorphous state of high polymers in general should be specially examined. We shall only point out here that the crystalline (ordered) high polymer structures obtained by the action of mechanical forces (stretching) and formed in the course of natural synthesis of the polymer cannot be regarded as more favorable than the amorphous state from the energy aspect.

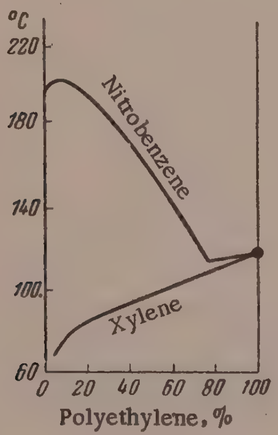

Fig. 3. Equilibrium diagrams for polyethylene with xylene and nitrobenzene (after Richards).

For high polymers with monomer units of simple structure the energy barrier is relatively low, and such polymers crystallize not only from solution but also in the solid state. A good example of this is provided by polyethylene.

It is evident that the relationships between the amorphous and crystalline states represented in Fig. 2 are also applicable to systems containing high polymers. Figure 2,1 corresponds to the case in which the region of amorphous separation into two phases lies in the very low temperature region. Here crystalline equilibrium ought to be attained first. However, polymers which crystallize with difficulty traverse the equilibrium curve without change of the phase state. In the case of deeper cooling, down to the region of amorphous phase separation, separation into two amorphous phases is preceded by vitrification of the system, which makes phase separation impossible in practice. Separation in accordance with Fig. 2,1 may be realized only for crystalline high polymers, as is shown by the behavior of polyethylene in xylene, studied by Richards [10].

Figure 2,2 probably represents the behavior of systems of the type gelatin–water, acetylcellulose–benzyl alcohol, starch–water, etc., i. e., systems in which gel formation occurs in the range of normal temperatures. The true position of the crystalline equilibrium curves for such systems cannot be determined owing to the impossibility of crystallization in practice.

The systems represented by Fig. 2,3 have been studied little, since many high polymers do not melt without chemical decomposition. This applies, at least, to most polymers which have polar groups and are difficult to crystallize. An example of such a system with an easily crystallizable polymer – polyethylene – is provided by the system with nitrobenzene as "solvent," which was also studied by Richards [10].

Richards' data are reproduced in Fig. 3; it is seen that the system polyethylene–xylene corresponds to the case shown in Fig. 2,1 and the system polyethylene–nitrobenzene to the case shown in Fig. 2,3.

In conclusion it must be pointed out that high polymer gels have another important characteristic ; their high deformability may be caused not only by peculiarities in their physical structure (a lamellar system with "elastic walls") which is also found in gels of low molecular substances, but also by the flexibility of the macromolecules. It is known that polymers such as rubber have high elasticity owing to the possibility of more or less free rotation about the individual valency bonds in the chain molecule. Thus, when a mechanical force is applied to a high polymer gel, two mechanisms of elastic extension are superposed. For the polymers described as "rigid" the predominant mechanism is deformation of a lamellar system, while in "flexible" polymers, especially under large loads, the predominant deformation is that caused by straightening of the macromolecules which are coiled when in the equilibrium state.

Calculation of the extension obtainable in the gel model described in this paper shows that the maximum extension is 157% relative to the initial length. In practice the extension at break is considerably less than this. At the same time, rubber-like polymers may show reversible extensions of several hundred per cent.

Therefore it would not be correct to attempt to explain the high elasticity of rubber solely on the assumption that it has a two-phase structure, just as it is not correct to ignore the mechanism of deformation of a lamellar structure for cases in which the system is in a state of imperfect separation into two phases, i. e., when it is in the gel state.

SUMMARY

1. On the principle that the two forms of equilibrium – crystalline and amorphous – are mutually independent, the mechanism of separation of a two-component system into two amorphous phases and of gel formation is considered.

2. A gel is defined as a system with imperfect or uncompleted phase separation, consisting of two phases in equilibrium with respect to composition. One of these phases, which approximates to a solid in its properties, forms a continuous framework which includes isolated regions of the other phase (of low viscosity).

3. The special characteristics of the formation of gels and gel-like precipitates in low molecular (mainly inorganic) substances and in high polymers are discussed.

4. The distinction between the elasticity of gels and the high elasticity of rubber-like polymers is noted.

LITERATURE CITED

[1] S. Papkov, Colloid J. 18, 72 (1956). [Original Russian pagination. See C. B. Translation].

[2] P. Weimarn, J. Russ. Chem. Soc. 38, 263, 466 (1906); 47, 4133 (1915); M. Volmer, Kinetik der Phasenbildung (Dresden-Leipzig, 1939).

[3] See H. B. Weiser, Inorganic Colloid Chemistry, v. 2, 3 (N. Y., 1934) p. 8.

[4] Z. Berestneva and V. Kargin, Progr. Chem. 24, 249 (1955).

[5] P. Kobeko, Amorphous Substances (Acad. Sci. USSR Press, Moscow-Leningrad, 1952).

[6] A. Shekhter, S. Roginsky, and S. Sakharova, Bull. Acad. Sci. USSR, Div. Chem. Sci. 205 (1948).

[7] I. Efremov, Colloid J. 16, 264 (1954). [Original Russian pagination. See C. B. Translation].

[8] S. Papkov, J. Phys. Chem. 18, 546 (1954).

[9] S. Papkov, V. Kargin and Z. Rogovin, J. Phys. Chem. 10, 607 (1937).

[10] R. B. Richards, Trans. Faraday Soc. 41, 127 (1945); 42, 10 (1946).

Received March 27, 1956

Moscow

INVESTIGATIONS OF THE STRUCTUROMECHANICAL PROPERTIES OF ETHYLCELLULOSE SOLUTIONS AND THE EFFECT OF OXIDATION ON THESE PROPERTIES

T. I. Samsonova and L. V. Ivanova-Chumakova

Ethylcellulose – the cellulose ether formed by the reaction of ethyl chloride with alkali cellulose – has good resistance to the effects of low temperatures and to chemical attack by alkalies, salt solutions, and water. However, if it is subjected to the action of oxygen, especially at elevated temperatures, ethyl cellulose is oxidized and develops considerable brittleness. Comparisons of the properties of different grades of ethylcellulose and of changes caused by oxidation are important owing to its very extensive use in industry. In addition to studies of the chemical changes which occur in the oxidation of ethylcellulose [1, 2] and determinations of molecular weight and its distribution [3], considerable interest attaches to investigations of the structuromechanical properties of its solutions, which characterize intermolecular interaction.

The usual method [4] for determination of tensile strength and maximum deformation of films gives sharply different results for oxidized and unoxidized ethylcelluloses, but does not reveal differences in the properties of original unoxidized samples of different degrees of substitution, probably because this method provides a better measure of the bond strengths in the molecular chains than of the intensity of intermolecular interaction. By the methods for studying the mechanical properties of dissolved substances used in the present investigation it is possible to detect differences between the original samples.

The solutions were prepared from two commercial grades of ethylcellulose, K and NI, corresponding to different degrees of hydroxyl group substitution (with ethoxyl group contents of 44.5% for K and 48.5 for NI), but with the same intrinsic viscosity $[\eta] = 2.3$ and average molecular weight of the order of $66 \cdot 10^3$. As the presence of mineral impurities has a great influence on the properties of ethylcellulose, especially in solution [5, 6], the commercial ethylcellulose samples were purified by passage of the dilute solutions through purified active carbon followed by precipitation of the ethylcellulose. The ethylcellulose samples were oxidized by the action of heat in a stream of oxygen: NI at 120° for 3 hours 20 minutes to an intrinsic viscosity $[\eta] = 1.3$ and average molecular weight $41 \cdot 10^3$ (ethoxyl content 46.9%), to give NI of the first degree of oxidation, while to obtain a higher degree of oxidation with $[\eta] = 0.6$ and average molecular weight $25 \cdot 10^3$ (ethoxyl content 35.5%) it was heated at the same temperature for 5 hours, giving NI of the second degree of oxidation.

Ethylcellulose grade K was oxidized by the action of heat at 125° for 2 hours 15 minutes, to give $[\eta] = 0.87$; the average molecular weight was $27 \cdot 10^3$ (ethoxyl content 41.5%).

The solvents used for making the ethylcellulose solutions were benzyl alcohol (η = 0.056 poise) and dibutyl phthalate (η = 0.206 poise). Benzyl alcohol is a good solvent for all grades of ethylcellulose; moreover, its volatility is low (b. p. 205.4°), which simplifies its use for filling the liquid seal in the instrument [7].

Because of the low volatility of dibutyl phthalate (b. p. 340°) and the total absence of any film formation on the surface of its solutions after prolonged exposure to air, such solutions could be studied without steps being taken to protect them against evaporation.

The elasticoviscous properties of the ethylcellulose solutions were studied in a rotational instrument with small coaxial cylinders, described in a previous paper [7]. The concentration ranges were from 3 to 10% in dibutyl phthalate, and from 5 to 18.5% in benzyl alcohol. All the experiments were performed at 22.2° ± 0.2.

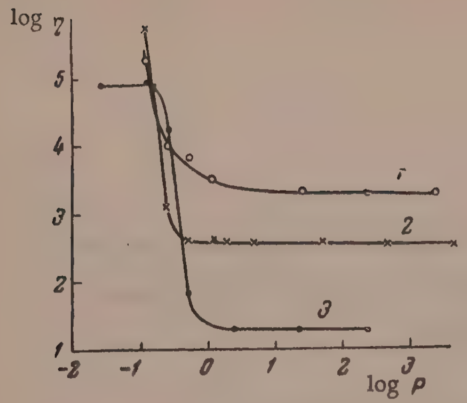

Fig. 1. Variation of effective viscosity with stress for 18.5% solutions of NI ethylcellulose in benzyl alcohol at 22.2°: 1) NI, η_m = 1900 poises; 2) NI of the first degree of oxidation, η_m = 320 poises; 3) NI of the second degree of oxidation, η_m = 9 poises.

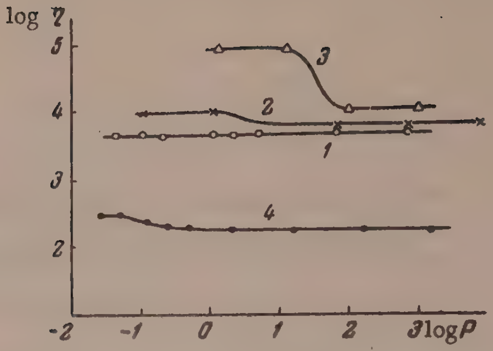

Fig. 2. Variation of effective viscosity with stress for 18.5% solutions of K ethylcellulose in benzyl alcohol at 22.2°: 1) in the first week of aging, $\eta = 4.3 \cdot 10^3$; 2) the same solution after two weeks of aging; 3) the solution after one and a half months of aging; 4) oxidized K, η = 125 poises.

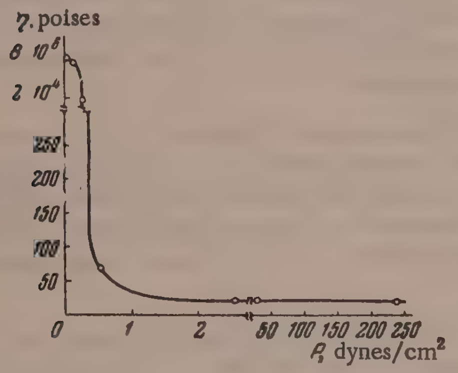

Fig. 3. Variation of effective viscosity with stress for 18.5% solution of NI ethylcellulose, of the second degree of oxidation, in benzyl alcohol at 22.2°.

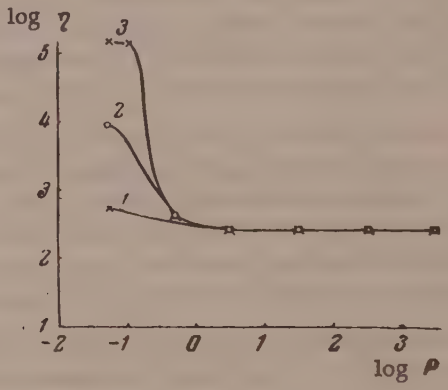

Fig. 4. Variation of effective viscosity with stress for 10% solution of K ethylcellulose in benzyl alcohol at 22.2° after aging for: 1) one day, 2) two days, 3) three weeks.

Measurements were made both of the kinetics of the growth and decrease of the deformation on application and removal of small stresses by rotation of the upper end of the dynamometer thread through a certain angle, and of the equilibrium stresses established in the flowing systems when the outer cylinder was rotated by means of a motor. These measurements were used to plot curves for the variations of effective viscosity in steady flow with the acting stress; these are shown in Figs. 1, 2, and 3 for 18.5% solutions of ethylcellulose in benzyl alcohol. Other concentrations of the same ethylcellulose samples (for example, 10% of K, and 5 and 10% of NI), because of their high fluidity, proved to be less suitable for studies of this relationship, but the results for these in general confirm the other findings. The data presented show that there is a very sharp difference between the behavior of low-substituted (K) and high-substituted ethylcellulose solutions.

The first striking feature is the very different decrease in the viscosities of NI and K ethylcellulose solutions with increase of stress over a certain narrow range: for NI, from $\eta_0 = 1.7 \cdot 10^5$ to $\eta_m = 1.9 \cdot 10^3$ poises (Fig. 1, Curve 1), i. e., by a factor of about 100; and for K, from $\eta_0 = 9.3 \cdot 10^3$ to $\eta_m = 5.8 \cdot 10^3$ poises (Fig. 2, Curve 2), which is less than a two-fold decrease. The similar viscosities at the lower ends of the curves show that the properties of both types of systems become similar after structural breakdown, but the structural buildup during preliminary rest differs. Studies of the changes in the properties of the solutions during prolonged standing in the instrument showed that in the case of NI ethylcellulose, and especially of its oxidation products, maximum structure develops in a relatively short time (~ 2 days), as indicated by constant and high viscosity values, while solutions of K ethylcellulose do not show any significant structural changes in the same period of time. This is convincingly shown by the course of Curve 1 (Fig. 2), all the points on which ($\eta = 4.4 \cdot 10^3$ poises) were obtained for the same sample in the course of one week. Repeated experiments on the same sample after 2 weeks, with small stresses of up to 1 dyne/cm^2 revealed the formation of some additional structure, corresponding to an increased viscosity $\eta = 9.3 \cdot 10^3$ poises.

Together with the data obtained after the sample had been held for one and a half months in the instrument (Fig. 2, Curve 3; $\eta_0 = 7.8 \cdot 10^4$), this shows that structure formation also occurs in solutions of K ethylcellulose, but much more slowly than in NI ethylcellulose. With 10% of K ethylcellulose in the solution (Fig. 4) this process is no longer as slow, probably because of the freer movement of the molecular segments in the less concentrated solution. Curves 1, 2, and 3 (Fig. 4) correspond to different aging times of the samples in the instrument before the start of the experiment, and they show that viscosity in flow with undestroyed structure becomes 17 times as high even on the second day (from $\eta_0 = 5.0 \cdot 10^2$ to $\eta_m = 8.8 \cdot 10^3$ poises), and after 20 days it reaches $1.4 \cdot 10^5$ poises. The fact, revealed by these investigations, that structure buildup in 18.5% solutions of NI ethylcellulose is completed in not more than two days, while in K ethylcellulose it does not develop to any appreciable extent in the same period, was taken into account in studying the characteristics of each individual system (Figs. 1, 2, 3). This is particularly important because each such series of tests was performed on the same sample, kept for a long time in the instrument, since it was not possible either to change the sample before each experiment or to stir it. Such stirring would require additional time before the start of our extremely lengthy experiments, for relaxation of the stresses which would arise. Since the stress was removed in all the experiments after the necessary deformation had been developed and the system reached complete equilibrium, the sample could be used for the next experiment. However, if structural breakdown took place, the system was allowed to age before the next experiment. It must also be pointed out that tests at different stresses were always performed in the sequence from smaller to larger stresses. With this procedure the viscosity increases found on the curves cannot be attributed to structural buildup in the system in the course of time.

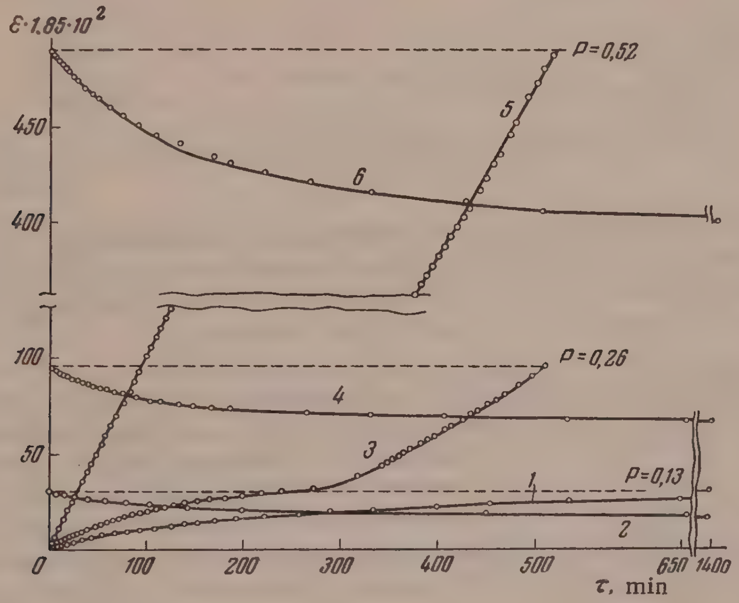

Fig. 5. Increase and decrease of deformations in 18.5% NI ethylcellulose solution in benzyl alcohol at 22.2°: 1,3,5) increase of deformation at stresses P = 0.13, 0.26, and 0.52 dyne/cm^2; 2,4,6) decrease of deformation for the same stresses, respectively.

In addition to this relatively rapid structural buildup and its rapid breakdown in flow under very high stresses, 18.5% solutions of NI ethylcellulose were also found to have structural instability under low stresses. This was shown by the fact that, between low and high stresses, intermediate stresses were found (Figs. 5, 6, Curves 3) at which the properties of the system changed abruptly in the course of the deformation, in the direction of structural breakdown [8]. The two viscosity values, calculated from the flow rates before breakdown and after steady flow has been established in the disrupted structure, coincide with the η(P) curve in the region in which it shows an abrupt, almost vertical drop over a certain fairly narrow range of stresses. Similar breakdown was not found in experiments at higher stresses, but in such experiments the viscosity of the system was close to its lower limit right at the start of the deformation. On the other hand, if stresses below these intermediate values (0.13 dyne/cm^2, Fig. 5 and 0.12 dyne/cm^2, Fig. 6) were used, then changes took place in the system in the course of the experiments which must be attributed to restoration, during flow, of the structure previously broken down to some extent when the external stress was applied. It may be assumed that abrupt application or removal of a stress equally break down the structure to some extent both at the start of loading and at the start of unloading. If the development and decrease of the elastic deformation take approximately the same course, it is possible from the total time for the development of the deformation and the magnitude of the residual deformation to calculate the average rate of true flow, which in such systems is much higher at low stresses than the rate of flow at the end of loading, i. e., after a time greater than the time required for complete dissipation of the elastic deformation. It must be pointed out that the same effect was found in repeated experiments, performed on the same sample after it had been at rest for some time without any preliminary destruction. The reproducibility of the results obtained for any one stress showed that no significant irreversible changes occur in solutions of NI ethylcellulose in the process. Therefore the discrepancy between the true flow rates at the beginning and end of the development of deformation indicates that the structure may have been broken down at the instant the load was applied.

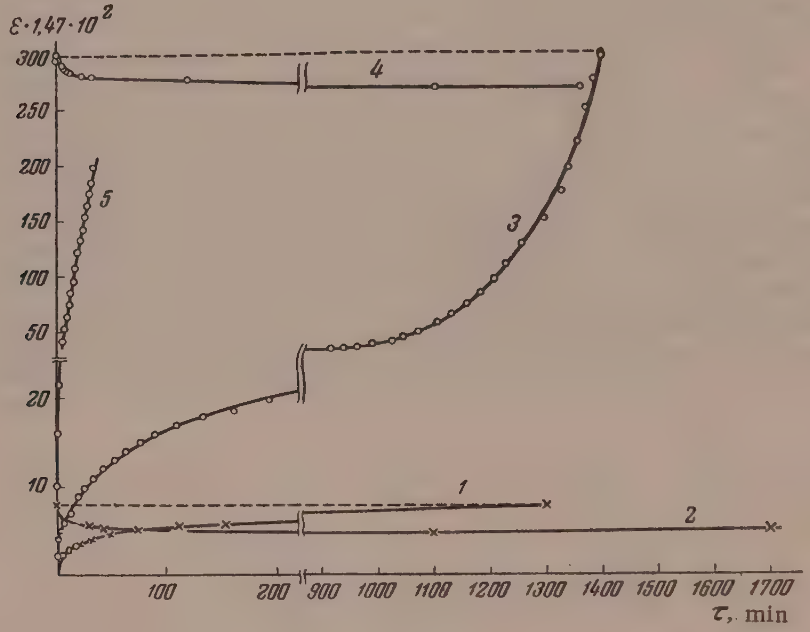

Fig. 6. Increase and decrease of deformation in 18.5% solutions of NI ethylcellulose of the first degree of oxidation in benzyl alcohol at 22.2°: 1,3,5) increase of deformation at stresses P = 0.12, 0.24, and 0.48 dynes/cm^2; 2,4,6) decrease of deformation for the same stresses, respectively.

The data for viscosity calculations in such experiments were based on their final periods, when, after a sharp retardation of the flow rate owing to structure formation in flow, on about the second day of the experiment, a constant flow rate became established, corresponding to a constant time, measured in tens of hours, for displacement by one scale division.

Figures 1 and 2 show that the effective viscosity is much higher for oxidized than the original (unoxidized) ethylcellulose samples, and the minimum viscosity is less for higher degrees of oxidation. This is fully in agreement with molecular weight data [3] indicating that oxidation shortens the chain length. In addition to the lower viscosity limit, η_m = 19 poises, an upper limit, $\eta_0' = 7.8 \cdot 10^4$ poises (Table 1, Fig. 3) was determined for NI ethylcellulose of the second degree of oxidation. For the other samples of NI ethylcellulose only a transition into the high viscosity region was found, but the maximum could not be determined because the low rates of flow already reached (one division per day or longer) did not allow of the use of even lower rates and therefore even longer observation periods.

TABLE 1

Viscosity of 18.5% Solution of NI Ethylcellulose (Second Degree of Oxidation) in Benzyl Alcohol

P, dynes/cm^2	0.026	0.13	0.26	0.52	2.55	23.67	239.2
$\frac{d\varepsilon}{d\tau}$, sec^{-1}	$0.33 \cdot 10^{-6}$	$0.18 \cdot 10^{-5}$	$0.15 \cdot 10^{-4}$	$0.77 \cdot 10^{-2}$	0.1239	1.239	12.395
η, poises	$7.8 \cdot 10^4$	$7.2 \cdot 10^4$	$1.7 \cdot 10^1$	67.5	20.6	19,2	19.1

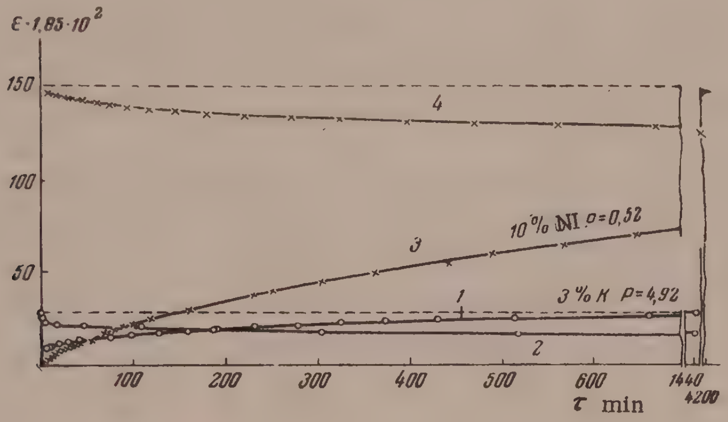

Fig. 7. Increase (1, 3) and decrease (2, 4) of deformation in solutions of ethylcellulose in dibutyl phthalate at 22.2°: 1,2) 3% solution of K ethylcellulose, stress P = 4.92 dynes/cm^2; 3,4) 10% solution of NI ethylcellulose, stress P = 0.52 dyne/cm^2.

The ethylcellulose solutions showed elastic behavior during the unloading part of the experiment; i. e., there were considerable elastic after-effects — a certain decrease of the deformation, as shown in Figs. 5-7. Therefore solution concentrations were chosen [7] at which the deformation would develop and decrease correctly under the experimental conditions used. The optimum conditions were such that, as the solution concentration was increased, a system with an excessively long period of development of elastic deformation should not be obtained, as this would hinder development of the process to completion, but at the same time the degree of molecular interaction in solution should be enough to retard the residual flow to such an extent that it should not greatly obscure the elastic deformation. In a rotational instrument with a dynamometer of the thread type observations of deformation kinetics under constant stress are difficult for systems of low viscosity, as the rapid development of residual deformation makes it impossible to maintain and record the acting stress with a high degree of accuracy. However, the accuracy to which any possible external stresses are removed from the system is important in studying the kinetics of the decrease of elastic deformation. The best conditions are obtained for this if the development of deformation equivalent to 50-100 microscope scale divisions leading to steady flow requires a force provided by rotation of the dynamometer thread (usually the thinnest because of the low concentration) through an angle of not less than 200-300°. This relation between the angle of rotation of the inner cylinder and the thread torsion angle is necessary because any additional twisting [9] may cause errors in determination of the stresses. The magnitude of such an error should not exceed a very small fraction of the given stress. Otherwise it would be difficult, at the end of the fall of deformation, to avoid the action of external stresses giving deformation rates of the same order of magnitude, in addition to the internal elastic after-effect forces in the sample itself.

It did not prove possible to fulfill these optimum conditions satisfactorily in experiments on solutions of different ethylcellulose samples in benzyl alcohol, thereby finding the correct and exact course of the development and decrease of elastic deformation. However, when the solvent was changed to dibutyl phthalate, which resulted in greater interaction between the molecular chains at low concentrations, these conditions were approached, and it proved possible to obtain a fuller and more correct development of the elastic deformation (under strictly constant stress), and also more accurate readings of its decrease, especially at the end of the process.

TABLE 2

Calculation of the Constant k for the Kinetics of Elastic Deformation from Experimental Data on Solutions in Dibutyl Phthalate

3%K; $t = 22°$; $P = 4{,}9$ dynes/cm^2			10% NI $t = 22°$; $P = 0.52$ dynes/cm^2			10% NI $t = 45°$; $P = 0.52$ dynes/cm^2		
Time after unloading min.	Elastic deformation in scale divisions	k in scale divisions in min $\cdot 10^3$	Time after unloading min.	Elastic deformation in scale divisions	k in scale divisions in min $\cdot 10^3$	Time after unloading min.	Elastic deformation in scale divisions	k in scale divisions in min $\cdot 10^3$
0	9	—	0	30	—	0	44	—
48	5	26	7.5	27	21	2	40	9
108	4	21	12	26	23	3.7	33	12
188	3	22	18	25	25	6.1	36	13
303	2	21	26	24	26	7.8	35	13
578	1	23	35	23	27	9.7	34	13
910	0.3	24	46	22	27	11.8	33	13
—	—	—	61	21	27	14.5	32	13
—	—	—	77	20	27	17.5	31	13
—	—	—	95	19	27	21	30	13
—	—	—	119	18	27	25	29	13
—	—	—	148	17	27	29.5	28	13
—	—	—	181	16	26	35	27	13
—	—	—	222	15	26	41.5	26	12
—	—	—	272	14	25	48	25	12
—	—	—	325	13	25	65	23	11
—	—	—	400	12	24	86	21	11
—	—	—	472	11	23	114	19	10
—	—	—	564	10	23	131	18	9
—	—	—	670	9	23	176	16	9
—	—	—	824	8	21	234	14	8
—	—	—	1004	7	20	—	—	—
—	—	—	1234	6	20	—	—	—

Table 2 gives, in accordance with the relationship established previously [10], calculations of the constant k for the kinetics of elastic deformation, based on experimental data for solutions in dibutyl phthalate (Fig. 7),

$$k = -\frac{\varepsilon_m \ln \frac{\varepsilon_e}{\varepsilon_m} + \varepsilon_m - \varepsilon_e}{\tau},$$

where ϵ_m is the maximum value of the elastic deformation for the given stress; ϵ_e is the elastic deformation remaining at a given time instant; τ is the time of decrease of the deformation (recovery time).

As is seen from Table 2, the values of k are satisfactorily constant; for convenient calculation from the available data they are given in Table 2 in terms of microscope scale divisions per time in minutes (scale div./min.$^{-1}$). However, for comparison of the values for different samples and temperatures the average value must be expressed as an absolute quantity, and also reduced to a stress of 1 dyne/cm^2 [10].

The formula for this conversion is

$$a = \frac{k \cdot 0{,}54 \cdot 10^{-2}}{60 \cdot P} \left(\frac{\mathrm{cm}^2}{\mathrm{dyne} \cdot \mathrm{sec}}\right).$$

where a is the absolute constant for the development of elastic deformation with time, independent of the stress; $0.54 \cdot 10^{-2}$ is the relative deformation corresponding to one scale division; 60 is the conversion factor to give the time in seconds; P is the stress acting during development of the deformation, in dynes/cm^2.

Conversion of the data in Table 2 gave the values of a given in Table 3. They are in full agreement with the ordinary influence of temperature, resulting in accelerated deformation with increase of temperature, and also with out data on the greater deformability of NI solutions in comparison with K ethylcellulose solutions, as shown, for example, in Fig. 7. The curves in Fig. 7 for 10% solutions of NI ethylcellulose show that, in a given time, considerably greater deformations, both residual and elastic, develop in such solutions than in 3% solutions of K ethylcellulose, despite the fact that the acting stress in the latter case was almost 10 times the stress used in the case of NI ethylcellulose. The probable reason for this difference in properties is that the greater intermolecular interaction in the original K ethylcellulose prevents solvation of the molecular chains by dibutyl phthalate molecules to a greater extent than in NI ethylcellulose [11]. Therefore the length of the free regions of the chain is less in K ethylcellulose, leading to lower deformability.

TABLE 3

Constant a (Independent of the Stress) for Solutions of K and NI Ethylcellulose: Solutions in Dibutyl Phthalate

Solutions in dibutyl phthalate	3% K	10% NI	
Dissolving temperature	22°	22°	45°
a in poises^{-1}	$0.42 \cdot 10^{-6}$	$0.43 \cdot 10^{-5}$	$1.9 \cdot 10^{-5}$

SUMMARY

1. The elasticoviscous properties of ethylcellulose solutions of different degrees of substitution (K and NI) and solutions of oxidized ethylcellulose have been studied.

2. A difference has been found between the rates of structure formation in 18.5% solutions of K and NI ethylcelluloses in benzyl alcohol, resulting in sharply different decreases of the effective viscosities of such solutions, aged for the same periods, over a certain narrow range of stress increases.

3. It is shown that the minimum constant viscosities of such solutions are lower for oxidized than unoxidized samples, and lower for the more highly substituted NI ethylcellulose than for K. This corresponds to the higher molecular weights of K than NI, and of unoxidized than oxidized ethylcelluloses [3].

4. Solutions of ethylcellulose in dibutylphthalate were shown to conform to a relationship previously established [10], by means of which the decrease of elastic deformation with time can be characterized by a single constant.

We offer our sincere gratitude to Academician P. A. Rebinder for valuable advice during discussions of this work, and also to Associate Member of the Academy of Sciences USSR, S. N. Danilov for guidance in selection of the materials.

LITERATURE CITED

[1] L. F. McBurney, Ind. Eng. Chem. 41, 1251, 1256 (1949).

[2] O. P. Kuzmina and V. I. Kurlyankina, Proc. Acad. Sci. USSR 114 (1957).

[3] T. I. Samsonova and S. Ya. Frenkel, Colloid J. 19, 2 (1957).*

[4] P. P. Kobeko, Amorphous Substances (Acad. Sci. USSR Press, 1952).

[5] O. G. Efremova and S. A. Glikman, Sci. Mem. Saratov State Univ. 30, 55 (1952).

[6] E. V. Evans and H. M. Spurlin, J. Am. Chem. Soc. 72, 4751 (1950).

[7] L. V. Ivanova-Chumakova and P. A. Rebinder, Colloid J. 18, 429 (1956).*

[8] A. A. Trapeznikov, Colloid J. 12, 73 (1950).

[9] A. S. Kolbanovskaya and P. A. Rebinder, Colloid J. 12, 194 (1950).

[10] L. V. Chumakova and P. A. Rebinder, Proc. Acad. Sci. USSR 81, 239 (1951); Colloid J. 18, 540 (1956).*

[11] S. M. Lipatov and S. I. Meerson, Colloid J. 12, 2 (1950).

Received November 28, 1956

Institute of Physical Chemistry, Acad. Sci. USSR,
Division of Disperse Systems, Moscow
Institute of High Molecular Compounds, Leningrad

---

* [Original Russian pagination. See C. B. Translation.]

THE THEORY OF FLOW OF PLASTIC DISPERSE SYSTEMS

N. V. Tyabin and G. V. Vinogradov

Numerous flow processes in plastic disperse systems do not directly conform to the Newton and Shvedov–Bingham equations, but a theory of such flow processes has not yet been developed. The lack of such a theory makes impossible even approximate mathematical calculations relating to various deformations of plastic disperse systems in heterogeneous tangential stress fields, to say nothing of flow in the complex stressed state, when normal as well as tangential stresses act on the system.

Experimental viscosimetric data are generally represented in the form of rheological flow curves which show the variation of the average velocity gradient $\overline{D}$ with the shearing stress τ_R at a capillary wall or the inner cylinder in a capillary viscosimeter. As the result of the experimental investigations performed during the last ten years, mainly by Vinogradov, Pavlov, and Sinitsyn, on the flow of plastic disperse systems in capillary and rotational viscosimeters, the nature of the functional relationship $\overline{D} = \varphi(\tau_R)$ for many plastic disperse systems is known over velocity gradient ranges covering 6-8 orders of magnitude. The Weissenberg–Rabinowitsch method, developed for capillary [1] and rotational [2,3] viscosimeters, can be applied to data on the flow of such media in heterogeneous tangential stress fields to calculate the true, characteristic flow curves $D_R = \varphi(\tau_R)$, where D_R is the velocity gradient in a layer of radius R, for example at a capillary wall or at the wall of the cylinder in a rotational viscosimeter. We shall write this last equation in the form: $D = \varphi(\tau)$. The functions $\overline{D} = \varphi(\tau_R)$ and $D = \varphi(\tau)$ can be written in polynomial form, such as

$$\tau = a_0 + a_1 D + a_2 D^{n_2} + a_3 D^{n_3} + \ldots + a_n D^{n_n}, \tag{1}$$

where a_i are constant coefficients and n_i are exponents; $0 < n_i < 1$.

However, the constant coefficients and exponents in this equation have no physical meaning. Substitution of values of the tangential stresses found from this equation into the equation for the motion of a continuous medium gives equations for the flow of the medium, in the form of nonlinear differential equations difficult to solve. It is therefore more convenient first to simplify the equation for the flow of a plastic disperse system; this will simplify considerably the solution of the original differential equations, and therefore also the mathematical calculations necessary for the solution of practical problems of flow of disperse systems.

In order to simplify the equation for the flow of a plastic disperse system, i.e., to reduce it to linear equations of the Newton or Shvedov–Bingham type, we shall first evaluate the deviation of the flow Equation (1) from these equations: $\tau = a_1 D$ or $\tau = a_0 + a_1 D$, following from Equation (1). For a given accuracy E% for the calculation of the tangential stress, we can write that, at a certain velocity gradient $D = D_x$ the nonlinear part of the polynomial (1) will be equal to

$$a_2 D_x^{n_2} + a_3 D_x^{n_3} + \ldots + a_n D_x^{n_n} = \frac{\tau_x E}{100}. \tag{1a}$$

Substituting τ_x from Equation (1) for $D = D_x$, we have the equation

$$a_0 + a_1 D_x + \frac{100 - E}{E} a_2 D_x^{n_2} + \frac{100 - E}{E} a_3 D_x^{n_3} + \ldots + \frac{100 - E}{E} a_n D_x^{n_n} = 0, \tag{2}$$

solution of which gives D_x, which is the velocity gradient to which Equation (1) should be approximated in the form of Shvedov–Bingham equations. We shall term D_x the approximation limit. For $D > D_x$ a plastic disperse system obeys the Shvedov–Bingham law within the given limits of accuracy. If $a_0 \leq \tau_X E/100$, the plastic system flows according to Newton's law $\tau = a_1 D$.

We shall now consider an analytical graphical method for approximation of the flow curve to linear functions or chords in the zone in which $D \leq D_X$. Let the graph for the functional relationship $D = \varphi(\tau)$ over a certain range of values of τ and D be represented by the Curve AB (Fig. 1). Through the points $C(\tau_0 - \Delta\tau_0, D_0)$ and $F(\tau_0 + \Delta\tau_0, D_0)$, where $\Delta\tau_0 = \tau_0 E/100$, we draw the Curves CE and EG, the respective equations for which are

$$D = \varphi_1(\tau) \quad (2) \qquad \text{and} \qquad D = \varphi_2(\tau) \qquad (3)$$

Curves CE and FG determine the error zone CEFG on the graph. In the error zone we can replace any curve by a linear segment without exceeding the permissible error limits. We replace a section of the curve by a chord, drawn tangentially to one of the curves of the error zone, in this instance the Curve CE. The equation of the tangent to the Curve CE at the point $K(\tau_1, D_1)$ passing through the point $F(\tau_0 + \Delta\tau_0, D_0)$, will be:

$$D - D_0 = \varphi_1'(\tau_1)\,[\tau - (\tau_0 + \Delta\tau_0)]. \qquad (4)$$

Simultaneous solution of Equations (2) and (4) gives the coordinates of the point $K(\tau_1; D_1)$. The tangent FM will cut the Curve FG of the error zone at the point $M(\tau_2, D_2)$. By solving Equation (3) and $D_2 - D_0 = \varphi_1'(\tau_1)[\tau_2 - (\tau_0 + \Delta\tau_0)]$ simultaneously, we find the coordinates of the point $M(\tau_2, D_2)$ as the positive roots of these equations nearest to the values of τ_1 and D_1. We have thus replaced the curve AB by the chord AM in the first region. By drawing a new tangent from the point M to the left curve of the error zone, and finding by an analogous procedure the coordinates of the point of intersection of this tangent with our curve, we obtain a new chord. By continuing this approximation process over the section of the curve from D to D_X we represent it by sections of linear chords, i.e., we replace the functional relationship $D = \varphi(\tau)$ by a set of linear functions $D = \varphi_i(\tau)$, valid over a definite range of tangential stress variations from τ_i to τ_{i+1}.

The equations for the approximated straight lines or the equations for the tangents to the curve CE the error zone may be regarded as equations for the viscoplastic flow of the medium over a definite range of tangential stresses or velocity gradients, or as Shvedov–Bingham equations: $\tau = \theta_i + \eta_i D$, where, as usual, θ_i represents the tangential stresses cut off by extrapolated straight lines along the abscissa axis, which we shall term the maximum shearing stresses, and η_i are the plastic viscosity coefficients (Fig. 1).

The critical values of the tangential stresses at which the Shvedov–Bingham law for the flow changes (i.e., the constants θ_i and η_i change) in consequence of a transition from one flow zone to another we shall term the boundary shearing stresses τ_{0i}. It is evident that the values of τ_{0i} are determined from the condition: when $D_i = D_{i+1}$, $\tau_i = \tau_{i+1} = \tau_{0i}$, and hence

$$\tau_{0i} = \frac{\theta_i \eta_{i+1} - \theta_{i+1}\eta_i}{\eta_{i+1} - \eta_i} \quad (i = 1, \ldots, n-1). \qquad (5)$$

At some definite surface in the flow zone the tangential stresses will be equal to the boundary shearing stresses. In accordance with the foregoing, we shall give the name of the boundary shearing stress surfaces to the surfaces in the flow zone in which the flow law changes. All the flow zone will thus be divided by the boundary shearing stress surfaces into a series of zones, the number of which will be determined by the number of Shvedov–Bingham or Newton equations approximating to the flow equation for the given medium. It must be pointed out that, on the basis of this approximation method, flow may extend over a limited region of the plastic disperse system, and in the rest of the space the medium will be as if in a solid state. The flow zone is separated from the solid zone by a maximum shearing stress surface at which the tangential stress equals the extrapolated value of the maximum shearing stress θ_1. At the boundary and the maximum shearing stress surfaces, the conditions of continuity and equality of the tangential and normal stresses and of the flow velocity components of the medium are satisfied. Thus, the flow of a plastic disperse system will be described by a system of differential equations for the flow of viscoplastic [4] and viscous media.

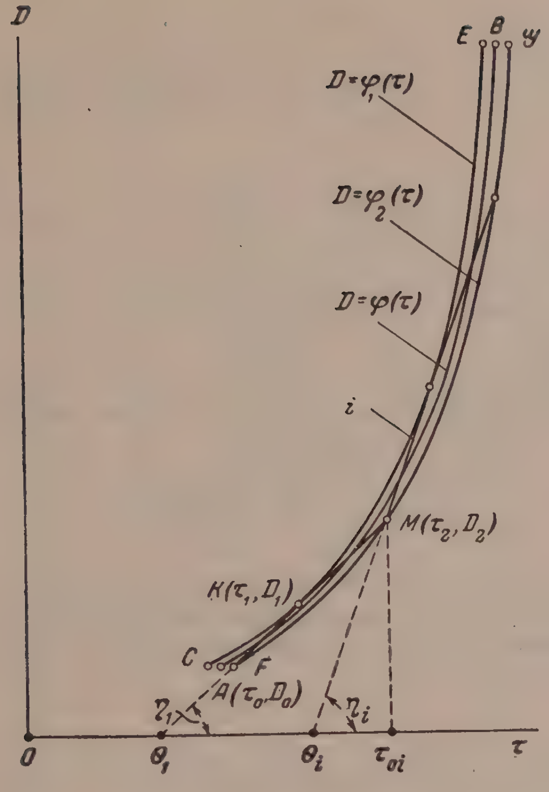

Fig. 1. Approximate representation of nonlinear flow of a plastic disperse system in the form of Shvedov–Bingham equations.

As an application of the proposed method, we shall consider the approximation of the laws of flow for plastic greases, "solidols", the flow of which has been studied by Pavlov [5] in capillary and rotational viscosimeters. The laws for the flow of solidol in a capillary viscosimeter, determined by Pavlov, are given in Table 1, and empirical data for the flow of solidol in a rotational viscosimeter of Pavlov's design are given in Table 2.

Since the experimental data were determined to an accuracy not exceeding 5%, we shall approximate the flow laws with an accuracy of 5%.

Determining the approximation limit of Equation (6) on the basis of Equation (1a), we can write:

$$30\bar{D}_x^{\,1/2} = {}^5/_{100}\,(4\bar{D}_x + 30\bar{D}_x^{\,1/2} + 20).$$

Solving this equation, we find the approximation limit for Equation (6): $\bar{D}_x = 1700$ sec.$^{-1}$; therefore this equation should be simplified in the gradient range from $\bar{D}_0 = 29$ sec.$^{-1}$ to $\bar{D}_x = 1700$ sec.$^{-1}$. When $\bar{D} > D_x$, the flow equation for the medium will be: $\tau_R = 4\bar{D} + 20$. However, when $\bar{D} = \bar{D}_x$, $\theta = 20$ dynes/cm^2 is ~ 0.3 % of the tangential stress, and therefore when $\bar{D} > \bar{D}_x$ solidol (80°) must be regarded as a viscous liquid, the flow equation for which will be: $\tau_R = 4\bar{D}$. For analytical approximation of Equation (6) when $\bar{D} < \bar{D}_x$, we find the equations for the Curves CE and FG of the error zone (Fig. 1):

$$\tau_R = 3{,}83\,\bar{D} + 28{,}8\,\bar{D}^{1/2} + 19; \tag{9}$$

$$\tau_R = 4{,}25\,\bar{D} + 31{,}6\,\bar{D}^{1/2} + 21. \tag{10}$$

TABLE 1

Laws for the Flow of Solidol, Made with Spindle Oil Distillate, in a Capillary Viscosimeter

t° C	Initial values		Final values		Flow equation	Approximation limit $\bar{D}_x$ sec.$^{-1}$	Equation numbers
	$\bar{D}$, sec.$^{-1}$	$\tau_R \cdot 10^{-3}$ dynes/cm^2	$\bar{D}$, sec.$^{-1}$	$\tau_R \cdot 10^{-3}$ dynes/cm^2			
80	29	0.227	11 750	47.7	$\tau_R = 4\bar{D} + 30\bar{D}^{1/2} + 20$	1700	(6)
20	0.083	4.72	1 170	39.4	$\tau_R = 6\bar{D} + 2800\bar{D}^{1/2} + 3500$	—	(7)
–45	0.032	55.6	13	541	$\tau_R = \bar{D} + 2850\bar{D}^{1/2} + 7200$	1920	(8)

Through the initial point of the Curve FG of the error zone, with the coordinates

$$\tau_{02} = 0{,}23 \cdot 10^3 + \frac{\tau_{02} \cdot 5}{100} = 242 \frac{\text{dynes/}}{\text{cm}^2}; \quad D_{02} = 29 \ \text{sec}^{-1}$$

we draw the tangent to the curve represented by Equation (9); from this we find the value of $\bar{D}$, and substitute it into equation (4), so obtaining

$$\bar{D} - 29 = \frac{\bar{D}_1^{1/3}}{3{,}83\,\bar{D}_1^{1/3} + 9{,}6} (\tau_R - 242). \tag{11}$$

We solve Equations (11) and (9) simultaneously to find the coordinate of the point of contact $\bar{D}_1 = 166$ sec.$^{-1}$, and then, from Equation (9), $\tau_1 = 813$ dynes/cm^2.

TABLE 2

Experimental Data for the Flow of Tallow Solidol in Rotational Viscosimeter at 50°

n r.p.m.	D sec.$^{-1}$	$\tau \cdot 10^{-3}$ dynes/cm^2		
		τ_{exptl}	$\tau + \frac{5}{100}\tau$	$\tau - \frac{5}{100}\tau$
0.192	0.47	0.86	0.90	0.82
0.96	2.35	1.69	1.77	1.60
4.8	11.76	2.71	2.85	2.58
24	58.8	3.27	3.43	3.11
120	294	4.76	5.00	4.52
600	1470	7.95	8.34	7.55

The equation to the tangent (11) then becomes:

$$\bar{D} - 29 = 0{,}242 \ (\tau_R - 242). \tag{12}$$

Hence, the Equation (6) for flow of solidol at $\bar{D} < 1700$ sec.$^{-1}$ can be approximated by the Shvedov–Bingham equation (12), which can be written in the usual form as

$$\tau_R = 122 + 4\bar{D}. \tag{12a}$$

Determining the approximation limit of Equation (6) in the form of this Shvedov–Bingham equation, we write the expression:

$$122 = \frac{5}{100} (122 + 4\bar{D}_{x1}),$$

from which we find $\bar{D}_{x1} = 580$ sec.$^{-1}$.

Thus, solidol at 80° flows according to the Shvedov–Bingham law in the velocity gradient region $\bar{D} \leq 580$ sec.$^{-1}$, while in the zone in which $\bar{D} \geq 580$ sec.$^{-1}$ it flows according to the Newton law $\tau_R = 4\bar{D}$. We determine the approximation limit of equations (7) and (8) by a similar procedure. Equation (7) should be approximated over the whole range of $\bar{D}$ and τ_R studied.

A much more convenient and rapid method is the graphical method for approximation to a flow curve in the form of linear portions corresponding to the Shvedov–Bingham law. The graphical approximation can be performed with sufficient accuracy on 3-4 graphs for the relationship $\bar{D} = \varphi(\tau_R)$, plotted on different scales chosen so as to cover the whole flow zone without decreasing the accuracy of the method. Figure 2 shows a graphical approximation of the equation for the flow of solidol in a capillary viscosimeter at 20° (7), on three different scales. Table 3 gives approximation data for Equation (7) in the form of Shvedov–Bingham equations. In this case the Shvedov–Bingham equations will be the equations to the tangents, while the abscissas of the points of intersection of the tangents with the second curve of the error zone will give the boundary shearing stresses. The limits within which the given expression for the Shvedov–Bingham law is valid will be termed the upper and lower boundary shearing stresses and the boundary velocity gradients.

A comparison of the analytically derived expressions for the Shvedov–Bingham equation with the equations obtained graphically shows that they coincide completely. Figure 3 gives the graphical approximation of empirical data on the flow of solidol in a rotational viscosimeter (see Table 2), analyzed by the Weissenberg–Rabinowitsch method [2,3].

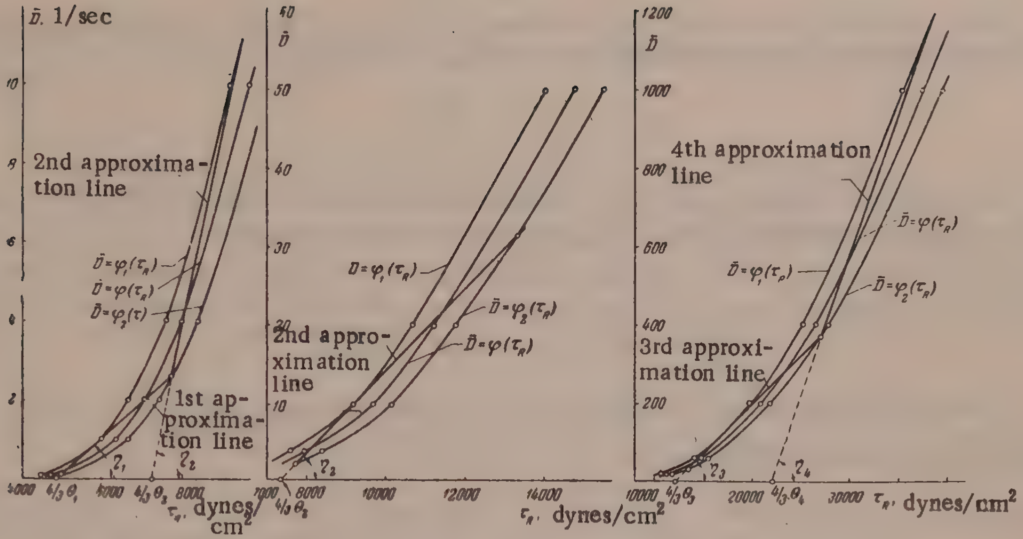

Fig. 2. Graphical approximation of the curve for the flow of solidol in a capillary viscosimeter, on three different scales.

TABLE 3

Group of Shvedov–Bingham Equations Approximating to the Law for the Flow of Solidol in a Capillary Viscosimeter

Lower boundary		$\tau_R = \frac{4}{3}\theta + \eta\bar{D}$	$\tau = \theta + \eta D$	Upper boundary	
velocity gradients $\bar{D}$, sec.$^{-1}$	shearing stresses $\tau_R \cdot 10^{-3}$, dynes/cm^2			velocity gradients $\bar{D}$, sec.$^{-1}$	shearing stresses $\tau_R \cdot 10^{-3}$, dynes/cm^2
0.083	3.68	$\tau_R = 4875 + 1084\bar{D}$	$\tau = 3650 + 1084\ D$	2.30	7.73
2.30	7.73	$\tau_R = 7250 + 193\bar{D}$	$\tau = 5430 + 193\ D$	31.5	13.4
31.5	13.4	$\tau_R = 1200 + 40.6\bar{D}$	$\tau = 9000 + 40.6\ D$	385	27.0
385	27.0	$\tau_R = 22000 + 14.0\bar{D}$	$\tau = 16500 + 14.0\ D$	—	—

The proposed method for simplification of the flow equations of plastic disperse systems can be used for calculations relating to various cases of flow of such systems in a heterogeneous field of tangential shearing stresses. Here we shall consider the flow of plastic disperse systems in round cylindrical pipes. This case is of great importance in viscosimetry and technology.

Suppose that a plastic disperse system flows in conditions of pure shear through a tube of radius R and length L under the action of a pressure difference Δp at the ends of the tube. The flowing medium will contain a heterogeneous field of tangential stresses, determined by the expression

$$\tau = \Delta pr/2L. \qquad (13)$$

The boundary stress surfaces will be coaxial cylindrical surfaces of radii r_i. These are given by Equations (5) and (13):

$$r_i = \frac{2L\tau_{0i}}{\Delta p} = \frac{2L}{\Delta p}\,\frac{\theta_i\eta_{i+1} - \theta_{i+1}\eta_i}{\eta_{i+1} - \eta_i} \quad (i = 1,\ldots,n-1). \tag{14}$$

In the center, the medium will move at constant velocity in the form of a continuous cylinder, the radius r_0 of which is determined by Equation (13), as when $r = r_0$, $\tau = \theta_1$, then

$$r_0 = \frac{2L\theta_1}{\Delta p}. \tag{15}$$

As was shown by Tyabin [4], the law of velocity distributions in the flow of a viscoplastic medium which obeys the Shvedov–Bingham law in the i-th layer of the tube is represented by

$$v_i = -\frac{1}{\eta_i}\left(\frac{\Delta p}{L}\frac{r^2}{4} - \theta_i r\right) + C_i \ln r + N_i. \tag{16}$$

The tangential stress in the i-th layer in the tube is found from the expression $\tau_i = \theta_i - \eta_i \frac{dv_i}{dr}$. Finding $\frac{dv_i}{dr}$ from Equation (16), we have:

$$\tau_i = \frac{\Delta pr}{2L} - \eta_i \frac{C_i}{r}. \tag{17}$$

Comparison of Equations (13) and (17) shows that the constant C_i in Equation (17) is equal to zero. Before consideration of the general case, we shall examine the flow through a tube of a disperse system the rheological flow curve for which can be approximated in the form of two expressions of the Shvedov–Bingham equation. In this case (Fig. 4) there will be one cylindrical surface of boundary shearing stress, the radius of which will be

$$r_1 = \frac{2L}{\Delta p}\,\frac{\theta_1\eta_2 - \theta_2\eta_1}{\eta_2 - \eta_1}.$$

The velocity distributions in the two viscoplastic layers will be given by Equation (16)

$$v_1 = -\frac{1}{\eta_1}\left(\frac{\Delta p}{L}\frac{r^2}{4} - \theta_1 r\right) + C_1 \ln r + N_1;$$
$$v_2 = -\frac{1}{\eta_2}\left(\frac{\Delta p}{L}\frac{r^2}{4} - \theta_2 r\right) + C_2 \ln r + N_2.$$

In order to find the velocity distribution, it is necessary to find the integration constants in these equations. Assuming that the plastic disperse system adheres to the tube walls, we have for $r = R$, $v_2 = 0$; it follows from the condition of velocity continuity at the boundary shearing stress surface that when $r = r_1$, $v_1 = v_2$. From the condition of continuity of the tangential stresses, as was shown above, we find that the constants $C_1 = C_2 = 0$. Then, determining N_1 and N_2, we have from the boundary conditions:

$$N_1 = -\frac{1}{\eta_2}\left(\frac{\Delta p}{L}\frac{r_1^2}{4} - \theta_2 r_1\right) + \frac{1}{\eta_1}\left(\frac{\Delta p}{L}\frac{r_1^2}{4} - \theta_1 r_1\right) + N_2,$$
$$N_2 = \frac{1}{\eta_2}\left(\frac{\Delta p}{L}\frac{R^2}{4} - \theta_2 R\right).$$

The amount of plastic disperse system flowing through the round tube per second is given by the expression

$$q = \pi r_0^2 v_0 + 2\pi \int_{r_0}^{r_1} v_1 r dr + 2\pi \int_{r_1}^{R} v_2 r dr,$$

where $v_0 = v_1(r_0)$ is the velocity of the continuous core. Substituting the values for the velocities and integrating, we have:

$$q = \frac{\pi\Delta p}{8L\eta_2}(R^4 - r_1^4) + \frac{\pi\Delta p}{8L\eta_1}(r_1^4 - r_0^4) - \frac{\pi\theta_2}{3\eta_2}(R^3 - r_1^3) - \frac{\pi\theta_1}{3\eta_1}(r_1^3 - r_0^3). \quad (18)$$

For the flow of a plastic disperse system, the curve for which can be approximated in the form of a broken line consisting of n sections, we can determine the integration constants as above, and find that $C_i = 0$ and $N_i = \text{const}$. Without giving the full calculation, we can, analogously to Equation (18), write the expression for the amount of medium flowing per second in the pipe:

$$q = \frac{\pi\Delta p}{8L} \sum_{i=1}^{i=n} \frac{1}{\eta_i}(r_i^4 - r_{i-1}^4) - \frac{\pi}{3} \sum_{i=1}^{i=n} \frac{\theta_i}{\eta_i}(r_i^3 - r_{i-1}^3). \quad (19)$$

When this expression is used, it must be assumed that when $i = 1$, $r_{i-1} = r_0$, while when $i = n$, $r_i = R$, r_0 and r_i are determined by Formulas (15) and (14). Substitution of the values of r_0 and r_i gives:

$$q = \frac{2\pi L^3}{\Delta p^3} \sum_{i=1}^{i=n} \frac{(\tau_{0i}^4 - \tau_{0i-1}^4) - {}^4/_3\,\theta_i(\tau_{0i}^3 - \tau_{0i-1}^3)}{\eta_i},$$

where for $i = 1$, $\tau_{0i-1} = \theta_1$, and for $i = n$, $\tau_{0i} = \Delta pR/2L$.

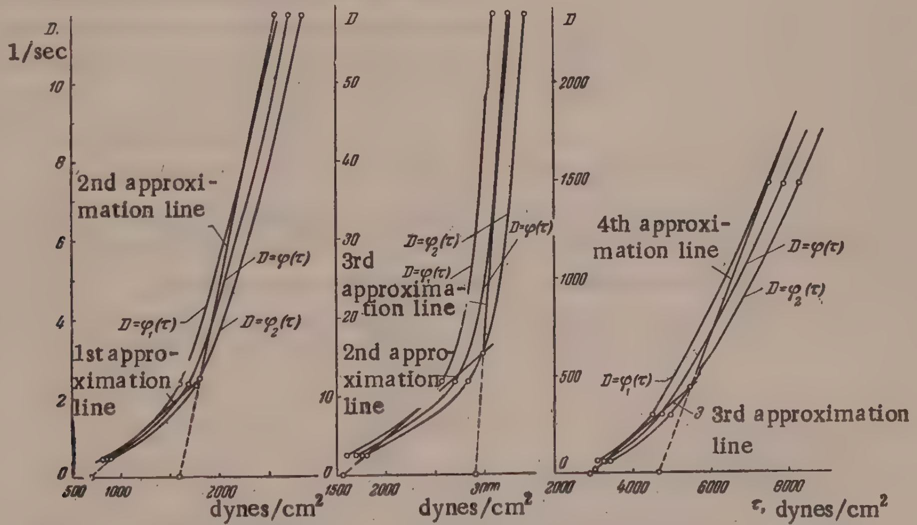

Fig. 3. Graphical approximation of experimental data for the flow of solidol in a rotational viscosimeter, on three scales.

When the curve for the flow of a disperse system is represented by one straight line, i.e., when the disperse system conforms to the Shvedov–Bingham equation, Equation (19) becomes the Buckingham equation for the flow of a viscoplastic medium in a tube. In this case n = 1, and we have:

$$q = \frac{\pi\Delta p}{8L\eta_1}(R^4 - r_0^4) - \frac{\pi}{3}\frac{\theta_1}{\eta_1}(R^3 - r_0^3) = \frac{\pi R^4\Delta p}{8L\eta_1}\left[1 - \frac{4}{3}\frac{r_0}{R} + \frac{1}{3}\left(\frac{r_0}{R}\right)^4\right].$$

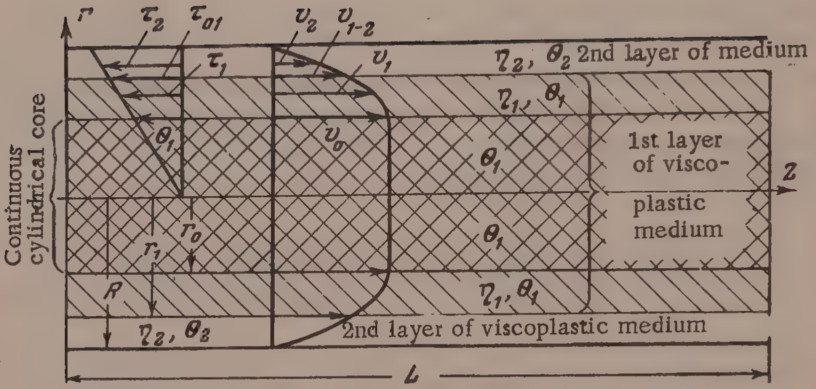
r
τ2
τ01
υ2
υ1-2
τ1
υ1
η2, θ2 2nd layer of medium
η1, θ1
Continuous cylindrical core
θ1
υ0
θ1
1st layer of visco-plastic medium
z
r0
r1
θ1
R
η1, θ1
η2, θ2
2nd layer of viscoplastic medium
L

Fig. 4. Flow of a plastic disperse system in a round tube for the case in which the flow curve is approximated by two Shvedov–Bingham equations.

SUMMARY

1. An approximation method has been developed for representing nonlinear equations for flow of plastic disperse systems in the form of groups of Shvedov–Bingham and Newton linear equations. In this way the flow of disperse systems can be represented by differential equations for the flow of viscous and viscoplastic media.

2. The approximation method has been applied to experimental data on the flow of solidol greases in capillary and rotational viscosimeters. It is shown that the curve for the flow of solidol can be represented by several Shvedov–Bingham equations and a Newton equation over a range of 5-6 tenth-powers.

3. The flow of a plastic disperse system in a cylindrical tube has been considered, when the flow can be approximately represented by n Shvedov–Bingham equations. An expression relating the amount of medium flowing per second and the pressure difference at the tube ends has been derived.

The authors express their sincere gratitude to V. P. Pavlov for kindly supplying experimental data on the flow of solidols.

LITERATURE CITED

[1] B. Rabinowitsch, Z. phys. Chem. A145, 1 (1929).

[2] G. E. Alves, D. F. Bourher, and K. L. Pigford, Chem. Eng. Progress 8, 385 (1952).

[3] V. G. Lebedev and G. V. Vinogradoy, Colloid J., 17, No. 1, 38 (1955). *

[4] N. V. Tyabin, Colloid J., 13, No. 1 (1951).

[5] V. P. Pavlov, Candidate's Dissertation (Moscow, 1949); G. V. Vinogradov and V. P. Pavlov, Symposium, Low Temperature Properties of Petroleum Products (Moscow, 1949).

Institute of Petroleum
Academy of Sciences USSR
Moscow

Received July 5, 1956

AN ELECTROCHEMICAL STUDY OF BENTONITE SUSPENSIONS

1. ACTION OF SODIUM HYDROXIDE ON SUSPENSIONS OF ELECTRODIALYZED ASKANGEL

I. A. Uskov and E. T. Uskova

The principal properties of clays greatly depend on the state of the surface of their particles and on the processes which occur in the surface layers of these particles. The state of the surface is largely determined by the electrokinetic potential. Several studies of the electrokinetic properties of clays have been reported [1], but the question is still far from solved. Some workers regard clay as consisting of salts of silicic, aluminosilicic, and ferrisilicic acids [2]. The clay particles then become negatively charged in water owing to dissociation of molecules in the surface layer. Others [3] regard clay as an amphoteric electrolyte, containing sufficiently dissociated acid (silicic acid) and basic (sesquioxide) groups. The particle charge is a certain statistical value representing the aggregate values of the positive and negative charges arising by dissociation of the surface molecules. The view also exists that particles in clay suspensions carry two different double layers simultaneously [4]; one belonging to plane surfaces and the other to fractures and edges. These layers may even differ in sign; this is indicated by electronographs [5] which show that negatively charged gold micelles are adsorbed only at the edges of kaolinite and montmorillonite particles.

To determine the causes of charge formation on clay particles, Kargin [6] studied mixed gels of silicic acid and sesquioxides as clay models. He attributes charge formation to molecular adsorption of electrolyte from solution, but does not deny the possibility of chemical interaction between the surfaces of the disperse phase particles and the dispersion medium.

In the present investigation the chemical nature of the ionogenic complex in electodialyzed bentonite has been studied by means of potentiometric and conductometric titrations by sodium hydroxide. The variation of the electrokinetic potential with the composition of the ionogenic complex was also studied.

Material studied. The Caucasian bentonite, askangel, was soaked in ten times its own bulk of distilled water for several days. The swollen mass was rubbed through a sieve with 4,900 holes per 1 cm^2. A 2% suspension was allowed to settle for 2-3 minutes, and the sediment was discarded.

The suspension was treated with 0.05 N hydrochloric acid by repeated decantation to a negative reaction for calcium. Excess hydrochloric acid was first removed by decantation with water, and when peptization of the sediment began, by electrodialysis. The electrode potential of the electrodialyzer was 160 v, and the central compartment was 6 cm wide. The electrodialysis was continued for a month with overnight breaks. The electrical conductivity of the suspension was $2 \cdot 10^{-6}$ $ohm^{-1}cm^{-1}$.

It was assumed that as the result of this treatment all the exchangeable cations and anions of the bentonite had been replaced by hydrogen and hydroxyl ions respectively, i.e., that hydrogen bentonite had been prepared.

Measurement methods. The hydrogen bentonite was subjected to conductometric and potentiometric titrations. These methods have been successfully used by many workers [7] for determinations of the composition of ionogenic complexes in sols. It was found in preliminary experiments that the electrical conductivity and pH of the suspensions varied appreciably for several days after addition of alkali. The titrations were therefore performed by determinations of the parameters which became established by the seventh day after addition of alkali.

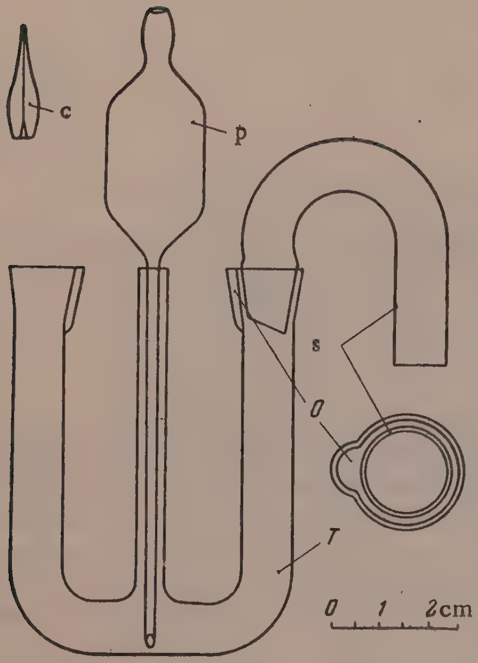

Fig. 1. Electrophoresis apparatus: T) U-tube; S) siphon tube filled with agar gel (second siphon tube not shown); 0) orifice for air outlet; P) pipet for introducing the suspension into the apparatus; C) capillary tube to serve as air brake, joined to the pipet by means of a rubber tube.

The pH measurements were performed with the aid of an antimony electrode; the electromotive force was determined by the compensation method with the "Etalon" potentiometer. The antimony electrode was calibrated against buffer solutions the pH of which had been determined by means of the quinhydrone and hydrogen electrodes. The electromotive force was regarded as constant when the value found did not differ from the previous one by more than 1-2 units in the fourth figure. The readings were taken one minute after stirring of the suspension.

The conductance was determined by the Kohlrausch method with smooth platinum electrodes and an alternating current generator; the temperature was maintained at 20° ± 0.05.

The electrokinetic potential was measured by the electrophoretic method in an apparatus based on a similar design described by Chaikovsky [8]. A diagram of the apparatus is given in Fig. 1.

The siphons are connected by means of ground glass joints with grooves for the escape of air displaced from the apparatus by the suspension (introduced by means of a pipet). The use of ground glass joints ensures that the interelectrode distance is strictly constant. The lower end of the pipet is cut obliquely, and the upper end is closed by a capillary so chosen that the time to fill the apparatus is 10-15 minutes. Before each determination the apparatus was treated in hot chromic mixture, washed in running water, and steamed for 15-20 minutes. All the glassware used was cleaned similarly.

As has been shown by one of us [9], the use of agar in saturated potassium chloride solution for filling the siphons is inadmissible, as it results in changes in the conductance of the auxiliary liquid owing to penetration of KCl into it. The siphons were therefore filled with 2% agar solution in distilled water.

Solutions of hydrochloric acid of the same conductivity as the suspension were used as auxiliary liquids. For alkaline suspensions the auxiliary liquid was prepared from sodium hydroxide solutions. The potential gradient in the suspension and auxiliary liquid was calculated with allowance for the potential drop in the siphons. The total resistance R of the circuit was calculated by Ohm's law. The resistance $\underline{r}$ of the siphons was measured separately. The potential drop between the siphons, i.e., in the suspension and auxiliary liquid, is

$$E = V\frac{R-r}{R},$$

where V is the potential at the instrument terminals.

The electrophoretic mobilities were determined by measurements, with the aid of a microscope, of the time required for the boundary between the liquid and the suspension to move through 1 mm. 5-6 such determinations were performed in one direction (without the current being switched off). As a rule the rate of electrophoresis did not vary in the course of an experiment, i.e., while the suspension boundary moved through 5 mm; this can be seen in Fig. 2. All the readings were taken at the rising boundary.

The electrokinetic potential was calculated from the Smoluchowski equation. As reported by Kruyt and Overbeek [10], the Smoluchowski equation is valid for suspensions. Surface conductance and relaxation effects can be ignored in this case.

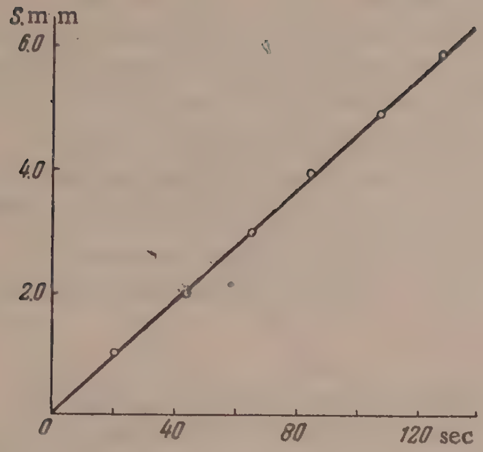

Fig. 2. Displacement of the boundary hydrogen bentonite suspension and auxiliary liquid in the electrophoresis cell.

Results of the Determinations

Potentiometric titrations showed that suspensions of electrodialyzed askangel behave as mixtures of two weak acids (Fig. 3). The stronger of these is neutralized at pH 7.9, and the weaker at pH 10.3; their dissociation constants, calculated from potentiometric titration data, are $7 \cdot 10^{-6}$ and $5 \cdot 10^{-10}$ respectively.

The curve suggests that two different acids, and not one dibasic acid, are present. The suspension contains 650 microequiv. of the first acid and 250 microequiv. of the second per 1 g of the dry material.

The stronger acid is evidently one of the polysilicic acids present in the surface layers of bentonite particles; it dissociates to give hydrogen ions, as is shown by the low pH value of 4 for the electrodialyzed suspension. The dissociation of the second acid is suppressed, as its degree of dissociation is 10^4 times smaller than that of the first.

Nikolsky and Paramanova [11] have shown that aluminate formation occurs at pH 10.0-10.5. Since bentonite contains a considerable amount of alumina and the second acid is neutralized at pH 10.3, there is good reason to believe that this is aluminic acid; evidently aluminum hydroxide, which is converted into aluminate at high pH values, is present on the surfaces of electrodialyzed bentonite particles.

Conductometric titration confirms the hypothesis that two acids are present on the surfaces of electrodialyzed bentonite particles. The conductometric titration curve in Fig. 3 shows three fairly distinct linear regions. The first additions of sodium hydroxide to the hydrogen bentonite suspension produce a slow increase of conductivity. This region corresponds to addition of 0-600 microequiv. of sodium hydroxide per 1 g of dry hydrogen bentonite. The conductivity over the region corresponding to 600-800 microequiv./g increases much more steeply than over the preceding region. Further additions of hydroxide, above 800 microequiv./g, result in a still more rapid conductivity increase. This type of curve is typical of conductometric titrations of mixtures of two weak acids, and is in agreement with the potentiometric titration data. An interesting facts is that the inflexions on the conductometric and potentiometric titration curves almost coincide (Fig. 3).

Results of the electrokinetic potential measurements are shown in Fig. 4. Additions of small amounts of sodium hydroxide produce only a small increase of the electrokinetic potential. From 500 microequiv./g the potential rises steeply, passes through a maximum at 700 microequiv./g, and falls just as steeply to the original values at 830 microequiv./g. Further addition of alkali results in a further decrease of the zeta potential. This complex variation of the electrokinetic potential with the amount of sodium hydroxide added to the suspension can be explained on the basis of the potentiometric and conductometric data.

The surface layer of the particles in the original hydrogen bentonite suspension consists of silicic (or aluminosilicic) acid and aluminum hydroxide. The presence of the acid is indicated by the first break on the conductometric titration curve. The existence of aluminum hydroxide in the surface layer is shown by the second break and inflexion on the same curve. The negative charge of the particles id determined by the dissociation of silicic acid (or the acid groups of the aluminosilicate); dissociation of aluminum hydroxide (or the corresponding groups of the aluminosilicate) accounts for the possibility of a positive charge. The negative value of the zeta potential indicates the predominant significance of the acid in the formation of the electric double layer on the particles.

Addition of small amounts of sodium hydroxide results in substitution of H ions in the outer layer of the double layer by Na ions, and the pH of the suspension increases in consequence. Despite the fact that the very mobile H^+ ions are replaced by the less mobile Na^+ ions, the electrical conductivity not only does not diminish, but even increases. This can only be explained by a considerably higher degree of dissociation of the salt formed, in comparison with the corresponding acid, which makes the outer layer of the double layer more diffuse.

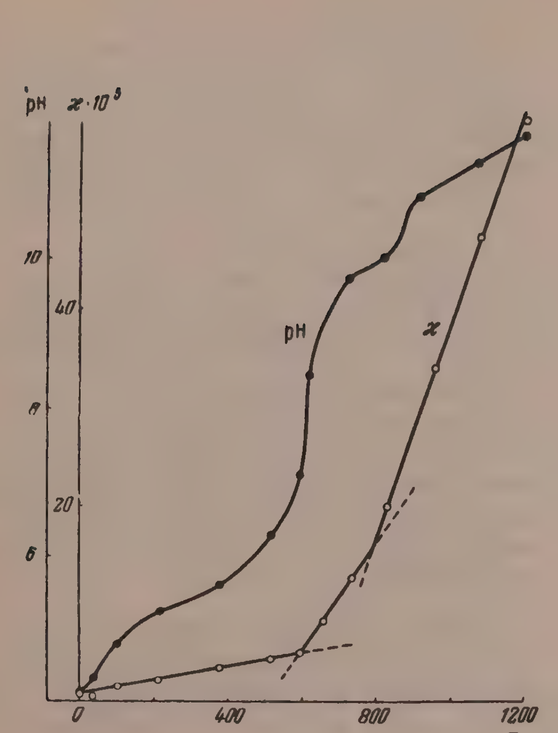

Fig. 3. Curves for potentiometric (pH) and conductometric (κ) titration of 0.55% suspension of hydrogen bentonite with sodium hydroxide; m is the number of microequivalents of NaOH per 1 g dry material.

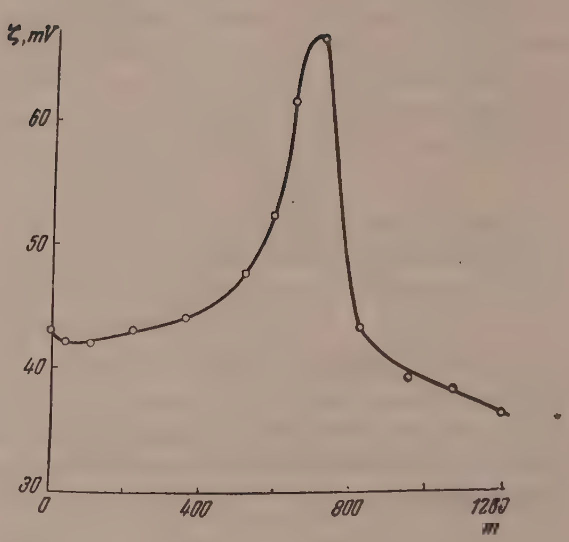

Fig. 4. Variation of the electrokinetic potential of 0.55% bentonite suspension with the amount of sodium hydroxide added.

At the same time the dissociation of aluminum hydroxide, already low, is suppressed; this ultimately results in an increase of negative charge.

The sharp increase of zeta potential coincides with the point at which the acid is neutralized and a salt which dissociates readily is formed, favoring development of the diffuse double layer. However, the zeta potential does not decrease on further addition of sodium hydroxide. On the contrary, it increases even more steeply. This can be explained by the amphoteric nature of aluminum hydroxide. At high pH values sodium aluminate is formed, which dissociates to a greater extent than sodium silicate (see the conductometric titration curve). Formation of aluminate ions on the particle surfaces results in an increase of the positive charge and a rise of the zeta potential.

The increase of potential does not continue up to the formation of the maximum amount of aluminate. It is known that aluminate can exist only in the presence of large amounts of alkali. Excess of electrolyte leads to a sharp increase in the ionic strength of the solution, as shown by the steep ascent of the conductometric titration curve in this region. As a result the diffuse layer is compressed and the electrokinetic potential decreases. However, the "double stabilization" is so strong that even at the high pH values of 10-12 the potential remains considerable (over 35 mv).

A hypothesis concerning the structure of the surface layer of the bentonite particle can be advanced on the basis of these results. The inner layer of the electric double layer in hydrogen bentonite is composed of $HSiO_3^-$ ions and, in much smaller amounts, of $Al(OH)^+_2$ ions. The outer layer contains predominantly hydrogen ions and some hydroxyl ions. The particle as a whole has a negative charge.

In neutral and weakly acid media (pH 7-9), $Al(OH)_2^+$ ions disappear from the inner layer owing to suppression of the main dissociation of aluminum hydroxide. All the silicic acid in the surface layer is converted into its acid sodium salt, dissociation of which results in an increase of the amount of $HSiO_3^-$ ions on the particle surface. The negative charge of the particle greatly increases as the result of the considerable dissociation of this salt. In the outer layer the hydrogen ions are replaced by sodium ions. These are held less strongly than H^+ ions by the particle surface, making the outer layer of the electric double layer more diffuse.

In an alkaline medium (pH 9-10) the inner layer of the double layer of a sodium bentonite particle contains, in addition to $HSiO_3^-$ ions, also AlO_2^- ions, which leads to an even greater increase of the charge on the particle. The outer layer contains a corresponding number of sodium ions. Formation of the easily dissociated sodium aluminate results in an increase of the surface charge. Further additions of sodium hydroxide do not cause any changes in the ionogenic complex, but merely compress the diffuse region of the outer layer of the electrical double layer of the bentonite particle.

This view of the mechanism of the effects produced by addition of alkali to suspensions of hydrogen bentonite is a development of Mattson's theory on the ampholytoid structure of clay particles, and provides experimental confirmation for these views.

The composition of the ampholytic complex of the bentonite particle is in reality much more complicated, but its amphoteric character remains.

SUMMARY

1. It has been shown by potentiometric and conductometric titrations that the surface layer of electrodialyzed bentonite particles is composed of 2/3 silicic acid and 1/3 aluminum hydroxide.

2. The electrokinetic potential of electrodialyzed bentonite suspensions as a function of the amount of alkali added has been measured by an electrophoretic method.

3. Small additions of sodium hydroxide produce only a slight increase of the zeta potential of hydrogen bentonite particles. Starting with additions of 500 microequiv./g, the potential rises sharply, passes through a maximum at 700 microequiv./g, and then falls to the original value at 830 microequiv./ g. Addition of sodium hydroxide in excess of this amount causes a further fall of zeta potential. An explanation for the dependence of the electrokinetic potential on the amount of sodium hydroxide added is advanced.

4. The surface layer of the bentonite particle is amphoteric in character. The inner layer of the electric double layer of the hydrogen bentonite particle consists of $HSiO_3^-$ and in part of $Al(OH)_2^+$ ions, while the outer layer consists mainly of H^+ ions with a much smaller amount of OH^- ions. The inner layer of the electric double layer of the sodium bentonite particle consists of $HSiO_3^-$ and AlO_2^- ions, and the outer layer, of sodium ions.

The authors express their deep gratitude to A. V. Dumansky for valuable advice and comments on the manuscript.

LITERATURE CITED

[1] P. Tuorila, Koll.-Z. 44, 11, (1928); I. I. Zhukov and M. N. Sokolova, J. Russ. Chem. Soc., 61, 1081 (1929); A. Buzagh, Koll.-Z. 47, 223, 1949; S. Mattson Soil. Sci. 28, 179, 337 (1929); I. N. Antipov-Karataev, T. F. Antipova-Karataeva, and A. N. Yasinovsky, Colloid J., 1, 333 (1935); E. A. Hauser, A. J. Jonson, J. Am. Ceram. Soc. 25, 223 (1942); E. A. Hauser, Trans. Faraday Soc. 44, 287 (1945); A. H. Beavers, B. L. Larson, Soil Sci. Soc. Am. Proc. 17, No. 1, 22 (1953).

[2] K. K. Gedroits, Selected Works (State Agric. Lit. Press, 1955), 1; N. I. Gorbunov, Sorptive Capacity of Soils and Its Nature (Agric. Press, Moscow, 1948).

[3] S. Mattson, Soil Colloids (Agric. Press, Moscow, 1938).

[4] H. Olphen, Rec. Trav. Chim. Pays-Bas. 69, 1308 (1950).

[5] P. A. Thiessen, Z. Elektrochem. 48, 675 (1942).

[6] M. E. Shishniashvili and V. A. Kargin, Colloid J., 8, 101 (1946); V. A. Kargin and A. L. Batsanadze, Colloid J., 8, 269 (1946).

[7] W. Pauli, E. Schmidt, Z. phys. Chem. 129, 199 (1927); W. Pauli, Koll. Chem. Beih. 17, 256 (1923); W. Pauli, E. Walko, Electrochemie der Kolloide (1932); A. I. Rabinowitsch and R. Burstein, Biochem. Z. 32, 187 (1927); A. I. Rabinowitsch and V. A. Kargin, Trans. Karpov Chem. Inst., 8, 33 (1928); J. Phys. Chem., 1, 65 (1930).

[8] S. Chaikovsky, Colloid J., 5, 131 (1939).

[9] O. D. Kurilenko and E. T. Shechkova, Ukrain. Chem. J., 16, 501 (1950).

[10] H. R. Kryut, Colloid Science (IL, 1955) p. 291.

[11] B. P. Nikolsky and V. I. Paramonova, J. Phys. Chem. 2, 687 (1931).

The T. G. Shevchenko State University
Kiev
Ukrainian Academy of Agricultural Sciences

Received May 15, 1956

ACTION OF THE BASIC SALT ALUMINUM OXYCHLORIDE ON THE STRUCTUROMECHANICAL (THIXOTROPIC) PROPERTIES OF ASKANGEL SUSPENSIONS

E. D. Uznadze and M. E. Shishniashvili

Studies of the mechanism of the action of electrolytes on structure formation in bentonite suspensions are of independent scientific significance, and are also important in relation to the correct utilization of such suspensions in the complex conditions of oil well drilling. The better the structuromechanical and thixotropic properties of a clay suspension used in oil well drilling, the more successful is the elimination of difficulties caused by losses of the suspension through pores in the strata and sand. The structurizing electrolytes used in drilling practice must cause the formation of thixotropic suspensions, increasing both the strength of the structure and the rate of its buildup. Structurizing electrolytes which mainly cause changes in the hydrophilic nature of the clay particles (electrolytes containing the alkali cations K, Na, and Li, or electrolytes containing the multivalent cations Ca, Al, Fe, etc.) do not produce any substantial increase of the thixotropic structure formation in bentonite suspensions and are therefore not very effective in preventing losses of the circulating clay suspension in drilling processes.

The purpose of the present investigation was to seek possible ways of increasing the strength of thixotropic structures in bentonite suspensions, with the ultimate aim of using them in complicated drilling conditions.

A basic aluminum salt – aluminum oxychloride, $[Al_2(OH)_5]Cl$ [1] was used for increasing the structural strength of the suspensions; its effective action on the electrochemical properties of mineral colloidal solutions [2], and also its significant influence on the structuromechanical properties of bentonite suspensions, even when used in very small amounts [3], has been demonstrated.

The existing method for the preparation of this salt is very laborious and requires the expenditure of many chemical reagents with a low yield of the final product. We therefore developed a direct method for preparation of aluminum oxychloride from a readily available raw material – aluminum hydroxide.

Aluminum hydroxide was prepared in an aqueous medium by the following reaction: $2Al(OH)_3 + HCl \rightarrow [Al_2(OH)_5]Cl + H_2O$. It was shown in preliminary experiments that the yield of aluminum hydroxide greatly varies with the degree of dilution of the acid and with variations of the relative proportions of water and aluminum hydroxide. To find the optimum conditions, equal amounts of aluminum hydroxide were dissolved in hydrochloric acid solutions of different concentrations: 1; 0.75; 0.5; 0.2 and 0.1 N. It was found that the purest salt is obtained by treatment of aluminum hydroxide with 0.2 and 0.1 N solutions of HCl; treatment of the gel with 0.5 N HCl gives a less pure salt and a low yield.

The glassy aluminum oxychloride was chemically analyzed to determine its composition.

The concentrations of chloride ions and complex $[Al_2(OH)_5]^+$ cations were determined by potentiometric titration with glass and silver electrodes. The concentrations of the ions, calculated from the inflexions on the curves, showed that the aluminum–chlorine ratio is close to unity.

To determine the composition of the complex cation, the number of hydroxyl groups bound with aluminum in the complex cation was determined, and the number of water molecules combined in a molecule of the glassy aluminum oxychloride was also found. It was shown by a method [4] based on the formation of the salt Na_3AlF_6 by the action of sodium fluoride on the aluminum cation that the complex cation of aluminum oxychloride obtained from aluminum hydroxide contains five hydroxyl groups [3].

The number of water molecules of the glassy aluminum oxychloride was found from the difference between the theoretical content of Al_2O_3 in this salt and the content as given by chemical analysis. This difference, calculated per 1 mole of the salt, corresponds to 6 moles of water [3].

Thus it may be assumed that the aluminum oxychloride molecule contains five hydroxyl groups and has the composition $[Al_2(OH)_5]Cl$; it is probably bound with not more than six molecules of water.

In order to study the structure of this peculiar salt, experiments were carried out to obtain it in the crystalline state. The method used consisted of crystallization of the salt from alcoholic solution with gradual dehydration of the alcohol by metallic calcium.

Microscopical examination of the monocrystals of aluminum oxychloride so obtained showed that the salt crystallizes in the monoclinic system. The crystal structure was confirmed by electron diffraction diagrams.

The material studied was bentonite clay of Askan origin. The experiments were performed on a 3.3% suspension of a highly disperse askangel fraction (enriched askangel) with a water yield W = 8.5 ml and relative viscosity of 25 seconds as determined by the SPV-5 instrument.

The effect of aluminum oxychloride on the structuromechanical properties of askangel suspensions was studied by a method based on model analysis with the aid of the modified Veiler–Rebinder apparatus [5,6]. This method gives the most complete quantitative characterization of the structuromechanical properties of structurized systems.

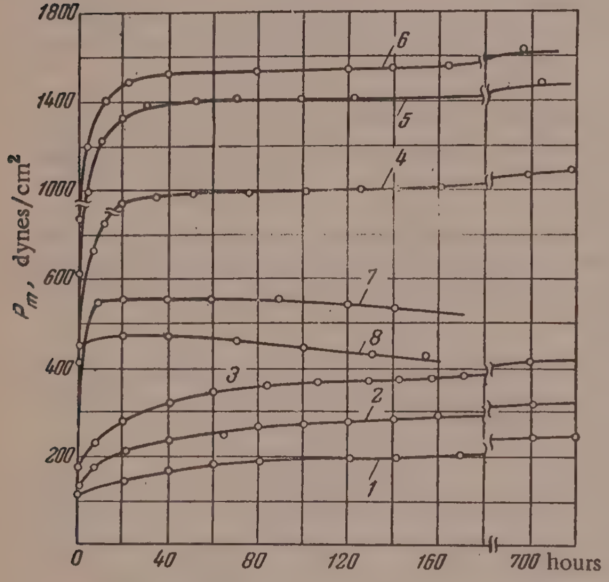

Fig. 1. Kinetics of thixotropic buildup in 3.3% askangel suspension with various contents of aluminum oxychloride: 1) askangel suspension without additions; ditto, with additions of: 2) 0.015%; 3) 0.034%; 4) 0.07%; 5) 0.14%; 6) 0.28%; 7) 0.42%; 8) 0.56% $[Al_2(OH)_5]Cl$.

A study was made of the changes in thixotropic structure formation in askangel suspensions on addition of various amounts of aluminum oxychloride. The question of the reversibility of the thixotropic structure formation process was also studied.

Figure 1 shows kinetic curves for thixotropic buildup in natural askangel suspensions containing from 0.015 to 0.56% of aluminum oxychloride on the volume of the suspension. These curves show that thixotropic strengthening of askangel suspensions increases with increasing amounts of aluminum oxychloride, reaching a maximum value for 0.28% of the electrolyte. On further increase of the amount of added electrolyte the maximum shearing stress of the suspension decreases considerably with time (Fig. 1, Curves 7,8).

Curves 4,5, and 6 (Fig. 1) show that during the first 10-20 hours the maximum shearing stress for the suspension (P_m) increases with time; subsequently the strength of the thixotropic structure remains practically unchanged. Thixotropic buildup in these suspensions is largely completed in 80 hours.

The measure of thixotropy used was the relative strengthening or the coefficient of thixotropy, $K_T = P_m - P_0) / P_0$, where P_m is the maximum shearing stress at a given instant; P_0 is the initial maximum shearing stress or the initial strength of the structure.

The Table (p. 371) gives the experimental data from which the thixotropy coefficients were calculated; the variation of the thixotropy coefficients with the aluminum oxychloride contents in the suspension is shown in Fig. 2.

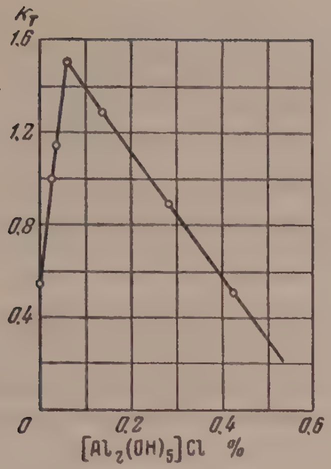

Fig. 2. Variation of K_T with aluminum oxychloride content for a 3.3% askangel suspension.

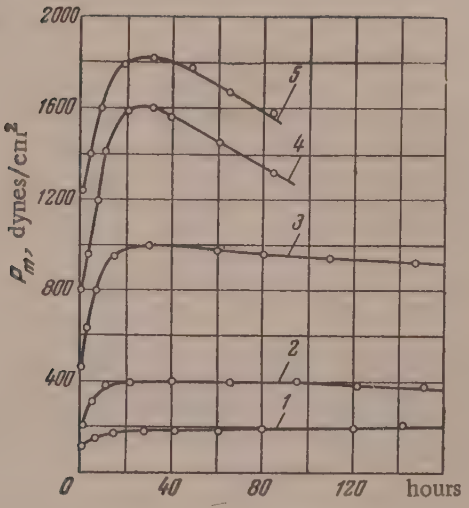

Fig. 3. Variation of the maximum shearing stress for a 3.3% askangel suspension as a function of $AlCl_3$ content: 1) without additions; with additions of: 2) 0.015%; 3) 0.034%; 4) 0.07%; 5) 0.14% $AlCl_3$.

It follows from the Table and Fig. 2 that the coefficient of thixotropy K_T of the askangel suspension first increases with increasing amounts of added electrolyte, reaching a maximum value with 0.07% of aluminum oxychloride in the suspension, and then decreases rapidly.

The variation of K_T is probably caused by changes in the composition of the askangel exchange complex owing to specific adsorption of the complex cation of the basic aluminum salt, causing considerable changes in the electrokinetic properties of the suspension. The structures formed have high thixotropic properties, probably owing to formation of stable coagulation structures.

Coefficient of Thixotropy K_T of a 3.3% Suspension of Natural Askangel as a Function of the Aluminum Oxychloride Content (Buildup time 80 hours)

Suspension studied	P_0 in dynes/cm^2	P_m in dynes/cm^2	$K_T = \frac{P_m - P_0}{P_0}$
Natural askangel	128	200	0.56
Ditto with 0.015% aluminum oxychloride	140	280	1.00
Ditto with 0.034% aluminum oxychloride	168	365	1.17
Ditto with 0.07% aluminum oxychloride	400	1000	1.50
Ditto with 0.14% aluminum oxychloride	605	1400	1.31
Ditto with 0.28% aluminum oxychloride	840	1570	0.90
Ditto with 0.42% aluminum oxychloride	356	538	0.51
Ditto with 0.56% aluminum oxychloride	470	470	—

For a comparison of the effect of aluminum oxychloride as a structurizing electrolyte, experiments were also carried out with askangel suspensions containing aluminum chloride added in equimolecular amounts in the form of 1 N solutions.

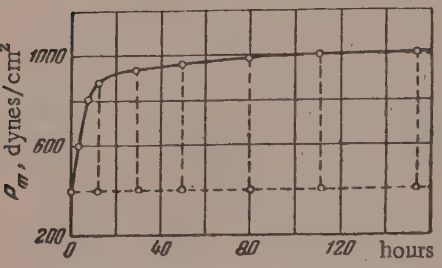

Fig. 4. Kinetics of thixotropic buildup in 3.3% askangel suspension containing 0.07% of aluminum oxychloride (broken lines indicate breakdown of structure).

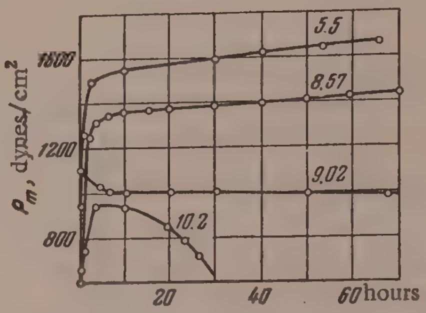

Fig. 5. Kinetics of thixotropic buildup in 3.3% askangel suspension containing aluminum oxychloride, at different pH values (shown on the curves).

As Fig. 3 shows, addition of 0.034% $AlCl_3$ to askangel suspensions produces a slight increase of structural strength. Further increases of the amount of electrolyte added raise the structural viscosity, and the strength of the structure diminishes appreciably with time. Thus, aluminum chloride causes the formation of nonthixotropic structures in askangel suspensions as the result of its hydrophobizing action leading to formation of compact aggregates with visible coagulation of the system.

Experiments on the reversibility of thixotropic structure formation were carried out on a 3.3% suspension of natural askangel, containing 0.07% aluminum oxychloride on the volume of the suspension. During the determinations of the structural buildup with time, the structure was periodically destroyed mechanically and its strength determined.

The structural network in the suspension is totally broken down by mechanical destruction, but it is built up again with time to its maximum value (Fig. 4), indicating the formation of reversible and very stable thixotropic structures in presence of aluminum oxychloride.

As the structuromechanical properties of clay suspensions under the action of various electrolytes depend also on the pH of the medium [6], our next task was to study thixotropic structure formation in askangel suspensions containing aluminum oxychloride at various equilibrium pH values of the suspensions. The original suspensions were treated with 0.1 N solutions of NaOH and HCl to give pH values of 5.5, 9.02, and 10.20 (the pH of a suspension of natural askangel is 8.57). 0.14% of aluminum oxychloride on the volume of the suspension was then added, in the form of 1 N solution.

The maximum shearing stress P_m or the strength of the structure increases considerably with decreasing pH of the suspension (Fig. 5). By decreasing the pH of the suspension it is possible to decrease the consumption of aluminum oxychloride considerably, with a simultaneous increase of the strength of the thixotropic structure. For example, for a suspension of natural askangel containing 0.07% of aluminum oxychloride at pH 8.62, $P_0 = 400.2$ dynes/cm² and $P_m = 1000.9$ dynes/cm², while for an askangel suspension containing 0.034% of aluminum oxychloride with equilibrium pH 5.5, $P_0 = 450$ dynes/cm² and $P_m = 1370.0$ dynes/cm².

The more effective action of the basic aluminum salt as a structurizing electrolyte at pH 5.5 should be attributed to the fact that this salt is the more stable in these conditions. At lower pH values, and also at pH values of 8.62 and over in the natural askangel suspension, the action of the $[Al(OH)_5]^+$ cation becomes less effective, probably owing to its hydrolysis at high pH and partial decomposition at low pH values.

Figure 6 shows a curve for thixotropic buildup in a 3.3% suspension of natural askangel having pH 5.5 and containing 0.034% aluminum oxychloride. The maximum shearing stress P_m for this suspension is considerably higher than for a suspension containing 0.07% aluminum oxychloride at initial pH 8.62 (Fig. 4). It also follows from Fig. 6 that after mechanical breakdown of this suspension the structural network is completely destroyed, indicating the formation of reversible thixotropic structures.

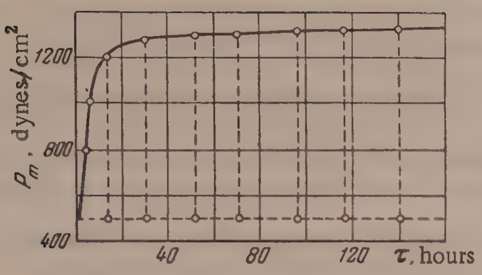

Fig. 6. Kinetics of thixotropic buildup in 3.3% askangel suspension containing 0.034% aluminum oxychloride at pH 5.5 (broken lines represent breakdown of structure).

The action of aluminum oxychloride as a structurizing electrolyte in askangel suspensions apparently consists mainly of a considerable decrease of the electrokinetic factor determining the stability of the suspension. As was shown in earlier investigations [2], the zeta potential of highly purified soil sols is decreased considerably by the addition of small amounts of aluminum oxychloride, while further increase of the added salt concentration results in complete charge reversal in the sols. The decrease of the electrokinetic potential of the negatively charged askangel particles in all probability favors an increase of the forces of attraction between the individual particles and induces latent coagulation, i.e., formation of larger aggregates from which the continuous thixotropic structures are probably formed. The appreciably hydrophilic nature of the $[Al(OH)_5]^+$ cation prevents the individual askangel particles, separated by very thin layers of the dispersion medium, from forming compact aggregates. The formation of a continuous network of clay particles, the bonds between which are weakened by the presence of very thin hydrate shells and also by the presence of larger clay particles, determines the formation of completely reversible thixotropic structures.

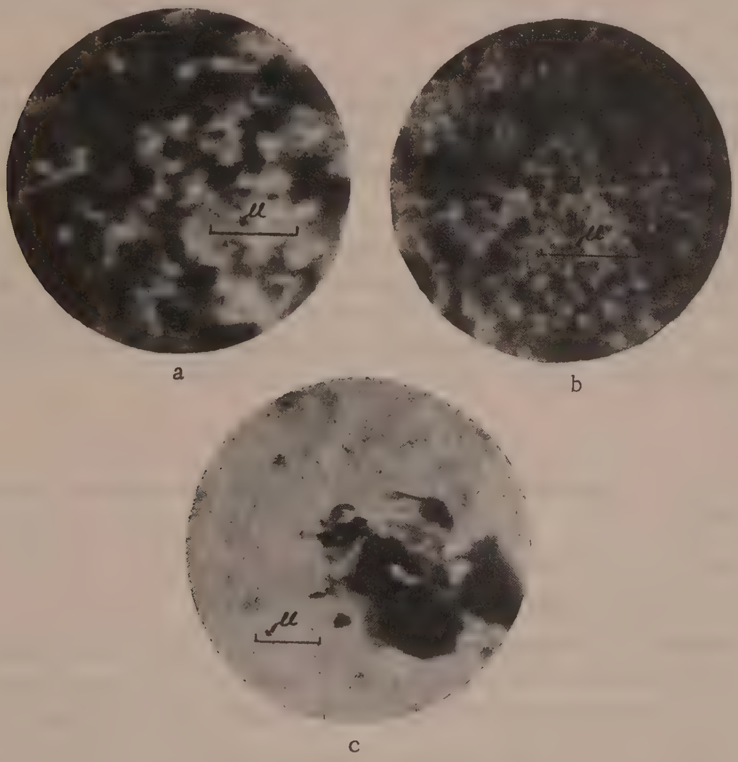

Fig. 7. Electron micrographs of suspensions; a) natural askangel; b) ditto, containing 0.0048% aluminum oxychloride; c) ditto, containing 0.048% aluminum oxychloride.

When the amount of the added electrolyte is increased, the forces of attraction between the particles increase so much, probably owing to charge reversal, that visible coagulation occurs. The compact aggregates formed readily separate from the dispersion medium, and the system gradually loses strength and thixotropic characteristics. When aluminum chloride is added to an askangel suspension, hydrophobization (dehydration) of the particle surfaces occurs in addition to a change in the electrokinetic stability factor. This results in visible coagulation, the structural viscosity greatly increases, and the strength of the structure diminishes. Thixotropic structure formation therefore does not take place in such suspensions.

Thus, the use of aluminum oxychloride as a structurizing electrolyte in natural askangel suspensions leads, on the one hand, to a considerable decrease of clay consumption in the production of the drilling mud, and on the other, to formation of thixotropically reversible suspensions which can be used in the complicated conditions of deep drilling.

As the effectiveness of the structurizing electrolyte used depends to a considerable extent on the acid or alkaline properties of the drilled rock, aluminum oxychloride is suitable for use in drilling weakly acidic or neutral strata. The use of this electrolyte in drilling may be of considerable practical importance.

Thixotropic structure formation in askangel suspensions, and in suspensions treated with aluminum oxychloride, was also studied with the aid of the electron microscope. This method was used for making visual observations of thixotropic structure formation in askangel suspensions.* A highly disperse suspension, prepared by prolonged settling of a dilute suspension of askangel, was used. The concentration of the final suspension was 0.236%.

The electron micrographs (Fig. 7) show clearly that the bentonite particles are not anisodiametric in form, and do not form long chains or plane laminar networks as usually described in the literature. The askangel particles are rather rounded, often with characteristically diffuse outlines, probably because of the high degree of swelling in water. At a number of points in the micrographs bonds can be detected between the finest individual particles, forming types of chains; spatial distribution of these chains probably results in the formation of a structural network penetrating the whole suspension (Fig. 7,a).

Electron microscope investigations of a highly disperse askangel suspension containing 0.0048% of aluminum oxychloride on the volume of the suspension, showed that formation of completely reversible thixotropic structures is accompanied by the appearance of structural chains consisting of appreciably larger clay particles (Fig. 7,b). With 10 times this amount of added electrolyte the structural chains disappear and large aggregates are formed, leading to visible coagulation of the system (Fig. 7,c).

Thus, the mechanism of structure formation in askangel suspensions on addition of aluminum oxychloride essentially consists of the formation of structural networks composed of larger aggregates (secondary formations) of particles than those in the original suspension. This increase of particle size in structure formation in askangel can be regarded as the initial stage of latent coagulation. The appreciable hydrophily of the complex $[Al_2(OH)_5]^+$ cation prevents further coagulation.

SUMMARY

1. Aluminum oxychloride is prepared by the treatment of freshly precipitated aluminum hydroxide with 0.2 and 0.1 N HCl solutions.

2. The complex cation of aluminum oxychloride contains five hydroxyl groups, and the aluminum oxychloride molecule is combined with not more than 6 molecules of water.

3. Aluminum oxychloride is an effective structurizing electrolyte which can be used as an additive to bentonite suspensions used in complicated drilling of acid or neutral strata. Addition of aluminum oxychloride to askangel suspensions produces a considerable increase in the strength of the thixotropically reversible structure.

4. The amount of aluminum oxychloride required to give the optimum structuromechanical properties in askangel suspensions is 0.07% on the volume of the suspension, while for similar suspensions with equilibrium pH 5.5 the amount is decreased to 0.034%.

5. Structure formation in askangel suspensions in presence of aluminum oxychloride mainly consists of the formation of structural networks composed of larger aggregates (secondary formations) of askangel particles.

---

*This section of the work was carried out with the assistance of A. N. Mumladze, scientific assistant at the laboratory.

This increase of askangel particle size should be regarded as the initial stage of latent coagulation.

LITERATURE CITED

[1] M. E. Shishniashvili, V. A. Kargin, and A. L. Batsanadze, Trans. Inst. Chem. Acad. Sci. Georgian SSR 7, 33 (1946); J. Phys. Chem., 21, 3 (1947); Z. Ya. Berestneva and V. A. Kargin, J. Phys. Chem., 10, 533 (1937); V. A. Kargin and N. Ogandzhanova, J. Phys. Chem., 10, 782 (1937).

[2] M. E. Shishniashvili and E. M. Nanobashvili, Report of the Acad. Sci. Georgian SSR, 1-2 (1945); Trans. Inst. Chem. Acad. Sci. Georgian SSR 9 (1948).

[3] E. D. Uznadze and M. E. Shishniashvili, Trans. Inst. Chem. Acad. Sci. Georgian SSR 14 (1956).

[4] V. A. Chernov, The Nature of Soil Acidity (Izd. AN SSSR, Moscow—Leningrad, 1947).

[5] E. E. Segalova and P. A. Rebinder, Colloid J., 13 (1951); S. Ya. Veiler and P. A. Rebinder, Colloid J., 11, 8 (1949).

[6] E. I. Kobakhidze, Candidate's Dissertation (Inst. Chem. Acad. Sci. Georgian SSR, 1955).

The P. G. Melikishvili Institute of Chemistry
Academy of Sciences, Georgian SSR
Laboratory of Colloid Chemistry
Tbilisi

Received June 5, 1956

EVALUATION OF RUBBER—SOLVENT INTERACTION

A. G. Shvarts

It is known that the solution (or swelling) of rubbers is accompanied by a decrease in the free energy ΔF of the rubber—solvent system

$$\Delta F = \Delta H - T\Delta S, \tag{1}$$

where ΔH is the enthalpy change; ΔS is the entropy change, and T is the absolute temperature.

If F decreases continuously during the swelling, the result is unlimited swelling or solution. If F passes through a maximum with increase of swelling, the swelling is limited. This latter case is characteristic of vulcanizates.

The equilibrium swelling can be theoretically calculated from the Flory equation [1]:

$$\ln\left(1 + \frac{1}{Q_\infty}\right) - (Q_\infty + 1)^{-1} - \mu (Q_\infty + 1)^{-2} - \\ - \frac{1}{m_c}\left[(Q_\infty + 1)^{-\frac{1}{3}} - \frac{1}{2}(Q_\infty + 1)^{-1}\right] = 0, * \tag{2}$$

where Q_∞ is the equilibrium degree of swelling, expressed as the ratio of the volume increase of the swollen specimen to the volume of the dry specimen after swelling; $m_c = M_r/\rho_r V_s$; V_s is the molar volume of the solvent in cubic centimeters per mole; ρ_r is the density of the rubber in grams per cubic centimeter; M_r is the molecular weight of a segment of the molecular chain between adjacent cross links; μ is a parameter characterizing intermolecular interaction between the rubber and the solvent. The enthalpy increment ΔH on mixing increases with increasing μ. The intermolecular interaction parameter μ depends on the ratio of the square roots of the cohesive energy densities for the rubber and the solvent [4,5].

$$\mu = \mu_s + \frac{V_s\,(\delta_r - \delta_s)^2}{RT}, \tag{3}$$

where δ_r and δ_s are the square roots of the cohesive energy densities of the rubber and solvent respectively. These are generally known [4,5] as the solubility parameters. The value of the parameter for the solvent can be calculated from its latent heat of vaporization (ΔH_V) at the given temperature:

$$\delta_s = \sqrt{\frac{\Delta H_V - RT}{V_s}}, \tag{4}$$

---

* Two other equations [2,3] are known which connect Q_∞ with the density of the vulcanization network and a parameter characterizing rubber—solvent interaction. However, Equation (2) is the one most commonly used.

in Equation (3) $\mu_s = 1/\gamma$, where γ is the number of solvent molecules surrounding one segment of the rubber molecule. It is generally assumed that γ is constant for all rubbers [5]. On the basis of literature data it is assumed in the present paper that $\gamma = 4$.

We must point out that Equation (3) is valid for systems with the same nature of intermolecular interaction forces (for example, nonpolar rubber – nonpolar solvent). Equation (2) shows that the interaction of solvents with rubbers and vulcanizates depends on the absolute values of μ and m_c. It should be noted that the parameter μ depends on the chemical nature of the rubber units and is independent of the molecular weight of the polymer, and therefore it characterizes the interaction both of the rubber itself and of its vulcanizates with the solvent.

It has been shown in a number of investigations [6,7] that for limited swelling of unvulcanized rubber, $\mu > 0.5$. Therefore, for a rough evaluation of the solvent power of a particular solvent it is sufficient to compare the values of the solubility parameters for the rubber and the solvent.

Values of the solubility parameters of certain rubbers and solvents, taken from the literature and calculated, are given in Tables 1 and 2.

TABLE 1

Values of the Solubility Parameter δ in (cal./cc)$^{1/2}$ for Various Rubbers

Rubber	Literature data		Calculated
	Gee [5]	Scott [4]	
Natural	7.98	8.35	8.22
Sodium butadiene	—	8.45	8.35
Divinyl–styrene (Buna S type), 15% styrene	—	8.55	—
Ditto, 25%	8.1	8.60	8.45
Ditto, 40%	—	8.70	—
Polychloroprene (Neoprene GN type)	8.2	9.25	9.00
Divinyl – acrylonitrile (Buna N type)	—	9.50	9.70

TABLE 2

Range of Solubility Parameters for Solvents of Different Chemical Classes, Calculated from the Heats of Vaporization at 25°

Solvents	Range of values of δ_s (cal./cc)$^{1/2}$
Paraffin hydrocarbons	6.75* — 7.55
Low molecular aromatic hydrocarbons	9.15 — 8.80
Ethers	7.90 — 7.45
Esters	10.15 — 8.00
Ketones	9.9 — 7.6
Nitriles	11.9 — 9.4
Monohydric alcohols	16.5 — 10.3

---

* The values of δ_s on the left refer to solvents of lower molecular weight.

It follows from Equation (3) that the value of μ decreases, and the solvent power of a given solvent therefore increases, with decreasing absolute difference between the solubility parameters of the rubber and the solvent. However, some classes of solvents, such as hydrocarbons, ethers, and ketones, may have similar solubility parameters (Table 2) but different solvent powers; i.e., Equation (3) is not applicable to the general case of solution of rubbers in different solvents. Gul [8] showed that this is because Equation (3) does not take into account the differences in the intermolecular forces acting between different rubbers and solvents. Some authors [4] propose the introduction of a correction factor K > 1 into Equation (3) for describing the interaction of rubbers with different solvents

$$\mu = \mu_s + \frac{K \cdot V_s (\delta_r - \delta_s)^2}{RT}. \qquad (5)$$

The factor K is to be calculated from experimental values of μ found with the aid of Equation (2) from the degrees of swelling of the same vulcanizate in different solvents. However, this calculation method is laborious and is valid for only a few solvents. In the present paper a method is proposed for graphical determination of μ from Equation (5), applicable to the interaction of a number of rubbers with solvents of different chemical classes. Since the correction factor K takes differences in the nature of the intermolecular forces into account, it is to be expected that K will have the same value for a given rubber and solvents of the same chemical nature.

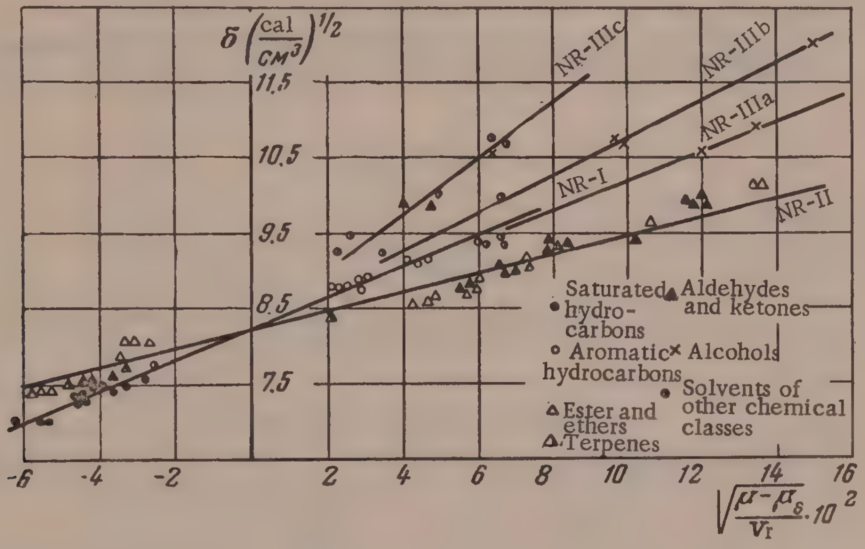

Fig. 1. Variation of δ_s with $\sqrt{(\mu - \mu_s)/V_s}$ for natural rubber; $\delta_r = 8.22$ (cal./cc)$^{1/2}$, $\mu_s = 0.25$.

We write Equation (5) in the form:

$$\delta_s = \delta_r \pm \sqrt{RT/K} \cdot \sqrt{(\mu - \mu_s)/V_s}. \qquad (6)$$

For systems with intermolecular interaction forces of the same character RT/K = const. Therefore for such systems Equation (6) represents a linear relationship between $\sqrt{(\mu - \mu_s)/V_s}$ and δ_s. A line of this type cuts off an intercept numerically equal to the solubility parameter δ_r of the rubber along the ordinate axis.

Data on the swelling of filled and unfilled vulcanizates in a large number of solvents [4,5,9-12] (the solvents are listed in Table 3) were used to calculate values $\sqrt{(\mu - \mu_s)/V_s}$ from Equation (2). The values so found were plotted graphically (Figs. 1-5). It was found that the parameter μ, characterizing intermolecular interaction, is independent of the loading of the rubber. Figure 1 shows points for the swelling of three different filled and three unfilled natural rubber vulcanizates in about 50 solvents. Figure 2 gives data for swelling of three divinyl–styrene rubbers containing 25% styrene (Buna S type) in 28 solvents, and Fig. 3, for three polychloroprene rubbers (Neoprene GN type) in 25 solvents. Figure 4 refers to swelling of one sodium butadiene rubber in 7 solvents, and Fig. 5, to one divinyl–acrylonitrile rubber (Buna N type) in 9 solvent.

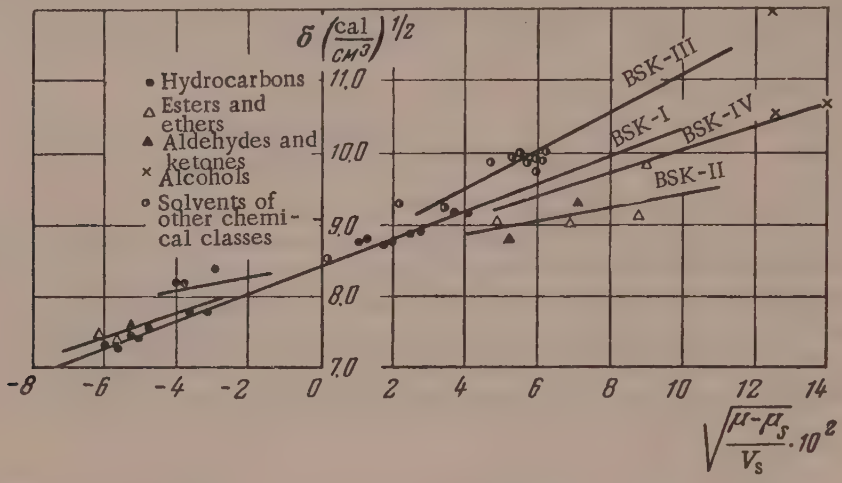

Fig. 2. Variation of δ_s with $\sqrt{(\mu-\mu_s)/V_s}$ for divinyl–styrene rubber with ~25% styrene; $\delta_r = 8.45$ (cal./cc)$^{1/2}$; $\mu_s = 0.25$.

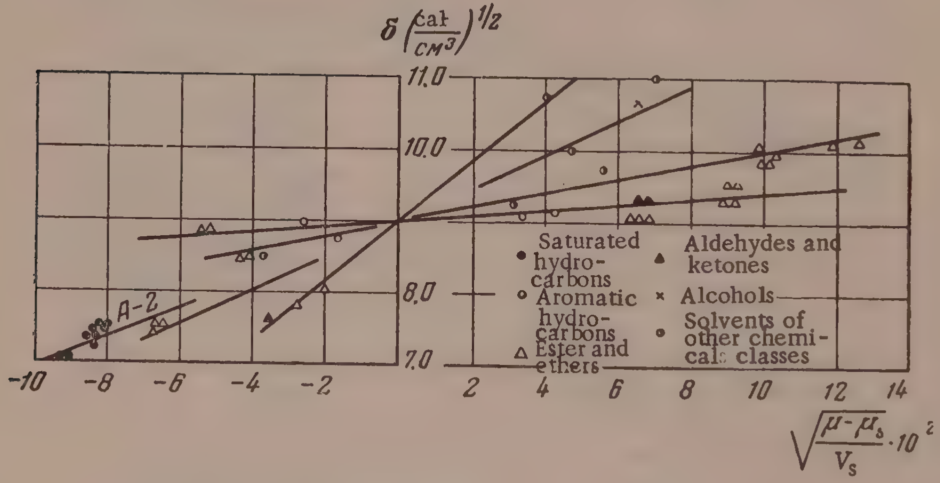

Fig. 3. Variation of δ_s with $\sqrt{(\mu-\mu_s)/V_s}$ for chloroprene rubber of the Neoprene type; $\delta_r = 9.00$ (cal./cc)$^{1/2}$; $\mu_s = 0.25$. Designations of the curves (reading downward on the right of the diagram): A-5, A-4, A-3, A-1.

The graphs show that all points corresponding to systems with intermolecular interaction of the same character lie on one straight line. Several lines intersect at one point, thus determining the exact value of the solubility parameter of the given rubber (Table 1).

The accuracy with which the position of the straight lines determining the interaction of rubbers with solvents of different chemical classes is fixed increases with increasing amounts of experimental data used for plotting these graphs (for example, 115 points were plotted for natural rubber in Fig. 1).

TABLE 3

Lists of Solvents Used in Calculations of the $\delta_s - \sqrt{(\mu - \mu_s)/V_s}$ Relationships Shown in Figs. 1-5

Symbol on graph	Solvents
	Fig. 1, natural rubber
NR –I	Saturated and aromatic hydrocarbons
NR -II	Methyl ethyl ketone, diisopropyl ketone, mesityl oxide, methyl formate, diethyl ether, ethyl acetate, n-amyl acetate, propyl acetate, n-butyl acetate, n-butyl n-butyrate, isobutyl n-butyrate, limonene, isoprene, butyraldehyde, acetone
NR- IIIa	Nitriles; alcohols: tertiary butyl, amyl, n-propyl; nitromethane
NR -IIIb	Dioxane, chloroform; alcohols: hexyl, benzyl
NR -IIIc	Alcohols: heptyl, octyl; cyclohexane, dichloroethane, carbon tetrachloride, styrene, acetyl chloride, notrobenzene
	Fig. 2, divinyl — styrene rubber
BSK -I	Saturated and aromatic hydrocarbons; limonene, dichloroethane, carbon tetrachloride
BSK -II	Cyclohexane, cyclohexene, methyl ethyl ketone, mesityl oxide, ethyl acetate, n-amyl acetate
BSK -III	Styrene, chloroform, dioxane, carbon disulfide, benzyl alcohol
BSK -IV	Isoprene, methylcyclohexane, ethyl ether, hexyl alcohol, octyl alcohol, acetone
	Fig. 3, polychloroprene
A-1	Benzene, toluene, methyl ethyl ketone, ethyl formate, methyl acetate, ethyl acetate, n-propyl acetate
A-2	n-Pentane, n-hexane, n-heptane
A-3	Chloroform, carbon tetrachloride, dichloroethane, xylene, methyl formate, n-butyl acetate, acetone
A-4	Dioxane, aniline, ethyl ether, hexyl alcohol
A-5	Nitrobenzene, diisopropyl ketone, n-butyl n-butyrate, isobutyl n-butyrate
	Fig. 4, sodium butadiene rubber
SKB-1	n-Hexane, n-heptane, benzene, toluene, p-xylene, ethylbenzene, carbon tetrachloride
	Fig. 5, divinyl — acrylonitrile rubber
SKN-1	n-Hexane, n-heptane, cyclohexane, benzene, toluene, p-xylene, ethylbenzene, chloroform, carbon tetrachloride

It is seen in Fig. 1 that the points corresponding to saturated and aromatic hydrocarbons lie along one straight line. The points for all the ketones, esters, and ethers given in Table 3 also lie on one straight line. The behavior of alcohols is different.

In the action of alcohols on natural rubber the nature of the intermolecular interaction changes with increasing molecular weight of the alcohol. As a result, the points corresponding to swelling of NR vulcanizates in tertiary butyl, amyl, and n-propyl alcohols lie on one straight line, and the points for n-heptyl and n-octyl alcohols on another.

Of the data used, only the point for the interaction of NR with cyclohexane did not lie on one of these lines for NR. The interaction of polychloroprene rubbers with solvents could not be represented by straight lines specific for given homologous series. Points representing interaction of polychloroprene rubbers with different

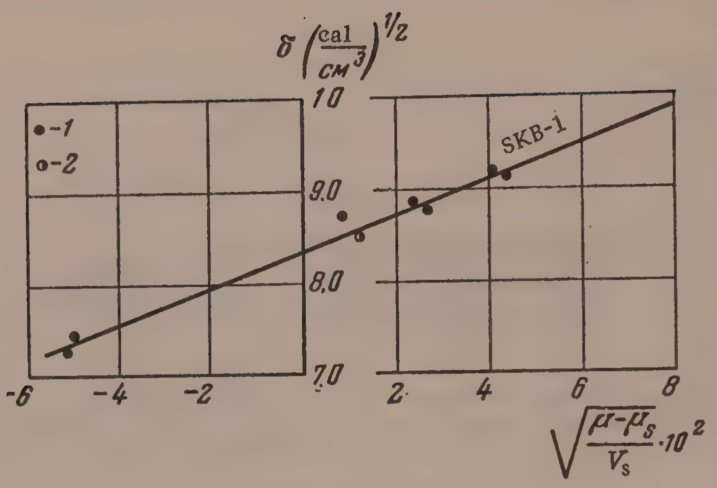

Fig. 4. Variation of δ_s with $\sqrt{(\mu - \mu_s)/V_s}$ for sodium butadiene rubber SKB-I; $\delta_r = 8.35$ (cal./cc)$^{1/2}$; $\mu_s = 0.25$: 1) hydrocarbons; 2) carbon tetrachloride.

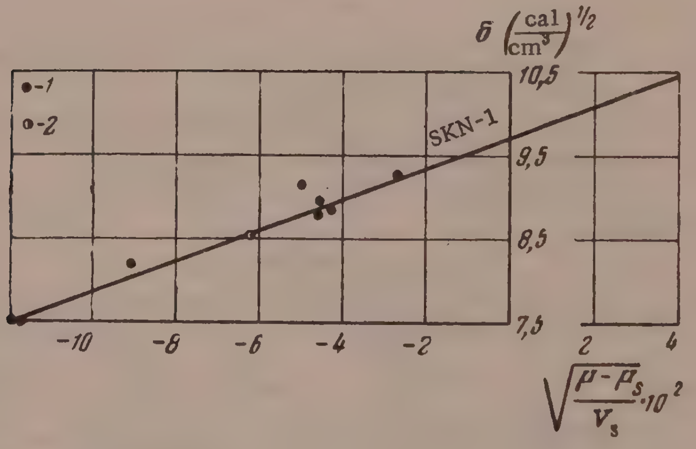

Fig. 5. Variation of δ_s with $\sqrt{(\mu - \mu_s)/V_s}$ for divinyl—acrylonitrile rubber SKN-I of Buna N type; $\delta_r = 9.70$ (cal./cc)$^{1/2}$; $\mu_s = 0.25$: 1) hydrocarbons; 2) carbon tetrachloride.

esters or ethers lay on different lines. The regular transition from one line to another, found for the swelling of NR in alcohols, is not shown in this case. The probable explanation is the insufficient accuracy of the data used. Further investigations are needed for a complete characterization of the behavior of polychloroprene.

The straight lines in Fig. 1 can be used to evaluate the interaction of natural rubber not only with the solvents listed in Table 3, but also with their homologs; the lines for polychloroprene (as given in Fig. 3) can be used only for determining its interaction with the solvents given in Table 3.

The data in Fig. 3 show that for determination of the parameter μ it is not always possible to make use only of the difference between the absolute values of the solubility parameters of the solvent and the rubber. For example, for ethyl formate the solubility parameter $\delta_s = 9.43$ (cal./cc)$^{1/2}$, for isobutyl n-butyrate $\delta_s = 7.78$

$(\text{cal./cc})^{1/2}$, and for polychloroprene $\delta_s = 9.00\ (\text{cal./cc})^{1/2}$. It seems at first sight that polychloroprene should swell better in ethyl formate than in isobutyl n-butyrate, but it follows from Fig. 3 that μ for the system polychloroprene–ethyl formate is 0.95, and for the system polychloroprene – isobutyl n-butyrate it is 0.46, so that the solvent power of isobutyl n-butyrate is much greater.

Let us consider the swelling of vulcanized SKS-30 rubber (composition in parts by weight: rubber 100, sulfur 0.5, diphenylguanidine 0.3) in solvents of approximately the same molecular volume but with different types of intermolecular forces (Table 4).

TABLE 4

Swelling of SKS-30 Rubber Vulcanizates

Solvents	Molar volume in cc/mole	Solubility parameter δ_s in $(\text{cal./cc})^{1/2}$	Parameter μ	Maximum swelling Q_∞
Carbon tetrachloride	96.5	8.50	0.250	41.0
m-Xylene	123.0	8.80	0.292	34.5
Toluene	107.0	8.90	0.312	34.6
Benzene	89.5	9.15	0.375	31.4
Dichloroethane	78.7	9.75	0.624	21.1
n-Heptane	146.0	7.45	0.648	6.91
n-Amyl acetate	147.0	9.10	0.912	3.30
Ethyl acetoacetate	127.0	10.00	1.550	0.30

It is seen from Table 4 that the maximum swelling of the vulcanizate decreases with increase of μ, and that the different character of the intermolecular forces in n-amyl acetate and benzene leads to quite different values of μ although the values of δ_s for these solvents are approximately the same.

To determine the solvent power of a given solvent at normal temperature it is necessary to:

1) calculate δ_s by means of Equation (4) from tabular data on heats of vaporization at 20-25°;

2) find the value of $\sqrt{(\mu - \mu_s)/V_s}$ in one of the graphs (from a known ordinate on the line for solvents of the appropriate homologous series);

3) calculate μ by the formula:

$$\mu = 0.25 + \left[\left(\sqrt{\frac{\mu - \mu_s}{V_s}}\right)^2 \cdot V_s\right]. \qquad (7)$$

When the value of μ is known, Equation (2) can be used to determine the maximum swelling of any vulcanizate, with known density of the spatial network, in the given solvent.

SUMMARY

1. The influence of differences in the nature of the intermolecular forces in different solvents on their solvent powers has been examined.

2. A graphical method is proposed for evaluation of the influence of the nature of the intermolecular forces of the solvent on the maximum swelling of vulcanizates.

3. For a given rubber and a given chemical class of solvents, the relationship between δ_s and $\sqrt{(\mu - \mu_s)/V_s}$ is linear. Lines for different classes of solvents intersect at one point which represents δ_r, the solubility parameter for the rubber.

The author expresses his deep gratitude to Prof. B. A. Dogadkin and to V. E. Gul for guidance and help in the investigation.

LITERATURE CITED

[1] P. Flory, J. Chem. Phys. 18, No. 1, 108 (1949.

[2] P. Flory, J. Chem. Phys. 11, 521 (1943).

[3] Kuhn, Pasternack, Kuhn, Helv. Chim. Acta 30, 1705 (1947).

[4] R. Scott and M. Magat, J. Pol. Sci. 4, 555 (1949).

[5] G. Gee, article in Symposium "Chemistry of Large Molecules" No. 1, (IL, 1948).

[6] J. Hildebrand, and R. Scott, Solubility of Nonelectrolytes, (N.Y., 1950).

[7] V. E. Gul, Trans. All-Union Conf. Colloid Chem. (Kiev, 1950).

[8] V. E. Gul, Colloid J., 13, 99 (1951).

[9] G. Whitby, A. Evans, and D. Pasternack, Trans. Faraday Soc. 38, 259, (1942).

[10] G. Gee, Trans. IRI 18, 266 (1943).

[11] F. Rosbler, and R. White, Rub. Age 61, 313 (1947).

[12] F. Rostler, et al., Rub. Age 59, 299 (1946).

Tire Institute
Moscow

Received June 5, 1956

INVESTIGATION OF THE ADSORBABILITY OF CARBOHYDRATE SOLUTIONS BY A POLAROGRAPHIC METHOD

M. S. Shulman

It is known that the polarographic maxima on current–potential curves are suppressed by adsorbed surface-active substances. The suppression of the polarographic maximum increases with increasing adsorption.

Heyrovsky [1,2] showed that oxygen dissolved in an electrolyte is readily reduced at a dropping electrode, giving two polarographic waves. The first wave is produced by reduction of oxygen to hydrogen peroxide, and the second, an extended wave, is the result of reduction of hydrogen peroxide to water or to hydroxyl ions. The first oxygen wave forms a sharp maximum which is suppressed by surface-active substances.

The suppressing effects of surface-active substances are studied by measurement of the polarographic wave height of oxygen dissolved in potassium chloride solution. Heyrovsky [2] considers that the suppressing power is characterized by the dilution at which the substance suppresses the greatest oxygen maximum in 0.0014 N KCl solution by one half. Frumkin [3] has established a number of laws relating to the formation of maxima on polarographic curves.

Variation of the Height of the Oxygen Wave in 0.02 N KCl Solution on Addition of Carbohydrate Solutions

% of carbohydrate present in 0.02 N KCl solution	Height of oxygen maximum wave in mm after addition of 1% solution						
	starch paste	dispersed starch	dextrin	glucose	maltose	sucrose	arabinose
0	212	212	212	212	112	212	212
0.0004	209	—	198	—	—	—	—
0.0008	203	—	—	—	—	—	—
0.0016	184	189	—	—	—	—	—
0.0032	175	—	—	—	—	—	—
0.0064	138	118	—	—	—	—	—
0.0080	—	—	112	212	122	—	—
0.016	76	74	—	—	—	153	212
0.024	—	—	—	—	118	—	206
0.032	57	55	47	—	115	149	199
0.048	42	—	41	—	—	—	—
0.064	39	—	—	—	—	—	—
0.08	35	—	—	192	97	144	182
0.096	35	35	35	—	—	—	—
0.12	35	—	—	—	92	—	177
0.20	—	—	—	185	86	—	—

The purpose of the present investigation was to study the adsorption of solutions of certain carbohydrates (native and dispersed starch, dextrins, glucose, maltose, and arabinose) by measurement of the oxygen wave height.

The polarograph designed by the State Institute of Nonferrous Metals was used for the investigations. All the determinations were performed on 0.02 N potassium chloride solution; different amounts of 1% solutions of the carbohydrates studied were added to 25 ml quantities of this solution by means of a micropipet.

The potential range was from 0 to 2.4 v. All the determinations were carried out at 18-20°. Galvanometer readings were taken at 0.15 v intervals. The sensitivity of the galvanometer was $^{1}/_{500}$.

The results are given in the Table.

It follows from the results that glucose and arabinose have little effect on the height of the oxygen maximum wave; sucrose has a greater effect, and the action of maltose is still more appreciable.

Carbohydrates of high molecular weight (dextrins, starch paste, and dispersed starch) have the same adsorbability. The diagram shows the changes in the height of the oxygen wave after additions of potato starch to 0.02 N KCl solution. It is seen that maximum adsorption occurs with a starch content of 0.06-0.08% in the solution.

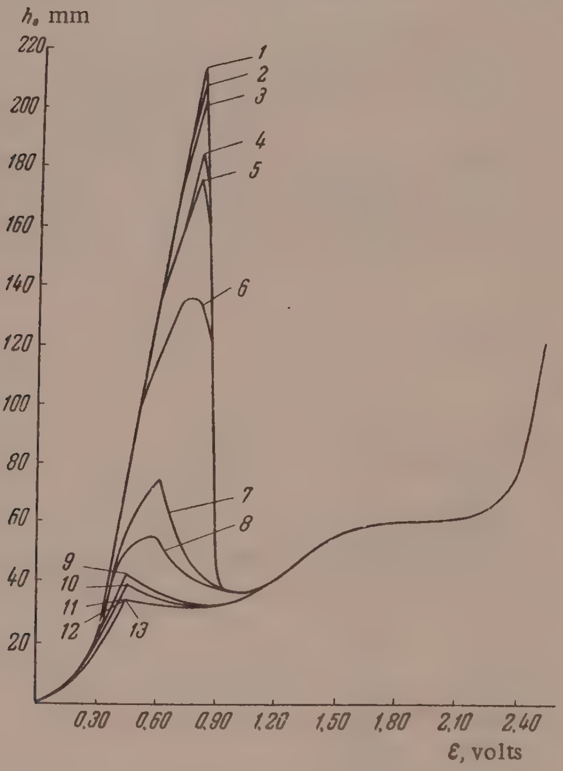

Variation of the maximum on polarographic curves for 0.02 N KCl solution after addition of potato starch solution: 1) no addition; 2) 0.0004%; 3) 0.0008%; 4) 0.0016%; 5) 0.0032%; 6) 0.0064%; 7) 0.016%; 8) 0.032%; 9) 0.048%; 10) 0.064%; 11) 0.08%; 12) 0.096%; 13) 0.12%.

Analogous results were obtained by Sokolov [4], who studied the suppression of the oxygen maximum by additions of normal and disaggregated gelatin. The curves for the suppression of the oxygen maximum by normal and disaggregated gelatin were found to coincide completely, indicating that they were adsorbed equally on mercury.

SUMMARY

1. Polymeric carbohydrates – dextrins, starch paste, and dispersed starch – are adsorbed equally on a mercury surface.

2. Glucose and arabinose have little effect on the height of the oxygen wave; maltose lowers the polarographic maximum appreciably.

LITERATURE CITED

[1] J. Heyrovsky, Trans. Faraday Soc. 19, 785 (1924).

[2] J. Heyrovsky, Polarographic Technique (IL, Moscow, 1951).

[3] A. N. Frumkin, Supplement to Chapter VIII of I. Kolthoff and J. Lingane, Polarography (Goskhimizdat, 1948).

[4] I. Ya. Sokolov, Colloid J., 4, 533 (1938).

All-Union Scientific Research Institute
for the Alcohol Industry
Moscow

Received May 18, 1956

INDUSTRIAL UNIT FOR PRODUCTION OF EMULSIONS BY MEANS OF AN LIQUID WHISTLE (JET)

S. I. Sinkova and S. A. Puzyrev

Various types of equipment are used for the production of emulsions; the commonest are stirrer devices, centrifugal emulsifiers, and colloid mills [1]. All such equipment has various disadvantages, and some of the devices are of complex construction and require the expenditure of considerable amounts of energy for emulsification.

The purpose of the present communication is to describe an ultrasonic unit the operation of which is based on the production of ultrasonic vibrations by means of a liquid jet.

It is known that ultrasonic vibrations have a strong emulsifying effect. However, the practical applications of this effect have been very restricted because piezoelectric and magnetostriction vibrators used for producing ultrasonic vibrations require a high frequency generator. Moreover, with the use of such vibrators the radiating surfaces are rather small (30-100 cm^2) so that only very small volumes of liquid can be treated. The radiating surface in piezoelectric vibrators is limited by the natural dimensions of native quartz crystals. For treatment of large volumes, the radiating surface can be increased by the use of a large number of single crystals. However, because of the high cost of polished crystals, this method cannot be widely used. The use of a large number of magnetostriction vibrators also involves great difficulties. The cost of units using either method is very high. All this accounts for the fact that emulsification by means of ultrasonics has not been adopted industrially.

The production of relatively powerful ultrasonic vibrations in liquids by means of a hydrodynamic vibrator – an ultrasonic liquid jet – is based on the following principle: a liquid stream emerging under high pressure at a high speed through a narrow jet impinges on a metal plate with oblique edges (the "knife") situated in front of the jet and fixed at four points (Fig. 1). The plate vibrates under the impact of the liquid jet; the vibration frequency depends on the velocity of the liquid stream and the distance between the jet and the plate. The distance between the jet and the edge of the plate (l) must be one half of the wave length ($\lambda/2$) of the fundamental vibration emitted by the source, as the vibration nodes must be at the points where the stream emerges from the jet and where it hits the plate

$$l = \frac{\lambda}{2} = \frac{u}{2\nu}, \qquad (1)$$

where u is the velocity of sound in the given liquid and ν is the vibration frequency.

For intense ultrasonic vibrations to be produced it is necessary to obtain resonance of the system, for which the fundamental frequency ν' of the plate must coincide with the frequency as defined in Equation (1). The fundamental frequency of the plate is given by the equation

$$\nu' = \frac{\varepsilon^2 \pi b}{4\sqrt{3}a} \sqrt{\frac{Eg}{D}}, \qquad (2)$$

where ν' is the fundamental frequency of the plate; a is the length of the plate; b is the thickness of the plate; E is Young's modulus; D is the density; g is the acceleration due to gravity; ϵ is a factor (for the fundamental vibration $\epsilon = 0.5969$).

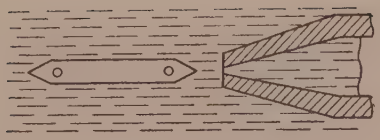

Fig. 1. Diagram of arrangement of jet and "knife".

By varying the dimensions or the length of the plate it is possible to select a definite fundamental vibration frequency of the plate and, by varying the distance between the jet and the plate and regulating the speed of the stream, it is possible to produce resonance in the system. The frequencies of the vibrations produced by the jet are of the same order as the frequencies of magnetostriction vibrators, i.e., 20-30 kilocycles/second; the power is 100-180 w.

In contrast to other ultrasonic generators, direct conversion of mechanical into ultrasonic energy is effected by means of the ultrasonic liquid jet.

An emulsification apparatus with the use of a liquid jet has been designed by Pollman and Janovski [2] and was described in detail in the book by Garlinskaya and Bezzubov [3]. The unit used by the present authors differs from the apparatus described by Pollman and Janovski. Different design variations both of the whole apparatus and of the jet were tried, the basic principle being that of the liquid jet. After prolonged researches and trials, the design shown in Fig. 2 was chosen.*

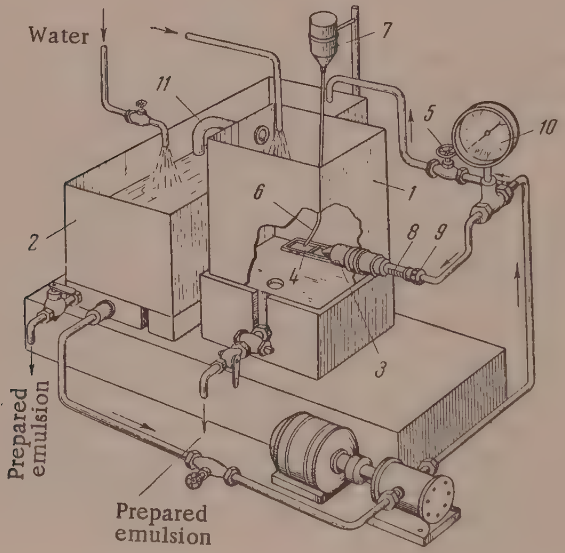

Fig. 2. Ultrasonic liquid jet apparatus for production of emulsions.

The whole unit is a closed system consisting of two reservoirs 1 and 2 connected by pipes through which the liquid is circulated by a pump.

The right tank 1 contains the liquid jet 3. The slit orifice of the jet is 0.5 mm wide and 1 cm long. The speed of the stream leaving the jet is regulated by variation of the pressure by means of the valve 5. The pressure is indicated by the manometer 10. A tube 6 with a clip, through which the liquid for emulsification is fed from the vessel 7, leads to the "knife" 4, formed by the edge of the plate.

---

* The authors express their deep gratitude to S. V. Andreev, A. P. Sviridov, and G. M. Shkarlat for help and advice in designing and constructing the unit.

The distance between the jet and the knife is regulated by means of a screw 9 and the scale 8, situated outside the tank. Before the unit is started up, both tanks are filled with a definite volume of water (20, 60-100 liters), the pump is switched on, and a pressure of 5-12 atmosphere is set up by means of the valve 5, the correct distance between the jet and the knife being adjusted by means of the screw 9. The clip on the inlet tube 6 is then opened and a definite volume of the liquid to be emulsified is let in. The design of the jet is such that the liquid passes through the zone of maximum action of the ultrasound and is instantly emulsified. Very vigorous agitation also occurs in this zone. The concentration of the emulsion formed depends on the volume of water previously put into the tanks, and on the amount of liquid introduced for emulsification. The emulsion formed in the reservoir 1 passes through the pipe 11 into reservoir 2 and again enters the first reservoir through the jet, with continuous addition of the emulsified liquid. Emulsions with concentrations of up to 20% and over can be made in this way.

The emulsions produced are generally finely dispersed (droplet size 0.5–4 μ) and are stable even in absence of emulsifiers. The output of the unit can be increased severalfold by connecting several jets in parallel to the pump, in the same reservoir. The unit can also easily be used for continuous emulsification. For this, fresh water must be fed continuously into the second tank, while the prepared emulsion is continuously removed from the first.

Among the emulsions prepared by means of this unit, emulsions of various organosilicon compounds have been obtained without the use of emulsifiers; some of these cannot be produced with the use of stirrers rotating at 3000 revolutions/minute, even with the use of emulsifiers (gelatin, etc.). An ultrasonic unit with one jet can produce 60-100 liters of emulsions of these compounds in a few minutes.

Because of its high rate of output, simplicity, and cheapness, this unit can be recommended for industrial use.

LITERATURE CITED

[1] W. Clayton, Emulsions (IL, Moscow, 1950).

[2] Pollman, Janovski, Z. ang. Phys., 1, 222 (1948).

[3] E. I. Garlinskaya and A. D. Bezzubov, Ultrasound and its Utilization in the Food Industry.

Central Scientific Research Institute
for Cellulose and Paper Industry
Leningrad

Received June 2, 1956

DISCUSSIONS

THE EQUILIBRIUM STATE OF HIGH-POLYMER GELS

(ON THE SUBJECT OF THE COMMENTS BY A. V. NIKOLAEV, R. E. NEIMAN, AND O. V. NEIMAN, COLLOID J. 19, 121 (1957)*

S. M. Lipatov and S. I. Meerson

The problem of gel formation is again becoming very important because several new polymers (polyacrylates, polyvinyl chloride, polystyrene, etc.) of interest for fiber production form solutions only in a small number of liquids and only at high temperatures. On cooling, such solutions form gels in the same manner as has been shown earlier for gelatin, agar, and other natural polymers. The mechanism of gel formation by these new polymers is identical with the mechanism of gelatin gel formation; in both cases the gel at definite concentrations is not in a state of equilibrium, but clearly defined aging of the gel occurs, leading to syneresis – separation of the system into two phases. The analogy between gelation and crystallization developed in our publications over a number of years [1] is now not only confirmed as an analogy, but in a number of papers gelation is identified with crystallization.

Many theories of gelation have existed in the past [2]. Here we may mention two viewpoints, each of which still has its supporters. In our publications we assumed the possibility of complete saturation of the polar groups in the macromolecules by solvent molecules, and the process of structure formation was regarded as interaction between the polymer molecules by means of their polar or generally unsolvated groups [3]. In the other view [4], supported by the authors of the comments on our paper, it is assumed that polar groups may interact with each other in consequence of desolvation of such groups during gelation.

Let us consider the main points put forward by the authors [4].

I. They state that gelation of solutions, and therefore fusion of gels, is not accompanied by heat effect. There are neither theoretical nor experimental grounds for this assertion. Although the authors refer to the care taken in their experiments, the papers [5,6] do not contain experimental data on gelatin gels, while the data on agar are unconvincing. On the assumption that the gelation process consists of two stages: a) gelation without phase separation, the author attribute the absence of a heat effect of gelation to the fact that at the first stage "the nonequilibrium, gel which has not separated into layers should not have a structural network" (p. 132). In this case either there are no bonds between the macromolecules or the bonds are weak and there is no heat effect, while in case (b) phase separation occurs and heat may be evolved.

The authors evidently are not aware that the very first instant of gelation is accompanied by microseparation of the system and interaction between the molecules. Therefore there is no reason for associating the evolution of heat with phase separation in the system. This is also clear from the fact that a 12% solution, which exists as a solution at 40°, forms an equilibrium gel on cooling, which does not separate out in course of time. Earlier we showed that gelation proceeds in stages, each of which is associated with strengthening of the gel structure with time.

1. Solution → gel I + g_1. 2. Gel I → gel II + g_2. Gel II → syneresis + g_3. The total heat effect of the process is equal to the sum of these effects. The authors put forward a scheme according to which the first process is not accompanied by a heat effect, all the heat being evolved at the second stage. They describe this as a new scheme in principle. It is seen from this scheme (p. 130, Fig. 1) that when the solution is cooled from T_2 to T_1 the gel formed has a higher heat content than the solution at temperature T_2 (?). This does not

---

* [Original Russian pagination. See C. B. Translation, p. 129].

correspond to reality, as gelation of solutions below 12% concentration is also accompanied by a heat effect.

The authors themselves realize that the heat effect of gelation which they could not detect must exist. Thus, at the end of the article (p. 132) it is stated that a definite number of local bonds may be formed during gelation; "this process should be accompanied by heat and volume effects." To escape from this confused situation, the authors assume that gelation is accompanied by simultaneous desolvation and interaction between the particles by their desolvated groups.

The desolvation concept is new in principle only in that it is now introduced into the authors' explanations, although quite recently they considered that "there can be no changes in the hydration or structure of the sol and gel, as each of these processes would be accompanied by a heat effect or volume change" (p. 351). It is seen that previously there was no mention of any compensation of two opposing effects. If this veiwpoint is accepted, the conclusions should be quite different from those drawn by the authors. Indeed, if gelation was accompanied by desolvation and formation of bonds between the macromolecules of the desolvated groups, heat absorption should occur, and not compensation of two heat effects. This follows from the fact that hydration and solution of gelatin have a positive heat effect, as in the equation $Q = g - c$, $g > c$. Consequently the reverse process of desolvation and bond formation between the macromolecules should be accompanied by absorption of heat. In reality heat is not absorbed. If it is assumed that $g = c$, as is done by the authors, the formation of very stable bonds must be postulated, as hydrogen bonds are formed in the hydration of gelatin.

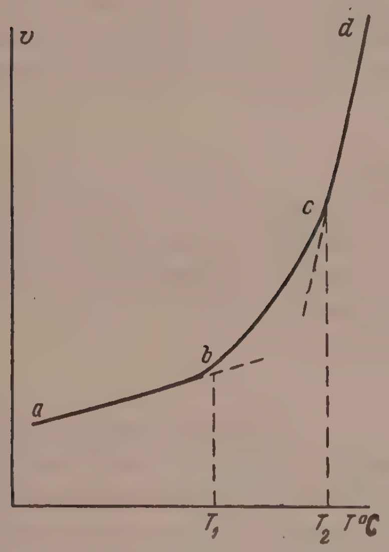

Fig. 1. Schematic graph of the relationship v = = f (T) for gelatin gels.

The authors state further that "in phase separation the number of bonds between the macromoles increase sharply," as a result of which heat should be evolved. The question of the nature of these bonds arises. If desolvation and compensation of two effects is presumed here also, why do the authors assume evolution of heat in syneresis? Or do other groups take part in intermolecular interaction in this case?

It is clear on theoretical grounds that spontaneous gelation should proceed with a decrease of free energy. Since in gelation the large number of possible configurations of the macromolecules is decreased and $\Delta S < 0$ gelation can only proceed spontaneously if $\Delta H < 0$ and $|\Delta H| > |T\Delta S|$. Hence it follows that the gelation process must be accompanied by a heat effect. Finally, if we assume that desolvation occurs spontaneously during gelation, we must assume the existence of two spontaneous processes of opposite sign – solvation (in swelling) and desolvation (in gelation).

Since a gel is formed during gelation and subsequent separation of the system, the composition of which coincides with the composition of the swollen gel, and gelation and syneresis return the system to its original state, the assumption that desolvation occurs in gelation is unfounded. *

II. The authors state further that the gelation process is not accompaned by a volume effect. We cannot agree with this either. N. N. Puchkova has made numerous measurements in our laboratory of the thermal expansion of gelatin gels over a wide range of concentrations.

The results may be schematically represented by Fig. 1. The $v = f(T)$ curve shows two characteristic points. At T_1 the change of gel volume is associated with the start of fusion, which is completed at T_2. If these results are compared with the data published by Neiman [7] on gelatin gels, it is seen that he ignores the

---

* Recently calorimetric studies have been carried out in our laboratory of the solution of gelatin gels of different compositions in urea solutions at 20 and 50°. The results not only confirm that the gelation process is exothermic, but make possible a quantitative evaluation of the heat effect (≈ 9 cal./g for a 20% gelatin gel). The results of these determinations are to be published in the near future.

the volume changes over the intervals ab and cd and considers only the region bc. Two straight lines are drawn in this region, intersecting at 37-39°. The author states that "beyond the limits of the indicated range there is a deviation from linearity, in the direction of both high and low temperatures." It is not clear why the author neglects these "deviations from linearity." However, the erroneous conclusion is drawn from this that no volume change occurs during fusion of a gel On the basis of our data it can be claimed that the gel—sol transition is accompanied by a volume change at $T_1—T_2$, and this region always corresponds to fusion of the gel.

Incidentally, the paper [8] contains data for the relationship log τ = f (1/(T) where τ is the relaxation time for the gel volume. It is shown that a certain temperature, which the authors call the "melting point" of the gel, corresponds to the intersection of two straight lines, one of which represents the state of the gel, and the other, of the solution. The difference between the activation energies is 42-40 kcal./mole. Even from these data it follows that there should be a heat effect of gelation, and a characteristic point on the v = f (T) curve corresponding to the "melting point."

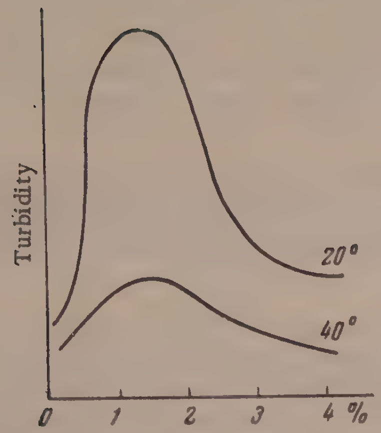

Fig. 2. Variation of turbidity of gelatin gels with concentration.

III. The authors consider two examples in confirmation of their views concerning the absence of heat and volume effects on gelation. One is the thermogram for heating and cooling of borate glass, and the other relates to volume effects in coagulation of $Fe(OH)_3$. The authors assert in the case of the first example that the vitrification of fused glass is not accompanied by a heat effect. However, Botvinkin [9] has shown experimentally that the heat of vitrification of boric anhydride is 26.7 cal./mole. This result is obtained from the heat capacity of glass as a function of temperature. With regard to the second example, it is sufficient to note certain contradictions in the publications by the authors of the discussion paper. For example, it is stated [10] that "coagulation of $Fe(OH)_3$ sol is practically unaccompanied by a volume effect," and the general conclusion is drawn that "volume effects in sol—gel transitions (peptization, coagulation) are zero." However, in the discussion paper we read: "therefore there is no doubt that the volume effect of the sol—gel transition ... while in the shrinkage because of condensation of a gel by the action of a coagulant (analogously to syneresis) it may be comparable with the effect in phase transition". Because of all the foregoing we must disagree with the authors of the discussion papaer and consider their viewpoint to be erroneous.

IV. Mechanism of gel formation. If the force field on the molecules is heterogeneous i.e., if polar and hydrocarbon bonds exist between the macromolecules, solution of the polymer is possible if both types of bond are overcome as the result of interaction with the solvent

$$Q = (g_p - c_p) + (g_n - c_n),$$

where g_p and g_n represent the solvation of polar and nonpolar groups respectively, and c_p and c_n are the bond energies between such groups. If the solvent solvates only one type of group, for example polar, and $g_p > c_p$ while $g_n = 0$, the swelling process is accompanied by evolution of heat, but it is limited, as the energy of the structure, which depends on c_n, has not been overcome. If a quantity of heat equivalent to c_n is supplied to the swollen polymer, a solution is formed which, when cooled to the original temperature, forms either a structurized solution or a gel (depending on the concentration). In either case aggregation occurs in a very short time. The number of aggregates is large, and this can be determined very exactly by light scattering, and also by the heat-effect. Figure 2 shows curves for light scattering at two different temperatures; these curves clearly show the conditions for aggregate formation. As was shown by us in 1936 [11], aggregation precedes gelation only in relatively dilute systems; at gelatin concentrations above 2% aggregation becomes progressively less necessary for gel network formation, as the number of macromolecules becomes large enough for formation of direct bonds between them. As was already stated above, liquid droplets which may be detected microscopically are exuded during the first stages of gel formation, i.e., separation of the system commences and continues in time up to syneresis. It is therefore quite wrong to assume that a network is formed only in phase separation, just as it is wrong to believe that all the heat of gelationis liberated during the first instant of gel formation, or that gelation always leads to complete phase separation of the system with formation of a gel of equilibrium composition.

Gelation proceeds in a complicated manner, differently for different polymers: if gelation is accompanied by chemical effects, as in starch, the phase separation is irreversible. Phase separation in gelatin is completely reversible, while when a polyethylene gel undergoes such separation steric hindrances arise and the system does not return to its original equilibrium state.

The aggregates formed in gelation are fairly stable, and two processes may be distinguished in the fusion of a gel: 1) fusion of the network, and 2) fusion of the aggregates. Examination of the change of light scattering on increase of temperature shows that the aggregates disappear (fuse) over a very narrow temperature range. This and a number of similar facts gives reason to consider gelation as a process analogous to crystallization.

In recent years publications have appeared in which gel formation is regarded as crystallization. Richards [12] showed that when a solution of polyethylene in xylene is cooled, crystallites are formed and aggregate into spherulites. Boedtker and Doty [13] showed, for gelatin solutions, that the aggregates formed are crystallites and their formation has the same origin as gel formation. The presence of crystalline structures in gels is proved not only by the liberation of heat and increase of volume, but by the appearance of sharp rings on X-ray diagrams of gelatin films obtained from gels. Similar effects have recently been found in gels of carboxymethylcellulose and of polyvinyl chloride. Doty stresses that fusion of gels consists of two stages: 1) fusion of the network, accompanied by liberation of the aggregates, and 2) fusion of the aggregates themselves. As was shown by us, formation of not very concentrated gels is preceded by aggregation, and therefore a freshly prepared gel can, in agreement with Doty, be regarded as a precipitate in a weak gel. It follows from the foregoing that stable bonds are formed between macromolecules or their aggregates during gelation, and the authors [4] now admit this, and consider that heat is evolved in the earliest stages of gelation, but it is used to compensate the desolvation process.

It is clear that there are no grounds for assuming desolvation, and therefore the mechanism suggested by the authors to replace ours, which is based on erroneous assumptions, contradicts both experimental data and theory in its very basis.

LITERATURE CITED

[1] S. M. Lipatov, J. Russ. Chem. Soc., 59, 471 (1927); 40-55 (1929); Physical Chemistry of Colloids (Moscow, 1948).

[2] S. M. Lipatov, Problems of Gelation of Lyophilic Colloids, (VSNITO, Zelinsky University, 1937).

[3] S. M. Lipatov, J. Gen. Chem., 3, 694 (1933).

[4] A. V. Nikolaev, R. E. Neiman, and O. V. Neiman, Colloid J., 19, No. 1, 121 (1957).

[5] A. V. Nikolaev, G. I. Golub, and P. Osetrov, Colloid J., 8, 345 (1946).

[6] R. E. Neiman and O. V. Neiman, Colloid J., 9, 203 (1947).

[7] R. E. Neiman, Colloid J., 14, No. 2, 108 (1952). [Original Russian pagination. See C. B. Translation].

[8] R. E. Neiman, Colloid J., 16, No. 4, 281 (1954). [Original Russian pagination. See C. S. Translation].

[9] O. K. Botvinkin, Physical Chemistry of Silicates, (Moscow, 1951) p. 261.

[10] R. E. Neiman and R. I. Sukhorukova, Colloid J., 12, No. 5, 363 (1950).

[11] S. M. Lipatov, Problems of Gelation of Lyophilic Colloids (1937).

[12] R. B. Richards, Trans. Faraday Soc., 42, 10 (1946).

[13] H. Boedtker and P. Doty, J. Phys. Chem. 58, 968 (1954); 17, 89 (1955).

Moscow

Received March 3, 1957

PROBLEMS RELATING TO THE MECHANISM OF THE FRICTION OF RUBBER

S. B. Ratner

Scientific studies of rubber friction are of recent origin and enough data for drawing definite conclusions concerning its mechanism are not yet available. However, since a discussion on the mechanism of rubber friction is already in progress [1-3], it is necessary to point out that it is rational to compare the friction of rubber with three other allied phenomena which are better understood: a) friction of ordinary solids; b) flow of viscous liquids; c) deformation of rubber itself.

Friction of rubber and of solids. In contrast to solids, rubber in the course of friction undergoes high-elastic rather than plastic deformation, and creeps like a caterpillar around projections, "flowing" around them [4]. Despite the reversible character of high-elastic deformation, it resembles irreversible plastic deformation in two respects: the possibility of large displacements and the existence of irreversible energy losses (similar to those accompanying friction). It is therefore not surprising that many factors influence the friction of rubber and of oridnary solids similarly. In relation to the role of the load [5,6] this is not disputed by Bartenev [1]

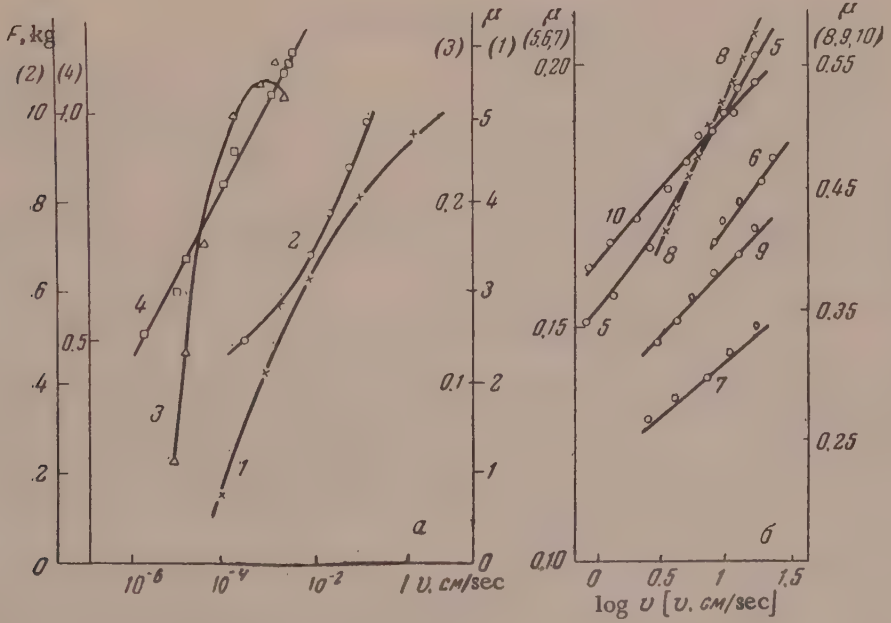

Fig. 1. Variation of the force F (or coefficient μ) of friction with the logarithm of the sliding velocity for rubber (a) and other materials (b) [7]; 1) rubber on glass [9]; 2) on glass [7]; 3) on steel [10]; 4) on steel [3]; 5) pine wood on walnut wood; 6) steel on steel; 7) bronze on steel; 8) leather on steel; 9) the same, after rubbing in; 10) aluminum on steel [7].

However, despite his assertions [1], the influence of sliding velocity v (Fig. 1) is also analogous: the frictional coefficient μ of rubber also generally increases with increasing v (Fig. 1,a), like that of other bodies (leather, wood, metals – Fig. 1,b); often in accordance with the same [7,9] Shallamach–Many equation: $\mu = a + b \log v$. Even cases in which the $\mu - v$ curve passes through a maximum are known both for rubber [10, 11] and for metals [12-14]

These data cover the velocity range from 10^{-12} to 10^{2} cm/second, in which the positions of rubber, wood, and metals are sometimes displaced according to differences in their "relaxation" rates. The data in Curves 2 and 5-11 (Fig. 1), obtained without vibration or heating of the surfaces, are especially reliable. Increase of contact time increases the static friction of rubber and of solids.

Thus, the laws of friction of rubber and of solids are analogous in many respects (the role of temperature is discussed below) which shows that there are similar features in the respective mechanisms.

Friction of rubber and viscous flow. The role of deformation. It is possible, following Schallamach [9, 11], to attempt to demonstrate the analogy between the friction of rubber and the flow of viscous liquids, on the on the assumption that in the sliding of rubber thermal motion RT aids the tractional force F to overcome the activation barrier E. Schallamach presented experimental data which provided the basis for his molecular kinetic theory of rubber friction, represented by the equation

$$v = v_0 \exp [-(E - \alpha F)/RT].$$

However, in addition to a certain resemblance between the formulas for friction and flow, experience indicates considerable differences between these phenomena These are: absolute static friction [15]; maxima on F–v (see [11]) and also Curve 3 in Fig. 1); minima on F–T curves [16]. Let us consider these effects, found for the friction of rubber and contrary to the mechanism of flow.

Schallamach did not consider his formula valid when $v \to 0$. However, on the basis of his idea (similarity between friction and flow) it is possible to apply the Eyring equation [17] for viscous flow to the friction of rubber:

$$v = v_1 \exp (E/RT) \sinh(\alpha F/RT).$$

Now F = 0 when v = 0, as should be the case in flow. Bartenev [18] reached the conclusion that the static friction of rubber (in contrast to solids) is zero in this way, ignoring the difference between the mechanisms of flow and friction. He formerly admitted this himself when he wrote [18] that his concepts "do not essentially differ from the analogous molecular mechanism of viscous flow postulated by Frenkel and Eyring" (p. 1161), so that "by considering the jumps in the light of the simplified Frenkel–Eyring scheme . . . we obtain a simple but inexact equation analogous to the Eyring equations for viscous flow" (p. 1162).

Thus, Bartenev considered that the flow equation is inexact (and not inapplicable to friction), and therefore he attempted to introduce a refinement by solving [18] a two-dimensional flow problem, whereas Eyring [17] solved the one-dimensional (see equation above) and three-dimensional problems. This mathematical distinction does not bring about any essential change; it does not convert an equation for flow into an equation for friction. After my criticism [2], Bartenev added [3] that the distinction lies in the fact that in friction, i.e., "in internal friction the area of actual contact coincides with the area of nominal contact, and in external friction it does not" (p. 627). This, however, contradicts his own assertion [1] that the role of the contact area bears no relation to the nature of the effect or its kinetics.

Another distinction (not considered by Bartenev) is important: in friction, rubber is displaced as a whole, which may decrease the energy of interaction (and therefore E) on increase of the velocity. Therefore F may reach a maximum and then decrease on considerable increase of v (as the rubber will not have time to come into close contact with the support), in agreement with the experimental data mentioned above [10, 11].

From this standpoint, and also with the deformation of rubber during friction taken into consideration, it is possible to explain other experimental facts not accounted for by the flow mechanism: it is possible to correlate the existence of static friction in rubber with the existence of an equilibrium modulus (in addition to adhesion forces), and the appearance of a minimum on the F(T) curve for the static friction of rubber with competition between increasing deformation and decreasing rigidity with increase of temperature.

The influence of temperature on the force of kinetic friction increases with decreasing E, according to the equation:* $F = E/\alpha$, which follows from the Schallamach equation when $\underline{v}$ = constant. Therefore for rubber, when E is not large, the temperature has a strong influence on friction, in contrast to its weak influence on the firction of solids. A similar conclusion follows from a comparison of the effects of temperature on the deformability of rubber and of solids.

Thus, on the basis of all the known facts, it is inadmissible to ignore the differences in principle between rubber friction and viscous flow. The existence of such facts, and of points of resemblance between the friction of rubber and of solids (and also of the characteristic role played by the deformation of rubber in friction) does not justify the assumption that the phenomena are identical, but poses the task of further comparisons and investigation of their mechanisms on the basis of carefully planned experiments.

Certain Errors in the Discussion Articles [1,3].

a) Bartenev [3] quotes Z. E. Styran's data on the F−v relationship for one sample of rubber and writes: "The graph shows that the frictional force tends to zero with unlimited decrease of the velocity" (p 626). However, this is incorrect, as can be easily seen if the same data are plotted in F−log $\underline{v}$ coordinates (Curve 4, Fig. 1). It is seen from the graph that the Schallamach equation is applicable to these data, which are analogous to other known data. However, it cannot be concluded from Fig. 1,a that $F \to 0$ when $v \to 0$ (i.e., when $\log v \to -\infty$). This is so because, if extrapolation to $F = 0$ is admissible, we have $v \neq 0$, while if it is inadmissible there are no grounds for Bartenev's assertion.

Bartenev [3] accuses me of not noting the fact that the Deryagin formula was first extended by I. V. Kragelsky (p. 628). This is untrue, as our papers [4,19] make appropriate reference to the work of Kragelsky [20].

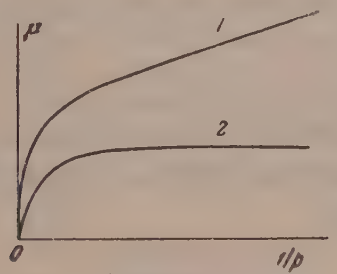

Fig. 2. Frictional coefficient of rubber as a function of the reciprocal load, after Bartenev [21].

b) Bartenev writes [3]: "Ratner [2] formulates assertions which are ascribed to me; . . . they are not taken from my papers but are formulated by Ratner" (p. 629). This refers to the following points made by Bartenev in [1,18]: the influence of velocity on the frictional force is always different in principle for rubber and for solids (p. 249); the static friction of rubber is zero (p. 1163); the frictional force is strictly proportional to the actual contact area (p. 250); roughness of the support influences the friction of rubber only by increasing the contact area (p. 250). Lack of space makes it impossible to give quotations which show that these formulations of ours, which Bartenev now [3] admits to be erroneous, reflected his views correctly [1,18,21].

We shall consider one example only. Bartenev [3] writes that in examining the paper [1], Ratner [2] made "numerous errors in so doing. It is asserted, for example, that in my paper the law of friction is considered when $p \to \infty$." (p. 628). However, my assertion is shown to be correct by Fig. 2, which reproduces Fig. 2 from [21], in which Bartenev gives $\mu - 1/p$ curves starting with $1/p = 0$ (zero, and not some other boundary of the load range under consideration, is specifically shown on the abscissa axis), i.e., from $p = \infty$. This, as he now admits himself [3] "is incorrect, as the law of friction was derived as a linear approximation in a limited load range" (p. 628).

It is seen from this discussion that many important questions relating to the friction of rubber are as yet unsolved; their solution requires further collection and generalization of facts.

---

* This equation describes data [16] on static friction over a narrow temperature range, since it passes through a minimum. However, Bartenev [3] takes only some values from our data, ignoring the minimum and the subsequent increase of F; he erroneously asserts that I wrote [16] the equation $F = A \exp(U/RT)$, whereas I used not the total frictional force F but only one term F_0.

LITERATURE CITED

[1] G. M. Bartenev, Colloid J., 18, 249 (1956).*

[2] S. B. Ratner, Colloid J., 370 (1956).*

[3] G. M. Bartenev, Colloid J., 18, 626 (1956).*

[4] B. V. Deryagin and S. B. Ratner, Proc. Acad. Sci. USSR, 103, No. 6, 1021 (1955).

[5] B. V. Deryagin, S. B. Ratner, and M. F. Futran, Proc. Acad. Sci. USSR, 92, No. 6, 1137 (1953).

[6] A. Schallamach, Proc. Phys. Soc. B65, 657, (1952).

[7] C. Many, Am. J. Phys. 20, 203, (1952).

[8] Roth, Driscoll, Holt, Rubb. Chem. Techn. 16, 155, (1953).

[9] A. Schallamach, Proc. Phys. Soc. B66, 386 (1953).

[10] J. Hurry and J. Prock, Ind. Rubb. J. 128, No. 5, 619 (1953).

[11] A. Schallamach, Koll.-Z. 141, No. 3 (1955).

[12] J. Burwell, and E. Rabinowicz, J. Appl. Phys. 24, No. 2, 136 (1953).

[13] P. Konti, Sulla resistenza di Attrito Royal Acad. de Lincei, II, (1875).

[14] I. V. Kragelsky and V. S. Shchedrov, Development of the Science of Friction (Izd. AN SSSR, 1956).

[15] S. B. Ratner and V. V. Lavrentyev, Proc. Acad. Sci. USSR, 108, No. 3 (1956).

[16] S. B. Ratner, Proc. Acad. Sci. USSR, 93, No. 1, 47 (1953).

[17] A. Tobolsky, R. Powell, and H. Eyring in Chemistry of Large Molecules, vol. 2 (IL, Moscow, 1948) p. 206.

[18] G. M. Bartenev, Proc. Acad. Sci. USSR, 96, 1161 (1954).

[19] S. B. Ratner and V. V. Lavrentyev, J. Tech. Phys., No. 4, 147 (1956).

[20] I. V. Kragelsky, Trans. II All-Union Conf. on Friction and Wear in Machines, 3 (1949).

[21] G. N. Bartenev, Proc. Acad. Sci. USSR, 103, No. 6 (1955).

Received October 18, 1956

---

* [Original Russian pagination. See C. B. Translation.]

CONCERNING THE DISCUSSION ON THE FRICTION OF RUBBER

G. M. Bartenev

The article [1] which opened the discussion raised the following problems: 1) the nature of friction, and 2) the law of the friction of rubber, since there is no agreed opinion in the literature concerning the nature of the effect, and some very varied and contradictory laws of friction are put forward.

In Ratner's second article, published in this issue, the molecular mechanisms of the friction of rubber and of the flow of liquids are confused as before. The similarity between friction and viscous flow, pointed out in our paper [2], lies in a common molecular-kinetic activation mechanism for the transition of the kinetic units through the barrier, which is also found for other processes, such as ionic conductance, diffusion, etc. Differences between these processes follow from differences in the structure and in the nature of the thermal motion of rubber and liquids. Therefore the actual mechanisms and the molecular models of these processes are different.

In Fig. 1 in Ratner's paper he compares two graphs for two essentially different friction regions (low velocities for rubber and high velocities for metals), which is inadmissible, since the distinction between the external friction of rubber and of metals, which we emphasized, is found only in the region of low sliding velocities, where no vibration or heating of the surface occur. Ratner states that the author of the paper erroneously extrapolated the data to infinitely large loads. A graph is given (Fig. 2), taken from the paper [3], in which the curve, in Ratner's opinion, is drawn from $1/p = 0$, i.e., from $p = \infty$. It was however, stated in our paper [3] that the relationship between the coefficient of friction and normal pressure was derived for $1/p > 10^{-4}$ cm^2/kg. It is evident that it is impossible to show this on a graph drawn to an ordinary scale for normal pressures from 0.1 to 100 kg/cm^2.

We still consider that: 1) the friction of rubber is a molecular-kinetic activation process, determined by its structure; 2) the static friction of rubber is therefore an arbitrary magnitude which depends on the accuracy of the determinations and the experimental conditions; 3) the analytical form of the law of rubber friction is basically determined by the dependence of the actual contact area on the load; 4) the Deryagin binomial equation cannot be applied to the friction of rubber; 5) the Ratner equation does not represent the dependence of the coefficient of friction on the load.

LITERATURE CITED

[1] G. M. Bartenev, Colloid J., 18, No. 2, 249 (1956); 18, No. 5, 626 (1956).*

[2] G. M. Bartenev, Proc. Acad. Sci. USSR, 96, No. 6, 1161 (1954).

[3] G. M. Bartenev, Proc. Acad. Sci. USSR, 103, No. 6, 1017 (1955).

[4] S. B. Ratner, Proc. Acad. Sci. USSR, 83, 443 (1952); 86, 121 (1952); Colloid J., 18, 272 (1956);* 19, 394 (1957).*

Received April 1, 1957

---

*[Original Russian pagination. See C. B. Translation.]

APPLICABILITY OF THE BINOMIAL LAW OF FRICTION TO THE FRICTION OF RUBBER

B. V. Deryagin

One point made by G. M. Bartenev, which he regards as proved, is that the binomial law of friction is not applicable to the friction of rubber. It is first necessary to stress the danger of confusing two essentially different laws under the name of a binomial law of friction:

1. The law for total friction

$$F = F(N), \tag{1}$$

which relates the frictional force F to the load N; an example of this is provided by Coulomb's empirical law of friction

$$F = AN + B,$$

where A and B are constants.

2. The elementary (elemental, in I. V. Kragelsky's terminology) law of friction, which connects the frictional and adhesion forces per unit area of true contact

$$\frac{F}{S} = \Psi\left(\frac{N}{S}\right). \tag{2}$$

The relationship which usually exists between S and N, and which may depend on the form of the bodies, must be known before it is possible to determine the form of Equation (2) when the form of Equation (1) is known from experimental data.

By suitable choice of the form of the relationship $S = S(N)$ it is possible to obtain most varied forms of Equation (2); for example, as described in [1], a mononomial law of friction $F/S = \text{const}$. It is evident that if the $S = S(N)$ function is chosen differently it is possible to obtain a binomial law $F/S = \mu(N/S + p_0)$ or any other elementary law of friction. Conversely, it follows that it is by no means proved by G. M. Bartenev [1] that the binomial elementary law of friction is inapplicable.

As regards positive proofs of the applicability of the binomial elementary law of friction to rubber, this question is discussed by me, with reference to new experimental data, in articles now in the press.

LITERATURE CITED

[1] G. M. Bartenev, Proc. Acad. Sci. USSR, 103, No. 6 (1955).

Received May 15, 1957

Editorial note: In publishing the papers by S. B. Ratner, G. M. Bartenev, and B. V. Deryagin, the editor closes the discussion on the friction of rubber.

LETTER TO THE EDITOR

USE OF ION-EXCHANGE RESINS FOR PURIFYING QUARTZ SUSPENSIONS

K. V. Chmutov and O. G. Larionov

Fine quartz suspensions made by vibratory grinding are often contaminated by metallic particles corresponding in chemical composition to the structural parts of the vibratory mill and containing iron, chromium, manganese, etc. Such suspensions must be made free from these contaminations in preparation for laboratory use. Treatment of the ground material with acids followed by washing and decantation takes a great deal of time, as the suspension settles very slowly. Washing on filters is also ineffective, as the quartz particles pass through the filter paper in large amounts.

This last fact, the poor retention by filters, was utilized by us for purification of quartz suspensions. After the metal particles have been dissolved in acid, the suspension together with the dissolved impurities is filtered through a column containing a granular cation exchange resin in the H form. The suspension passes through the column almost completely, while the salt cations remain in the resin layer.

The purification technique was as follows. A quartz suspension containing 100 g of dry material, with a solid–liquid ratio of 1 : 4, was placed in a conical flask containing a mixture of hydrochloric (50 ml) and nitric (10 ml) acids. Part of the acid was removed by 2 hours of boiling. The suspension was diluted to two liters with water and passed through a column containing KU-2 cation exchange resin in the H form. The height of the layer was 20 cm, the diameter of the column was 4 cm, and the resin grain size was 1 mm. After the layer was exhausted (reaction for iron) it was regenerated by 4 N HCl solution and washed with water to a neutral reaction to methyl orange; a new portion of solution was then passed through, etc.

If a coarse suspension is used, the upper layer of the adsorbent may become clogged with settling particles. To avoid this, the solution above the top layer can be agitated by a current of air. The use of the "fluidized layer" principle with the suspension fed in at the bottom of the column is rational, but more complicated technically, and cannot be recommended for purification of small amounts of suspension.

A static method can also be used, the suspension being shaken with a certain amount of cation exchange resin and filtered through a gauze filter on a Buchner funnel. This operation must be repeated several times with fresh portions of resin.

If a dry powder is required, excess hydrochloric acid is removed by evaporation and drying. If the suspension is to be used, it is simpler to remove the acid by similar filtration of the suspension through a column containing an anion exchange resin in the OH form.

Institute of Physical Chemistry
Academy of Sciences USSR
Chromatography Laboratory
Moscow

Received March 3, 1957

SIGNIFICANCE OF ABBREVIATIONS MOST FREQUENTLY ENCOUNTERED IN SOVIET PERIODICALS

FIAN	Phys. Inst. Acad. Sci. USSR.
GDI	Water Power Inst.
GITI	State Sci.-Tech. Press
GITTL	State Tech. and Theor. Lit. Press
GONTI	State United Sci.-Tech. Press
Gosenergoizdat	State Power Press
Goskhimizdat	State Chem. Press
GOST	All-Union State Standard
GTTI	State Tech. and Theor. Lit. Press
IL	Foreign Lit. Press
ISN (Izd. Sov. Nauk)	Soviet Science Press
Izd. AN SSSR	Acad. Sci. USSR Press
Izd. MGU	Moscow State Univ. Press
LEIIZhT	Leningrad Power Inst. of Railroad Engineering
LET	Leningrad Elec. Engr. School
LETI	Leningrad Electrotechnical Inst.
LETIIZhT	Leningrad Electrical Engineering Research Inst. of Railroad Engr.
Mashgiz	State Sci.-Tech. Press for Machine Construction Lit.
MEP	Ministry of Electrical Industry
MES	Ministry of Electrical Power Plants
MESEP	Ministry of Electrical Power Plants and the Electrical Industry
MGU	Moscow State Univ.
MKhTI	Moscow Inst. Chem. Tech.
MOPI	Moscow Regional Pedagogical Inst.
MSP	Ministry of Industrial Construction
NII ZVUKSZAPIOI	Scientific Research Inst. of Sound Recording
NIKFI	Sci. Inst. of Modern Motion Picture Photography
ONTI	United Sci.-Tech. Press
OTI	Division of Technical Information
OTN	Div. Tech. Sci.
Stroiizdat	Construction Press
TOE	Association of Power Engineers
TsKTI	Central Research Inst. for Boilers and Turbines
TsNIEL	Central Scientific Research Elec. Engr. Lab.
TsNIEL-MES	Central Scientific Research Elec. Engr. Lab.—Ministry of Electric Power Plants
TsVTI	Central Office of Economic Information
UF	Ural Branch
VIESKh	All-Union Inst. of Rural Elec. Power Stations
VNIIM	All-Union Scientific Research Inst. of Meteorology
VNIIZhDT	All-Union Scientific Research Inst. of Railroad Engineering
VTI	All-Union Thermotech. Inst.
VZEI	All-Union Power Correspondence Inst.

Note: Abbreviations not on this list and not explained in the translation have been transliterated, no further information about their significance being available to us. — Publisher.

COLLOID JOURNAL OF THE U.S.S.R. IN ENGLISH TRANSLATION

May-June, 1956

TABLE OF CONTENTS

	Page	Russ. page
1. Heats of Swelling and Solution of Polymers in Relation to Molecular Weights and Temperature. K. S. Akhmedov and S. M. Lipatov	263	257
2. Two Stages of the Network Formation Process in Polymers. G. M. Bartenev	267	261
3. The Electrochemistry of High Polymer Dispersions. 4. Influence of Cations of Different Valencies on the Electrokinetic Potential of Synthetic Latex Globules. S. S. Voyutsky and R. M. Panich	273	268
4. Adhesion of High Polymers. 3. Effects of the Size, Shape, and Polarity of High Polymer Molecules on Their Adhesion to Cellophane. S. S. Voyutsky, A. I. Shapovalova, and A. P. Pisarenko	279	274
5. Studies of the Physical Chemistry of Agar. 2. Theory and Practice of Agar Fractionation. S. A. Glikman and I. G. Shubtsova	285	281
6. The Effect of Swelling on the Strength of Vulcanizates. B. A. Dogadkin, D. L. Fedyukin, and V. E. Gul	291	287
7. Elastic Deformation of Wood. Yu. M. Ivanov	297	293
8. Thixotropic and Structuromechanical Properties of Askangel Suspensions in Relation to the Composition of the Exchange Complex. E. I. Kobakhidze, M. E. Shishniashvili, and N. N. Serb-Serbina	303	299
9. Properties of Thin Layers of Liquid Between Mica Plates. G. A. Korchinsky	311	307
10. Investigation of the Mechanical Properties of Plastic Disperse Systems in Conditions of Uniaxial Extension and Compression. E. P. Mosikhin and G. V. Vinogradov	315	311
11. Electron Microscope and X-ray Investigations of Disperse Phases in Organosols of Lead–Tin Alloys. E. M. Natanson, V. P. Chalyi, N. N. Kozachek and A. P. Kaban	323	319
12. Production of Titania–Silica Gels and Their Porous Structure. I. E. Neimark, A. I. Rastrenenko, and M. A. Piontkovskaya	329	324
13. Phase Equilibria in Colliod Systems. 1. Separation of A Homogeneous Solution Into Two Phases and the Gel Formation Process. S. P. Papkov	337	333
14. Investigation of the Structuromechanical Properties of Ethylcellulose Solutions and the Effect of Oxidation on These Properties. T. I. Samsonova and L. V. Ivanova-Chumakova	345	343
15. The Theory of Flow of Plastic Disperse Systems. N. V. Tyabin and G. V. Vinogradov	353	352
16. An Electrochemical Study of Bentonite Suspensions. 1. Action of Sodium Hydroxide on Suspensions of Electrodialyzed Askangel. I. A. Uskov and E. T. Uskova	361	361

COLLOID JOURNAL OF THE U.S.S.R. IN ENGLISH TRANSLATION

May-June, 1956

TABLE OF CONTENTS (continued)

Page | Russ. page

17. Action of the Basic Salt Aluminum Oxychloride on the Structuromechanical (Thixotropic) Properties of Askangel Suspensions. E. D. Uznadze and M. E. Shishniashvili 367 368

18. Evaluation of Rubber—Solvent Interaction. A. G. Shvarts 375 376

19. Investigation of the Adsorbability of Carbohydrate Solutions By a Polarographic Method. M. S. Shulman 383 384

20. Industrial Unit for Production of Emulsions by Means of An Ultrasonic Liquid Whistle (Jet). S. I. Sinkova and S. A. Puzyrev 387 387

Discussions

21. The Equilibrium State of High Polymer Gels. (On the Subject of the Comments by A. V. Nikolaev, R. E. Neiman, and O. V. Neiman, Colloid J. 19, 129(1957)) S. M. Lipatov and S. I. Meerson 391 390

22. Problems Relating to the Mechanism of the Friction of Rubber. S. B. Ratner 395 394

23. Concerning the Discussion on the Friction of Rubber. G. M. Bartenev 399 397

24. Applicability of the Binomial Law of Friction to the Friction of Rubber. B. V. Deryagin 401 398

Letter To The Editor

25. Use of Ion Exchange Resins for Purifying Quartz Suspensions. K. V. Chmutov and O. G. Larionov . . . . 403 ~~399~~

26. List of Abbreviations 405

BULLETIN OF THE
ACADEMY OF SCIENCES
OF THE USSR

(Izvestiya.)

in complete English translation

Contains outstanding work by the leading members of the Academy of Sciences, making it one of the most significant journals. A broad survey of Soviet chemical research, covering the general and inorganic, as well as the organic and biological fields.

SAMPLE PAPERS: Principles underlying new methods for the chemical treatment of complex iron and nickel ores; synthesis of alkenyl 2-chlorovinyl ketones; reaction of silacyclopentones and silacyclohexanes with concentrated sulfuric acid; investigation of the composition of the napthene part of the kerosene fraction of Tuimazin (Devonian) petroleum; synthesis of unsaturated organogermanium compounds.

Annual subscription, 12 issues,
approx. 1500 pages, $150.00.

Single articles available—Tables of Contents on request.

Organophosphorus. The No. 5, 1952, issue of the BAS is a special issue on organophosphorus, containing 30 articles, 175 pages, including 15 co-authored by A. E. Arbuzov . . . . $20.00.

CONSULTANTS BUREAU, INC.
227 WEST 17th STREET, NEW YORK 11, N. Y. — U.S.A.
Telephone: ALgonquin 5-0713 • Cable Address: CONBUREAU, NEW YORK

JOURNAL OF

ANALYTICAL CHEMISTRY

OF THE USSR

in complete English translation

The top Russian journal in this field, dealing with all phases of analysis, organic and inorganic, including metallurgy, petroleum, spectrochemistry. Sample articles: A simple rational design for the elementary cell of a counter current distribution apparatus; a potentiometric method of determining saponification numbers in solutions of petroleum resins; potassium tetraborate as a primary standard in acidimetry. Translation began with the 1952 volume. Annual subscription, 6 issues, approximately 800 pages, $80.00.

CONSULTANTS BUREAU, INC.

227 WEST 17th STREET, NEW YORK 11, N. Y.